EVOLVING STRATEGIES TOWARD THE SYNTHESIS OF CURCUSONE C

Thesis by

Austin C. Wright

In Partial Fulfillment of the Requirements for the Degree of

Doctor of Philosophy

California Institute of Technology

Pasadena, California

2020

(Defended January 27, 2020)

To my family

ACKNOWLEDGMENTS

I must first express gratitude to Professor Brian Stoltz for serving as my research advisor. His unconditional support of my constantly changing synthetic routes was instrumental in my development as a graduate student and, more importantly, as an independent researcher. I must also thank Professors Sarah Reisman, Jonas Peters, and Alison Ondrus for serving as my graduate committee members. Their constructive criticism throughout my time at Caltech has greatly influenced my graduate career.

My growth as an organic chemist has also been greatly impacted by several members of the Stoltz lab. As an incoming member, my understanding of all the intricate experimental procedures and theoretical concepts were shaped by Christopher Haley, with whom I collaborated on my first aryne paper. I must also profusely thank former post-doc Max Klatte for serving as my other *de facto* mentor during my mousy first year in the lab: his German-bred pragmatism helped me streamline my experimental technique, and his German-bred optimism helped me enjoy every minute of it. Later on, post-doc Caleb Hethcox proved to be another extremely useful educational resource, owing to his almost comprehensive knowledge of organic chemistry. Of course, Eric "E-Dubs" Welin must also be acknowledged for his important chemical insights both in the lab and at the bar. I'm sure he will make an outstanding addition to the faculty at UT Dallas.

I would be remiss to not also express gratitude to Chung Whan Lee for laying the groundwork for the synthesis of curcusone C, without which I would not have tackled this interesting target. I also have to acknowledge several other total synthesis specialists in the lab, particularly Beau Pritchett, Nicholas Hafeman, and Chris Reimann, whose collective input shaped my route and ultimately helped make it viable.

Beyond professional development, many of my fellow students were also excellent friends. First and foremost, I must thank Carson Matier for his constant positivity and silliness, which always managed to cheer me up. Fellow classmates Steven Loskot, David Schuman, and Alice Wong were also very kind friends and exemplary colleagues.

I have been privileged to have worked next to several outstanding hoodmates during my time at Caltech. Despite our clashing personalities and vastly different sanitary preferences for the fumehood, former graduate student Sam Shockley proved to be an invaluable friend. The astonishingly unhealthy former visiting student Yutaro Saito was truly a delight to work with, and I wish him the best of luck in his professorial pursuits. I must also mention former visiting student Rémi Lavernhe, whose seemingly unbreakable sense of humor and optimism quickly made him perhaps the most beloved member of the lab during his all-too-brief stay. Visiting student Max Kaiser unexpectedly imparted to me a fondness for chess, which I will certainly take with me beyond grad school.

Lastly, I must of course give thanks to my family. My mom in particular was always available for me.

ABSTRACT

Curcusone C is a tricyclic diterpenoid natural product possessing potent anti-cancer activities as well as a structurally unusual 2,3,7,8-tetrahydroazulene-1,4-dione skeleton. Herein, we report our evolving synthetic efforts toward the divergent total syntheses of *ent*-curcusone C and several structural congeners, which commenced with a Suzuki coupling of the peripheral carbon-based rings. Whereas the boronate partner was constructed from cyclopentenone, the halide partner could be elaborated from (*S*)-perillaldehyde. The alcohol coupling product was next esterified, then subjected to diazo transfer and cyclopropanation to produce a lactone. The resulting vinyl cyclopropane moiety was exposed to Kauffmann olefination conditions in order to form a divinylcyclopropane, which upon reductive lactone opening smoothly underwent a Cope rearrangement to establish the essential tricyclic core embedded in the curcusones.

Due to ongoing issues of scalability as well as unsatisfactory yields for the key cyclopropanation step, this route was ultimately abandoned, and an alternative strategy was devised which instead relied on a cross-electrophile coupling to join the peripheral rings. We further found that a central ring could be constructed via either Stetter annulation or ring-closing metathesis (RCM), accessing the tricyclic core of the curcusones in only 9 steps. Potential end-game strategies are further described.

We additionally report our experimental research into the acyl-amination of *in situ*-generated arynes using symmetrical imides. The difunctionalized aryl products could be further derivatized to synthetically useful indoles and quinolones via McMurray coupling and Camps cyclization, respectively.

PUBLISHED CONTENT AND CONTRIBUTIONS

Wright, A. C., C. W. Lee, B. M. Stoltz. (2019). "Progress toward the Enantioselective Synthesis of Curcusones A–D via a Divinylcyclopropane Rearrangement Strategy." In: *Organic Letters* 21, pp. 9658–9662. DOI: 10.1021/acs.orglett.9b03829.
A.C.W. Interpreted spectra, purified compounds, and wrote the manuscript.
Adapted for the contents of Chapter 1.

Wright, A. C., B. M. Stoltz. (2019). "Enantioselective construction of the tricyclic core of curcusones A–D via a cross-electrophile coupling approach." In: *Chemical Science* 10, pp. 10562–10565. DOI: 10.1039/C9SC04127C.
A.C.W. Interpreted spectra, purified compounds, and wrote the manuscript.
Adapted for the contents of Chapter 1.

Wright, A. C., C. K. Haley, et al. (2019). "Synthesis of Aryl Ketoamides via Aryne Insertion into Imides." In: *Organic Letters* 18, pp. 2793–2795. DOI: 10.1021/acs.orglett.6b00994.
A.C.W. Interpreted spectra, purified compounds, and wrote the manuscript.
Adapted for the contents of Chapter 2.

TABLE OF CONTENTS

Acknowledgments……iv
Abstract……vi
Published content and contributions……vii
Table of contents……viii
List of figures……x
List of schemes……xiii
List of tables……xiv
List of abbreviations……xv

Chapter 1 ***1***
Evolving Strategies Toward the Synthesis of Curcusone C

1.1 Introduction and Alternate Synthetic Strategies……1
1.1.1 Introduction……1
1.1.2 First Retrosynthetic Analysis: Divinylcyclopropane Rearrangement……3
1.1.3 Divinylcyclopropane Rearrangement……4
1.2 First Generation Approach……5
1.2.1 Limonene oxide Route……5
1.2.2 Perillaldehyde Route……8
1.3 Second Generation Route……13
1.3.1 Second Retrosynthetic Analysis: Cross-Electrophile Coupling……13
1.3.2 Cross-Electrophile Coupling……14
1.3.3 Construction of the Seven-Membered Ring via RCM……18
1.4 Endgame Strategies……21
1.5 Conclusion……25
1.6 Experimental Section……26
1.6.1 Materials and Methods……26
1.6.2 Preparative Procedures……28
1.7 Notes and References……58

Appendix 1 ***63***
Synthetic Summary Toward the Total Synthesis of Curcusone C

Appendix 2 ***72***
Spectra Relevant to Chapter 1: Evolving Strategies Toward the Synthesis of Curcusone C

Appendix 3 ***135***
X-Ray Crystallography Data Relevant to Chapter 1
A3.1 Crystal structure of **73**……135

Chapter 2 ***153***

Acyl-Amination of Arenes via Aryne Formation
2.1 Introduction and Background……153
2.2 Results and Discussion……155
2.3 Conclusion……159
2.4 Experimental Section……160

2.4.1 Materials and Methods……160
2.4.2 Preparative Procedures……161
2.5 Notes and References……172

Appendix 4 ***174***
Spectra Relevant to Chapter 2: Acyl-Amination of Arenes via Aryne Formation

Appendix 5 ***197***
Notebook Cross-Reference

Comprehensive Bibliography……206
Index……212
About the Author……216

LIST OF FIGURES

CHAPTER 1

Evolving Strategies Toward the Synthesis of Curcusone C

Figure 1.1.1. Reported Structures of Curcusones A–J……..……..2
Figure 1.2.1. Synthetic Evolution of Cyclohexene Coupling Fragments……..……9
*Figure 1.3.1. Uncooperative Halide Electrophiles Studied for the α-Alkylation of **65**……..……15*

APPENDIX 2

Spectra Relevant to Chapter 1: Evolving Strategies Toward the Synthesis of Curcusone C

*Figure A2.1 ^{1}H NMR (500 MHz, $CDCl_3$) of compound **28**……...73*
*Figure A2.2 Infrared spectrum (Thin Film, NaCl) of compound **28**……..……74*
*Figure A2.3 ^{13}C NMR (126 MHz, $CDCl_3$) of compound **28**……..……74*
*Figure A2.4 ^{1}H NMR (400 MHz, $CDCl_3$) of compound **31**……..……75*
*Figure A2.5 Infrared spectrum (Thin Film, NaCl) of compound **31**……..……76*
*Figure A2.6 ^{13}C NMR (101 MHz, C_6D_6) of compound **31**……..……76*
*Figure A2.7 ^{1}H NMR (400 MHz, C_6D_6) of compound **87**……..……77*
*Figure A2.8 Infrared spectrum (Thin Film, NaCl) of compound **87**……..……78*
*Figure A2.9 ^{13}C NMR (101 MHz, C_6D_6) of compound **87**……..……78*
*Figure A2.10 ^{1}H NMR (400 MHz, C_6D_6) of compound **33**……..……79*
*Figure A2.11 Infrared spectrum (Thin Film, NaCl) of compound **33**……..……80*
*Figure A2.12 ^{13}C NMR (101 MHz, $CDCl_3$) of compound **33**……..……80*
*Figure A2.13 ^{1}H NMR (500 MHz, $CDCl_3$) of compound **34**……..……81*
*Figure A2.14 Infrared spectrum (Thin Film, NaCl) of compound **34**……..……82*
*Figure A2.15 ^{13}C NMR (126 MHz, $CDCl_3$) of compound **34**……..……82*
*Figure A2.16 ^{1}H NMR (400 MHz, C_6D_6) of compound **38**……..……83*
*Figure A2.17 Infrared spectrum (Thin Film, NaCl) of compound **38**……..……84*
*Figure A2.18 ^{13}C NMR (101 MHz, C_6D_6) of compound **38**……..……84*
*Figure A2.19 ^{1}H NMR (400 MHz, C_6D_3) of compound **39**……..……85*
*Figure A2.20 Infrared spectrum (Thin Film, NaCl) of compound **39**……..……86*
*Figure A2.21 ^{13}C NMR (101 MHz, C_6D_6) of compound **39**……..……86*
*Figure A2.22 ^{1}H NMR (400 MHz, C_6D_6) of compound **88**……..……87*
*Figure A2.23 Infrared spectrum (Thin Film, NaCl) of compound **88**……..……88*
*Figure A2.24 ^{13}C NMR (101 MHz, $CDCl_3$) of compound **88**……..……88*
*Figure A2.25 ^{1}H NMR (400 MHz, CD_2Cl_2) of compound **40**……..……89*
*Figure A2.26 Infrared spectrum (Thin Film, NaCl) of compound **40**……..……90*
*Figure A2.27 ^{13}C NMR (101 MHz, CD_2Cl_2) of compound **40**……..……90*
*Figure A2.28 ^{1}H NMR (400 MHz, $CDCl_3$) of compound **41**……..……91*
*Figure A2.29 Infrared spectrum (Thin Film, NaCl) of compound **41**……..……92*
*Figure A2.30 ^{13}C NMR (101 MHz, $CDCl_3$) of compound **41**……..……92*
*Figure A2.31 ^{1}H NMR (400 MHz, $CDCl_3$) of compound **42**……..……93*
*Figure A2.32 Infrared spectrum (Thin Film, NaCl) of compound **42**……..……94*
*Figure A2.33 ^{13}C NMR (101 MHz, $CDCl_3$) of compound **42**……..……94*

Figure A2.34 ^{1}H *NMR (500 MHz,* $CDCl_3$*) of compound* ***43*** *95*
Figure A2.35 *Infrared spectrum (Thin Film, NaCl) of compound* ***43*** *96*
Figure A2.36 ^{13}C *NMR (126 MHz,* $CDCl_3$*) of compound* ***43*** *96*
Figure A2.37 ^{1}H *NMR (500 MHz,* $CDCl_3$*) of compound* ***21*** *97*
Figure A2.38 *Infrared spectrum (Thin Film, NaCl) of compound* ***21*** *98*
Figure A2.39 ^{13}C *NMR (126 MHz,* $CDCl_3$*) of compound* ***21*** *98*
Figure A2.40 ^{1}H *NMR (500 MHz,* $CDCl_3$*) of compound* ***44*** *99*
Figure A2.41 *Infrared spectrum (Thin Film, NaCl) of compound* ***44*** *100*
Figure A2.42 ^{13}C *NMR (126 MHz,* $CDCl_3$*) of compound* ***44*** *100*
Figure A2.43 ^{1}H *NMR (500 MHz,* $CDCl_3$*) of compound* ***19*** *101*
Figure A2.44 *Infrared spectrum (Thin Film, NaCl) of compound* ***19*** *102*
Figure A2.45 ^{13}C *NMR (126 MHz,* $CDCl_3$*) of compound* ***19*** *102*
Figure A2.46 ^{1}H *NMR (500 MHz,* $CDCl_3$*) of compound* ***45*** *103*
Figure A2.47 *Infrared spectrum (Thin Film, NaCl) of compound* ***45*** *103*
Figure A2.48 ^{13}C *NMR (126 MHz,* $CDCl_3$*) of compound* ***45*** *104*
Figure A2.49 ^{1}H *NMR (500 MHz,* $CDCl_3$*) of compound* ***18*** *105*
Figure A2.50 *Infrared spectrum (Thin Film, NaCl) of compound* ***18*** *106*
Figure A2.51 ^{13}C *NMR (126 MHz,* $CDCl_3$*) of compound* ***18*** *106*
Figure A2.52 ^{1}H *NMR (500 MHz,* $CDCl_3$*) of compound* ***46*** *107*
Figure A2.53 *Infrared spectrum (Thin Film, NaCl) of compound* ***46*** *108*
Figure A2.54 ^{13}C *NMR (126 MHz,* $CDCl_3$*) of compound* ***46*** *108*
Figure A2.55 ^{1}H *NMR (500 MHz,* $CDCl_3$*) of compound* ***47*** *109*
Figure A2.56 *Infrared spectrum (Thin Film, NaCl) of compound* ***47*** *110*
Figure A2.57 ^{13}C *NMR (126 MHz,* $CDCl_3$*) of compound* ***47*** *110*
Figure A2.58 ^{1}H *NMR (500 MHz, DMSO-d6) of compound* ***49*** *111*
Figure A2.59 *Infrared spectrum (Thin Film, NaCl) of compound* ***49*** *112*
Figure A2.60 ^{13}C *NMR (126 MHz, DMSO-d6) of compound* ***49*** *112*
Figure A2.61 ^{1}H *NMR (500 MHz,* C_6D_6*) of compound* ***49*** *113*
Figure A2.62 *NOESY (600 MHz,* C_6D_6*) of compound* ***49*** *114*
Figure A2.63 ^{1}H–^{1}H *gCOSY NMR (600 MHz,* C_6D_6*) of compound* ***49*** *115*
Figure A2.64 ^{1}H–^{13}C *HSQC NMR (600 MHz,* C_6D_6*) of compound* ***49*** *116*
Figure A2.65 ^{1}H *NMR (500 MHz,* $CDCl_3$*) of compound* ***60*** *117*
Figure A2.66 *Infrared spectrum (Thin Film, NaCl) of compound* ***60*** *118*
Figure A2.67 ^{13}C *NMR (126 MHz,* $CDCl_3$*) of compound* ***60*** *118*
Figure A2.68 ^{1}H *NMR (500 MHz,* $CDCl_3$*) of compound* ***58*** *119*
Figure A2.69 *Infrared spectrum (Thin Film, NaCl) of compound* ***58*** *120*
Figure A2.70 ^{13}C *NMR (126 MHz,* $CDCl_3$*) of compound* ***58*** *120*
Figure A2.71 ^{1}H–^{13}C *HSQC NMR (400 MHz,* $CDCl_3$*) of compound* ***58*** *121*
Figure A2.72 ^{1}H *NMR (500 MHz,* $CDCl_3$*) of compound* ***67*** *122*
Figure A2.73 *Infrared spectrum (Thin Film, NaCl) of compound* ***67*** *123*
Figure A2.74 ^{13}C *NMR (126 MHz,* $CDCl_3$*) of compound* ***67*** *123*
Figure A2.75 ^{1}H *NMR (500 MHz,* $CDCl_3$*) of compound* ***68*** *124*
Figure A2.76 *Infrared spectrum (Thin Film, NaCl) of compound* ***68*** *125*
Figure A2.77 ^{13}C *NMR (126 MHz,* $CDCl_3$*) of compound* ***68*** *125*
Figure A2.78 ^{1}H *NMR (500 MHz,* $CDCl_3$*) of compound* ***57*** *126*
Figure A2.79 *Infrared spectrum (Thin Film, NaCl) of compound* ***57*** *127*
Figure A2.80 ^{13}C *NMR (126 MHz,* $CDCl_3$*) of compound* ***57*** *127*
Figure A2.81 ^{1}H *NMR (500 MHz,* $CDCl_3$*) of compound* ***63*** *128*
Figure A2.82 *Infrared spectrum (Thin Film, NaCl) of compound* ***63*** *129*
Figure A2.83 ^{13}C *NMR (126 MHz,* $CDCl_3$*) of compound* ***63*** *129*
Figure A2.84 ^{1}H *NMR (500 MHz,* $CDCl_3$*) of compound* ***72*** *130*
Figure A2.85 *Infrared spectrum (Thin Film, NaCl) of compound* ***72*** *131*
Figure A2.86 ^{13}C *NMR (126 MHz,* $CDCl_3$*) of compound* ***72*** *131*

Figure A2.87 *^{1}H NMR (500 MHz, $CDCl_3$) of compound **73**……132*
Figure A2.88 *Infrared spectrum (Thin Film, NaCl) of compound **73**……133*
Figure A2.89 *^{13}C NMR (126 MHz, $CDCl_3$) of compound **73**……133*
Figure A2.90 *^{1}H–^{13}C HSQC NMR (400 MHz, $CDCl_3$) of compound **73**……134*

CHAPTER 2

Acyl-Amination of Arenes via Aryne Formation

Figure 2.2.1 *Camps Cyclization of Insertion Products to Provide Quinolones……159*

APPENDIX 4

Spectra Relevant to Chapter 2: Acyl-Amination of Arenes via Aryne Formation

Figure A4.1 *^{1}H NMR (400 MHz, $CDCl_3$) of compound **109**……175*
Figure A4.2 *Infrared spectrum (Thin Film, NaCl) of compound **109**……176*
Figure A4.3 *^{13}C NMR (101 MHz, $CDCl_3$) of compound **109**……176*
Figure A4.4 *^{1}H NMR (400 MHz, $CDCl_3$) of compound **112**……177*
Figure A4.5 *Infrared spectrum (Thin Film, NaCl) of compound **112**……178*
Figure A4.6 *^{13}C NMR (101 MHz, $CDCl_3$) of compound **112**……178*
Figure A4.7 *^{1}H NMR (400 MHz, $CDCl_3$) of compound **104c**……179*
Figure A4.8 *Infrared spectrum (Thin Film, NaCl) of compound **104c**……180*
Figure A4.9 *^{13}C NMR (101 MHz, $CDCl_3$) of compound **104c**……180*
Figure A4.10 *^{1}H NMR (400 MHz, $CDCl_3$) of compound **104d**……181*
Figure A4.11 *Infrared spectrum (Thin Film, NaCl) of compound **104d**……182*
Figure A4.12 *^{13}C NMR (101 MHz, $CDCl_3$) of compound **104d**……182*
Figure A4.13 *^{1}H NMR (400 MHz, $CDCl_3$) of compound **104e**……183*
Figure A4.14 *Infrared spectrum (Thin Film, NaCl) of compound **104e**……184*
Figure A4.15 *^{13}C NMR (101 MHz, $CDCl_3$) of compound **104e**……184*
Figure A4.16 *^{1}H NMR (400 MHz, $CDCl_3$) of compound **106a**……185*
Figure A4.17 *Infrared spectrum (Thin Film, NaCl) of compound **106a**……186*
Figure A4.18 *^{13}C NMR (101 MHz, $CDCl_3$) of compound **106a**……186*
Figure A4.19 *^{1}H NMR (400 MHz, $CDCl_3$) of compound **106b**……187*
Figure A4.20 *Infrared spectrum (Thin Film, NaCl) of compound **106b**……188*
Figure A4.21 *^{13}C NMR (101 MHz, $CDCl_3$) of compound **106b**……188*
Figure A4.22 *^{1}H NMR (400 MHz, $CDCl_3$) of compound **106c**……189*
Figure A4.23 *Infrared spectrum (Thin Film, NaCl) of compound **106c**……190*
Figure A4.24 *^{13}C NMR (101 MHz, $CDCl_3$) of compound **106c**……190*
Figure A4.25 *^{1}H NMR (500 MHz, $CDCl_3$) of compound **106d**……191*
Figure A4.26 *Infrared spectrum (Thin Film, NaCl) of compound **106d**……192*
Figure A4.27 *^{13}C NMR (126 MHz, $CDCl_3$) of compound **106d**……192*
Figure A4.28 *^{1}H NMR (400 MHz, $CDCl_3$) of compound **107c**……193*
Figure A4.29 *Infrared spectrum (Thin Film, NaCl) of compound **107c**……193*
Figure A4.30 *^{13}C NMR (101 MHz, $CDCl_3$) of compound **107c**……194*
Figure A4.31 *^{1}H NMR (400 MHz, $CDCl_3$) of compound **107a**……195*
Figure A4.32 *^{1}H NMR (400 MHz, $CDCl_3$) of compound **107b**……196*

LIST OF SCHEMES

CHAPTER 1

Evolving Strategies Toward the Synthesis of Curcusone C

Scheme 1.1.1. Previous Synthetic Efforts by the Dai Group…….3
*Scheme 1.1.2. Retrosynthetic Analysis of ent-Curcusone C (ent-**3**) via Rearrangement……....4*
*Scheme 1.1.3. Proposed Divinylcyclopropane Rearrangement of **23**……..5*
*Scheme 1.2.1. 1st Generation Synthesis of Diazo **34**……..6*
*Scheme 1.2.2. Undesired hetero-Diels–Alder of enone **27**……...6*
*Scheme 1.2.3. 2nd Generation Approach toward ent-**1**–**4**……..8*
*Scheme 1.2.4. 3rd Generation Assembly of Bicycle **19**……10*
*Scheme 1.2.5. 3rd Generation Synthesis of Divinylcyclopropane **47**……..11*
*Scheme 1.2.6. Plausible Decomposition Pathway of Diazo **18**……..11*
*Scheme 1.2.7. Construction of Tricycle **49** by Lactone Opening and Rearrangement……...12*
*Scheme 1.2.8. Envisioned Oxidative Cleavage Sequence on Diol **49**……...12*
*Scheme 1.3.1. 2nd Generation Retrosynthesis of **3**……..14*
*Scheme 1.3.2. Synthesis of Coupling Partners **59** and **60**……..15*
Scheme 1.3.3. Proposed Mechanism for Reductive Cross-Coupling……17
Scheme 1.3.4. Further Optimization of the Reductive Coupling on Multigram Scale……17
*Scheme 1.3.5. Preparation of Stetter Precursor **57**……..18*
*Scheme 1.3.6. Unsuccessful Ring Expansion of Ene-dione **70**……...20*
*Scheme 1.3.7. Construction of Tricycle **73** via an RCM Approach……21*
*Scheme 1.4.1. Divergent Oxidation Strategies to Form Ene-dione **81**……23*
*Scheme 1.4.2. Divergent Advancement of **81** to Curcusones A–D……24*

CHAPTER 2

Acyl-Amination of Arenes via Aryne Formation

*Scheme 2.1.1. Classical Preparative Procedures for Benzyne (**91**) ……154*
Scheme 2.1.2. Aryne Insertion Methods……155
*Scheme 2.1.3. Derivatization of Aryl Ketoamides **97**……155*
*Scheme 2.2.1. Plausible Mechanism for Formation of Desired **102** and Byproduct **103**……156*

LIST OF TABLES

CHAPTER 1

Evolving Strategies Toward the Synthesis of Curcusone C

*Table 1.2.1. Unsuccessful Cyclopropanation of **34**……7*
*Table 1.2.2. Unsuccessful Attempts to Oxidize Tricycle **49**……13*
Table 1.3.1. Initial Optimization of the Cross-Electrophile Coupling……16
*Table 1.3.2. Optimization of the Catalytic Stetter Reaction on Ketoaldehyde **57**……19*

CHAPTER 2

Acyl-Amination of Arenes via Aryne Formation

Table 2.2.1. Reaction Optimization……156
Table 2.2.2. Imide Substrate Scope……157
Table 2.2.3. Aryne Substrate Scope……158

LIST OF ABBREVIATIONS

Å	Ångstrom
$[\alpha]_D$	specific rotation at wavelength of sodium D line
[H]	reduction
[O]	oxidation
Ac	acetyl
acac	acetylacetonate
Anal.	combustion elemental analysis
APCI	atmospheric pressure chemical ionization
app	apparent
aq	aqueous
AIBN	2,2'-azobisisobutyronitrile
Ar	aryl
atm	atmosphere
Bn	benzyl
BOX	bisoxazoline
bp	boiling point
br	broad
Bu	butyl
i-Bu	*iso*-butyl
n-Bu	butyl
t-Bu	*tert*-butyl

Bz	benzoyl
c	concentration for specific rotation measurements
ºC	degrees Celsius
ca.	circa
calc'd	calculated
CAN	ceric ammonium nitrate
cat	catalytic
Cbz	carbobenzyloxy
CI	chemical ionization
cm^{-1}	wavenumber(s)
Cp	cyclopentadienyl
Cy	cyclohexyl
d	doublet
D	deuterium
dba	dibenzylideneacetone
DBU	1,8-diazabicyclo[5.4.0]undec-7-ene
DCC	*N*,*N'*-dicyclohexylcarbodiimide
DCE	dichloroethane
DCM	dichloromethane
decomp	decomposition
DIBAL	diisobutylaluminum hydride
DMAP	4-dimethylaminopyridine
dmdba	bis(3,5-dimethoxybenzylidene)acetone

DMF	*N,N*-dimethylformamide
DMSO	dimethyl sulfoxide
dr	diastereomeric ratio
ee	enantiomeric excess
EI	electron impact
e.g.	exempli gratia
equiv	equivalent
ESI	electrospray ionization
exp	experimental
FAB	fast atom bombardment
FID	flame ionization detector
g	gram(s)
GC	gas chromatography
gCOSY	gradient-selected correlation spectroscopy
h	hour(s)
HMDS	1,1,1,3,3,3-hexamethyldisilazane
HMPA	hexamethylphosphoramide
HPLC	high-performance liquid chromatography
HSQC	heteronuclear single quantum coherence
hv	light
Hz	hertz
IBX	2-iodobenzoic acid
IC_{50}	median inhibition concentration (50%)

i.e.	id est
i-Pr	*iso*-propyl
IR	infrared (spectroscopy)
J	coupling constant
JohnPhos	(2-Biphenyl)di-*tert*-butylphosphine
kcal	kilocalorie
KHMDS	potassium hexamethyldisilazide
l	wavelength
L	liter, ligand
LDA	lithium hexamethyldisilazide
lit.	literature value
m	multiplet; milli
m	*meta*
m/z	mass to charge ratio
M	metal; molar; molecular ion
m-CPBA	*meta*-chloroperbenzoic acid
Me	methyl
MHz	megahertz
min	minute(s)
μ	micro
MM	mixed method
mol	mole(s)
MOM	methoxymethyl

mp	melting point
Ms	methanesulfonyl (mesyl)
MS	molecular sieves
n	nano
nbd	norbornadiene
NBS	*N*-bromosuccinimide
NMO	*N*-methylmorpholine *N*-oxide
NMR	nuclear magnetic resonance
NOE	nuclear Overhauser effect
NOESY	nuclear Overhauser enhancement spectroscopy
Nu	nucleophile
o	*ortho*
p	*para*
PCC	pyridinium chlorochromate
PDC	pyridinium dichromate
Ph	phenyl
pH	hydrogen ion concentration in aqueous solution
PhH	benzene
PhMe	toluene
Pin	pinacol
p*K*a	p*K* for association of an acid
PMB	*p*-methoxybenzyl
ppm	parts per million

PPTS	pyridinium *p*-toluenesulfonate
Pr	propyl
Py	pyridine
q	quartet
ref	reference
R	generic for any atom or functional group
rt	room temperature
s	singlet or strong or selectivity factor
sat.	saturated
S_N2	second-order nucleophilic substitution
sp.	species
t	triplet
TBAF	tetrabutylammonium fluoride
TBHP	*tert*-butyl hydroperoxide
TBS	*tert*-butyldimethylsilyl
TBSal	(6*Z*)-6-[(*tert*-butylamino)methylidene]cyclohexa-2,4-dien-1-one
TES	triethylsilyl
Tf	trifluoromethanesulfonyl (triflyl)
TFA	trifluoroacetic acid
THF	tetrahydrofuran
TIPS	triisopropylsilyl
TLC	thin-layer chromatography
TMEDA	*N,N,N',N'*-tetramethylethylenediamine

TMS	trimethylsilyl
TOF	time-of-flight
Tol	tolyl
Ts	*p*-toluenesulfonyl (tosyl)
UV	ultraviolet
v/v	volume to volume
w	weak
X	anionic ligand or halide
Xyl	xylyl

CHAPTER 1

Evolving Strategies Toward the Synthesis of Curcusone C[i]

1.1 INTRODUCTION AND ALTERNATE SYNTHETIC STRATEGIES

1.1.1 INTRODUCTION

Indigenous to Central America, the flowering plant *Jatropha curcas* has traditionally been used in the manufacturing of soaps and lamp oil but has also drawn attention due to its potential applications in the biodiesel industry.[1] *J. curcas* has also received notice by organic chemists owing to its structurally diverse array of diterpenoid secondary metabolites, which includes the curcusone

(i) This research was a collaborative effort between A. C. Wright and C. W. Lee, see: reference 6, reference 19, and reference 20.

family of natural products. This family comprises various synthetically challenging and biologically active rhamnofolane diterpenoid natural products. In 1986, Naengchomnong and coworkers first isolated curcusones A–D (**1**–**4**, Figure 1.1.1) and elucidated the structures of **2** and **3** via X-ray diffraction.[2] Over the ensuing three decades, several more members of this family were structurally identified and were further discovered to possess anticancer activity.[3] Among them, curcusone C (**3**) demonstrates the most potent and varied anticancer properties, including anti-proliferative activity against human hepatoma (IC_{50} in 2.17 uM), ovarian carcinoma (IC_{50} in 0.160 uM), and promyeolycytic leukemia (IC_{50} in 1.36 uM).[2]

Figure 1.1.1. Reported Structures of Curcusones A–J

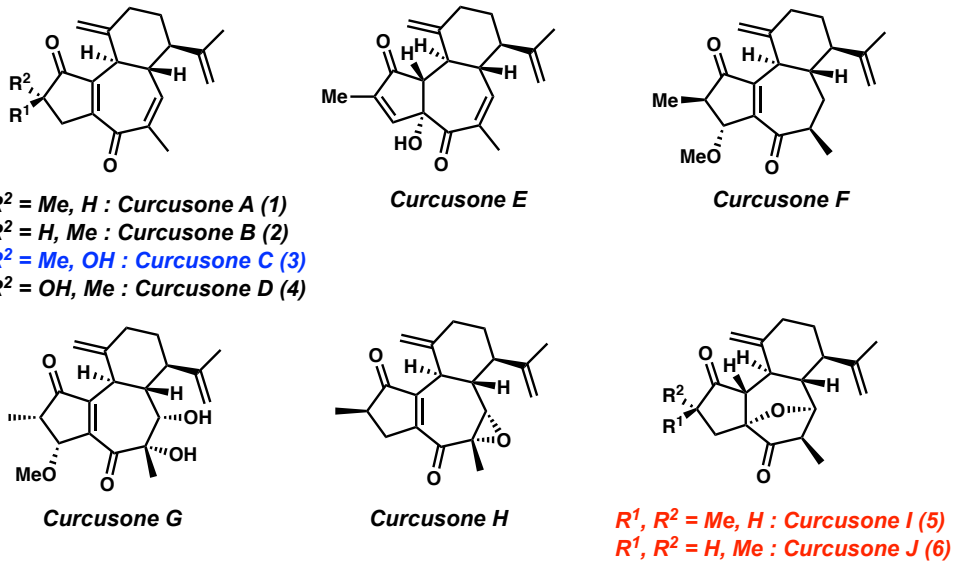

Despite these enticing biological features, **3** and all of its structural relatives have yet to surrender to any total synthesis campaigns. It is worthwhile to note that the Dai lab recently reported a synthesis of racemic oxo-bridged **5** and **6** over 21 steps (Scheme 1.1.1). Thus, they were able to elaborate known propargyl ether **7** to allene **8** over 3 steps. In the presence of a Au(I) catalyst, **8** undergoes a cascade sequence to deliver oxo-bridged **10** via transient furan **9**. They were further able to construct the eastern carbocyclic ring over 14 steps, providing late-stage *exo*-

methylene **14** via Diels–Alder adduct **13**. Lastly, they advanced **14** via α-methylation, desilylation, and oxidation, furnishing the reported structures of curcusones I (**5**) and J (**6**) in modest yields. Unfortunately, the stereochemistry of both of these putative natural product structures were found to have been incorrectly assigned by NMR.[4,5] We do not anticipate these issues with **3**, as its structure has been unambiguously determined by X-ray crystallography.[2]

Scheme 1.1.1. Previous Synthetic Efforts by the Dai Group

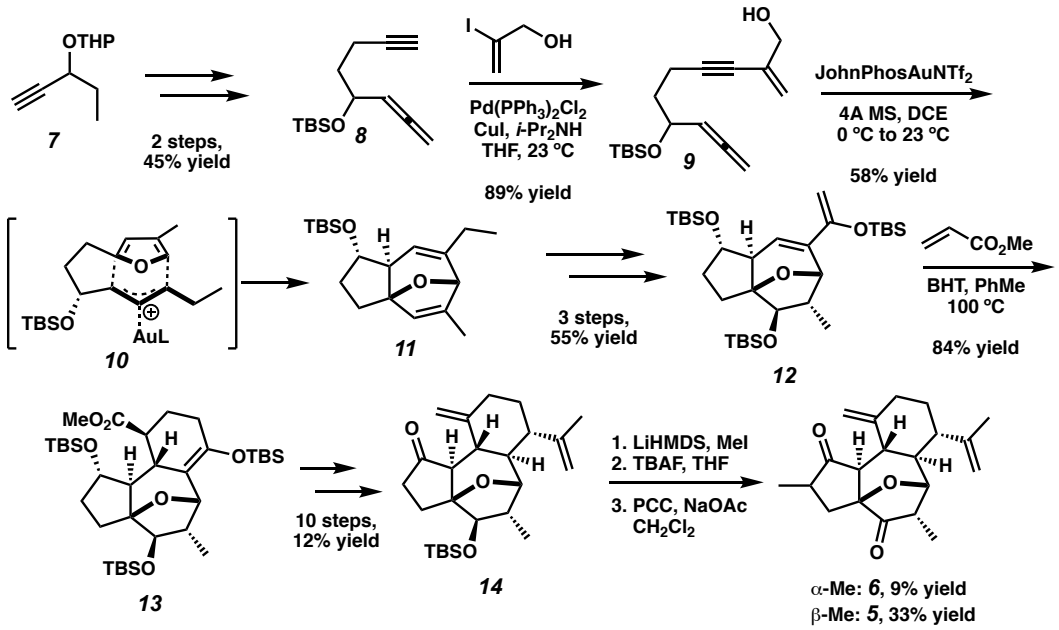

1.1.2 FIRST RETROSYNTHETIC ANALYSIS: DIVINYLCYCLOPROPANE REARRANGEMENT

After attempting several strategically related routes, our retrosynthesis eventually proposed that a late-stage α-functionalization would permit a divergent approach to the enantiomeric series of curcusones A–D (Scheme 1.1.2). As such, we envisioned performing an α-functionalization, oxidation, and olefination of silyl ether **15** (highlighted in red). The ene-dione moiety of **15** may be derived from ketoalcohol **16** by means of alcohol oxidation and acid- or base-promoted olefin

migration. The central seven-membered ring present in **16** could be assembled by a stereospecific divinylcyclopropane rearrangement and subsequent oxidative cleavage of hydroxymethylated cyclopropane **17**. We predicted that the cyclopropane moiety in **17** might be installed via intramolecular π-bond-cyclopropanation of a metallocarbenoid derived from diazo ketoester **18** followed by methylenation and reductive lactone opening. The diazo oxobutanoyl functionality in **18** (highlighted in red) could be incorporated by acylation and diazo transfer of alcohol **19**. Bicycle **19** may be accessed by a Suzuki cross-coupling of monocyclic fragments (+)-**20** and **21**, both of which could be derived from commercial materials.

*Scheme 1.1.2. Retrosynthetic Analysis of ent-Curcusone C (ent-**3**) via Rearrangement*

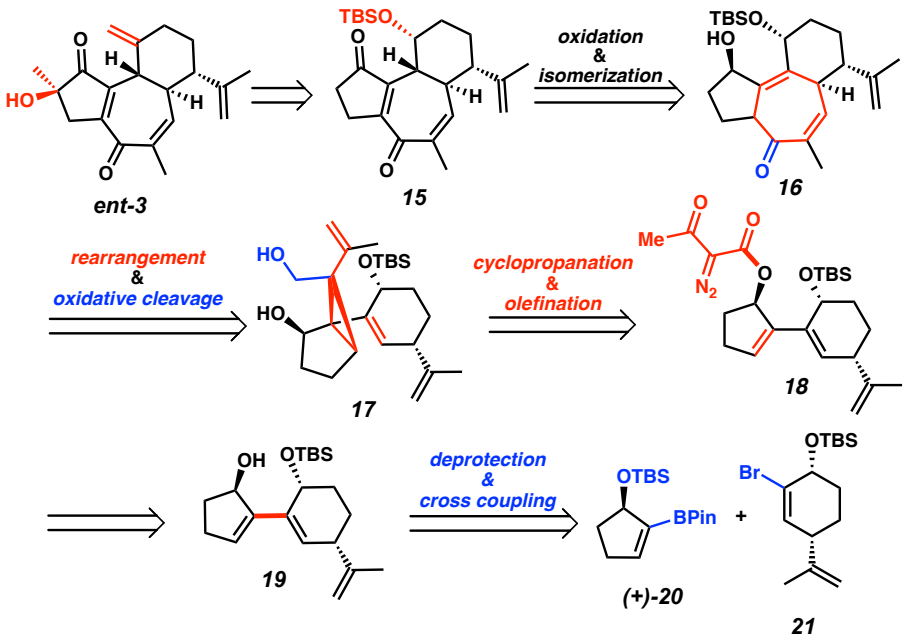

1.1.3 DIVINYLCYCLOPROPANE REARRANGEMENT

At the outset of our synthetic studies, we planned to incorporate the requisite *exo*-methylene of **3** prior to cross-coupling, affording desired cyclopropane **23** through intermediate diazo **22** (Scheme 1.1.3). Crucial to the success of our synthesis was a divinylcyclopropane rearrangement

to establish the structurally challenging central seven-membered ring. We presumed that this process would occur through a concerted Cope rearrangement via *endo* boat transition state **24**, providing tricycle **25** in a stereospecific fashion as dictated by the stereochemistry at C5 of **23**.

*Scheme 1.1.3. Proposed Divinylcyclopropane Rearrangement of **23***

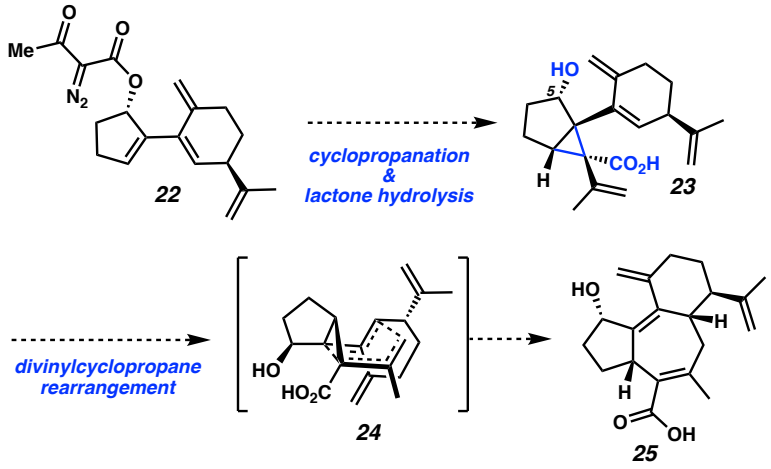

1.2 FIRST GENERATION APPROACH

1.2.1 LIMONENE OXIDE ROUTE

Upon first validating our route via model studies,[6] we next set out to deploy our technology on the actual system. We envisioned that the requisite bicycle **31** could be derived from a Suzuki coupling of boronate (–)-**20** and vinyl triflate **28** (Scheme 1.2.1). To this end, commercially available limonene oxide (**26**) was exposed to base-induced eliminative epoxide opening to provide an allylic alcohol, which could be further subjected to DMP oxidation[7] to afford enone **27** as well as an undesired hetero-Diels–Alder adduct (Scheme 1.2.2, highlighted in red). Following careful optimization, we eventually found that **27** could be elaborated to enol triflate **28** in satisfactory yields using KHMDS and Comins reagent.[8] Meanwhile, boronate partner (–)-**20** was

assembled from known vinyl bromide (–)-**30**[9] via CBS reduction, alcohol protection, and *O*-silylation. Pleasingly, Suzuki coupling of fragments (–)-**20** and **28** delivered requisite bicyclic diene **31**, which upon silyl deprotection, acetoacetylation, and diazo transfer delivered annulation precursor **34** via α-ketoester **33**.

*Scheme 1.2.1. 1st Generation Synthesis of Diazo **34***

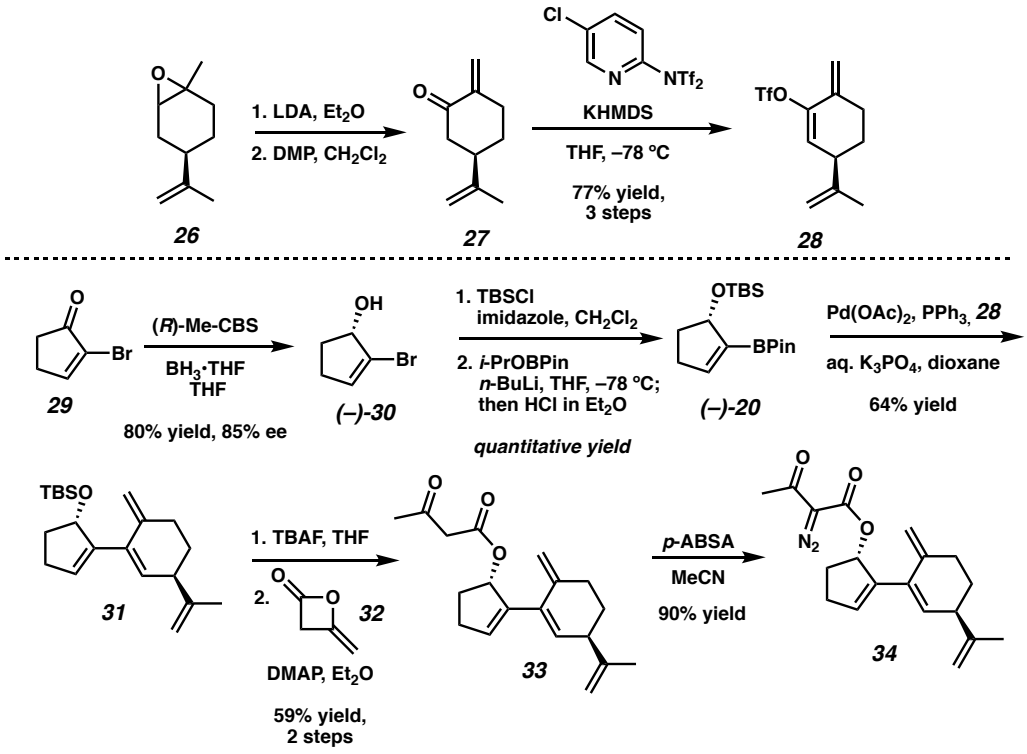

*Scheme 1.2.2. Undesired Hetero-Diels–Alder of Enone **27***

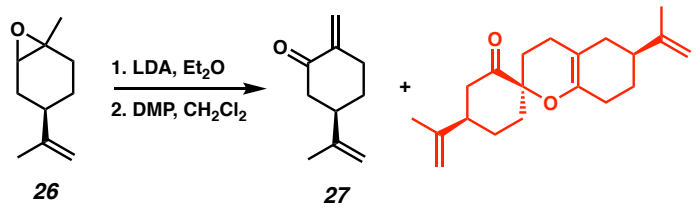

With diazo **34** in hand, we next investigated the critical cyclopropanation step (Table 1.2.1). Unfortunately, all attempts to advance **34** to **35** resulted in decomposition (Entries 1–3), a complex mixture of byproducts (Entry 4), or simply no reactivity (Entry 5). These combined issues necessitated a revision of our synthetic route. Given the success of our model system[6] toward similar cyclopropanation conditions, we speculated that the inability to execute this transformation on diazo **34** might be due to subtle stereoelectronic influences imparted by the presence of the proximal *exo*-methylene group (highlighted in red). In particular, the *exo*-methylene group may pose modest steric constraints on the system, preventing facile metallocarbenoid formation and subsequent cyclopropanation. It might also electronically deactivate the highly conjugated π system toward cyclopropanation, encouraging an unwanted decomposition pathway. In light of this, we instead chose to install a ketone functionality, which we suspected could be elaborated to the corresponding *exo*-methylene upon olefination. We eventually deduced that we could accomplish this by instead assembling the 6-membered-ring fragment from (*S*)-perillaldehyde.

*Table 1.2.1. Unsuccessful Cyclopropanation of **34***

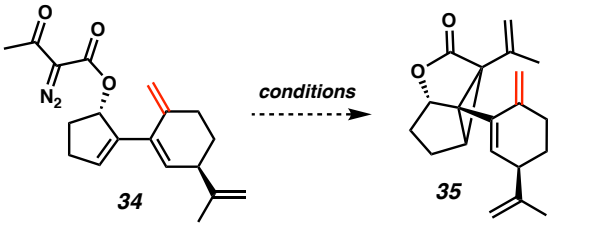

entry	catalyst	solvent	temperature	result
1[a]	$Cu(TBSal)_2$	PhMe	reflux	decomp
2[a]	$Cu(hfacac)_2$	PhMe	45 °C–75 °C	decomp
3[b]	CuOTf	PhMe	45 °C–75 °C	decomp
4[b]	$Rh_2(OAc)_4$	CH_2Cl_2	23 °C	complex mixture
5[b]	$Pd(OAc)_2$	Et_2O	0 °C	no reaction

[a] Reaction conditions: catalyst (5 mol %), solvent (0.05 M). [b] Reaction conditions: catalyst (10 mol %), solvent (0.05 M)

1.2.2 PERILLALDEHYDE ROUTE

Now targeting the enantiomeric series of curcusones A–D via coupling of enone fragment **38**, we assembled cyclohexenone **37** over three steps from (*S*)-perillaldehyde (**36**, Scheme 1.2.3) according to known methods.[10] An ensuing α-iodination of **37** using I_2 and pyridine provided desired iodoenone **38**, which itself could undergo the anticipated Suzuki coupling with boronate (+)-**20**[11] to furnish corresponding bicycle **39** in good yield. Silyl ether **39** could be advanced to α-ketoester **40** without event following deprotection and transacylation with diketene (**32**). Although the vital base-mediated diazo transfer and cyclopropanation sequence gratifyingly furnished desired enone **41**, significant amounts of unwanted olefin isomer **42** were also observed. Unfortunately, all efforts to perform a subsequent double olefination on the two ketones of **41** (highlighted in red) failed, prompting us to again reassess our route.

*Scheme 1.2.3. 2nd Generation Approach Toward ent-**1**–**4***

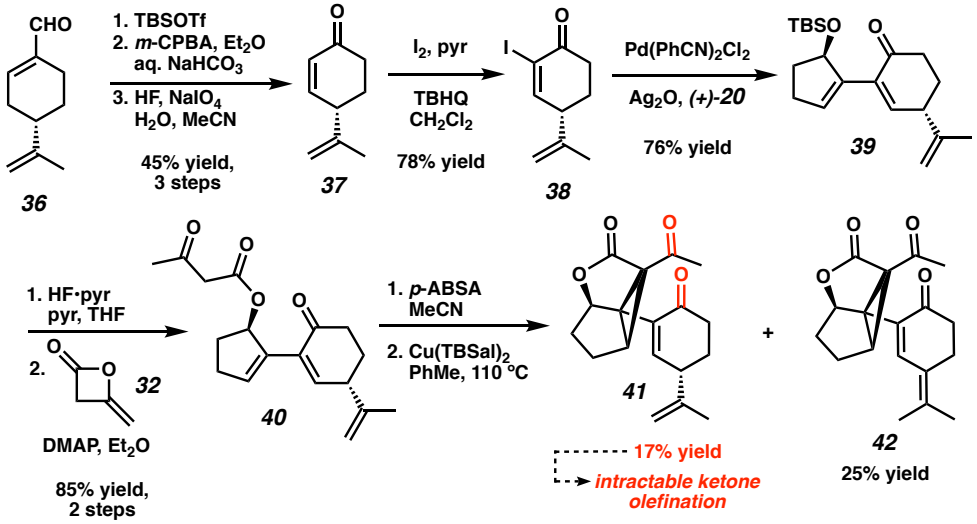

Considering the undesired isomerization pathways facilitated by the presence of the γ proton in enone **38** (Figure 1.2.1, highlighted in red), we finally decided to instead target a 1,2-reduced

and protected analogue of enone **38** (i.e., silyl allyl ether **21**, Scheme 1.2.4). This route commenced with bromination of **37** to afford bromoenone **43**, which could be non-selectively reduced in a 1,2-fashion and *O*-silylated to produce desired *cis* epimer **21** along with the undesired *trans* epimer in roughly equal portions. It is worthwhile to note that the thermodynamically[12] and kinetically[13] favored *trans* epimer was also investigated as a potential synthetic intermediate but was eventually found to be totally uncooperative toward cyclopropanation conditions due to exclusive decomposition. Moving forward, the redundancy of silyl protecting groups in both coupling partners motivated us to attempt deprotecting the boronate fragment prior to cross coupling. Unfortunately, after an exhaustive screening we found no silyl deprotection conditions that could accommodate the presence of the base- and acid-sensitive boronate functionality. Other protecting groups were also investigated with minimal success.[14] Interestingly, over the course of our efforts we eventually discovered that a cyclopentenol protection strategy could be avoided altogether by performing an unconventional double lithiation/boronate trapping procedure on (+)-**30** with pinacolborane to provide allyl alcohol **44**. With revised boronate **44** and bromide **21** in our possession, we next explored the crucial Suzuki coupling. Gratifyingly, standard coupling conditions afforded bicyclic alcohol **19** in good yield.

Figure 1.2.1. Synthetic Evolution of Cyclohexene Coupling Fragments

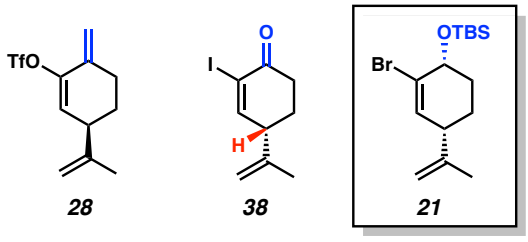

*Scheme 1.2.4. 3rd Generation Assembly of Bicycle **19***

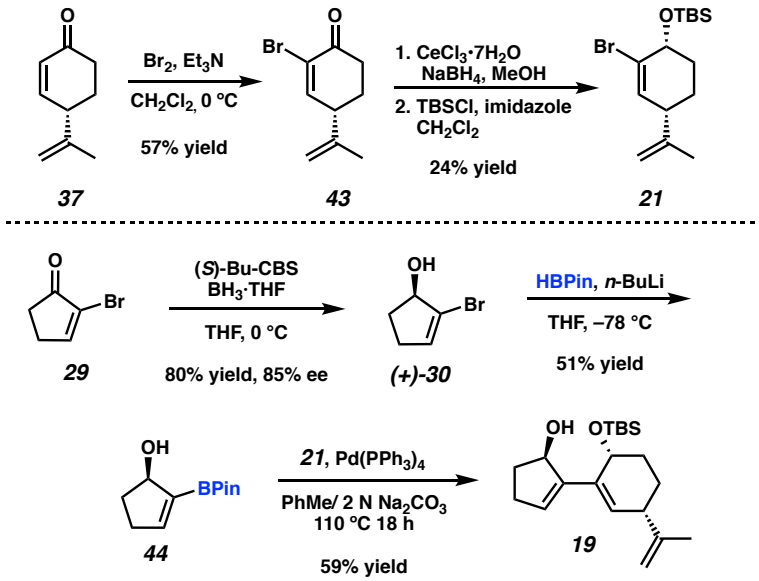

As expected, bicycle **19** could be readily advanced to cyclopropanation precursor **18** following esterification and diazo transfer (Scheme 1.2.5). We were further pleased to find that exposure of diazo **18** to previously optimized cyclopropanation conditions did indeed afford annulated product **46**, albeit only on small scales (i.e., 20 mg or less) and with substantial portions of an unwanted byproduct.[15] The sole byproduct of cyclopropanation encountered during our synthetic studies was identified as ketone **48,** whose formation may be explained by the radical-based fragmentation pathway described below (Scheme 1.2.6). However, we cannot rule out an alternative mechanism following intramolecular C–H insertion of a transient carbenoid to instead afford a β-lactone, which upon base-induced lactone opening and fragmentation would also produce ketone **48**.[16] With provision of cyclopropane **46**, we next aimed to append the second vinyl tether. After extensive studies, we discovered that methylenation of the ketone in **46** to olefin **47** could be achieved under Kauffmann olefination conditions,[17] thereby finally establishing the essential divinylcyclopropane system.

*Scheme 1.2.5. 3rd Generation Synthesis of Divinylcyclopropane **47***

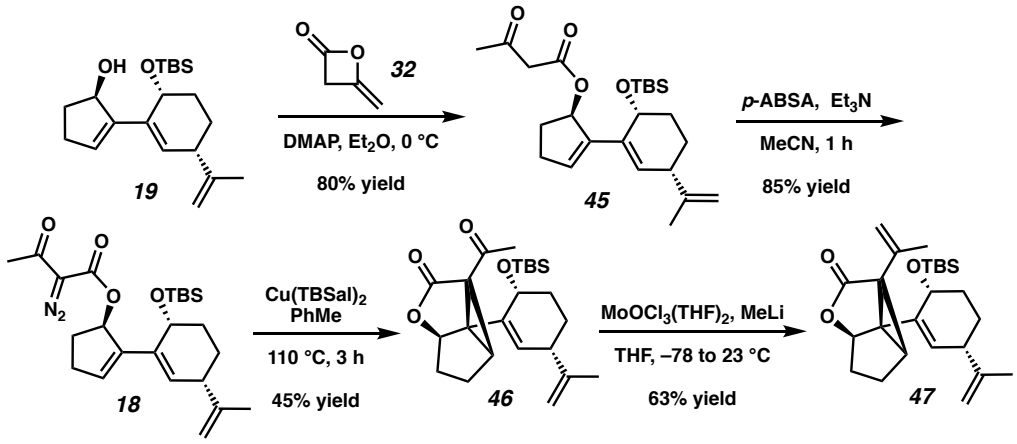

*Scheme 1.2.6. Plausible Decomposition Pathway of Diazo **18***

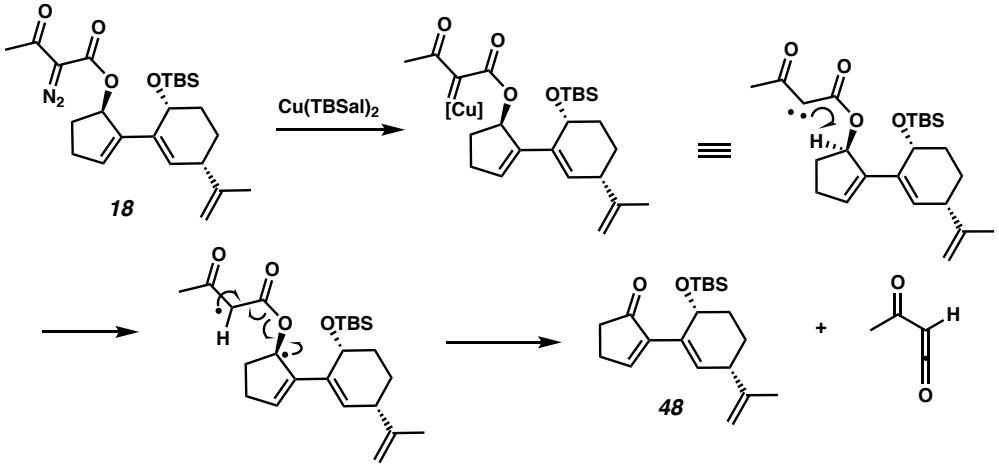

Upon accessing divinylated intermediate **47**, we set out to induce the pivotal rearrangement. To this end, reductive opening of the butyrolactone moiety of **47** provided envisioned diol **17** along with minor amounts of desired rearrangement product **49** (Scheme 1.2.7). Fortuitously, we found that this crude product mixture smoothly underwent the desired divinylcyclopropane rearrangement upon gentle heating to provide tricycle **49**, possessing the carbocyclic skeleton embedded in each of the curcusones.

*SCHEME 1.2.7. Construction of Tricycle **49** by Lactone Opening and Rearrangement*

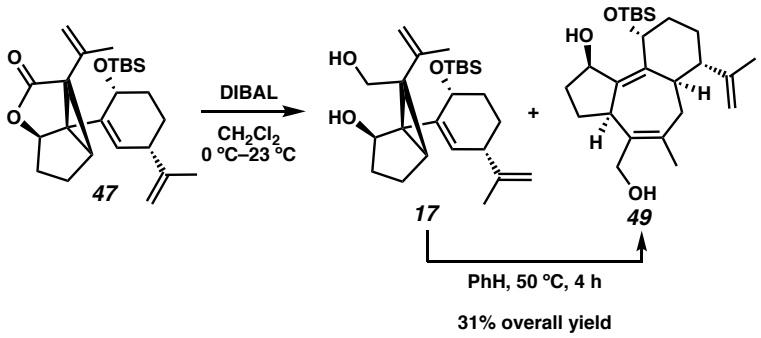

With the 5–7–6 carbon skeleton finally in hand, we were eager to elaborate diol **49** to ketoacid **50** via chemoselective oxidation of the primary alcohol (Scheme 1.2.8). In particular, we suspected that acid **50** may itself undergo the crucial oxidative cleavage via conversion to an acid chloride and subsequent carboxy-inversion and hydrolysis, delivering desired β,γ-unsaturated ketone **51**.[18]

*Scheme 1.2.8. Envisioned Oxidative Cleavage Sequence on Diol **49***

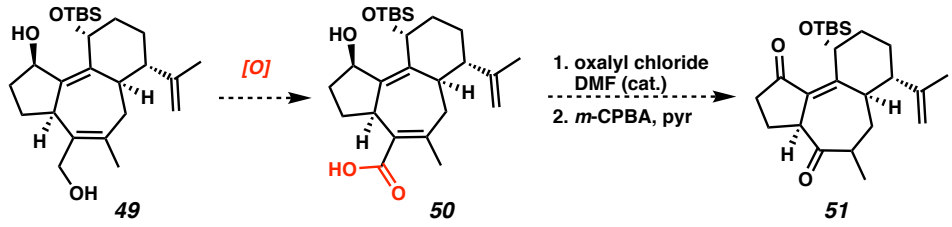

With an endgame strategy in mind, we were eager to initiate studies by performing a chemoselective oxidation of the primary alcohol of **49** (Table 1.2.2). We were however disappointed to find that all attempts to advance **49** to partially oxidized aldehyde **52** have thus far led to rapid decomposition, likely due to the exceptional instability of **49** toward oxidative conditions. Eventually, the combined difficulties posed by this substrate instability and by the prohibitively scale-dependent cyclopropanation step motivated us to embark on an entirely new route, which was since found to hinge on an RCM approach to assemble the central seven-membered ring.[19]

*Table 1.2.2. Unsuccessful Attempts to Oxidize Tricycle **49***

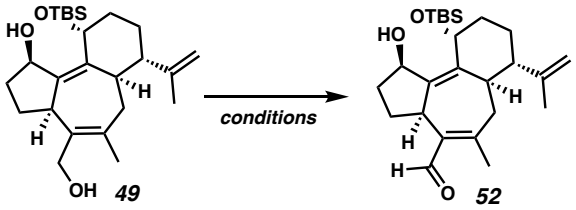

entry	conditions	result
1	DMP	decomp
2	$COCl_2$, DMSO; Et_3N	decomp
3	$[Cu(MeCN)_4]PF_6$, TEMPO, air	decomp
4	Cu(OTf)·PhH, TEMPO, air	decomp
5	MnO_2, CH_2Cl_2	decomp
6	PDC, CH_2Cl_2	decomp

1.3 SECOND GENERATION APPROACH

1.3.1 SECOND RETROSYNTHETIC ANALYSIS: CROSS-ELECTROPHILE COUPLING

Although we had initially aimed to construct the central seven-membered ring motif in **1**–**4** via a divinylcyclopropane rearrangement,[20] we found this route intractable due to the poor scalability of the key cyclopropanation step and to the oxidative instability of the frontier material. In a 2nd generation route, we envisioned that curcusone C and its structural relatives could be divergently assembled by α-functionalization of tricycle **53** (Scheme 1.3.1). The 2-methylcycloheptadienone moiety embedded in **53** may be derived from methylation and olefin migration of corresponding diosphenol intermediate **54**, which itself might be prepared by sequential dehydrogenation and oxygenation of 1,4-dione **55**. The central seven-membered ring found in **55** could be constructed via a one-carbon ring expansion of **56**. We suspected that the resulting six-membered ring in **56** may be installed by an intramolecular Stetter reaction of ketoaldehyde **57**. Intermediate **57** may itself be accessible by reduction and ketal cleavage of ester **58**. The carbon–carbon bond bridging the five- and six-membered ring systems of **58** could be

forged by a crucial cross-electrophile coupling of monocyclic bromide **59** and triflate **60,** which we envisioned could themselves each be accessed over only two steps from commercially available compounds.

*Scheme 1.3.1. 2nd Generation Retrosynthesis of **3***

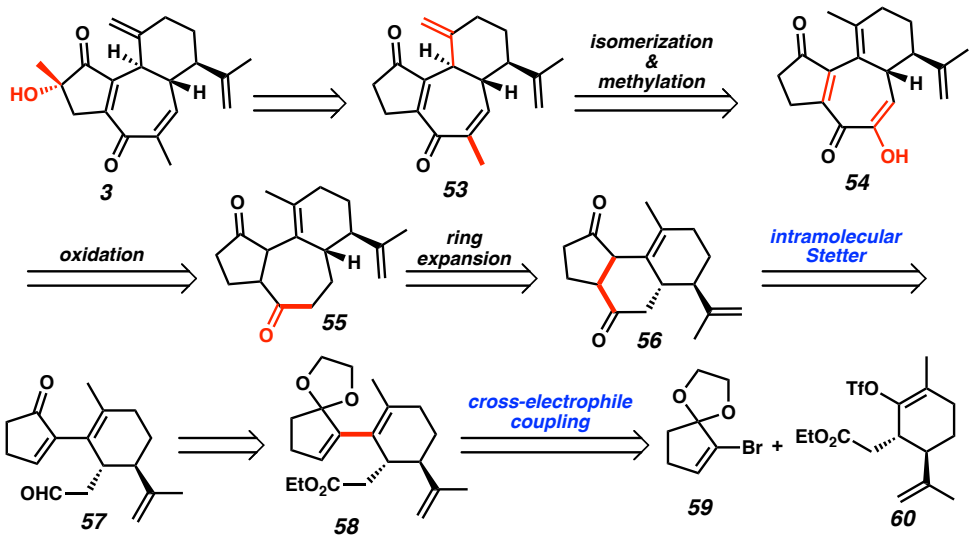

1.3.2 CROSS-ELECTROPHILE COUPLING

To achieve our first goal of constructing bicycle **58**, we set out to perform a reductive cross-coupling of electrophiles **59** and **60**. To this end, we synthesized vinyl triflate **60** by a two-step sequence involving a known α-alkylation of (*R*)-carvone[21] (**65**, Scheme 1.3.2, *vide infra*) followed by conjugate reduction of intermediate enone **66** and trapping of the resulting enolate with an electrophilic triflating agent. Numerous other carbon-based halide electrophiles such as dibromide **61**, β-bromoester **62**, and allyl iodide **63** were examined while exploring the critical α-alkylation step, but all unfortunately provided unsatisfactory yields and poor diastereoselectivities (Figure 1.3.1). Meanwhile, we found that bromide coupling partner **59** could be rapidly assembled in two steps according to known methods.[22]

Figure 1.3.1. Uncooperative Halide Electrophiles Studied for the α-Alkylation of ***65***

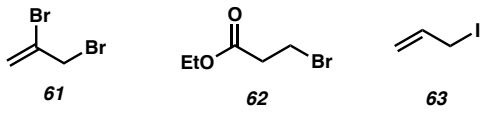

Scheme 1.3.2. Synthesis of Coupling Partners ***59*** *and* ***60***

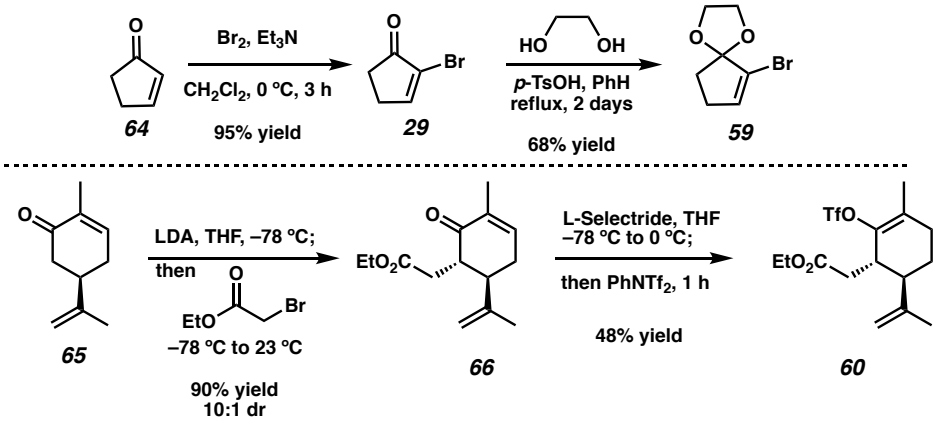

With both coupling partners now in hand, we directed our attention to the crucial cross-coupling step. Although we had initially intended to join the monocyclic fragments via traditional nucleophile–electrophile coupling approaches, we were dismayed to find that these strategies all failed to afford any product. Inspired by pioneering research from the Weix group[23] and our colleagues in the Reisman lab,[24] we decided to instead employ a reductive coupling strategy using a dual Pd/Ni catalytic system. To our delight, this system offered modest amounts of desired bicycle **58**, albeit with rapid decomposition of bromide **59** (Table 1.3.1, Entry 1). Control experiments omitting either the Pd or Ni catalysts resulted in no detectable product formation (Entries 2 and 3), revealing that both transition metals were indeed crucial to the reaction. Adjusting the choice of solvent (Entry 4), metal halide additive (Entries 5 and 6) and terminal reducing agent (Entry 7)[25] offered no improvement in yields. Increasing the equivalents of bromide **59** slightly benefitted product formation (Entry 8), likely due to the instability of **59** under the

reaction conditions. Gratifyingly, syringe pump addition of **59** over several hours resulted in markedly better yields with minimal substrate decomposition (Entry 9). We suspect this boost in yield is due to the consistently low concentration of **59** in solution, which might discourage undesirable hydrodehalogenation and homodimerization pathways.[26]

Table 1.3.1. Initial Optimization of the Cross-Electrophile Coupling

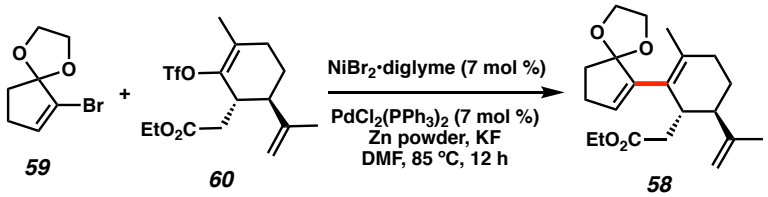

59 ***60*** ***58***

Entry	Deviation from standard procedure	Result
1	none	23% yield
2	No Pd	no product
3	No Ni	no product
4	dioxane instead of DMF	no product
5	NaI instead of KF	trace ***58***
6	no KF	trace ***58***
7	TDAE* instead of Zn	no product
8	4 equiv of ***59***	32% yield
9	syringe pump addition of ***59***	60% yield

*TDAE = tetrakis(dimethylamino)ethylene

Mechanistically, the reductive coupling is thought to commence with reduction of the Ni(II) and Pd(II) pre-catalysts. Next, a chemoselective oxidative addition of the active Pd(0) and Ni(0) catalysts will take place with the respective triflate and bromide partners (Scheme 1.3.3). Based on recent studies from the Weix group,[27] a subsequent transmetallation from Ni to Zn is thought to provide a transient organozinc species, which itself will undergo a second transmetallation to Pd to deliver a di-organopalladium species and a Zn(II) salt byproduct. Following this, reductive elimination of the Pd(II) intermediate furnishes the coupled product and regenerates the active Pd(0) catalyst. Meanwhile, reduction of the resultant Ni(II) salt with a stoichiometric Zn(0) reductant will turn over the Ni(0) catalyst. It is worthwhile to note that although we have so far

found no empirical evidence to suggest that the catalytic cycle of Ni occurs through single-electron insertion process, such a pathway cannot be definitively ruled out.

Scheme 1.3.3. Proposed Mechanism for Reductive Cross-Coupling

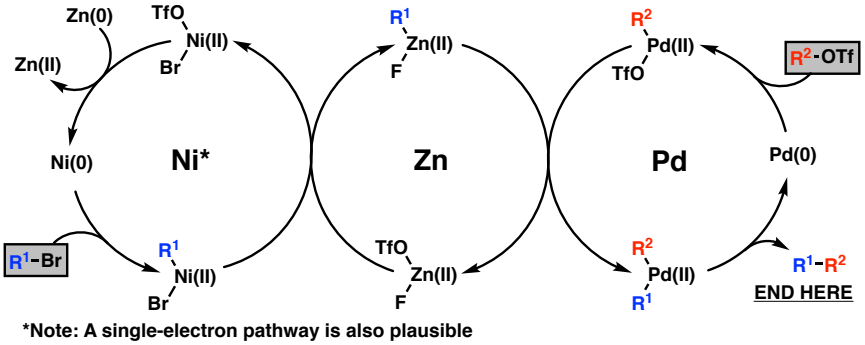

Upon scale-up, yields for this coupling process proved somewhat inconsistent due to a precipitous drop in reaction rates after roughly 50% conversion of triflate **60**. We hypothesized this to be caused by competitive coordination of the Lewis acidic Zn(II) byproduct to the essential fluoride additive, which serves as a bridging ligand during one or both of the proposed transmetallation events. In order to reverse this undesirable effect, we introduced ZnF_2 to the reaction and were pleased to find that this co-additive benefited both reproducibility and scalability, allowing us to reliably achieve 62–67% yields on multigram scale (Scheme 1.3.4). In stark contrast, simply increasing the stoichiometry of KF in the reaction generally lowered yields.

Scheme 1.3.4. Further Optimization of the Reductive Coupling on Multigram Scale

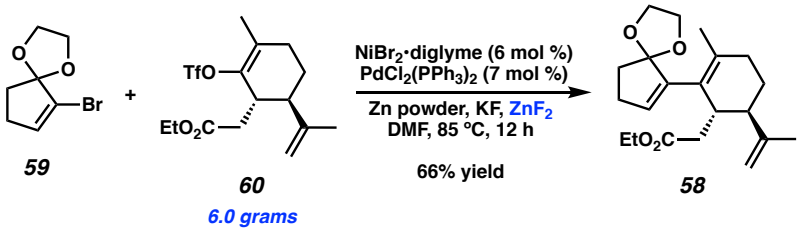

1.3.3 CONSTRUCTION OF THE SEVEN-MEMBERED RING BY RCM

With sufficient quantities of bicycle **58** now in hand, we focused our attention on the formation of the central seven-membered ring. The 1,4-dione synthon in targets **1**–**4** enticed us to pursue an umpolung Stetter disconnection. Although we initially planned to construct the seven-membered ring via one-carbon homologation of the carbonyl tether followed by Stetter annulation, all strategies relying on Wittig–Levine alkoxymethylenation,[28] α-alkoxycarbanion addition[29] and Van Leusen cyanation[30] offered either no reactivity or only trace product. As such, we instead envisioned performing a ring expansion[31] of corresponding Stetter adduct **56** (Scheme 1.3.1, *vide supra*). Thus, we eventually found that ester **58** could be readily elaborated to Stetter precursor **57** by means of Weinreb amidation, partial reduction with DIBAL, and acid-promoted ketal cleavage (Scheme 1.3.5).

*Scheme 1.3.5. Preparation of Stetter Precursor **57***

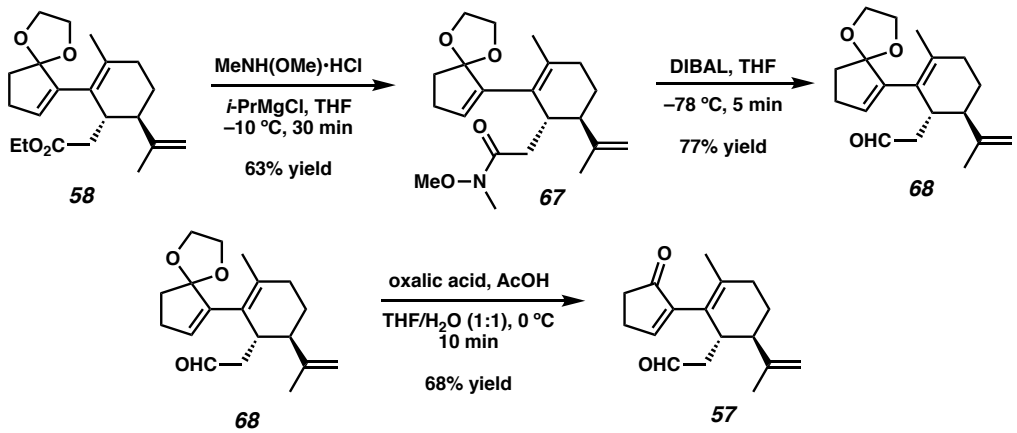

Now having rapid access to ketoaldehyde **57**, we explored the crucial Stetter annulation (Table 1.3.2). Fortuitously, exposure of **57** to NHC scaffold **69** in the presence of DBU did indeed furnish tricycle **56** in low yield and as a 1:1 mixture of diastereomers (Entry 1).[32,] Although the absolute stereochemistry of the two diastereomers could not be unambiguously elucidated, a comparison of

the relevant *J* values in the ^{1}H spectrum suggests that they possess the same relative stereochemistry at the 5–6 junction. Substitution of DBU with a metallo-base such as LiHMDS resulted primarily in 1,2-adduct formation (Entry 2),[33] likely due to the high oxophilicity of the lithium counter-cation. Altering the choice of catalyst only modestly improved yields but dramatically enhanced dr (Entry 3). Depression of temperature or catalyst loading resulted in sluggish reactivity and only modest improvements in dr (Entry 4). Eventually, a compromise was struck between yield and diastereoselectivity using 1,1,3,3-tetramethylguanidine (TMG, highlighted in blue) as the catalytic base (Entry 5), which provided **56** in fair yield and in 2:1 dr. To the best of our knowledge, this is the first instance of TMG conferring optimal yields and dr in an NHC-catalyzed Stetter reaction.

*Table 1.3.2. Optimization of the Catalytic Stetter Reaction on Ketoaldehyde **57***

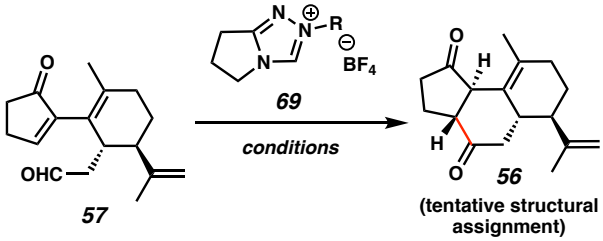

entry	R	catalyst loading	conditions	result*
1	Ph	30 mol %	DBU, dioxane 80 °C, 12 h	17% yield 1:1 dr
2	C_6F_5	30 mol %	LiHMDS, PhMe 70 °C, 12 h	1,2-adduct
3	C_6F_5	20 mol %	DBU, THF 30 °C, 30 min	24% yield 5:1 dr
4	C_6F_5	5 mol %	DBU, THF, 0 °C–23°C 12 h	incomplete conversion
5	C_6F_5	15 mol %	TMG, THF 23 °C–45 °C	50–60% yield 2:1 dr

*Relative stereochemistry at the 5–6 juncture was identified by ^{1}H NMR, however the absolute stereochemistry could not be determined.

With the 5–6–6 tricyclic core now installed, we next aimed to effect a one-carbon expansion of the central ring in **56**. Unfortunately, all attempts to perform nucleophilic addition into either

ketone moiety resulted in no reactivity, perhaps due to competing enolate formation. We eventually discovered that prolonged exposure of the diastereomeric mixture of **56** to strong acid resulted in a gradual olefin migration to stereoconvergently provide **70**, bearing the requisite ene-dione motif found in curcusones A–D (Scheme 1.3.6). Unfortunately, all attempts to expand the central ring of **70** to cycloheptenone **71** also failed, motivating us to reconsider our synthetic approach to the construction of the seven-membered ring.

*Scheme 1.3.6. Unsuccessful Ring Expansion of Ene-dione **70***

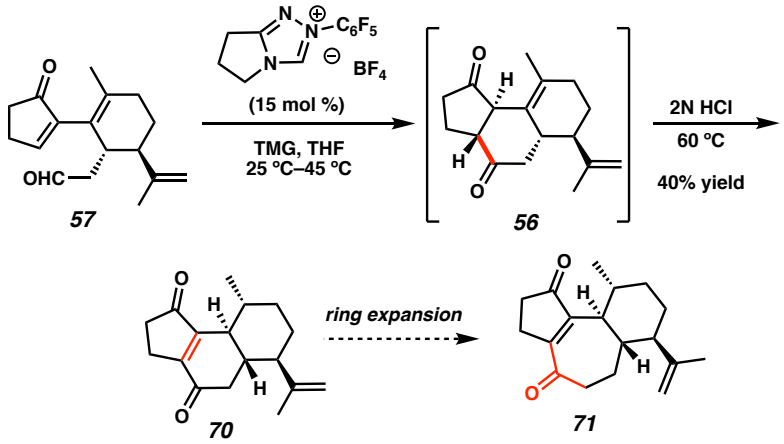

In a revised approach, we anticipated that the central ring might instead arise from a ring-closing metathesis (RCM) strategy. Thus, we conducted a one-pot olefination/ketal deprotection on common intermediate **68** to provide enone **72**, possessing the first necessary olefin tether (Scheme 1.3.7). We first planned to install the second olefin tether by means of Cu-mediated 1,4-addition to the enone of **72**, but all attempts to effect this transformation failed. To sidestep this roadblock, we instead chose to exploit a latent element of rotational symmetry in the cyclopentenone moiety. As such, we performed a sequential 1,2-vinylation of **72** to afford an intermediate *bis*-allylic alcohol, which upon Babler–Dauben oxidative rearrangement[34] by the action of PDC provided the desired dienone RCM precursor with good regioselectivity, albeit with

minor amounts of a chromatographically inseparable aldehyde isomer.[35] We were delighted to find that exposure of semi-crude RCM precursor to catalytic HGII smoothly delivered desired tricycle **73**, thereby providing rapid access to the carbocyclic core of curcusones A–D. We were incidentally pleased to find that the isopropenyl group in **73** (highlighted in red) proved to be inert toward RCM conditions, ensuring high topological selectivity for the desired ring closure. Interestingly, the crystal structure of **73** reveals that one of the double bonds (highlighted in purple) prefers to lie out of conjugation with the remainder of the π system, likely due to the considerable strain it imposes on the central ring.

*Scheme 1.3.7. Construction of Tricycle **73** via an RCM Approach*

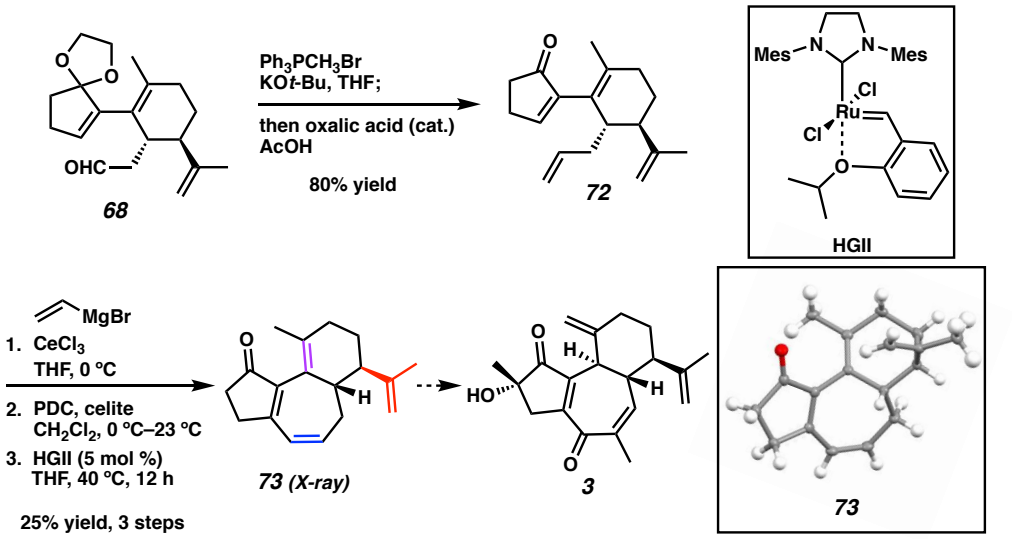

1.4 ENDGAME STRATEGIES

Now having the carbocyclic skeleton of targets **1**–**4** in our possession, we directed our efforts toward completing their respective syntheses. Considering the apparent coplanarity of the dienone framework of crystal structure **73** (Scheme 1.3.7, *vide supra*), we next aimed to install the second ketone motif in the seven-membered ring by leveraging the heightened electrophilicity at the γ-δ

unsaturation (highlighted in blue). To this end, we first attempted nucleophilic epoxidation using peroxide anion chemistry.[36] To our dismay, all attempts to effect this deceptively simple transformation have thus far failed due to a surprising lack of reactivity.

In light of our inability to directly oxygenate the desired olefin, we instead turned toward multi-step approaches such as hydroboration–oxidation chemistry to provide allylic alcohol **75**, as well as organocuprate addition to deliver methylated **74** (Scheme 1.4.1). Unfortunately, neither of these approaches proved fruitful due to a continued lack of reactivity at the desired olefin. To date, the only productive chemistry on recalcitrant substrate **73** was achieved by conjugate reduction with L-Selectride to provide putative enolate intermediate **76** as determined by proton quenching studies.[37] As such, our future plans will consist of attempting to trap out enolate **76** with an electrophilic reagent. Unfortunately, **76** has so far proven unreactive toward trapping with *N*-chlorosuccinimide and Davis oxaziridine **77**,[38] presumably due to the stability conferred on the enolate by its extensive conjugation. However, there are several highly activated analogues[39] of **77** which may prove reactive toward **76**. Assuming this oxidation event occurs, additional concerns of regioselectivity may arise owing to the three potentially nucleophilic sites in **76**. In the event that oxidation occurs α to the enolate **76** (highlighted in purple), α-ketoalcohol **78** intermediate will arise. Subsequent exposure of **78** to oxidative transposition conditions with PDC should deliver ene-dione **81**.[34] Alternatively, if oxidation occurs at the desired position of **76** (highlighted in blue), further oxidation of the resulting allylic alcohol should also furnish **81**. In the unlikely event that oxidation instead occurs at the most sterically and electronically deactivated position of **76** (highlighted in red), we will instead advance resultant tertiary alcohol **79** to intermediate **80** via electrophilic epoxidation. A Markovnikov reductive epoxide opening of **80** with Cp_2TiCl[40] and

subsequent alcohol oxidation with concomitant δ hydroxide elimination will again provide common intermediate **81**.

*Scheme 1.4.1. Divergent Oxidation Strategies to Form Ene-dione **81***

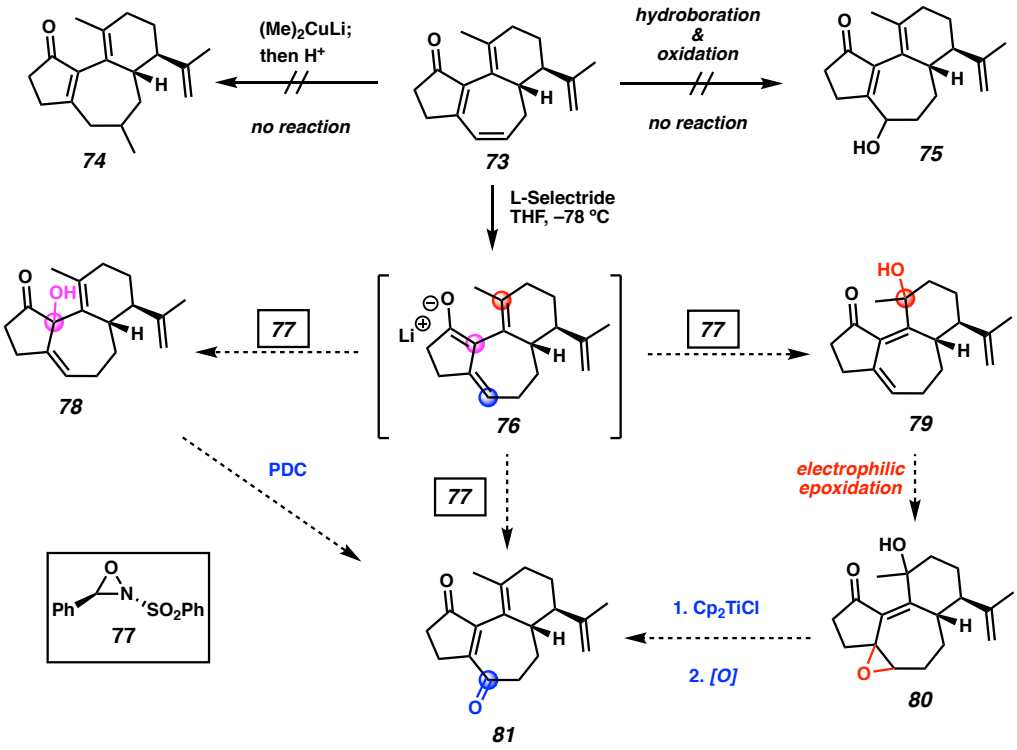

We suspect that the regioselectivity of a subsequent α-functionalization will be entirely dependent on the relative kinetic acidity of the protons α to both ketones (highlighted in blue and red). In the event that the cyclopentenone is more kinetically acidic, we will first install an α-methyl group to provide **82** as a mixture of epimers. On the other hand, if the cycloheptenone proves to be more kinetically acidic we will instead perform an α-hydroxylation to deliver epimers **83**. With intermediates **82** or **83** in our possession, we next aim to effect a base- or acid-mediated olefin migration in order to isomerize the cyclohexenyl olefin out of conjugation to deliver an *exo*-methylene. Although this isomerization event might be thermodynamically disfavored owing to the reduced substitution of the migrated olefin, the absence of more substituted olefin isomers

among the known members of the curcusones suggests that exocyclic olefin migration will offer a thermodynamic sink for this process. In the event that this is not the case, we will instead target *iso*-curcusones A–D. Following isomerization of **82** or **83**, we will next perform either α-hydroxylation or dehydration to deliver **84** or **85**, respectively. Late-stage intermediates **84** and **85** will be convergently advanced to curcusones A (**1**) and B (**2**) in as few as 15 total steps. Natural products **1** and **2** may be further subjected to α-hydroxylation, furnishing curcusones C (**3**) and D (**4**) in as few as 16 steps.

*Scheme 1.4.2. Divergent Advancement of **81** to Curcusones A–D*

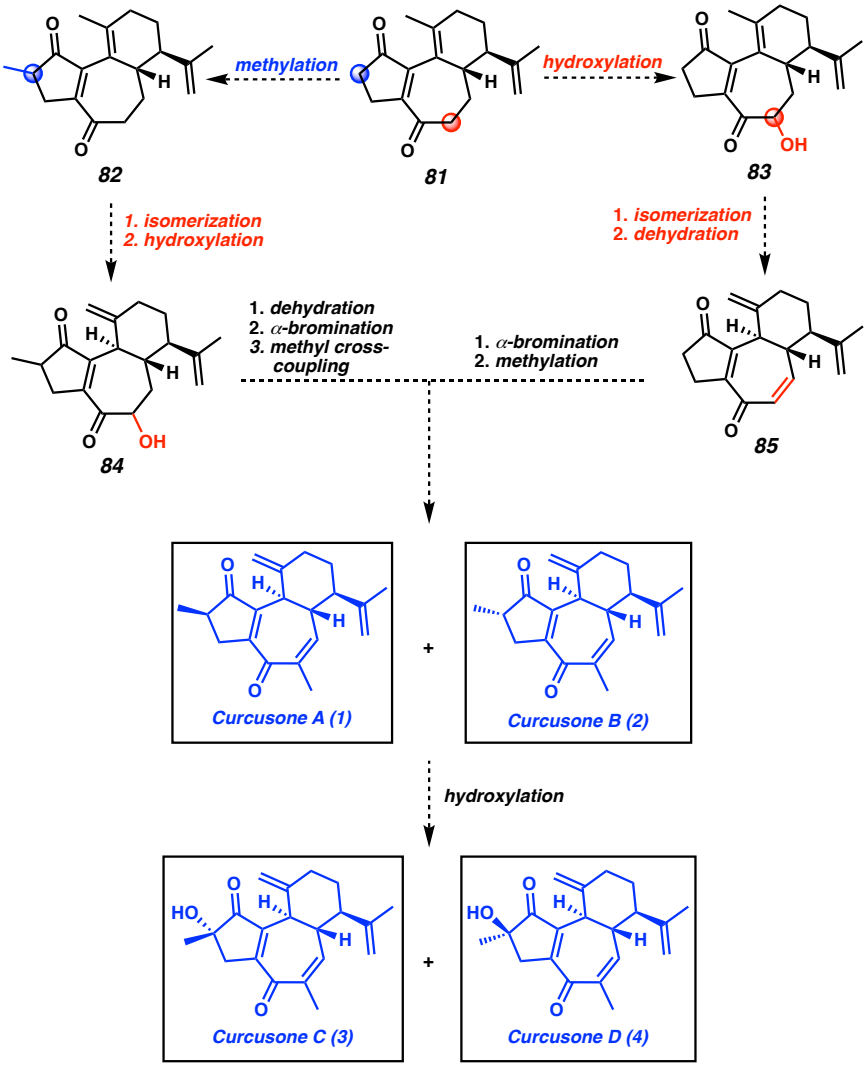

1.5 CONCLUSION

To summarize, we have disclosed our evolving strategies toward the first total synthesis of curcusone C. Our first-generation route hinged on a 1,1-divinylcyclopropane rearrangement, which was unfortunately found to be intractable owing to the highly scale- and substrate-dependent cyclopropanation step. As such, we eventually discovered an expedient and scalable route that instead relied on a cross-electrophile and RCM sequence in order to form crucial intermediate **73**, bearing the 5/7/6 carbocyclic skeleton embedded in the curcusones. Several alternative oxygenative strategies to advance **73** to curcusones A–D are currently under careful scrutiny in our group.

A1.6 EXPERIMENTAL SECTION

A1.6.1 MATERIALS AND METHODS

Unless stated otherwise, reactions were performed under an argon or nitrogen atmosphere using dry, deoxygenated solvents (distilled or passed over a column of activated alumina).[41] Et_3N, *i*-Pr_2NEt, *i*-Pr_2NH, pyridine, and *i*-PrOH were distilled from calcium hydride immediately prior to use. Commercially obtained reagents were used as received unless otherwise stated. *p*-ABSA,[42] $Cu(TBSal)_2$,[43] and $MoCl_3(THF)_2$[44] were prepared by known methods. Reactions were heated in an oil bath, and the temperatures were controlled by an IKAmag temperature modulator. Thin-layer chromatography (TLC) was performed using E. Merck silica gel 60 F254 precoated plates (0.25 mm) and visualized by UV fluorescence quenching, or potassium permanganate, iodine, or anisaldehyde staining. Silia*Flash* P60 Academic Silica gel (particle size 0.040-0.063 mm) was used for flash chromatography. ^1H and ^{13}C NMR spectra were recorded on a Varian Inova 600 (600 MHz and 151 MHz, respectively), Varian Inova 500 (at 500 MHz and 126 MHz, respectively), Bruker AV III HD spectrometer equipped with a Prodigy liquid nitrogen temperature cryoprobe (400 MHz and 101 MHz, respectively) and are reported relative to $CHCl_3$ (δ 7.26 and 77.16, respectively), C_6H_6 (δ 7.16 and 128.06, respectively), and CH_2Cl_2 (δ 5.32 and 53.84, respectively). Data for ^1H NMR spectra are reported as follows: chemical shift (δ ppm) (multiplicity, coupling constant (Hz), integration). IR spectra were recorded on a Perkin Elmer Paragon 1000 Spectrometer and are reported in frequency of absorption (cm^{-1}). HRMS were acquired from the Caltech Mass Spectral Facility using a JEOL JMS-600H High Resolution Mass Spectrometer in fast atom bombardment (FAB+) or electron ionization (EI+) mode or using an Agilent 6200 Series TOF with an Agilent G1978A Multimode source in electrospray ionization (ESI), atmospheric pressure chemical ionization (APCI) or mixed (MM) ionization mode. Optical

rotations were measured on a Jasco P-2000 polarimeter using a 100 mm path length cell at 589 nm.

1.6.2 PREPARATIVE PROCEDURES

26 *27*

Enone 27: To a flame-dried round-bottom flask with a magnetic stir bar were added diisopropyl amine (1.75 mL, 13.3 mmol, 1.1 equiv) and Et_2O (35 mL). A solution of *n*-BuLi (2.12 M in hexane, 6.84 mL, 14.5 mmol, 1.2 equiv) was added dropwise over a period of 30 min. A solution of epoxide **26** (2 mL, 12.1 mmol, 1.0 equiv) in Et_2O (7 mL) was added dropwise over a period of 30 min. The resulting mixture was allowed to warm up to 23 ºC and then stirred for 7 h. The reaction mixture was cooled in ice bath and water was added. The organic phase was separated and washed with 2 M aqueous HCl (10 mL), water (10 mL), saturated aqueous $NaHCO_3$ (10 mL) and brine (10 mL). The Et_2O extracts are combined, dried over $MgSO_4$, and evaporated to afford crude mixture. The residue was used for the next reaction without further purification. To a round-bottom flask equipped with a magnetic stir bar were added semi-crude allylic alcohol (124 mg, 0.815 mmol) and DCM (10 mL). Dess–Martin periodinane (440 mg, 1.06 mmol) was added to the mixture. The reaction was stirred for 3 h at 23 ºC. The reaction mixture was diluted with Et_2O (10 mL) and then a 1:1:1 mixture of saturated aqueous $Na_2S_2O_3$ (10 mL), saturated aqueous $NaHCO_3$ (10 mL), and water (10 mL) was added slowly. The resulting mixture was stirred for 20 min resulting in two clear layers. The organic layer was gathered, and the aqueous layer was extracted with Et_2O (30 mL x 3). The organic layers were combined and dried over Na_2SO_4, and evaporated to afford crude mixture (Caution, the solvent was only partially removed, as enone **27** dimerizes

easily.) The mixture was filtered through silica gel (8:1 pentane: Et_2O) and used in the next reaction without further purification. The characterization data matched those reported in the literature.[7]

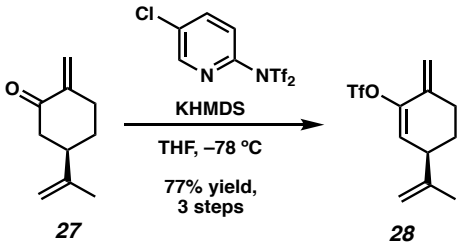

Vinyl triflate 28: To a flame-dried round-bottom flask equipped with a magnetic stir bar was added potassium bis(trimethylsilyl)amide (310 mg, 1.55 mmol, 1.6 equiv) in a nitrogen filled glove box. The flask was sealed with rubber septum and removed from the glove box, connected to a nitrogen inlet, and cooled to –78 ºC. A solution of semi-crude enone **27** (150 mg, 1 mmol, 1.0 equiv) in THF (10 mL) was added dropwise by syringe pump over 2 h. After the addition of enone **27** was completed, Comins reagent (652 mg, 1.66 mmol, 1.7 equiv) in THF (10 mL) was added dropwise. After stirring for 4 h at –78 ºC, the reaction mixture was poured into saturated aqueous $NaHCO_3$ (50 mL) and allowed to warm to 23 ºC. The mixture was extracted with Et_2O (30 x 3 mL). The combined organic layers were washed with brine (100 mL), dried over $MgSO_4$, and concentrated under reduced pressure. The residue was purified by flash column chromatography (25:1 hexanes: EtOAc) to afford triflate **28** (218 mg, 0.77 mmol, 77% yield over 3 steps); $R_f = 0.52$ (4:1, hexanes: EtOAc); ^{1}H NMR (500 MHz, $CDCl_3$) δ 5.82 (dd, J = 4.0, 1.7 Hz, 1H), 5.28 (s, 1H), 5.06–4.99 (m, 1H), 4.88 (t, J = 1.5 Hz, 1H), 4.77 (dt, J = 1.7, 0.9 Hz, 1H), 3.14–3.06 (m, 1H), 2.63–2.49 (m, 1H), 2.48–2.37 (m, 1H), 1.95–1.83 (m, 1H), 1.77 (s, 3H), 1.72–1.60 (m, 1H); ^{13}C NMR (126 MHz, $CDCl_3$) δ 149.5, 147.1, 145.8, 144.0, 139.5, 136.5, 136.0, 126.3, 123.9, 120.7, 119.9, 117.4, 112.8, 112.0, 111.1, 1102, 43.4, 29.6, 27.0, 21.3; IR (Neat Film, NaCl) 3084, 2947, 2869, 1648, 1608, 1447, 1436, 1422, 1428, 1373, 1245, 1214, 1143, 1129, 1066, 1045, 1017, 998,

978, 948, 755, 737 cm^{-1}; HRMS (FAB+) *m/z* calc'd for $C_{11}H_{12}F_3O_3S$ $[M+H-H_{\square}]^+$: 281.0459, found 281.0473; $[\alpha]_D^{25.0}$ 61.1° (*c* 0.25, $CHCl_3$).

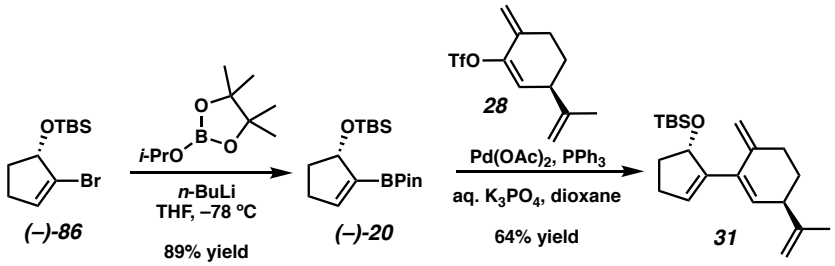

Bicycle 31: To a flame-dried round-bottom flask with a magnetic stir bar were added bromide (–)-**86** (6.0 g, 21.6 mmol, 1.0 equiv)[45] and THF (70 mL). The flask was cooled to –78 ºC and stirred for 10 min, after which *n*-BuLi (2.5 M in hexanes, 13 mL, 32.5 mmol, 1.5 equiv) was added dropwise. The reaction mixture was stirred at –78 ºC for 30 min and isopropyl pinacolyl borate (6.9 mL, 33.8 mmol, 1.6 equiv) was added. The reaction mixture was stirred at –78 ºC for 30 min and quenched with HCl solution (2 N in Et_2O, 16.3 mL, 32.5 mmol, 1.5 equiv). Following addition, the reaction mixture was diluted with Et_2O (70 mL) and warmed up to 23 ºC. The reaction mixture was filtered and concentrated under reduced pressure, and the resulting residue was used in the next reaction without further purification.

To a flame-dried round-bottom flask equipped with a magnetic stir bar were added semi-crude boronate (–)-**20** (2.65 g, 7.74 mmol, 1.1 equiv), triflate **28** (1.987 g, 7.04 mmol 1.0 equiv), palladium acetate (82 mg, 0.35 mmol, 5.0 mol %), triphenylphosphine (199 mg, 0.70 mmol, 10 mol %), and tribasic potassium phosphate (4.5 g, 21 mmol, 3.0 equiv). The mixture was evacuated and back filled with argon (x3), and to the reaction was added dioxane (25 mL) and water (2.5 mL). The reaction mixture was stirred at 23 ºC for 40 h, diluted with EtOAc (25 mL), washed with saturated aqueous NH_4Cl (25 mL), and dried over $MgSO_4$. The mixture was filtered and

concentrated under reduced pressure to afford crude mixture of **31** as a colorless oil. The resulting residue was purified by flash column chromatography (25:1 hexanes: EtOAc) to afford diene **31** (1.5 g, 4.54 mmol, 64% yield over triflate **28**) R_f = 0.95 (10:1, hexanes: EtOAc); ^{1}H NMR (400 MHz, C_6D_6) δ 5.88–5.84 (m, 1H), 5.70–5.68 (m, 1H), 5.02–4.93 (m, 2H), 4.93–4.88 (m, 2H), 4.85–4.81 (m, 1H), 2.97–2.91 (m, 1H), 2.51–2.30 (m, 4H), 2.16–2.02 (m, 2H), 1.80 (tt, *J* = 8.3, 4.0 Hz, 2H), 1.72–1.56 (m, 2H), 1.00 (s, 9H), 0.09 (s, 6H); ^{13}C NMR (101 MHz, C_6D_6) δ 148.5, 146.7, 143.4, 135.9, 132.7, 130.9, 111.0, 110.7, 78.7, 45.1, 34.8, 32.1, 29.3, 26.2, 26.0, 20.9, 18.4, –4.3, –4.5; IR (Neat Film, NaCl) 3435, 3080, 2956, 2929, 2856, 2360, 1725, 1645, 1472, 1463, 1362, 1258, 1095, 1020, 947, 865, 836, 801, 776 cm^{-1}; HRMS (FAB+) *m/z* calc'd for $C_{21}H_{33}OSi$ $[M+H–H_2]^+$: 329.2301, found 329.2297; $[\alpha]_D^{25.0}$ –38.3° (*c* 0.150, $CHCl_3$).

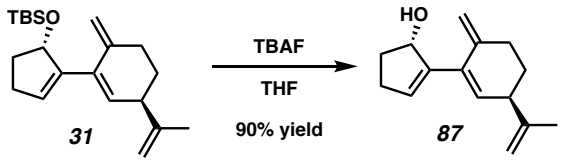

Alcohol 87: To a round-bottom flask with a magnetic stir bar were added silyl ether **31** (1.5 g, 4.54 mmol, 1.0 equiv) and THF (23 mL). To the mixture was added TBAF (1.0 M in THF, 7.7 mL, 7.7 mmol, 1.7 equiv) and stirred for 24 h at 23 ºC. The reaction mixture was quenched with sat. aq. NH_4Cl (20 mL) and extracted with Et_2O (3 x 10 mL). The organic layers were combined, dried over $MgSO_4$, and concentrated under reduced pressure. The residue was purified by flash column chromatography (3:1 hexanes: EtOAc) to afford allylic alcohol **87** (1.23 g, 5.69 mmol, 90% yield) as a colorless oil; R_f = 0.10 (10:1, hexanes: EtOAc); ^{1}H NMR (400 MHz, C_6D_6) δ5.84–5.79 (m, 1H), 5.76–5.71 (m, 1H), 5.11–5.05 (m, 1H), 4.95–4.86 (m, 3H), 4.85–4.80 (m, 1H), 2.92–2.81 (m, 1H), 2.43–2.21 (m, 3H), 2.19–1.98 (m, 2H), 1.85–1.68 (m, 2H), 1.66–1.45 (m, 4H), 1.21 (d, *J* = 5.8 Hz, 1H); ^{13}C NMR (101 MHz, C_6D_6) δ 148.6, 146.0, 143.4, 135.1, 132.2, 131.2, 128.4,

128.3, 128.2, 128.1, 127.9, 127.8, 111.2, 111.1, 78.0, 45.0, 33.9, 32. 5, 30.3, 29.5, 20.7; IR (Neat Film, NaCl) 3774, 3659, 3078, 3042, 2935, 2852, 2112, 1644, 1442, 1373, 1311, 1166, 1047, 930, 889, 843 cm^{-1}; HRMS (FAB+) *m/z* calc'd for $C_{15}H_{19}O_3$ $[M+H-H_2]^+$: 215.1436, found 215.1441; $[\alpha]_D^{25.0}$ –16.2° (*c* 0.150, $CHCl_3$).

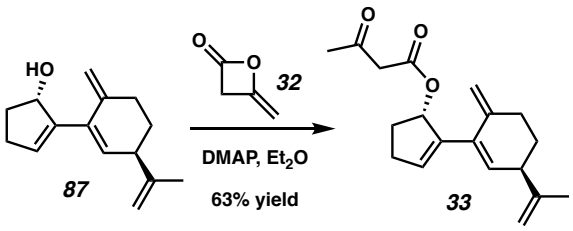

β-Ketoester 33: To a flame-dried round-bottom flask with a magnetic stir bar were added allylic alcohol **87** (1.23 g, 5.69 mmol, 1.0 equiv), 4-dimethylaminopyridine (35 mg, 0.29 mmol, 5.0 mol %) and Et_2O (20 mL). The flask was cooled to 0 ºC and stirred for 10 min. Diketene (**32**, 0.5 mL, 6.48 mmol, 1.1 equiv) was added dropwise. The reaction mixture was stirred 15 min at 0 ºC and then quenched by ice-cold water (10 mL). The mixture was extracted with Et_2O (3 x 15 mL). The combined organic layers were washed by brine (15 mL), dried over $MgSO_4$, and concentrated under reduced pressure. The crude oil was purified by flash column chromatography (10:1 hexanes: EtOAc) to afford β-ketoester **33** (1.07 g, 3.56 mmol, 63% yield) as a colorless oil; R_f = 0.40 (3:1, hexanes:Et_2O); ^1H NMR (400 MHz, C_6D_6) δ 6.23–6.15 (m, 1H), 5.82–5.80 (m, 1H), 5.80–5.77 (m, 1H), 5.05 (d, *J* = 2.1 Hz, 1H), 4.97–4.81 (m, 3H), 2.94 (s, 2H), 2.92–2.83 (m, 1H), 2.43–2.23 (m, 3H), 2.23–2.11 (m, 1H), 2.08–1.92 (m, 1H), 1.92–1.83 (m, 1H), 1.82–1.73 (m, 1H), 1.68 (s, 3H), 1.65 (s, 3H), 1.62–1.50 (m, 1H); ^{13}C NMR (101 MHz, C_6D_6) δ 199.0, 169.0, 166.9, 148.5, 143.2, 141.6, 134.9, 132.1, 111.2, 111.1, 81.3, 50.1, 45.0, 32.4, 31.1, 30.8, 29.54, 29.47, 20.8; IR (Neat Film, NaCl) 3629, 3078, 2935, 2855, 1727, 1644, 1440, 1360, 1315, 1238, 1149,

1029, 934, 895, 847, 802, 739 cm^{-1}; HRMS (FAB+) *m/z* calc'd for $C_{19}H_{25}O_3$ $[M+H]^+$: 301.1804, found 301.1814; $[\alpha]_D^{25.0}$ –41.8° (*c* 0.150, $CHCl_3$).

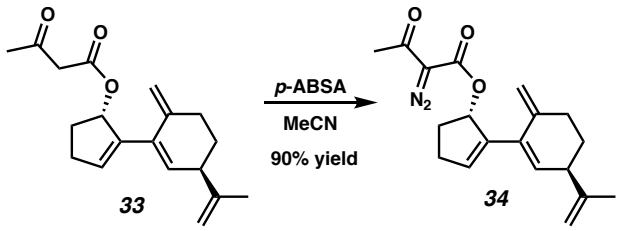

Diazo 34: To a round-bottom flask equipped with a magnetic stir bar were added β-ketoester **33** (1.07 g, 3.56 mmol, 1.0 equiv), MeCN (36 mL), and *p*-ABSA (1.3 g, 5.41 mmol, 1.5 equiv). Et_3N (1.5 mL, 10.75 mmol, 3.0 equiv) was added dropwise. The reaction mixture was stirred for 2 h at 23 ºC. The reaction mixture was filtered through a silica gel plug (pentanes: Et_2O 2:1) and concentrated under reduced pressure to afford diazo ester **34** (1.04 g, 3.19 mmol, 90% yield) as a yellowish oil; R_f = 0.44 (4:1, hexanes: EtOAc); ^1H NMR (500 MHz, $CDCl_3$) δ 6.06–5.98 (m, 2H), 5.61 (dd, *J* = 2.9, 1.5 Hz, 1H), 4.91–4.87 (m, 2H), 4.76 (dd, *J* = 2.0, 1.4 Hz, 1H), 4.74–4.69 (m, 1H), 2.93 (ddd, *J* = 9.1, 5.4, 3.2 Hz, 1H), 2.65–2.54 (m, 1H), 2.51–2.40 (m, 6H), 2.36–2.27 (m, 1H), 2.00–1.88 (m, 2H), 1.71 (dd, *J* = 1.4, 0.8 Hz, 3H), 1.60–1.52 (m, 1H); ^{13}C NMR (126 MHz, $CDCl_3$) δ 190.5, 161.4, 148.3, 142.9, 140.8, 135.2, 134.1, 132.1, 132.1, 110.9, 110.9, 82.2, 44.6, 31.9, 31.0, 30.7, 29.1, 28.4, 20.8; IR (Neat Film, NaCl) 3794, 3417, 3301, 3078, 2932, 2855, 2617, 2486, 2391, 2301, 2210, 2135, 1953, 1713, 1659, 1441, 1361, 1307, 1247, 1151, 1063, 1025, 965, 895, 847 cm^{-1}; HRMS (FAB+) *m/z* calc'd for $C_{19}H_{23}O_3N_2$ $[M+H]^+$: 327.1709, found 327.1725; $[\alpha]_D^{25.0}$ –6.7° (*c* 0.250, $CHCl_3$).

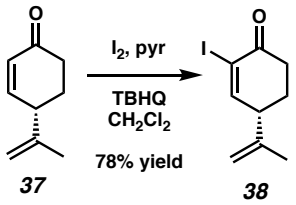

Iodoenone 38: To a round-bottom flask equipped with a magnetic stir bar were added ketone **37**[10] (200 mg, 1.47 mmol, 1.0 equiv), DCM (35 mL), and *tert*-butylhydroquinone (5 mg, 0.03 mmol, 2.0 mol %). A solution of iodine (700 mg, 2.76 mmol, 1.9 equiv) in pyridine (1.5 mL, 10.75 mmol, 7.3 equiv) was added. The reaction mixture was stirred for 2 h at 23 ºC. The reaction was diluted with Et_2O (20 mL) and water (20 mL) and quenched by saturated aqueous $Na_2S_2O_3$ (20 mL). The phases were separated, and the aqueous phases were extracted with DCM (3 x 20 mL). The combined organic phases were dried over $MgSO_4$, filtered and concentrated under reduced pressure. The crude product was purified by flash column chromatography (15:1, hexanes: EtOAc) to afford iodide **38** (300 mg, 1.14 mmol, 78% yield) as a yellowish oil; R_f = 0.40 (6:1, hexanes: EtOAc); ^{1}H NMR (400 MHz, C_6D_6)) δ 7.17 (d, *J* = 1.1 Hz, 1H), 4.62–4.55 (m, 1H), 4.47–4.43 (m, 1H), 2.36–2.22 (m, 2H), 1.92 (ddd, *J* = 16.2, 11.2, 4.8 Hz, 1H), 1.40–1.31 (m, 1H), 1.31–1.20 (m, 4H); ^{13}C NMR (101 MHz, C_6D_6) δ 190.5, 160.2, 144.5, 128.4, 128.3, 128.1, 127.9, 127.8, 112.8, 105.1, 47.5, 35.4, 27.7, 20.9; IR (Neat Film, NaCl) 3357, 3077, 2951, 2867, 1683, 1645, 1585, 1450, 1414, 1376, 1325, 1278, 1217, 1170, 1151, 1128, 1081, 1036, 971, 952, 89, 805, 713, 644 cm^{-1}; HRMS (FAB+) *m/z* calc'd for $C_9H_{12}OI$ $[M+H]^+$: 262.9933, found 262.9936; $[\alpha]_D^{25.0}$ –40.1° (*c* 0.44, $CHCl_3$).

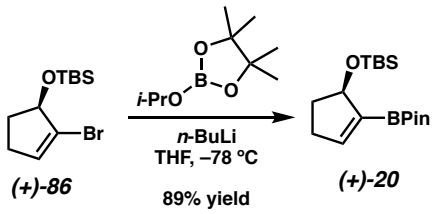

Boronate (+)-20: To a round-bottom flask equipped with a magnetic stir bar were added bromide (+)-**86** (1.04 g, 3.82 mmol, 1.00 equiv) and THF (15 mL). The flask was cooled to –78 ºC and stirred for 10 min. *n*-BuLi solution (2.5 M in hexanes, 2.3 mL, 5.75 mmol, 1.51 equiv) was added dropwise. The reaction mixture was stirred at –78 ºC for 30 min and isopropyl pinacolyl borate (1.2 mL, 5.88 mmol, 1.53 equiv) was added. The reaction mixture was stirred at –78 ºC for 30 min then quenched with HCl solution (2 N in Et_2O, 2.9 mL, 5.80 mmol, 1.52 equiv). Following addition, the reaction mixture was diluted with diethyl ether (15 mL) and warmed up to 23 ºC. The reaction mixture was filtered and was concentrated under reduced pressure to afford boronate (+)-**20** (1.1 g, 3.39 mmol, 89% yield) as a colorless oil. The characterization data matched those of *rac*-**20**. $[\alpha]_D^{25.0}$ 9.8° (*c* 1.35, $CHCl_3$).[20]

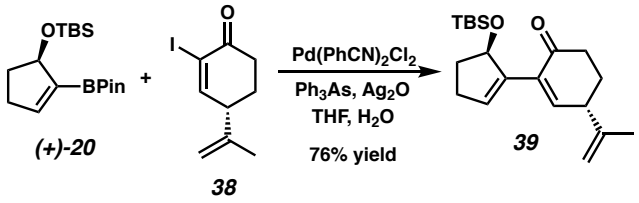

Bicycle 39: To a flame-dried round-bottom flask equipped with a magnetic stir bar were added boronate (+)-**20** (92 mg, 0.28 mmol, 1.5 equiv), iodide **38** (50 mg, 0.19 mmol, 1.0 equiv), silver oxide (70 mg, 0.30 mmol, 1.6 equiv), and triphenylarsine (6 mg, 0.02 mmol, 10 mol %). The mixture was evacuated and back-filled with argon (x3). The mixture was dissolved in dioxane (25 mL) and water (2.5 mL). To the mixture was added bis(benzonitrile)palladium chloride (4 mg,

0.01 mmol, 5.0 mol %). The reaction was stirred at 23 ºC for 6 h. The resulting mixture was filtered through celite with EtOAc and the solvent was removed under reduced pressure. The crude product was purified by flash column chromatography (20:1, hexanes: EtOAc) to afford bicycle **39** (48 mg, 0.144 mmol, 76% yield over **38**) as a white solid; R_f = 0.54 (6:1, hexanes: EtOAc); ^{1}H NMR (400 MHz, C_6D_6) δ 6.72 (dd, *J* = 3.4, 1.3 Hz, 1H), 6.26–6.17 (m, 1H), 5.33–5.25 (m, 1H), 4.76–4.74 (m, 1H), 4.72–4.70 (m, 1H), 2.72 (dt, *J* = 8.5, 4.1 Hz, 1H), 2.51–2.29 (m, 2H), 2.26–1.99 (m, 3H), 1.79–1.62 (m, 2H), 1.62–1.45 (m, 4H), 0.96 (s, 9H), 0.11 (s, 3H), 0.09 (s, 3H); ^{13}C NMR (101 MHz, C_6D_6) δ 197.0, 147.9, 146.2, 143.0, 135.7, 132.4, 128.3, 128.2, 128.1, 127.9, 127.8, 112.3, 78.5, 44.4, 38.1, 34.6, 30.6, 27.9, 26.2, 21.2, 18.3, –3.9, –4.4; IR (Neat Film, NaCl) 3348, 3078, 3042, 2929, 2893, 2855, 2737, 2708, 1687, 1683, 1649, 1472, 1463, 1451, 1388, 1375, 1360, 1314, 1287, 1251, 1218, 1189, 1157, 1141, 1064, 1006, 980, 941, 868, 836, 775, 735, 677 cm^{-1}; HRMS (FAB+) *m/z* calc'd for $C_{15}H_{19}O_3N_2$ $[M+H-H_2]^+$: 331.2093, found 331.2096; $[\alpha]_D^{25.0}$ –60.8° (*c* 0.44, $CHCl_3$).

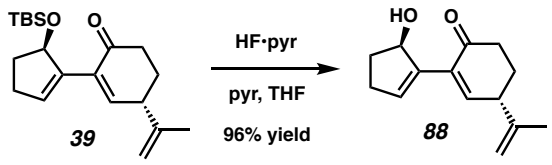

Alcohol 88: To a round-bottom plastic-coated flask equipped with a magnetic stir bar were added diene **39** (30 mg, 0.090 mmol, 1.0 equiv), THF (4 mL), and pyridine (0.05 mL, 0.62 mmol, 6.9 equiv). A solution of HF•pyr (pyridine 30%, hydrogen fluoride 70%, 0.1 mL, 50 equiv) was added dropwise. The reaction mixture was stirred for 18 h at 23 ºC. The reaction was diluted with Et_2O (4 mL) and neutralized with sat. aq. $NaHCO_3$ (10 mL). The phases were separated, and the aqueous phase was extracted with EtOAc (3 x 10 mL). The combined organic phases were dried over $MgSO_4$, filtered and concentrated under reduced pressure. The crude product was purified by

flash column chromatography (5:1, hexanes: EtOAc) to afford allylic alcohol **88** (19 mg, 0.087 mmol, 96% yield) as a colorless oil; R_f = 0.25 (2:1, hexanes: EtOAc); ^{1}H NMR (400 MHz, C_6D_6) δ 6.86–6.76 (m, 1H), 6.44–6.35 (m, 1H), 4.99–4.90 (m, 1H), 4.82–4.74 (m, 1H), 4.74–4.69 (m, 1H), 2.96 (s, 1H), 2.58 (dt, *J* = 8.7, 4.2 Hz, 1H), 2.54–2.43 (m, 1H), 2.36 (ddd, *J* = 16.3, 6.2, 4.3 Hz, 1H), 2.14–1.96 (m, 3H), 1.93–1.78 (m, 1H), 1.63–1.42 (m, 5H); ^{13}C NMR (101 MHz, C_6D_6) δ 198.9, 149.3, 146.2, 142.2, 135.2, 134.0, 112.4, 77.5, 44.3, 37.9, 34.0, 30.9, 27.8, 21.1; IR (Neat Film, NaCl) 3418, 3077, 3040, 2938, 2848, 1674, 1586, 1451, 1377, 1309, 1086, 1047, 990, 935, 895 cm^{-1}; HRMS (FAB+) *m/z* calc'd for $C_{14}H_{17}O_2$ $[M+H-H_2]^+$: 217.1229, found 217.1235; $[\alpha]_D^{25.0}$ –120.4° (*c* 0.33, $CHCl_3$).

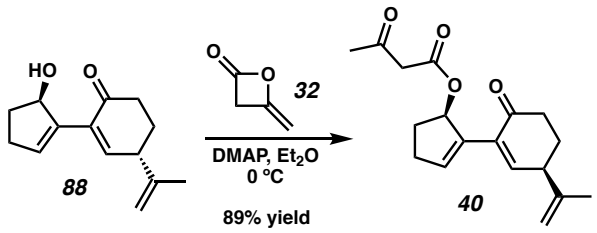

β-Ketoester 40: To a flame-dried round-bottom flask equipped with a magnetic stir bar were added allylic alcohol **88** (870 mg, 3.99 mmol, 1.0 equiv), 4-dimethylaminopyridine (50 mg, 0.41 mmol, 10 mol %), and Et_2O (20 mL). The flask was cooled to 0 ºC and stirred for 10 min. Diketene (**32**, 0.36 mL, 4.67 mmol, 1.2 equiv) was added dropwise. The reaction mixture stirred for 15 min at 0 ºC was then quenched with ice-cold water (20 mL). The mixture was extracted with Et_2O (3 x 20 mL). The combined organic layers were washed by brine (15 mL), dried over $MgSO_4$, and concentrated under reduced pressure. The crude oil was purified by flash column chromatography (4:1 hexanes: EtOAc) to afford β-ketoester **40** (1.07 g, 3.54 mmol, 89% yield) as a colorless oil; R_f = 0.40 (2:1 hexanes: Et_2O); ^{1}H NMR (400 MHz, CD_2Cl_2) δ 6.74–6.72 (m, 1H), 6.70–6.68 (m, 1H), 6.05 (dt, *J* = 7.5, 2.4 Hz, 1H), 4.89 (t, *J* = 1.5 Hz, 1H), 4.76–4.73 (m, 1H), 3.40–3.33 (m, 2H),

3.15 (dt, J = 8.7, 4.4 Hz, 1H), 2.65–2.27 (m, 5H), 2.18 (s, 3H), 2.17–2.09 (m, 1H), 1.98–1.81 (m, 2H), 1.79 (t, J = 1.2 Hz, 3H); ^{13}C NMR (101 MHz, CD_2Cl_2) δ 200.7, 198.5, 167.3, 148.8, 146.5, 138.1, 136.2, 133.1, 112.3, 81.4, 50.6, 44.4, 38.1, 31.7, 30.8, 30.3, 28.0, 21.4; IR (Neat Film, NaCl) 3655, 3643, 3080, 2943, 2850, 1726, 1640, 1554, 1450, 1356, 1315, 1256, 1146, 1088, 1029, 995, 900, 854, 778, 706, 634, 617 cm^{-1}; HRMS (FAB+) *m/z* calc'd for $C_{18}H_{23}O_4$ $[M+H]^+$: 303.1596, found 303.1594; $[\alpha]_D^{25.0}$ –30.6° (*c* 0.13, $CHCl_3$). (Note: the enol ether tautomer of β-ketoester **40** was predominant in CD_2Cl_2).

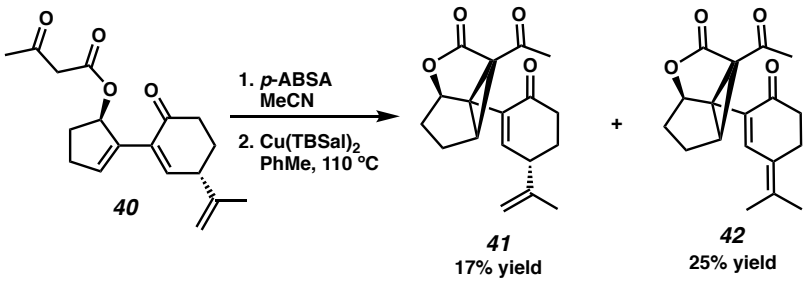

Cyclopropane 41: To a round-bottom flask equipped with a magnetic stir bar were added β-ketoester **40** (95 mg, 0.314 mmol, 1.0 equiv), MeCN (3 mL), and *p*-ABSA (113 mg, 0.47 mmol, 1.5 equiv). Et_3N (0.1 mL, 0.717 mmol, 2.3 equiv) was added dropwise. The reaction mixture was stirred for 2 h at 23 ºC. The reaction mixture was filtered through a Florisil (2:1, pentanes: Et_2O) then concentrated under reduced pressure. The residue was used in the next reaction without further purification.

To a flame-dried two-neck round-bottom flask equipped with a magnetic stir bar was added $Cu(TBSal)_2$ (8 mg, 0.019 mmol, 10 mol %) in a nitrogen-filled glove box. The flask was sealed with rubber septa and removed from the glove box. One of the rubber septa was replaced with a reflux condenser connected to a nitrogen inlet. A solution of semi-crude diazo ester (60 mg, 0.198 mmol, 1.0 equiv) in toluene (40 mL) was added. The reaction was heated to reflux in a 110 ºC oil

bath. After 3 h of stirring, the reaction mixture was cooled to 23 ºC and stirred for 15 min. The mixture was concentrated and purified by flash column chromatography (10:1 hexanes: EtOAc) to afford cyclopropane **41** (10 mg, 0.033 mmol, 17% yield) as a colorless oil; R_f = 0.40 (2:1 hexanes: EtOAc); ^{1}H NMR (400 MHz, $CDCl_3$) δ 6.79 (dd, *J* = 3.2, 1.1 Hz, 1H), 4.96–4.89 (m, 1H), 4.75–4.73 (m, 1H), 4.73–4.71 (m, 1H), 3.13 (dt, *J* = 8.3, 4.2 Hz, 1H), 2.96 (dd, *J* = 6.5, 1.0 Hz, 1H), 2.56 (ddd, *J* = 16.8, 6.5, 4.4 Hz, 1H), 2.44 (s, 3H), 2.40–2.26 (m, 2H), 2.21–2.00 (m, 2H), 2.00–1.78 (m, 6H); ^{13}C NMR (101 MHz, $CDCl_3$) δ 198.5, 198.2, 172.3, 153.8, 145.2, 131.7, 112.9, 85.7, 77.2, 59.2, 50.7, 43.7, 38.9, 38.6, 36.5, 29.9, 27.7, 23.9, 21.7; IR (Neat Film, NaCl) 3371, 3077, 2939, 1760, 182, 1651, 1488, 1439, 1362, 1339, 1309, 1242, 1223, 1190, 1160, 1136, 1085, 1067, 1006, 957, 912, 850, 817, 727, 703, 622, 612 cm^{-1}; HRMS (MM+) *m/z* calc'd for $C_{15}H_{19}O_3$ $[M+H]^+$: 301.1440, found 301.1450; $[\alpha]_D^{25.0}$ –56.8° (*c* 0.30, $CHCl_3$), and side product **42** (15 mg, 0.050 mmol, 25% yield) as a colorless oil; R_f = 0.05 (2:1 hexanes: EtOAc); ^{1}H NMR (400 MHz, $CDCl_3$) δ 7.32 (s, 1H), 4.75 (dd, *J* = 2.0, 1.1 Hz, 1H), 3.03 (dt, *J* = 6.5, 1.1 Hz, 1H), 2.75–2.60 (m, 2H), 2.54–2.35 (m, 6H), 2.10–2.01 (m, 1H), 2.01–1.96 (m, 3H), 1.96–1.84 (m, 5H); ^{13}C NMR (101 MHz, $CDCl_3$) δ 198.6, 198.2, 172.5, 144.5, 142.3, 126.3, 126.1, 85.8, 77.2, 60.1, 51.5, 38.5, 38.4, 37.1, 29.8, 25.6, 23.9, 22.2, 21.3; IR (Neat Film, NaCl) 3484, 3369, 3051, 2928, 2853, 2435, 2305, 2143, 1755, 1679, 1615, 1434, 1361, 1348, 1311, 1297, 1257, 1242, 1216, 1199, 1164, 1131, 1090, 1064, 1037, 1004, 966, 918, 888, 851, 822, 798, 753, 719, 667, 655, 633, 614 cm^{-1}; HRMS(FAB+) *m/z* calc'd for $C_{18}H_{21}O_4$ $[M+H]^+$: 301.1440, found 301.1434; $[\alpha]_D^{25.0}$ 53.1° (*c* 0.10, $CHCl_3$).

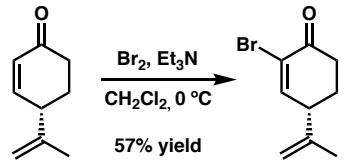

37 ***43***

Bromoenone 43: To a flame-dried round-bottom flask equipped with a magnetic stir bar were added ketone **37** (553 mg, 4.06 mmol, 1.0 equiv) and DCM (35 mL). The flask was cooled to 0 ºC and stirred for 10 min. A solution of bromine (0.24 mL, 4.66 mmol, 1.2 equiv) in DCM (5 mL) was added dropwise with vigorous stirring at 0 ºC. After the reaction became a reddish-brown color, Et_3N (0.6 mL, 4.30 mmol, 1.1 equiv) was added at 0 ºC. The cooling bath was removed, and the flask was allowed to warm to 23 ºC. After 30 min of stirring, the reaction was washed with water (40 mL). The aqueous phase was extracted with DCM (3 x 40 mL). The combined organic phases were dried over $MgSO_4$, filtered, and concentrated under reduced pressure. The crude product was purified by flash column chromatography (20:1 hexanes: EtOAc) to afford bromide **43** as a yellow oil (500 mg, 2.32 mmol, 57% yield); R_f = 0.45 (6:1 hexanes: EtOAc); ^{1}H NMR (500 MHz, $CDCl_3$) δ 7.29 (dd, *J* = 3.6, 0.9 Hz, 1H), 4.96–4.88 (m, 1H), 4.87–4.72 (m, 1H), 3.19–3.08 (m, 1H), 2.70 (ddd, *J* = 16.6, 7.0, 4.3 Hz, 1H), 2.51 (ddd, *J* = 16.6, 10.7, 4.5 Hz, 1H), 2.19 (ddtd, *J* = 12.8, 7.0, 4.7, 1.0 Hz, 1H), 1.99 (dddd, *J* = 13.5, 10.7, 8.2, 4.4 Hz, 1H), 1.79 (dd, *J* = 1.1 Hz, 3H); ^{13}C NMR (126 MHz, $CDCl_3$) δ 191.2, 153.1, 144.2, 124.0, 113.4, 46.1, 36.5, 27.6, 21.4.; IR (Neat Film, NaCl) 3853, 3650, 3371, 3035, 2953, 2869, 2360, 1694, 1646, 1595, 1451, 1417, 1377, 1327, 1278, 1218, 1172, 1153, 1132, 1085, 1037, 984, 958, 899, 816, 798, 786, 749, 716, 668, 650, 611 cm^1; HRMS (FAB+) *m/z* calc'd for $C_9H_{12}OBr$ $[M+H]^+$: 215.0072, found 215.0071; $[\alpha]_D^{25.0}$ 52.9° (*c* 0.30, $CHCl_3$).

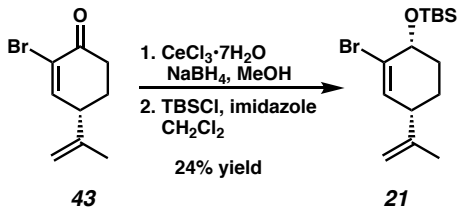

Silyl ether 21: To a round-bottom flask equipped with a magnetic stir bar were added bromoenone **43** (7.68 g, 35.7 mmol, 1.0 equiv) and MeOH (108 mL). The flask was cooled to 0 ºC, after which $CeCl_3 \bullet 7H_2O$ (13.3 g 35.7 mmol, 1.0 equiv) and $NaBH_4$ (1.35 g, 35.7 mmol, 1.0 equiv) were sequentially added over 5 min. The reaction was stirred at 0 ºC for 20 min, and the mixture was poured into sat. aq. NH_4Cl (300 mL). The aqueous phase was extracted with Et_2O (3 x 200 mL). The combined organic phases were dried over $MgSO_4$, filtered, and concentrated under reduced pressure. The crude product was passed through a plug of silica (20% EtOAc in hexanes) to afford crude alcohol as a colorless oil (7.01 g).

The semi-crude residue was dissolved in CH_2Cl_2 (81 mL), and imidazole (5.1 g, 74.3 mmol, 2.3 equiv) and TBSCl (8.3 g, 54.9 mmol, 1.7 equiv) were sequentially added. The resulting mixture was stirred at 23 ºC for 12 h, after which it was poured into brine (200 mL), extracted with CH_2Cl_2 (3 x 200 mL) dried over $MgSO_4$. The crude solution was concentrated *in vacuo* and purified by flash column chromatography (1% to 5% EtOAc in hexanes) to afford bromide **21** as a colorless oil (2.85 g, mmol, 24% yield); $R_f = 0.90$ (6:1 hexanes: EtOAc); ^{1}H NMR (500 MHz, $CDCl_3$) δ 6.03 (dd, J = 2.9, 0.8 Hz, 1H), 4.81–4.75 (m, 2H), 4.18 (td, J = 3.7, 1.2 Hz, 1H), 2.79–2.70 (m, 1H), 1.88–1.83 (m, 1H), 1.79–1.73 (m, 1H), 1.73–1.71 (m, 4H), 1.68–1.62 (m, 1H), 0.91 (s, 9H), 0.16 (s, 3H), 0.10 (s, 3H); ^{13}C NMR (126 MHz, $CDCl_3$) δ 147.1, 134.5, 126.3, 111.5, 70.6, 46.7, 32.7, 26.0, 22.2, 20.6, 18.3, –4.3, –4.5; IR (Neat Film, NaCl) 3077, 2950, 2929, 2885, 2856, 2738, 2709, 2360, 1918, 1793, 2738, 2709, 2360, 1918, 1793, 1684, 1648, 1472, 1462, 1448, 1436, 1407, 1388, 1375, 1361, 1300, 1280, 1251, 1219, 1194, 1171, 1126, 1084, 1064, 1025, 1006, 987, 960, 939,

914, 894, 880, 834, 814, 775, 729, 669, 639 cm^{-1}; HRMS (MM+) *m/z* calc'd for $C_{15}H_{19}O_3$ [M+H–H_2]$^+$: 331.0916, found 331.0902; $[\alpha]_D^{25.0}$ –22.6° (*c* 0.30, $CHCl_3$).

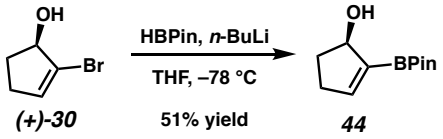

Boronate 44: To a round-bottom flask equipped with a magnetic stir bar was added (+)-**30** (326.0 mg, 2.00 mmol, 1.0 equiv) and THF (40 mL). The resulting solution was cooled to –78 ºC, and *n*-BuLi (2.3 M in hexanes, 4.60 mmol, 2.1 mL, 2.3 equiv) was added dropwise over several min. The resulting suspension was stirred vigorously for 15 min, and neat pinacolborane (0.80 mL, 5.00 mmol, 2.5 equiv) was added in one portion. The mixture was stirred vigorously for an additional 20 min, after which it was poured into sat. aq. NH_4Cl, extracted with Et_2O (3 x 50 mL), dried over Na_2SO_4, and concentrated *in vacuo*. The crude product was purified by flash column chromatography (4:1 hexanes: EtOAc) to afford boronate **44** (213.7 mg, 1.01 mmol, 51% yield) as a white solid; R_f = 0.10 (6:1 hexanes: EtOAc); ^{1}H NMR (400 MHz, $CDCl_3$) δ 6.70–6.63 (m, 1H), 5.05–4.95 (m, 1H), 2.64–2.51 (m, 1H), 2.41–2.18 (m, 2H), 1.71 (dddd, *J* = 13.7, 9.1, 5.5, 4.5 Hz, 1H), 1.28 (s, 12H); ^{13}C NMR (126 MHz, $CDCl_3$) δ 150.1, 83.6, 79.8, 33.2, 33.0, 26.0, 25.0; IR (Neat Film, NaCl) 3478, 3038, 2978, 2931, 2731, 2219, 1995, 1887, 1622, 1615, 1372, 1214, 1144, 1111, 1046, 1020, 964, 925, 854, 832, 759, 710 cm^{-1}; HRMS (FAB+) *m/z* calc'd for $C_{15}H_{19}O_3N_2$ [M+H–H_2]$^+$: 209.1349, found 209.1344; $[\alpha]_D^{25.0}$ –59.6° (*c* 0.80, $CHCl_3$).

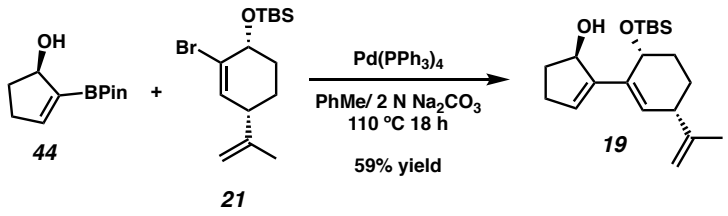

Bicycle 19: To a two-neck round-bottom flask equipped with reflux condenser and a magnetic stir bar were added boronate **44** (200 mg, 0.952 mmol, 1.6 equiv) and bromide **21** (200 mg, 0.605 mmol, 1.0 equiv). The mixture was evacuated and back-filled with argon (x3). Toluene (6 mL), tetrakis(triphenylphosphine)palladium(0) (21 mg, 0.018 mmol, 3.0 mol %), and 2 M aqueous Na_2CO_3 (6 mL) were added. The reaction was heated to reflux in a 110 ºC oil bath. After 18 h of stirring, the reaction mixture was cooled to 23 ºC and stirred for 15 min. The phases were separated and the aqueous phases were extracted with EtOAc (3 x 10 mL). The combined organic phases were washed with brine (10 mL), dried over $MgSO_4$, filtered and concentrated under reduced pressure. The crude product was purified by flash column chromatography (20:1 hexanes: EtOAc) to afford diene **19** (120 mg, 0.359 mmol, 59% yield) as a colorless oil; R_f = 0.40 (6:1 hexanes: EtOAc); ^{1}H NMR (500 MHz, $CDCl_3$) δ 5.85–5.81 (m, 2H), 4.95 (dt, *J* = 7.2, 2.5 Hz, 1H), 4.80–4.78 (m, 1H), 4.77 (dd, *J* = 2.0, 1.4 Hz, 1H), 4.43 (ddd, *J* = 3.6, 2.8, 1.3 Hz, 1H), 2.85–2.78 (m, 1H), 2.62–2.50 (m, 1H), 2.38–2.28 (m, 1H), 2.26–2.16 (m, 1H), 1.93–1.80 (m, 2H), 1.80–1.74 (m, 1H), 1.72 (dd, *J* = 1.5, 0.8 Hz, 3H), 1.68–1.58 (m, 2H), 0.85 (s, 9H), 0.09 (s, 3H), 0.05 (s, 3H); ^{13}C NMR (126 MHz, $CDCl_3$) δ 149.0, 145.1, 135.0, 130.7, 128.7, 110.9, 76.8, 65.1, 44.9, 33.7, 31.8, 30.7, 26.0, 22.4, 20.5, 18.3, –3.9, –4.2; IR (Neat Film, NaCl) 3601, 3412, 3072, 2929, 2855, 2737, 2708, 1924, 1647, 1472, 1463, 1436, 1407, 1389, 1375, 1360, 1334, 1305, 1252, 1218, 1024, 959, 934, 889, 835, 773, 723, 676 cm^{-1}; HRMS (MM+) *m/z* calc'd for $C_{20}H_{34}O_2NSiNa$ $[M+Na]^+$: 356.2220, found 357.2237; $[\alpha]_D^{25.0}$ –21.1° (*c* 0.10, $CHCl_3$).

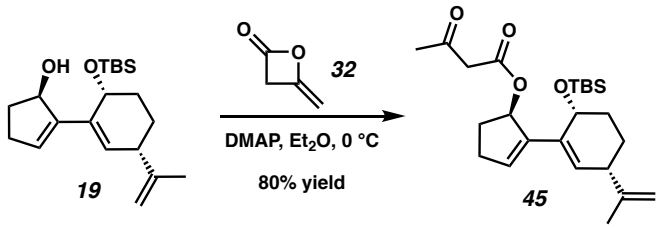

β-Ketoester 45: To a two-neck round-bottom flask with a magnetic stir bar were added bicyclic alcohol **19** (20 mg, 0.060 mmol, 1.0 equiv), and 4-dimethylaminopyridine (1.0 mg, 0.0082 mmol, 14 mol %) and Et_2O (1.5 mL). The flask was cooled to 0 ºC and stirred for 10 min. A solution of diketene (**32**, 0.07 mL, 0.907 mmol, 15.1 equiv) in Et_2O (2 mL) was added dropwise over several min. The reaction mixture was stirred for 15 min at 0 ºC then quenched by addition of ice-cold water (2 mL). The mixture was extracted with Et_2O (3 x 3 mL). The combined organic layers were washed with brine (3 mL), dried over $MgSO_4$, and concentrated under reduced pressure. The crude oil was purified by flash column chromatography (4:1 hexanes: EtOAc) to afford β-ketoester **45** (20 mg, 0.048 mmol, 80% yield) as a colorless oil; R_f = 0.45 (6:1 hexanes: Et_2O); ^{1}H NMR (500 MHz, $CDCl_3$) δ 6.18–5.98 (m, 2H), 5.62 (d, *J* = 2.8 Hz, 1H), 4.85–4.67 (m, 2H), 4.44 (t, *J* = 3.2 Hz, 1H), 3.36 (s, 2H), 2.77 (t, *J* = 8.6 Hz, 1H), 2.62–2.53 (m, 1H), 2.44–2.27 (m, 2H), 2.22 (s, 3H), 1.96–1.83 (m, 2H), 1.79–1.72 (m, 1H), 1.73–1.54 (m, 5H), 0.84 (s, 9H), 0.08 (s, 3H), 0.05 (s, 3H); ^{13}C NMR (126 MHz, $CDCl_3$) δ 200.8, 167.3, 148.8, 140.9, 134.4, 131.8, 130.4, 110.6, 79.8, 64.7, 50.4, 44.7, 31.7, 31.1, 30.8, 30.3, 25.9, 22.3, 20.4, 18.2, –3.8, –4.4; IR (Neat Film, NaCl) 2976, 2926, 2854, 1876, 1659, 1612, 1584, 1512, 1464, 1410, 1388, 1379, 1370, 1315, 1246, 1175, 1166, 1145, 1113, 1039, 967, 862, 819, 750, 688, 671 cm^{-1}; HRMS (MM+) *m/z* calc'd for $C_{24}H_{38}O_4SiNa$ $[M+Na]^+$: 441.2432, found 441.2441; $[\alpha]_D^{25.0}$ 4.4° (*c* 0.34, $CHCl_3$).

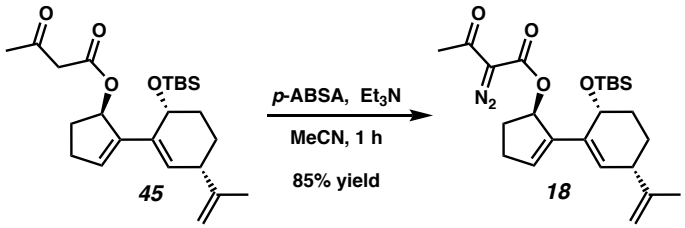

Diazo 18: To a round-bottom flask equipped with a magnetic stir bar were added β-ketoester **45** (20 mg, 0.048 mmol, 1.0 equiv), MeCN (2.5 mL), and *p*-ABSA (40.0 mg, 0.167 mmol, 3.5 equiv). Et_3N (0.03 mL, 0.215 mmol, 4.5 equiv) was added dropwise. The reaction mixture was stirred for 1 h min at 23 ºC and concentrated *in vacuo*. The resulting residue was passed through a silica gel plug (4:1 pentane:Et_2O) and concentrated under reduced pressure to afford diazo ester **18** (18 mg, 0.041 mmol, 85% yield) as a yellowish oil; R_f = 0.44 (4:1 hexanes: EtOAc); ^{1}H NMR (500 MHz, $CDCl_3$) δ 6.08 (dt, *J* = 1.66 Hz, 1.66 Hz, 7.75 Hz, 1H; ^{13}C NMR (126 MHz, $CDCl_3$) δ 190.47; IR (Neat Film, NaCl) 3408, 3073, 2929, 2855, 2362, 2139, 1713, 1661, 1652, 1472, 1464, 1366, 1312, 1250, 1195, 1150, 1086, 1064, 1025, 1006, 963, 938, 921, 895, 850, 834, 808, 773, 742, 676, 635 cm^{-1}; HRMS (MM+) *m/z* calc'd for $C_{24}H_{36}O_4N_2SiNa$ $[M+Na]^+$: 467.2337, found 467.2354; $[\alpha]_D^{25.0}$ –11.4° (*c* 0.31, $CHCl_3$).

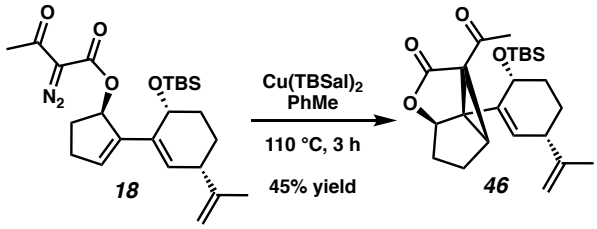

Cyclopropane 46: To a flame-dried two neck round-bottom flask equipped with a magnetic stir bar was added $Cu(TBSal)_2$ (3.0 mg, 0.0072 mmol, 16 mol %) in a nitrogen-filled glove box. The flask was sealed with rubber septa and removed from the glove box. One of the rubber septa was replaced with a reflux condenser connected to a nitrogen inlet. A solution of diazo ester **18**

(20 mg, 0.045 mmol, 1.0 equiv) in toluene (15 mL) was added. The reaction was heated to reflux in a 110 ºC oil bath. After 3 h of stirring, the reaction mixture was cooled to 23 ºC and stirred for 15 min. The mixture was concentrated and purified by flash column chromatography (10:1 hexanes: EtOAc) to afford cyclopropane **46** (8.4 mg, 0.020 mmol, 45% yield) as a white solid; R_f = 0.40 (6:1 hexanes: EtOAc); ^{1}H NMR (500 MHz, $CDCl_3$) δ 5.69 (d, *J* = 3.0 Hz, 1H), 5.09–5.00 (m, 1H), 4.81 (t, *J* = 1.7 Hz, 1H), 4.75–4.67 (m, 1H), 3.84–3.74 (m, 1H), 2.96 (dt, *J* = 6.3, 1.1 Hz, 1H), 2.76 (d, *J* = 7.6 Hz, 1H), 2.55 (s, 3H), 2.36–2.26 (m, 1H), 2.02 (dd, *J* = 13.0, 5.8 Hz, 1H), 1.96–1.85 (m, 1H), 1.82–1.70 (m, 5H), 1.69–1.52 (m, 3H), 0.90 (s, 9H), 0.09 (s, 6H); ^{13}C NMR (126 MHz, $CDCl_3$) δ198.4, 172.7, 147.7, 136.2, 132.9, 111.5, 86.4, 68.9, 65.1, 50.6, 43.7, 42.7, 38.3, 31.0, 30.4, 26.1, 23.9, 22.8, 21.0, 18.1, –3.8, –4.3; IR (Neat Film, NaCl) 2930, 2857, 1760, 1964, 1436, 1360, 1346, 1312, 1259, 1157, 1084, 1055, 1027, 1005, 983, 935, 896, 863, 832, 802, 774 cm^{-1}; HRMS (EI+) *m/z* calc'd for $C_{24}H_{36}O_4Si$ $[M\bullet]^+$: 416.2383, found, 416.2379; $[\alpha]_D^{25.0}$ –68.1° (*c* 0.10, $CHCl_3$).

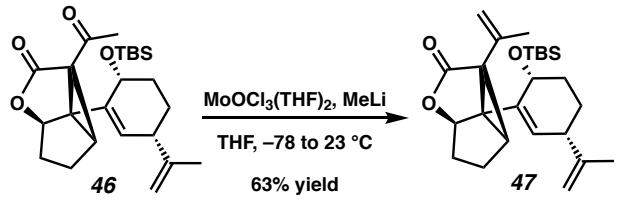

Divinylcyclopropane 47: To a flame-dried round-bottom flask equipped with a magnetic stir bar was added trichlorobis(THF) molybdenum(III) (750 mg, 2.08 mmol, 18.1 equiv) in a nitrogen-filled glove box. The flask was sealed with a rubber septum, removed from the glove box and connected to a nitrogen inlet. THF (3 mL) was added to the flask to generate a bright green solution. The flask was cooled to –78 ºC and stirred for 10 min. A solution of MeLi (1.6 M in Et_2O, 1.2 mL, 1.92 mmol, 16.7 equiv) was added dropwise to the reaction, resulting in a dark red

solution. After 1 h of stirring at –78 ºC, a solution of cyclopropane **46** (48 mg, 0.115 mmol, 1.0 equiv) in THF (1 mL) was added dropwise. The reaction was allowed to warm to ambient temperature and stirred for an additional 6 h. The reaction was quenched by addition of water (4 mL). The phases were separated, and the aqueous phase was extracted with Et_2O (3 x 4 mL). The combined organic phases were dried over $MgSO_4$, filtered, and concentrated under reduced pressure. The residue was purified by flash column chromatography (15:1 hexanes: EtOAc) to afford vinyl lactone **47** (30 mg, 0.0723 mmol, 63% yield) as a colorless oil; R_f = 0.50 (6:1 hexanes: EtOAc); ^{1}H NMR (500 MHz, $CDCl_3$) δ 5.51 (dd, *J* = 2.8, 0.9 Hz, 1H), 5.18–5.15 (m, 1H), 5.12–5.07 (m, 1H), 5.00–4.96 (m, 1H), 4.79 (dd, *J* = 2.0, 1.4 Hz, 1H), 4.73 (dt, *J* = 2.0, 0.9 Hz, 1H), 4.23–4.20 (m, 1H), 2.70 (ddd, *J* = 9.1, 5.9, 2.7 Hz, 1H), 2.44 (dt, *J* = 6.7, 1.3 Hz, 1H), 2.27–2.16 (m, 1H), 2.08–1.97 (m, 1H), 1.93–1.81 (m, 2H), 1.78–1.66 (m, 8H), 1.64–1.58 (m, 1H), 1.55–1.48 (m, 1H), 0.90 (s, 9H), 0.12 (s, 3H), 0.11 (s, 3H); ^{13}C NMR (126 MHz, $CDCl_3$) δ 174.9, 148.2, 136.5, 133.6, 133.5, 117.0, 111.2, 85.8, 67.5, 58.6, 49.1, 44.3, 38.9, 34.7, 31.5, 26.1, 23.5, 22.4, 22.3, 20.5, 18.1, –3.6, –4.4; IR (Neat Film, NaCl) 2953, 2857, 1766, 1645, 1463, 1343, 1254, 1197, 1159, 1079, 1057, 1024, 891, 864, 833, 775, 673 cm^{-1}; HRMS (MM+) *m/z* calc'd for $C_{25}H_{39}O_3Si$ $[M+H]^+$: 415.2663, found, 415.2697; $[\alpha]_D^{25.0}$ –35.4° (*c* 0.10, $CHCl_3$).

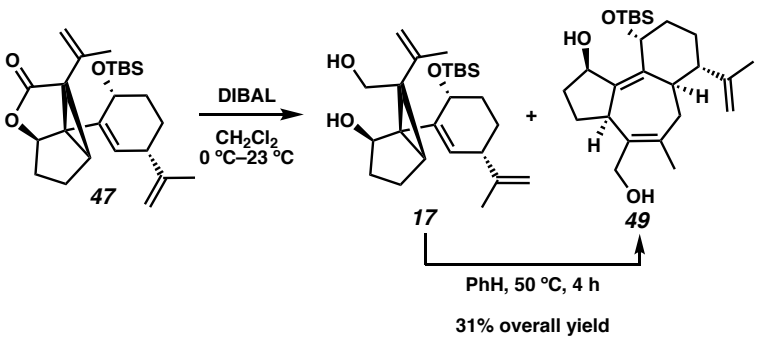

Tricycle 49: To a flame-dried round-bottom flask equipped with a magnetic stir bar were added vinyl lactone **47** (29 mg, 0.0699 mmol, 1.0 equiv) and DCM (14 mL). The flask was cooled to 0 ºC and stirred for 10 min. A solution of DIBAL (1 M in DCM, 0.35 mL, 0.35 mmol, 5.0 equiv) was added dropwise. The reaction mixture was slowly warmed up to 23 ºC and remained to stir for 24 h. The reaction was quenched by methanol (0.35 mL). Saturated aqueous potassium sodium tartrate solution (3 mL) was added to the mixture. The phases were separated, and the aqueous phase was extracted with DCM (5 x 10 mL). The combined organic phases were dried over $MgSO_4$, filtered, and transferred to round-bottom flask. The mixture was concentrated under reduced pressure and dissolved in benzene. The flask was immersed in a 50 ºC oil bath. After 4 h of stirring, the reaction was cooled to ambient temperature and concentrated under reduced pressure. The residue was purified by flash column chromatography (1:1 hexanes: EtOAc) to afford diol **49** as a white solid (9.0 mg, 0.215 mmol, 31% yield); R_f = 0.08 (3:1 hexanes: EtOAc); ^{1}H NMR (600 MHz, C_6D_6) 5.00 (dd, *J* = 4.1, 1.9 Hz, 1H), 4.92–4.89 (m, 1H), 4.87 (d, *J* = 2.2 Hz, 1H), 4.83 (d, *J* = 4.2 Hz, 1H), 4.16 (d, *J* = 11.3 Hz, 1H), 3.91 (d, *J* = 11.3 Hz, 1H), 3.56–3.49 (m, 1H), 3.06–3.00 (m, 1H), 2.85 (dd, *J* = 13.8, 4.5 Hz, 1H), 2.38 (dtd, *J* = 13.7, 11.8, 6.1 Hz, 1H), 2.28–2.13 (m, 2H), 2.04 (dd, *J* = 14.7, 11.4 Hz, 1H), 1.92–1.84 (m, 2H), 1.81 (d, *J* = 1.7 Hz, 3H), 1.77 (d, *J* = 1.2 Hz, 3H), 1.76–1.70 (m, 1H), 1.54 (tdd, *J* = 13.0, 4.3, 2.0 Hz, 1H), 1.51–1.37 (m, 2H), 1.01 (s, 9H), 0.08 (s, 3H), 0.08 (s, 3H); δ ^{13}C NMR (101 MHz, DMSO-d_6) 148.5, 140.1,

138.8, 137.8, 132.4, 111.9, 71. 3, 68.8, 57.9, 49.1, 42.1, 34.4, 34.0, 33.8, 29.3, 26.7, 26.6, 25.8, 25.7, 21.5, 17.7, –4.5, –4.7; IR (Neat Film, NaCl) 3342, 2929, 2856, 1645, 1451, 1254, 1163, 1079, 1033, 890, 836, 773, 739, 702 cm^{-1}; HRMS (FAB+) *m/z* calc'd for $C_{25}H_{41}O_3Si$ $[M+H-H_2]^+$: 417.2825, found 417.2833; $[\alpha]_D^{25.0}$ –27.6° (*c* 0.10, CH_3OH).

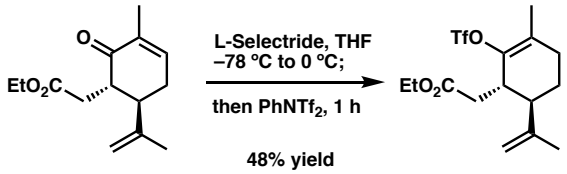

66 ***60***

Vinyl triflate 60: To a solution of **66** (8.00 g, 33.86 mmol, 1.0 equiv) in THF (113 mL, 0.3M) at –78 °C was added a 1M solution of L-Selectride in THF (33.9 mL, 1.0 equiv) over 1 min. The solution was stirred at –78 ºC for an additional 30 min. The septum was briefly removed, and solid *N*-phenyltriflimide (12.1 g, 33.9 mmol, 1.0 equiv) was quickly added in one portion. The resulting mixture was warmed to 0 °C. After stirring for an additional 30 min, the reaction was poured into sat. aq. NH_4Cl (300 mL) and extracted with Et_2O (3 X 500 mL). The combined organic layers were dried (Na_2SO_4), concentrated *in vacuo*, and purified by *careful* column chromatography (3% EtOAc in hexanes) to afford vinyl triflate **60** as a colorless oil (6.43 g, 48% yield); R_f = 0.6 (5% EtOAc in hexanes); $[\alpha]_D^{25}$ –27.6 (*c* 1, $CHCl_3$); ^1H NMR (500 MHz, $CDCl_3$) δ 4.83–4.81 (m, 2H), 4.10–4.06 (m, 2H), 2.92–2.87 (m, 1H), 2.63–2.60 (m, 1H), 2.44–2.36 (m, 2H), 2.16–2.13 (m, 2H), 1.77 (s, 3H), 1.69 (s, 3H), 1.70–1.69 (m, 2H), 1.66–1.62 (m, 4H), 1.22 (t, *J* = 7.1 Hz, 3H); ^{13}C NMR (126 MHz, $CDCl_3$) δ 171.2, 145.5, 143.4, 128.8, 118.4 (q, *J* = 321 Hz, CF_3) 112.6, 60.4, 47.5, 37.8, 35.0, 29.6, 25.2, 19.7, 17.3, 14.0; IR (Neat Film, NaCl) 2981.4, 2936.9, 1738.2, 1732.2,

1415.6, 1377.8, 1247.2, 1209.3, 1158.3, 1142.6, 1036.0, 947.8, 890.0, 813.3 cm^{-1}; HRMS (ESI-TOF) *m/z* calc'd for $C_{15}H_{21}F_3O_5SNa$ $[M+Na]^+$: 393.0954, found 393.0947.

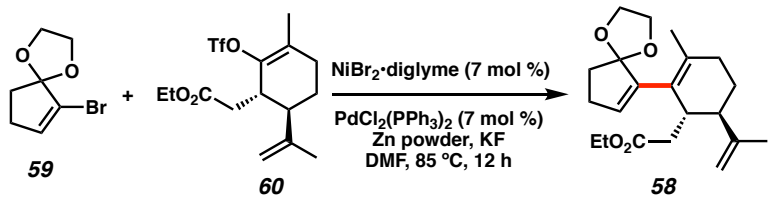

Bicycle 58: In a nitrogen-filled glovebox, a solution of $NiBr_2$•diglyme (169.3 mg, 6.0 mol %) precatalyst and bpy (75.0 mg, 6.0 mol %) in DMF (5 mL) was prepared and stirred vigorously for 10 min. Meanwhile, Zn^0 dust (2.09 g, 32.0 mmol, 4.0 equiv), KF (464.2 mg, 8.00 mmol, 1.0 equiv), $PdCl_2(PPh_3)_2$ (393.4 mg, 7.0 mol %), and ZnF_2 (1.65 g, 16.00 mmol, 2.0 equiv) were added to a 100 mL vial equipped with a cross-shaped stir bar. These solids were diluted with DMF (43 mL), and the resulting suspension was treated with a solution of vinyl bromide **59** (328.1 mg, 1.60 mmol, 0.20 equiv) and vinyl triflate **60** (2.96 g, 8.00 mmol, 1.0 equiv) in DMF (10 mL). The light green Ni(II)bpy solution was added to the vial, and the vial was capped with a septum and removed from the glove box. The reaction mixture was placed under a N_2 atmosphere and heated to 85 °C under vigorous stirring. Next, a pre-made solution of bromide **59** (1.97 g, 9.6 mmol, 1.2 equiv) in DMF (8 mL) was added to the heated mixture over 2 h via syringe pump. The reaction was stirred vigorously at 85 ºC for an additional 12 h, after which it was allowed to cool to 23 ºC. The resulting black slurry was poured into sat. aq. LiCl (500 mL), and it was extracted with Et_2O (500 mL x 4) until TLC confirmed no product remained in the aqueous layer. The combined organic layers were again extracted with brine (1 L), dried (Na_2SO_4), and concentrated *in vacuo*. (Note during extraction: The border between the organic and aqueous layers may be readily determined by olfactory analysis; If Zn(II) salts remain in the organic layer following extraction, they can be

easily removed by passage through a plug of silica (Et_2O as eluent).) The crude mixture was purified by column chromatography (15% EtOAc in hexanes) to afford bicycle **58** as a colorless oil (1.72 g, 62% yield); R_f = 0.55 (20% EtOAc in hexanes); $[\alpha]_D^{25}$ –122.8 (*c* 1, $CHCl_3$); ^{1}H NMR (400 MHz, $CDCl_3$) δ 5.71 (t, *J* = 2.5 Hz, 1H), 4.82–4.75 (m, 2H), 4.05 (q, *J* = 7.1 Hz, 2H), 3.97–3.91 (m, 4H), 2.80–2.76 (m, 1H), 2.62–2.58 (m, 1H), 2.38–2.36 (m, 2H), 2.27–2.22 (m, 2H), 2.08–1.95 (m, 5H), 1.71 (s, 3H), 1.65–1.63 (m, 4H), 1.24–1.21 (m, 3H); ^{13}C NMR (101 MHz, $CDCl_3$) δ 173.3, 147.8, 141.8, 136.1, 132.7, 127.9, 120.8, 110.9, 65.0, 64.4, 59.8, 45.5, 37.9, 37.4, 36.0, 30.0, 27.9, 25.0, 21.6, 20.4, 14.2; IR (Neat Film, NaCl) 2974.0, 2922.1, 2884.9, 1735.7, 1449.8, 1373.1, 1373.1, 1317.0, 1171.1, 1149.4, 1039.9, 1028.2, 946.5, 923.9, 888.5, 856.6, 850.4 cm^{-1}; HRMS (ESI-TOF) *m/z* calc'd for $C_{21}H_{30}O_4$ $[M+H]^+$: 347.2222, found 347.2215.

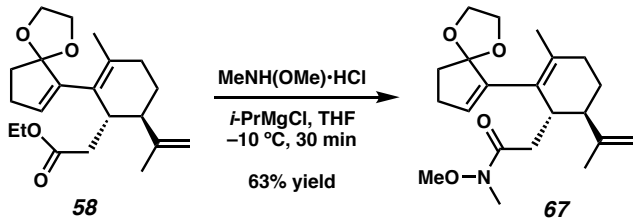

Weinreb amide 67: To a –10 °C solution of ester **58** (1.72 g, 4.96 mmol, 1.0 equiv) and MeNH(OMe)•HCl (1.07 g, 10.92 mmol, 2.2 equiv) in THF (50 mL) was slowly added a 2M solution of *i*-PrMgCl in THF (10 mL, 4.0 equiv) over several minutes. The reaction was stirred at –10 °C for 30 min then poured into sat. aq. NH_4Cl (50 mL), extracted with Et_2O (50 mL X 3), dried (Na_2SO_4), and concentrated *in vacuo*. The crude residue was purified by column chromatography (50% EtOAc in hexanes), concentrated, and stripped twice with hexanes (5 mL X 2) to provide amide **67** as a viscous clear oil (1.11 g, 63% yield); R_f = 0.40 (50% EtOAc in hexanes); $[\alpha]_D^{25}$ –118.5 (*c* 1, $CHCl_3$); ^{1}H NMR (500 MHz, $CDCl_3$) δ 5.75 (t, *J* = 2.5, 1H), 4.87 (s, 1H), 4.80 (s, 1H), 4.04–3.90 (m, 4H), 3.67 (s, 3H), 3.15 (s, 3H), 2.70 (m, 2.71–2.68, 1H), 2.42–2.38 (m, 1H), 2.35–

2.33 (m, 4H), 2.11–2.01 (m, 4H), 1.76 (s, 3H), 1.71–1.64 (m, 5H); ^{13}C NMR (126 MHz, $CDCl_3$) δ 174.4, 147.9, 142.3, 135.8, 132.3, 128.3, 120.7, 110.2, 64.9, 64.4, 61.1, 44.3, 36.7, 36.1, 35.1, 29.5, 27.9, 24.0, 21.6 (two resolved signals), 21.1; IR (Neat Film, NaCl) 2932.6, 1669.5, 1451.9, 1405.9, 1377.1, 1317.0, 1217.2, 1198.3, 1140.9, 1102.9, 1043.4, 1024.0, 1005.4, 948.9, 927.1, 890.5, 858.4 cm^{-1}; HRMS (ESI-TOF) *m/z* calc'd for $C_{21}H_{31}NO_4$ $[M+H]^+$: 362.2326, found 362.2314.

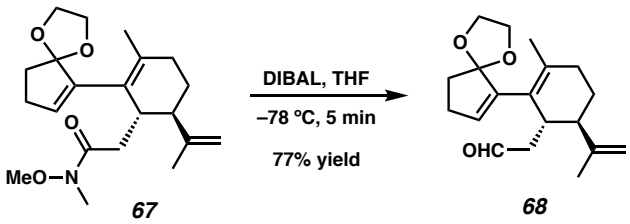

67 *68*

Aldehyde 68: To a –78 °C solution of amide **67** (1.13 g, 3.11 mmol, 1.0 equiv) in THF (31 mL) was added a 1M solution of DIBAL (3.72 mmol, 1.2 equiv) over 1 min. The solution was stirred at –78 °C for 5 min, after which it was poured into a combined solution of aq. $NaHCO_3$ (2 M, 100 mL) and sat. aq. Rochelle salt (100 mL). The biphasic mixture was vigorously stirred for 30 min, extracted with Et_2O (100 mL X 3), dried (Na_2SO_4), and concentrated *in vacuo*. The crude residue was purified by column chromatography (15% EtOAc in hexanes) to provide aldehyde **68** as a pale yellow oil (729 mg, 77% yield); R_f = 0.35 (5% EtOAc in hexanes); $[\alpha]_D^{25}$ —118.5 (*c* 1, $CHCl_3$); ^{1}H NMR (500 MHz, $CDCl_3$) δ 9.60 (s, 1H), 5.66 (t, *J* = 2.5 Hz, 1H), 4.79–4.78 (m, 2H), 3.92–3.88 (m, 4H), 2.88–2.83 (m, 1H), 2.49–2.48 (m, 1H), 2.40–2.34 (m, 3H), 2.08–2.03 (m, 5H), 1.68 (s, 3H), 1.67–1.64 (s, 5H); ^{13}C NMR (126 MHz, $CDCl_3$) δ 204.2, 147.5, 141.7, 136.8, 133.4, 127.7, 120.9, 111.7, 64.9, 64.5, 47.3, 47.2, 36.4, 35.9, 30.7, 27.9, 26.6, 20.1 (2 resolved signals); IR (Neat Film, NaCl) 2967.8, 2919.9, 2857.8, 2831.6, 2716.8, 1721.1, 1644.3, 1449.7, 1376.7, 1317.6, 1216.6, 1142.2, 1088.5, 1044.2, 1025.3, 948.2, 926.2, 892.1, 855.7 cm^{-1}; HRMS (ESI-TOF) *m/z* calc'd for $C_{19}H_{26}O_3Na$ $[M+Na]^+$: 325.1774, found 325.1764.

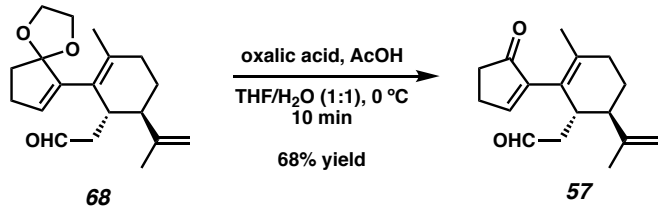

Enone 57: To a 0 °C solution of ketal **68** (345 mg, 1.34 mmol) in THF (10 mL) were sequentially added a pre-made solution of AcOH (0.8 mL, 13.40 mmol, 10 equiv) and H_2O (1 mL) followed by solid oxalic acid•dihydrate (169 mg, 1.0 equiv). The reaction was religiously monitored by TLC until deemed complete (ca. 5–10 min) after which it was quickly poured into ice-cold sat. aq. Na_2CO_3 (30 mL). (Note: prolonged reaction times result in rapid product decomposition.) The mixture was extracted with Et_2O (3 X 30 mL), dried (Na_2SO_4), and concentrated *in vacuo*. The crude residue was purified by column chromatography (20% EtOAc in hexanes) to provide enone **57** as a pale yellow oil (234.3 mg, 68% yield); R_f = 0.55 (30% EtOAc in hexanes); $[\alpha]_D^{25}$ 1.5 (*c* 1, $CHCl_3$); ^{1}H NMR (500 MHz, $CDCl_3$) δ 9.52 (s, 1H), 7.34 (t, *J* = 2.8 Hz, 1H), 4.82 (s, 2H), 3.00–2.93 (m, 1H), 2.65–2.63 (m, 2H), 2.43–2.41 (m, 2H), 2.31–2.23 (m, 2H), 2.17–2.09 (m, 2H), 2.03–2.01 (m, 1H), 1.70–1.67 (m, 5H), 1.50 (s, 3H); ^{13}C NMR (126 MHz, $CDCl_3$) δ 209.0, 202.8, 161.9, 147.1, 146.5, 134.1, 124.9, 112.2, 47.3, 47.1, 36.2, 34.5, 30.7, 26.8, 26.1, 21.1, 19.9; IR (Neat Film, NaCl) 3071.3, 2920.7, 2715.1, 1697.5, 1644.9, 1436.1, 1407.7, 1377.7, 1297.7, 1267.7, 1195.4, 1092.7, 1054.5, 1010.1, 928.3, 896.8, 790.2 cm^{-1}; HRMS (ESI-TOF) *m/z* calc'd for $C_{17}H_{22}O_2Na$ $[M+Na]^+$: 281.1512, found 281.1504.

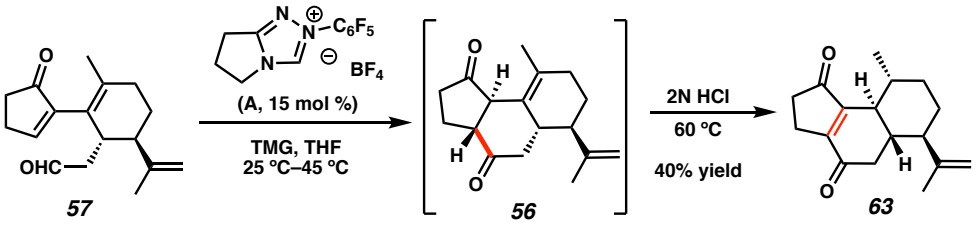

Tricycle 63: To a vial containing catalyst **A** (16 mg, 15 mol %) under N_2 was added a solution of enone **57** (75 mg, 0.29 mmol) in dioxane (5 mL). To the stirring reaction was added catalytic 1,1,3,3-tetramethylguanidine (TMG, 5 μL, 14 mol %). The resulting yellow solution was stirred at 23 °C for 1 h after which it was heated to 35 °C and stirred for an additional 1 h. The solution was further heated to 45 °C and stirred for 12 h. Upon completion, the resulting diastereomeric mixture was treated with 2N aq. HCl (5 mL) and heated to 60 °C until deemed complete by TLC (ca. 48 h). The reaction was diluted with H_2O (20 mL) and extracted with EtOAc (3 X 20 mL). (Note: the product will remain in the aqueous layer if neutralized with base). The combined organic layers were dried ($MgSO_4$), concentrated *in vacuo*, and purified by column chromatography (15% EtOAc in hexanes) to afford ene-dione **63** as a viscous yellow oil (31 mg, 41% yield; R_f = 0.65 (20% EtOAc in hexanes); $[\alpha]_D^{25}$ –111.5 (*c* 0.5, $CHCl_3$); ^{1}H NMR (500 MHz, $CDCl_3$) δ 4.81 (s, 1H), 4.76 (s, 1H), 2.93–2.58 (m, 6H), 2.28–1.98 (m, 4H), 1.84 (s, 3H), 1.71–1.54 (m, 7H); ^{13}C NMR (126 MHz, $CDCl_3$) δ 207.4, 199.5, 157.6, 151.6, 146.3, 142.6, 121.4, 112.3, 50.1, 45.6, 40.9, 36.0, 33.8, 27.1, 23.3, 22.2, 15.3; IR (Neat Film, NaCl) 2919.9, 2891.1, 1715.8, 1677.2, 1642.8, 1438.0, 1251.6, 1200.2, 114.3, 893.0 cm^{-1}; HRMS (ESI-TOF) *m/z* calc'd for $C_{17}H_{22}O_2$ $[M+H]^+$: 259.1698, found 259.1686.

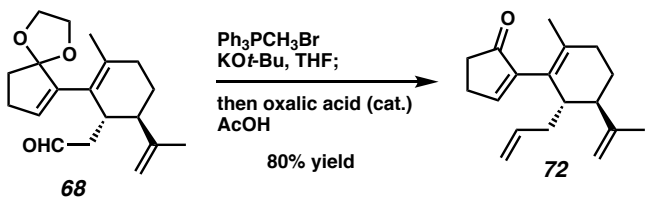

Olefin 72: To a 0 °C mixture of methyltriphenylphosphonium bromide (429 mg, 1.20 mmol, 1.5 equiv) in THF (4 mL) was added 1M KO*t*-Bu in THF (1.0 mL, 1.3 equiv). The reagent mixture was stirred for 10 min after which a solution of aldehyde **68** (242 mg, 0.8 mmol) in THF (4 mL) was added dropwise over 1 min. The reaction was stirred at 0 °C until deemed complete by TLC (ca. 1 h). Subsequently, a solution of AcOH in H_2O (1:1, 2 mL) was added, followed by solid oxalic acid•dihydrate (100 mg, 1.0 equiv). The resulting mixture was stirred at 0 °C until deemed complete by TLC (ca. 1 h) after which it was poured into 2N Na_2CO_3 (20 mL), extracted with Et_2O (3 X 20 mL), dried ($MgSO_4$), and concentrated *in vacuo*. The crude product was purified by column chromatography (15%–20% EtOAc in hexanes) to provide enone **72** as a pale yellow oil (174.1 mg, 85% yield); $R_f = 0.50$ (20% EtOAc in hexanes); $[\alpha]_D^{25}$ –31.9 (*c* 1, $CHCl_3$); ^{1}H NMR (500 MHz, $CDCl_3$) δ 7.31 (s, 1H), 5.61–5.51 (m, 1H), 4.90–4.75 (m, 4H), 2.63–2.61 (m, 2H), 2.50–2.42 (m, 1H), 2.41–2.40 (m, 2H), 2.20–2.13 (m, 1H), 2.05–2.00 (m, 3H), 1.68 (s, 3H), 1.67–1.60 (m, 2H), 1.48 (s, 3H); ^{13}C NMR (126 MHz, $CDCl_3$) δ 208.7, 160.4, 147.8, 146.8, 136.9, 133.3, 125.9, 115.9, 110.9, 43.9, 39.7, 36.2, 34.6, 30.2, 26.6, 25.1, 21.0, 20.4; IR (Neat Film, NaCl) 3071.6, 2974.8, 2924.2, 2859.1, 1703.5, 1642.8, 1440.1, 1406.5, 1375.8, 1297.7, 1255.9, 1195.0, 1093.5, 1001.1, 908.5, 889.4, 790.9 cm^{-1}; HRMS (ESI-TOF) *m/z* calc'd for $C_{18}H_{25}O$ $[M+H]^+$: 257.1905, found 257.1899.

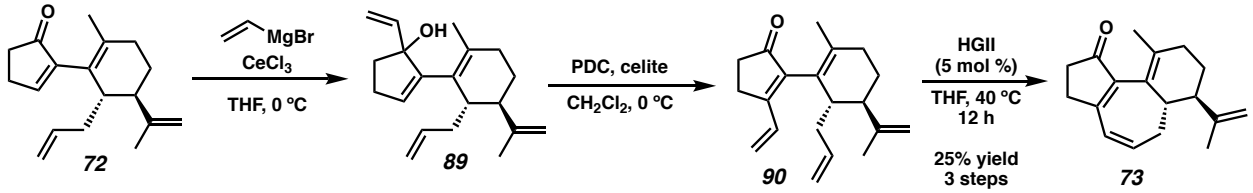

Tricycle 73: In a nitrogen-filled glovebox, anhydrous $CeCl_3$ (149 mg, 0.61 mmol, 1.0 equiv) was added to the reaction vessel. The vessel was sealed, removed from the glove box, and placed under a N_2 atmosphere. To the solid $CeCl_3$ was added a solution of enone **72** (183 mg, 0.61 mmol, 1.0 equiv) in THF (6 mL, 0.1M). The reaction was cooled to 0 °C and stirred for several min, after which it was treated with 1M vinylmagnesium bromide in THF (1.2 mL, 3.0 equiv). The reaction was stirred at the designated temperature until deemed complete by TLC (ca. 30 min). (Note: In cases where the reaction remained incomplete, an additional 1 equiv of vinyl Grignard solution was added). Upon completion, the reaction was quenched by addition of sat. aq. NH_4Cl, extracted with Et_2O (3 X 30 mL), dried (Na_2SO_4), and concentrated *in vacuo*. The crude residue was partially purified by passing through a plug of silica (20% EtOAc in hexanes) to provide *bis*-allyl alcohol **89** as a 1:1 mixture of diastereomers. The mixture was committed to the next reaction without further purification.

The crude mixture was dissolved in benchtop CH_2Cl_2 (6 mL) and cooled to 0 °C. Under air, the reaction was treated with PDC (451 mg, 1.20 mmol, 2.0 equiv) and celite (100 mg), and the mixture was allowed to warm to 23 °C over 2 h. Upon completion, the black mixture was passed through a plug of silica (CH_2Cl_2), concentrated *in vacuo*, and subjected to column chromatography (15% EtOAc in hexanes) to provide dienone **90** as a pale yellow oil (82 mg) that was satisfactorily pure for the next reaction.

A reaction vessel was charged with Hoveyda–Grubbs II catalyst (6.9 mg, 5 mol %). Upon purging with N_2, a solution of semi-pure dienone **90** (82 mg) in THF (10 mL) was added, and the

resulting solution was heated to 40 °C for 12 h. Upon completion, the solution was allowed to cool to 23 °C, and the catalyst was quenched by addition of ethyl vinyl ether (2 drops). After stirring for 5 min, the solution was concentrated *in vacuo*, and the resulting residue was purified by column chromatography (10%–20% EtOAc in hexanes) to provide tricycle **73** as a pale yellow oil (39 mg, 25% yield over 3 steps), which could be crystallized from hexanes (35 ºC to 4 ºC); R_f = 0.40 (20% EtOAc in hexanes); $[\alpha]_D^{25}$ –168.5 (*c* 1, $CHCl_3$); ^{1}H NMR (400 MHz, $CDCl_3$) δ 6.27–6.23 (m, 1H), 6.07–6.04 (m, 1H), 4.81–4.73 (m, 2H), 2.62–2.50 (m, 2H), 2.49–2.40 (m, 5H), 2.17–2.14 (m, 2H), 1.97–1.93 (m, 1H), 1.78–1.62 (m, 5H), 1.52 (s, 3H); ^{13}C NMR (126 MHz, $CDCl_3$) δ 206.3, 165.7, 147.3, 142.4, 141.2, 133.9, 125.7, 124.6, 111.2, 46.2, 41.6, 39.6, 35.3, 31.8, 30.0, 23.6, 22.8, 21.3; IR (Neat Film, NaCl) 3009.8, 2912.5, 1696.9, 1585.0, 1430.0, 1318.2, 1295.2, 1112.2, 894.9 cm^{-1}; HRMS (ESI-TOF) *m/z* calc'd for $C_{18}H_{22}ONa$ $[M+Na]^+$: 277.1563, found 277.1572.

1.7 NOTES AND REFERENCES

(1) Fairless, D. *Nature* **2007**, 652–655.

(2) Naengchomnong, W.; Thebtaranonth, Y.; Wiriyachitra, P.; Okamoto, K. T.; Clardy, J. *Tetrahedron Lett.* **1986**, *27*, 2439–2442.

(3) (*a*) Chianese, G.; Fattorusso, E.; Aiyelaagbe, O. O.; Luciano, P.; Schröder, H. C.; Müller, W. E. G.; Taglialatela-Scafati, O. *Org. Lett.* **2011**, *13*, 316–319; (*b*) Liu, J.-Q.; Yang, Y.-F.; Li, X.-Y.; Liu, E.-Q.; Li, Z.-R.; Zhou, L.; Li, Y.; Qiu, M.-H., *Phytochemistry* **2013**, *96*, 265–272; (*c*) Picha, P.; Naengchomnong, W.; Promratanapongse, P.; Kano, E.; Hayashi, S.; Ohtsubo, T.; Zhang, S. W.; Shioura, H.; Kitai, R.; Matsumoto, H.; Kawahara, K.; Puribhat, S.; Phanthumachinda, P. *J. Exp. Clin. Cancer Res.* **1996**, *15*, 177–183.

(4) Li, Y.; Dai, M. *Angew. Chem. Int. Ed.* **2017**, *56*, 11624–11627.

(5) Revised structures of curcusones I and J were recently proposed, see: Sarotti, A. M. *Org. Biomol. Chem.* **2018**, *16*, 944–950.

(6) Wright, A. C.; Lee, C. W.; Stoltz, B. M. *Org. Lett.* **2019**, *21*, 9658–9662.

(7) Wang, Q.; Fan, S. Y.; Wong, H. N. C.; Li, Z.; Fung, B. M.; Twieg, R. J.; Nguyen, H. T. *Tetrahedron Lett.* **1993**, *49*, 619–638.

(8) Comins, D. L.; Dehghani, A.; Foti, C. J.; Joseph, S. P. *Org. Synth.* **1997**, *74*, 77–80.

(9) Karaarslan, M.; Gokturk, E.; Demircan, A. *J. Chem. Res.* **2007**, 117–120.

(10) Seigel, C.; Gordon, P. M.; Razdan, R. K. *J. Org. Chem.* **1989**, *54*, 5428–5430.

(11) Coupling partner (+)-**20** was prepared using (*S*)-Me-CBS catalyst.

(12) Reversible Meerwein–Ponnderf–Verley reduction consistently favored the unwanted *trans* isomer, indicating that it is the thermodynamically favored epimer.

(13) All non-asymmetric and irreversible reactions resulted in the *trans* isomer as the predominant diastereomeric product, suggesting that its formation is kinetically favored.

(14) The fragile boronate functionality was incompatible toward most alcohol protection/deprotection strategies. The sole exception to this was found with PMB-based protecting groups, which could be delicately excised under pH-buffered conditions using DDQ.

(15) Similar decomposition pathways were observed during our campaign toward ineleganolide, see: Craig II, R. A. C.; Roizen, J. L.; Smith, R. C.; Jones, A. C.; Virgil, S. C. *Chem. Sci.* **2017**, 8, 507–514.

(16) Xu, X.; Deng, Y.; Yim, D. N.; Zavalij, P. Y.; Doyle, M. P. *Chem. Sci.* **2015**, *6*, 2196–2201.

(17) (a) Oesterreich, K.; Klein, I.; Spitzner, D. *Synlett* **2002**, 1712–1713; (b) Kauffmann, T.; Papenberg, M.; Wieschollek, R.; Sander, J. *Chem. Ber*. **1992**, *125*, 143–148.

(18) Denney, D. B.; Sherman, N. *J. Am. Chem. Soc.* **1965**, *30*, 3760–3761.

(19) Wright, A. C.; Stoltz, B. M. *Chem. Sci*. **2019**, *10*, 10562–10565.

(20) Lee, C. W.; Taylor, B. L. H.; Petrova, G. P.; Patel, A.; Morokuma, K.; Houk, K. N.; Stoltz, B. M. *J. Am. Chem. Soc.* **2019**, *141*, 6995–7004.

(21) Shi, L.-L.; Shen, H.-J.; Fang, L.-C.; Huang, J.; Li, C.-C.; Yang, Z. *Chem. Commun.* **2013**, *49*, 8806–8808.

(22) Smith, III, A. B.; Branca, S. J.; Pilla, N. N.; Guaciaro, M. A. *Org. Lett.* **1982**, *47*, 1855–1869.

(23) Ackerman, L. K. G.; Lovell, M. M.; Weix, D. J. *Nature* **2015**, *524*, 454–457.

(24) Poremba, K. E.; Kadunce, N. T.;Suzuki, N.; Cherney, A. H.; Reisman, S. E. *J. Am. Chem. Soc.* **2017**, *139*, 5684–5687.

(25) Anka-Lufford, L. L.; Huihui, K. M. M.; Gower, N. J.; Ackerman, L. K. G.; Weix, D. J. *Chem. Eur. J.* **2016**, *22*, 11564–11567.

(26) Everson, D. A.; Weix, D. J. *J. Org. Chem.* **2014**, *79*, 4793–4798.

(27) Olivares, A. M.; Weix, D. J. *J. Am. Chem. Soc.* **2018**, *140*, 2446–2449.

(28) Levine, S. G. *J. Am. Chem. Soc.* **1958**, *80*, 6150–6151.

(29) Still, W. C. *J. Am. Chem. Soc.* **1978**, *100*, 1481–1487.

(30) Oldenziel, O. H.; Van Leusen, D.; Van Leusen, A. M. *J. Org. Chem.* **1977**, *42*, 3114–3118.

(31) Kantorowski, E. J.; Kurth, M. J. *Tetrahedron* **2000***, 56*, 4317–4353.

(32) Marion, N.; Díez-González, S.; Nolan, S. P. *Angew. Chem. Int. Ed.* **2007**, *46*, 2988–3000.

(33) The following 1,2-adducts were obtained in roughly equal proportions:

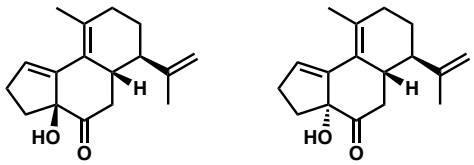

(34) (*a*) Babler, J. H.; Coghlan, M. J. *Synth. Commun.* **1976**, *6*, 469–474; (*b*) Dauben, W. G.; Michno, D. M. *J. Org. Chem.* **1977**, *42*, 682–685.

(35) The following aldehyde isomer was continually observed as a minor byproduct from the oxidative transposition:

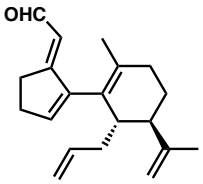

(36) Yu, M.; Danishefsky, S. J. *J. Am. Chem. Soc.* **2008**, *130*, 2783–2785.

(37) Although insufficient spectral data has yet been collected, we strongly suspect that the following enone product (highlighted in blue) arises from protic quenching of enolate **76**:

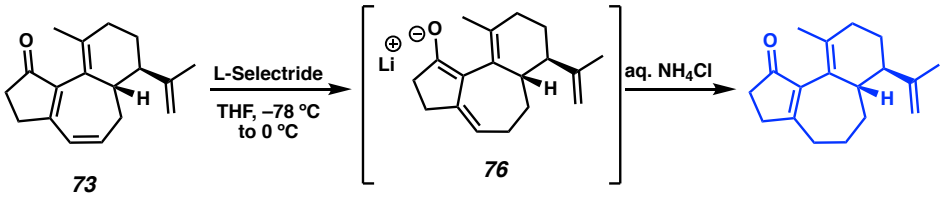

(38) Davis, F. A. *Tetrahedron* **2018**, *74*, 3198–3214.

(39) Williamson, K. S.; Michaelis, D. J.; Yoon, T. P. *Chem. Rev.* **2014**, *114*, 8016–8036.

(40) Morcillo, S. P.; Miguel, D.; Campana, A. G.; de Cienfuegos, L. A.; Justicia, J.; Cuerva, J. M. *Org. Chem. Front.* **2014**, *1*, 15–33.

(41) Pangborn, A. B.; Giardello, M. A.; Grubbs, R. H.; Rosen, R. K.; Timmers, F. J. *Organometallics* **1996**, *15*, 1518–1520.

(42) Davies, H. M. L.; Cantrell, R. W.; Jr.; Romines, R. K.; and Baum, S. J. *Org. Synth.* **1992**, 70, 93–100; *Coll. Vol. IX* **1998**, 422-426.

(43) Charles, R. G. *J. Org. Chem.* **1957**, *22*, 677–679.

(44) McUliffe, C. A.; Hosseiny, A.; McCullough, F. P. *Inorg. Chim. Acta* **1979**, *33*, 5–10.

(45) Khan, S.; Kato, N.; Hirama, M. *Synlett* **2000**, 1494–1496.

APPENDIX 1

Synthetic Summary Toward the Total Synthesis of Curcusone C

*Scheme A1.1. Retrosynthetic Analysis of ent-Curcusone C (ent-**3**) via Rearrangement*

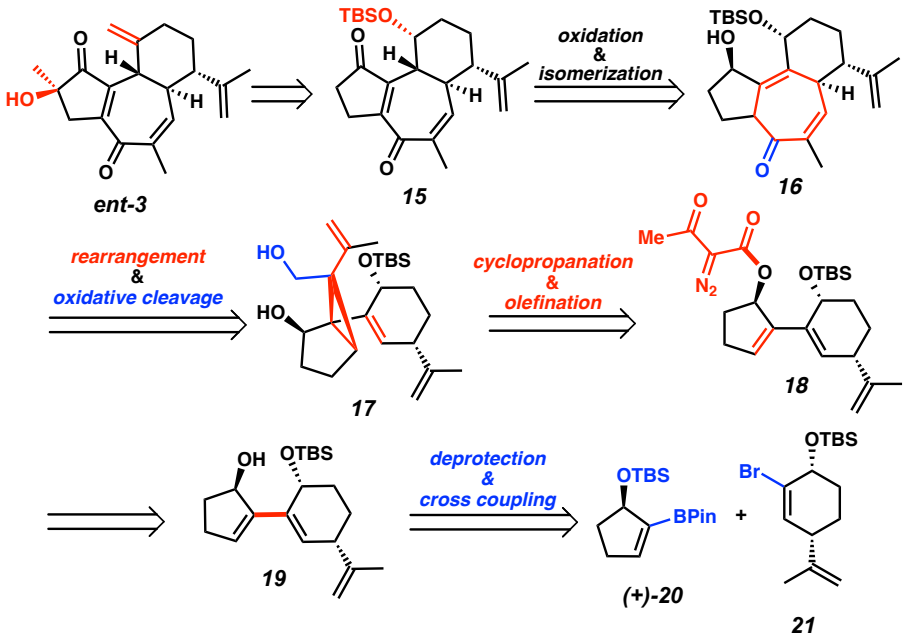

*Scheme A1.2. 1st Generation Synthesis of Diazo **34***

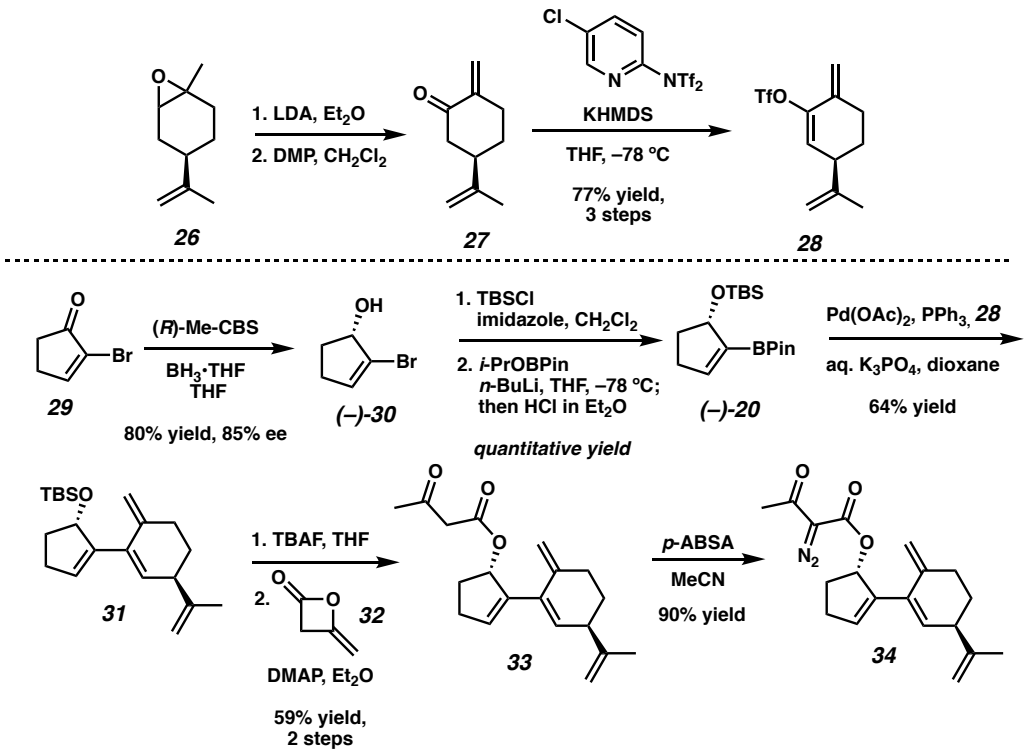

*Scheme A1.3. Undesired Hetero-Diels–Alder of Enone **27***

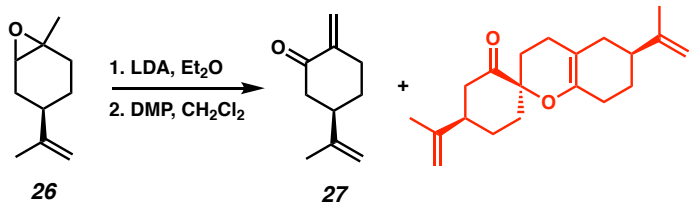

*Scheme A1.4. 2nd Generation Approach toward ent-**1–4***

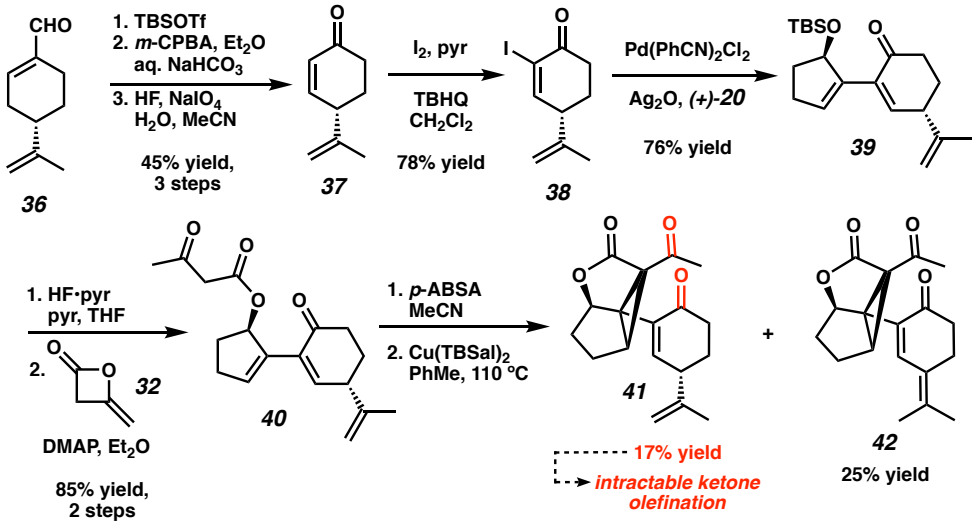

*Scheme A1.5. 3rd Generation Assembly of Bicycle **19***

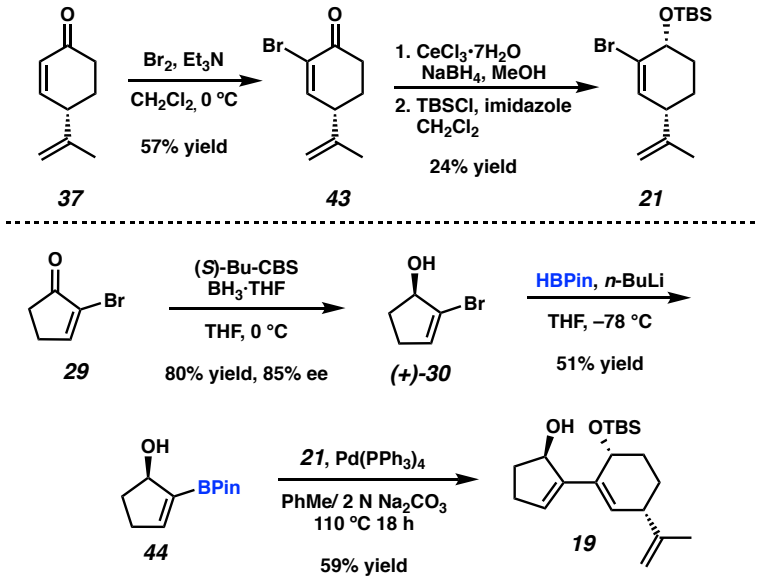

Scheme A1.6. 3rd Generation Synthesis of Divinylcyclopropane ***47***

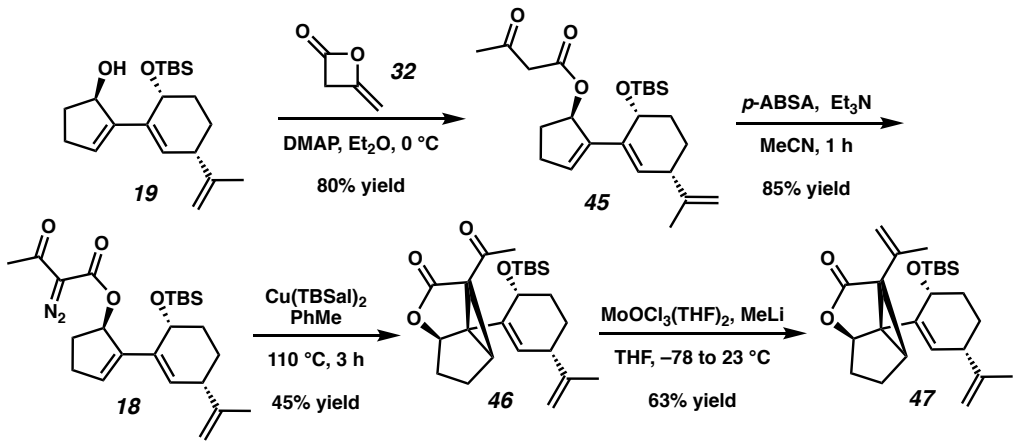

SCHEME A1.7. Construction of Tricycle ***49*** *by Lactone Opening and Rearrangement*

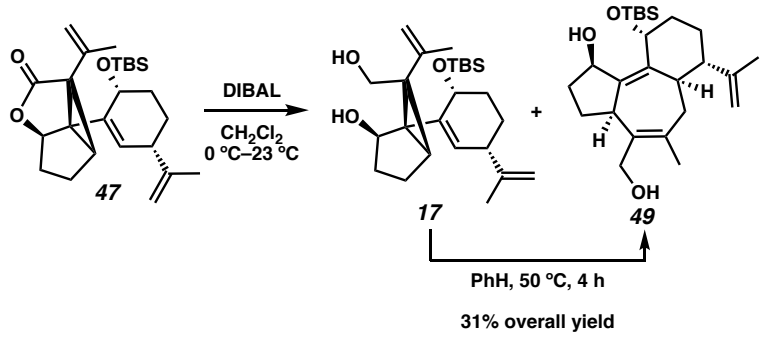

Scheme A1.8. Envisioned Oxidative Cleavage Sequence on Diol ***49***

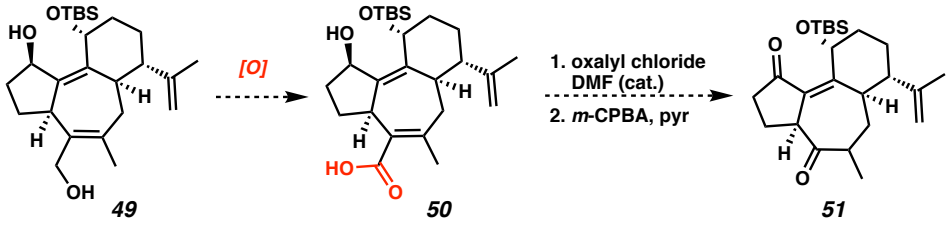

*Scheme A1.9. 2nd Generation Retrosynthesis of **3***

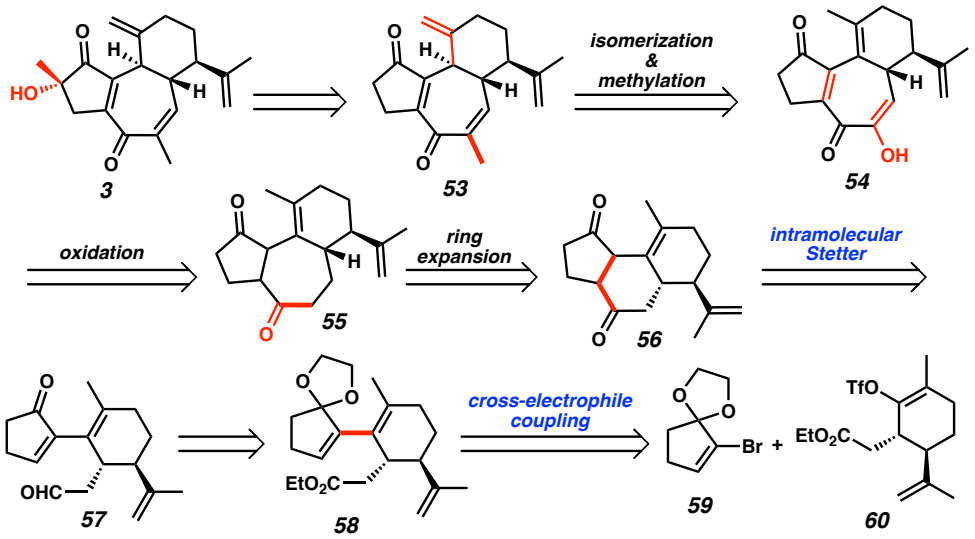

*Scheme A1.10. Synthesis of Coupling Partners **59** and **60***

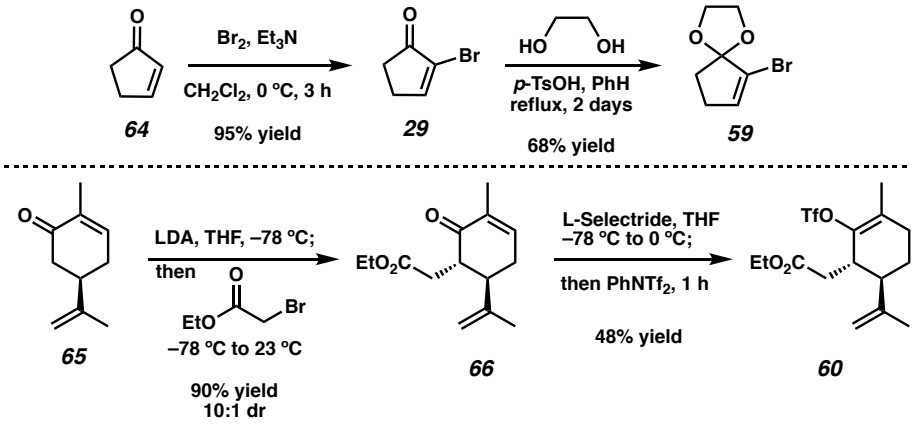

Table A1.1. Initial Optimization of the Cross-Electrophile Coupling

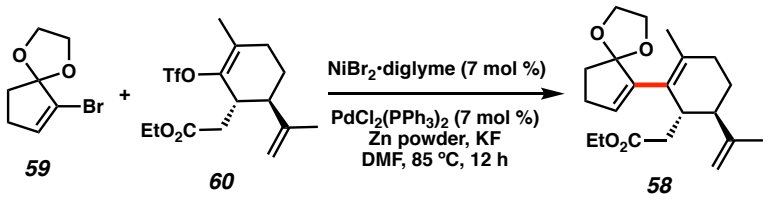

Entry	Deviation from standard procedure	Result
1	none	23% yield
2	No Pd	no product
3	No Ni	no product
4	dioxane instead of DMF	no product
5	NaI instead of KF	trace ***58***
6	no KF	trace ***58***
7	TDAE* instead of Zn	no product
8	4 equiv of ***59***	32% yield
9	syringe pump addition of ***59***	60% yield

*TDAE = tetrakis(dimethylamino)ethylene

Scheme A1.11. Further Optimization of the Reductive Coupling on Multigram Scale

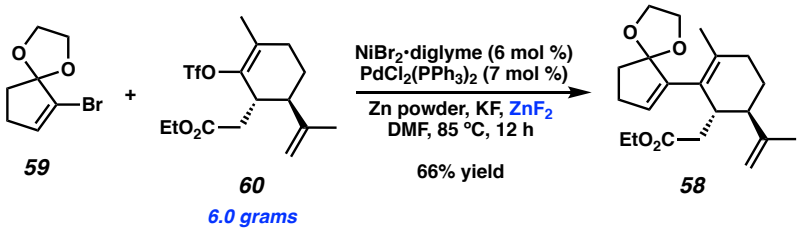

*Scheme A1.12. Preparation of Stetter Precursor **57***

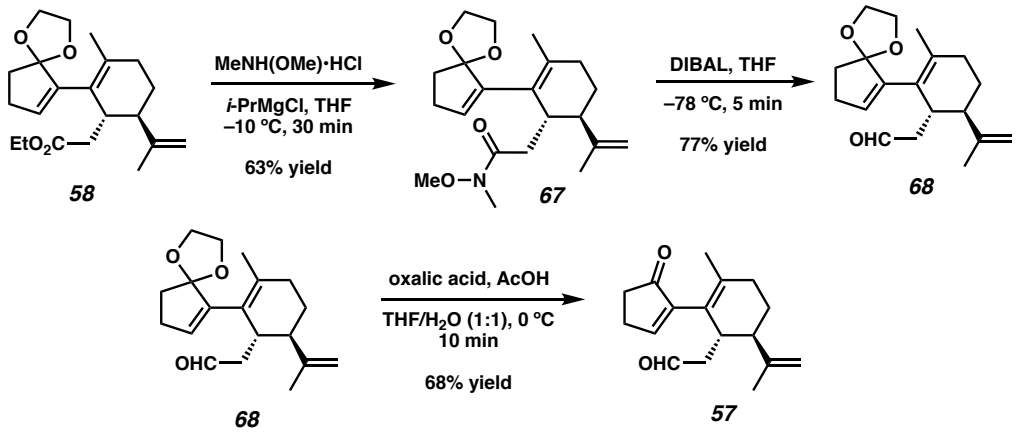

*Table A1.2. Optimization of the Catalytic Stetter Reaction on Ketoaldehyde **57***

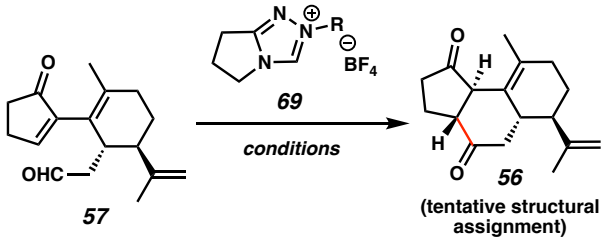

entry	R	catalyst loading	conditions	result*
1	Ph	30 mol %	DBU, dioxane 80 °C, 12 h	17% yield 1:1 dr
2	C_6F_5	30 mol %	LiHMDS, PhMe 70 °C, 12 h	1,2-adduct
3	C_6F_5	20 mol %	DBU, THF 30 °C, 30 min	24% yield 5:1 dr
4	C_6F_5	5 mol %	DBU, THF, 0 °C–23°C 12 h	incomplete conversion
5	C_6F_5	15 mol %	TMG, THF 23 °C–45 °C	50–60% yield 2:1 dr

*Relative stereochemistry at the 5–6 juncture was identified by ^{1}H NMR, however the absolute stereochemistry could not be determined.

*Scheme A1.13. Unsuccessful Ring Expansion of Ene-dione **70***

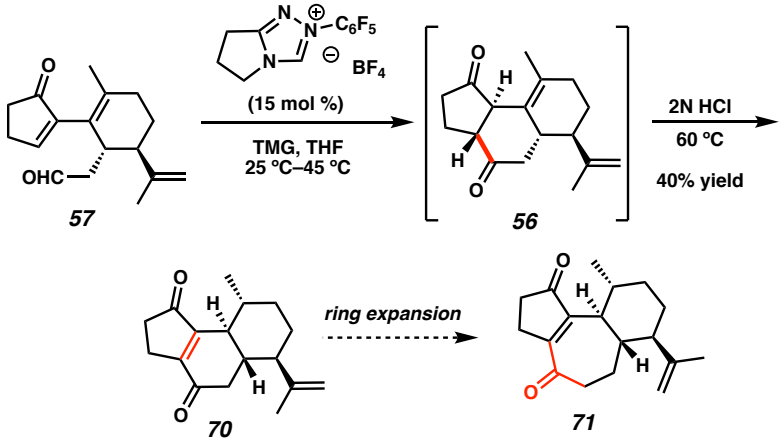

*Scheme A1.14. Construction of Tricycle **73** via an RCM Approach*

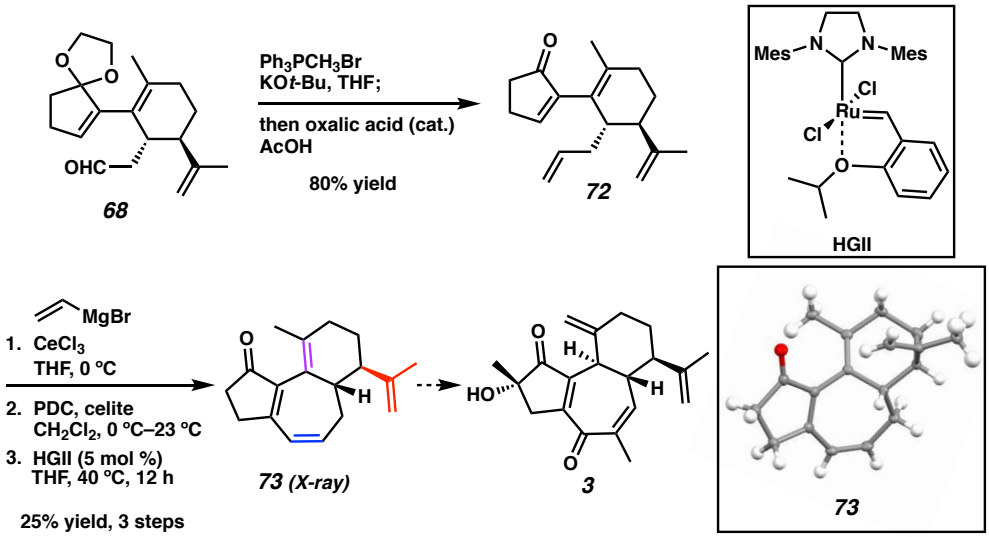

*Scheme A1.15. Divergent Oxidation Strategies to Form Ene-dione **81***

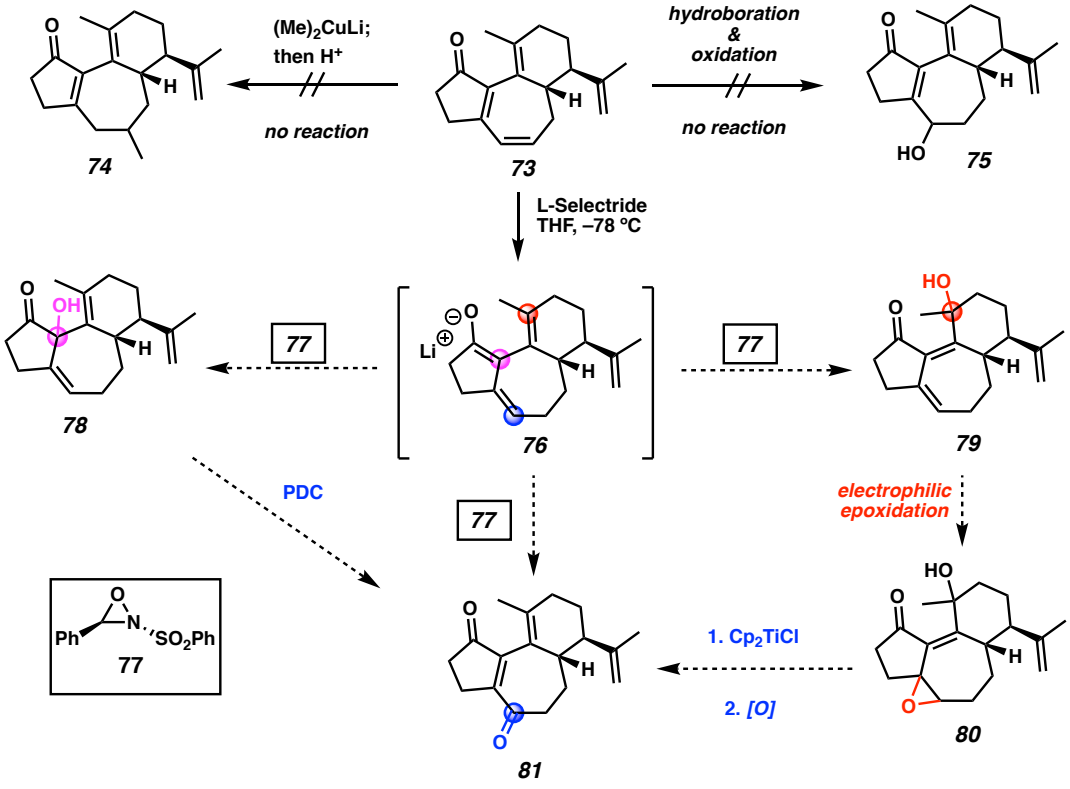

*Scheme A1.16. Divergent Advancement of **81** to Curcusones A–D*

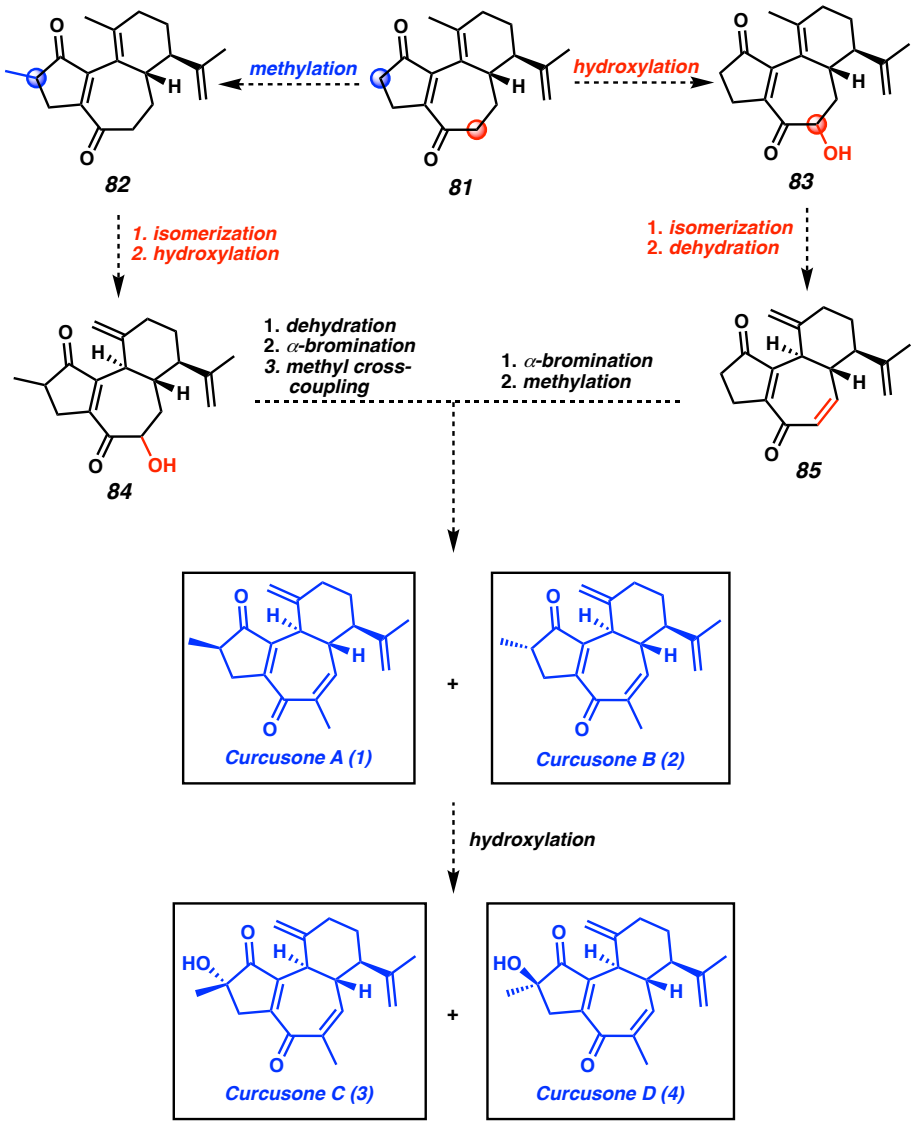

APPENDIX 2

Spectra Relevant to Chapter 1:

Evolving Strategies Toward the Synthesis of Curcusone C

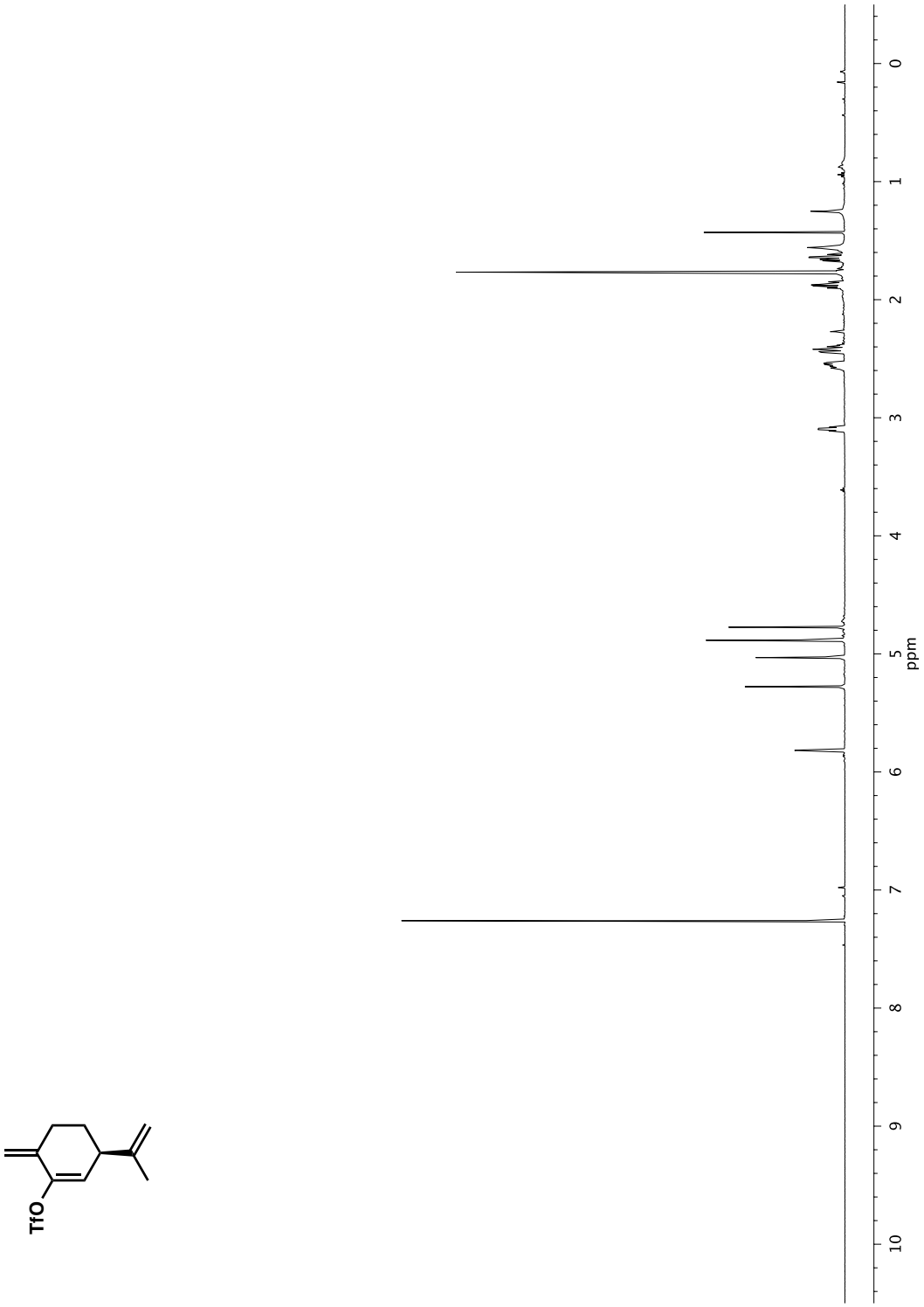

Figure A2.1 ^{1}H NMR (500 MHz, $CDCl_3$) of compound **28**

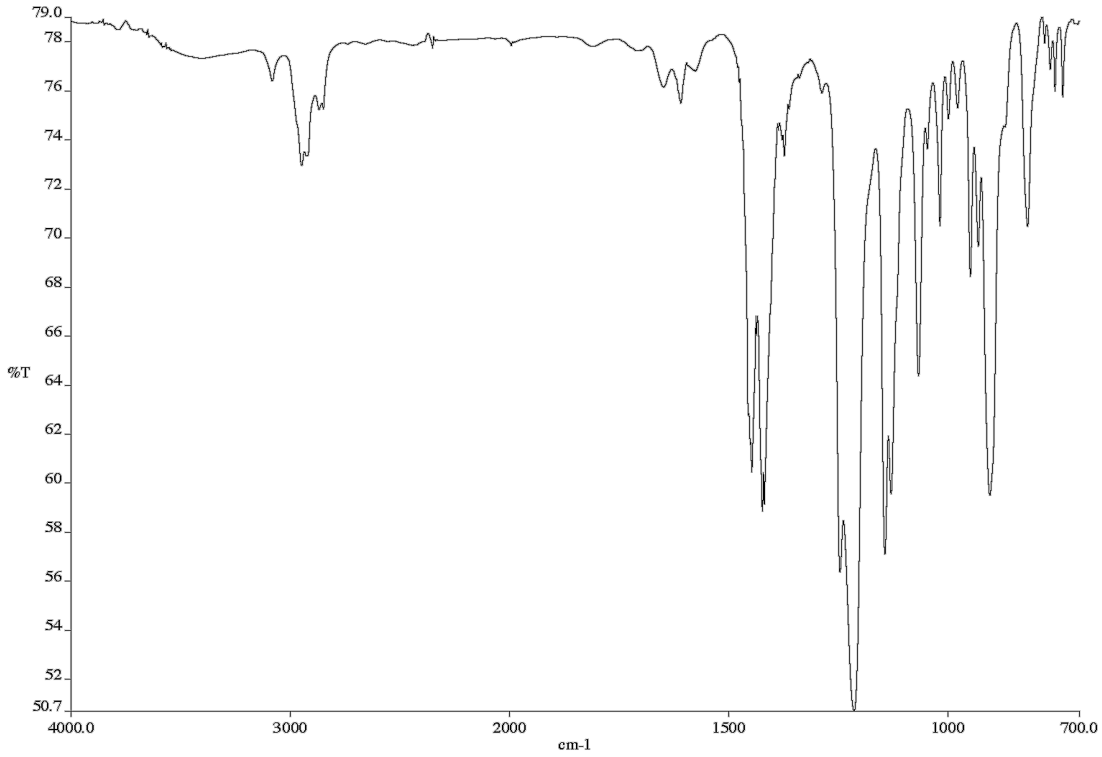

Figure A2.2 Infrared spectrum (Thin Film, NaCl) of compound **28**

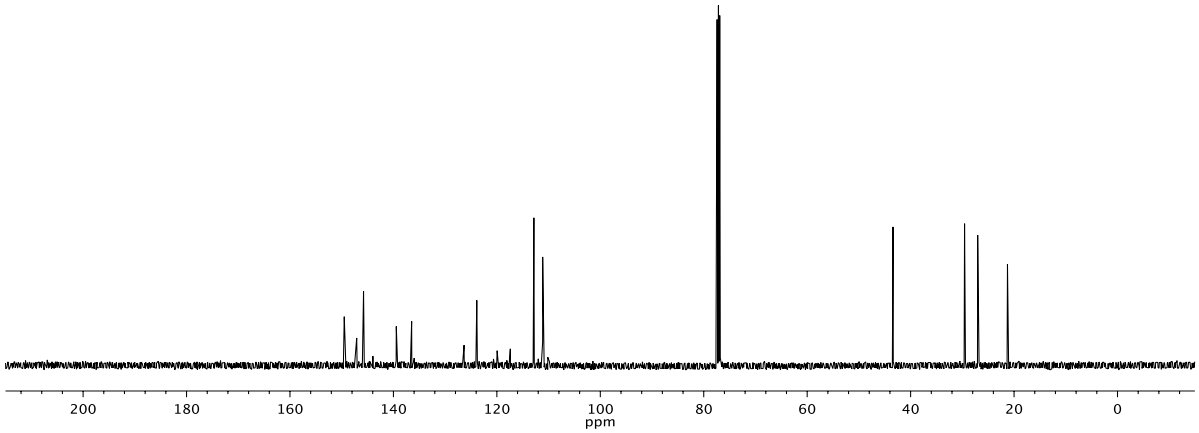

Figure A2.3 ^{13}C NMR (126 MHz, $CDCl_3$) of compound **28**

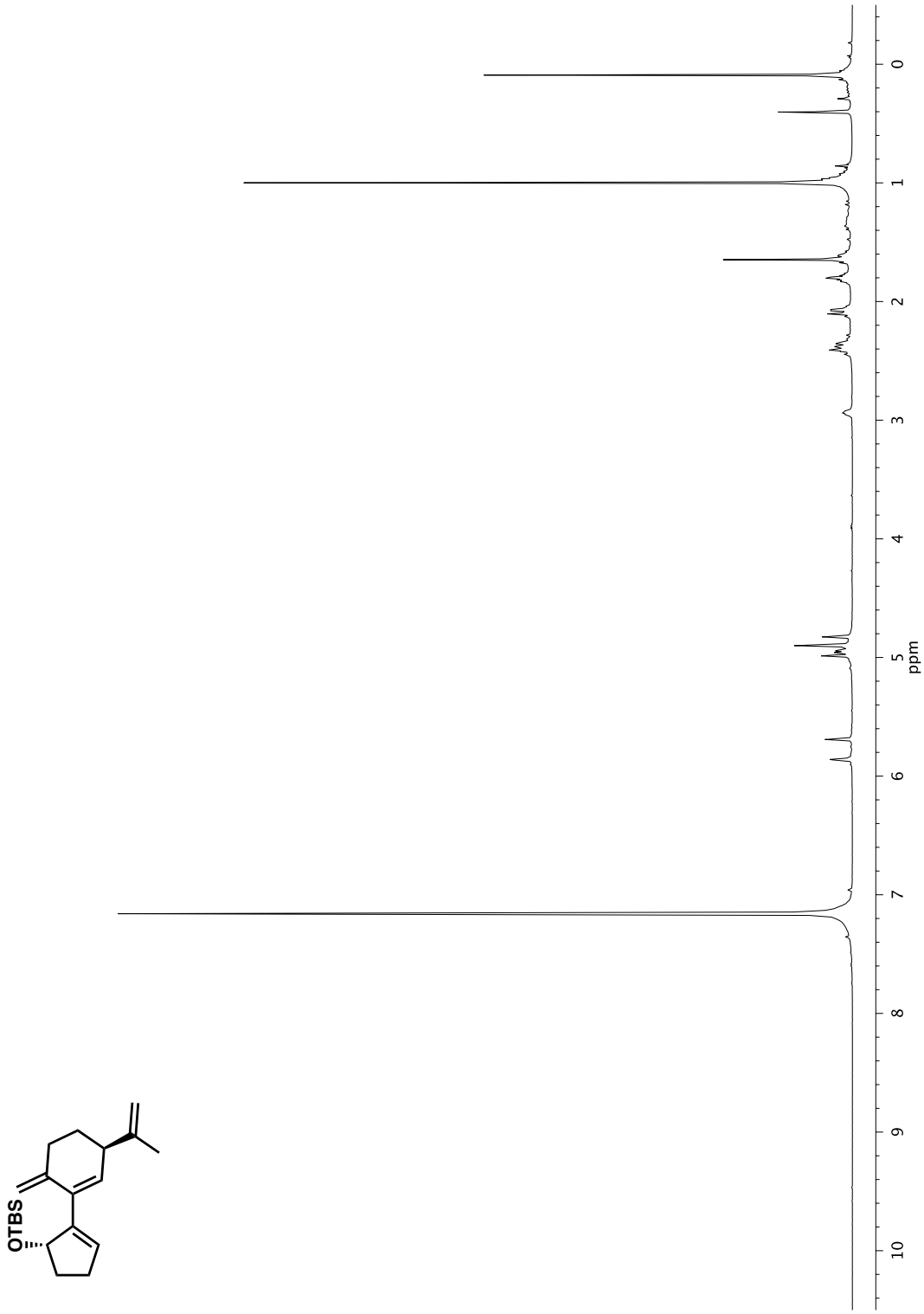

Figure A2.4 ^{1}H NMR (400 MHz, $CDCl_3$) of compound **31**

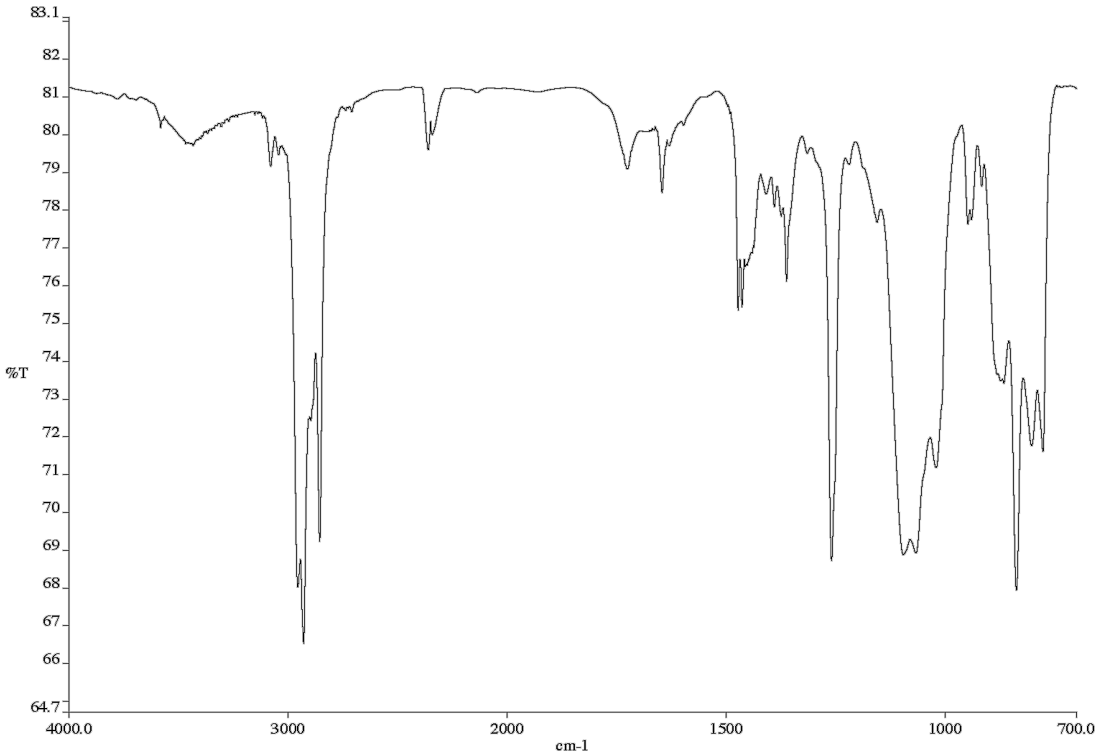

Figure A2.5 Infrared spectrum (Thin Film, NaCl) of compound **31**

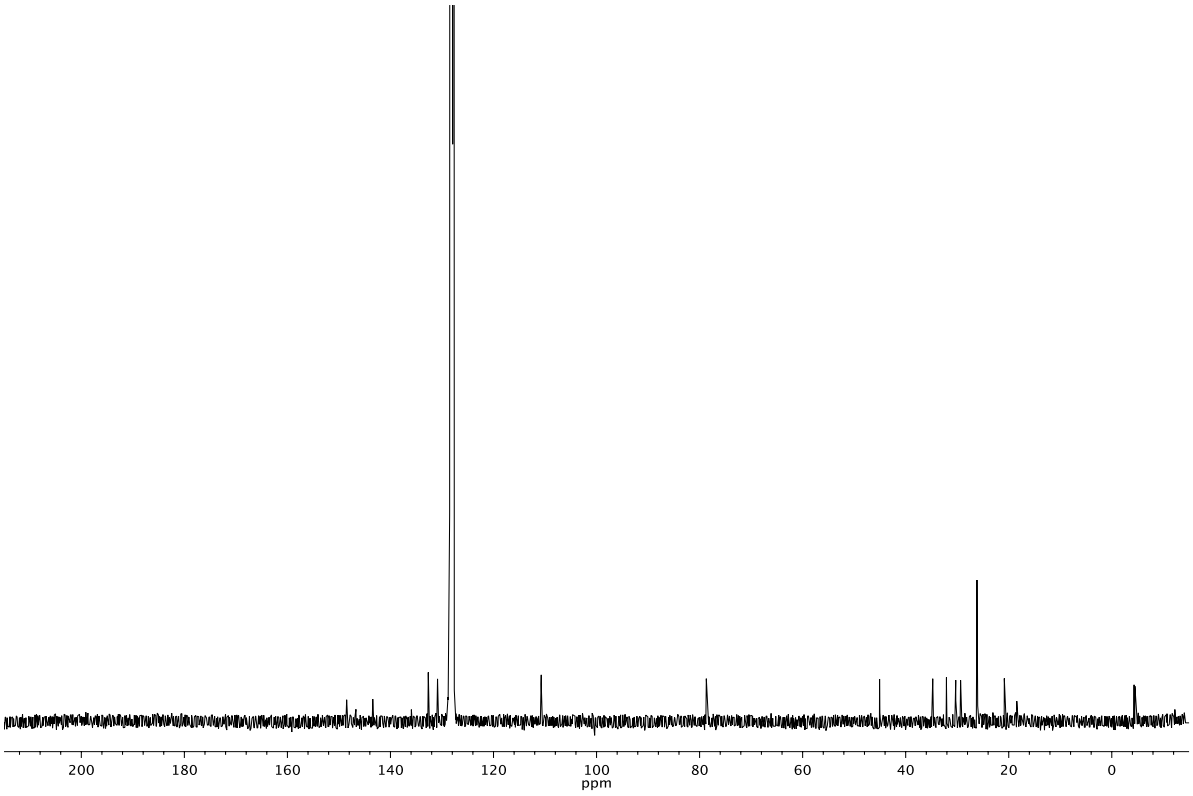

Figure A2.6 ^{13}C NMR (101 MHz, C_6D_6) of compound **31**

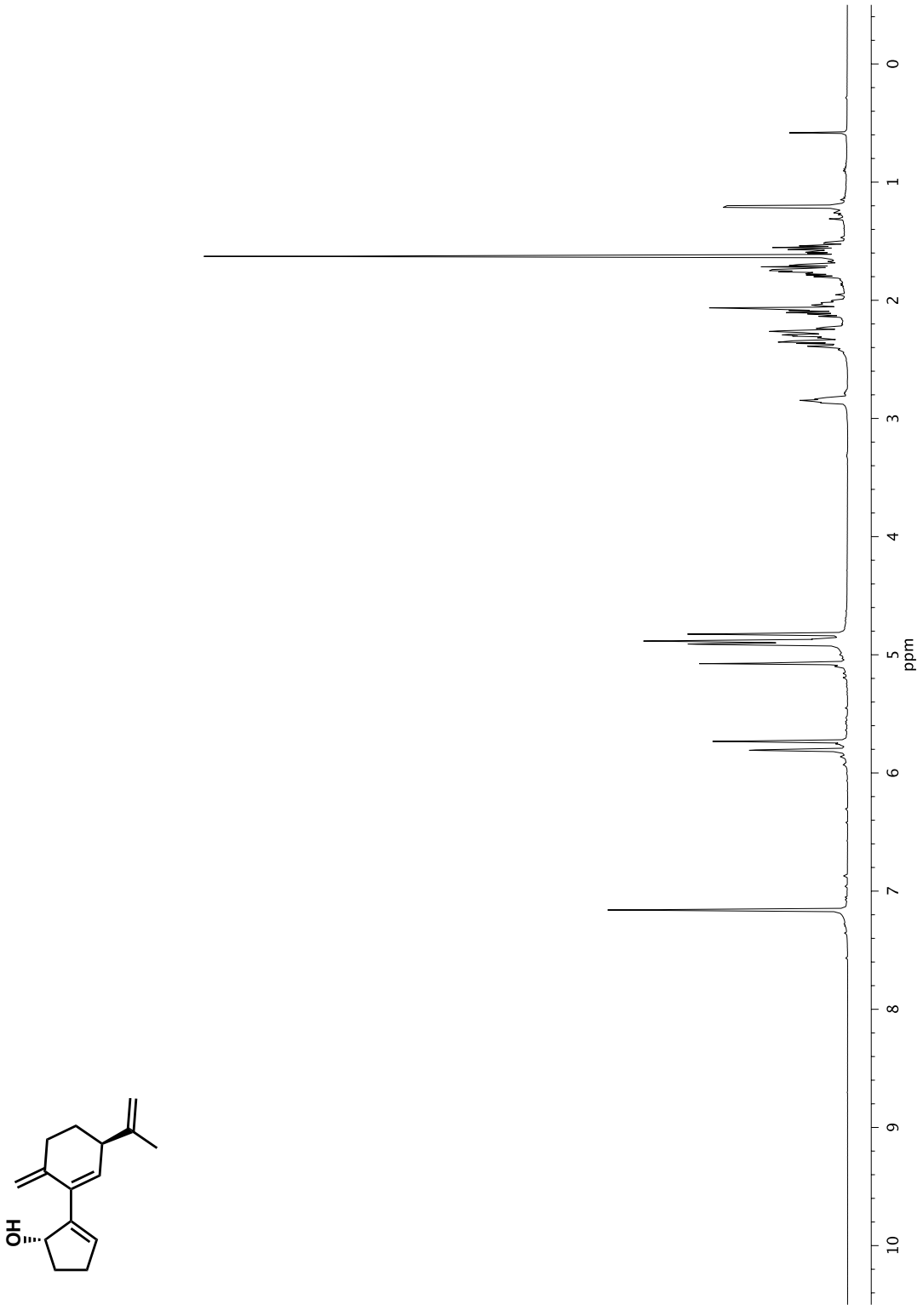

Figure A2.7 ^{1}H NMR (400 MHz, C_6D_6) of compound **87**

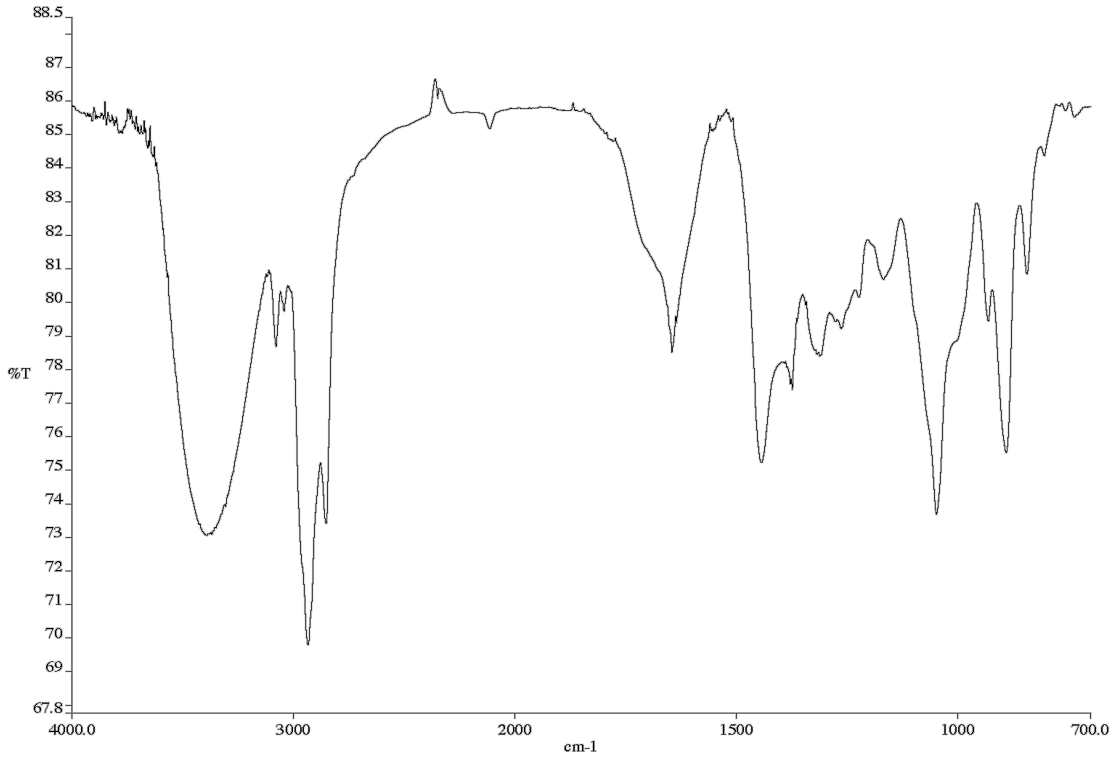

Figure A2.8 Infrared spectrum (Thin Film, NaCl) of compound **87**

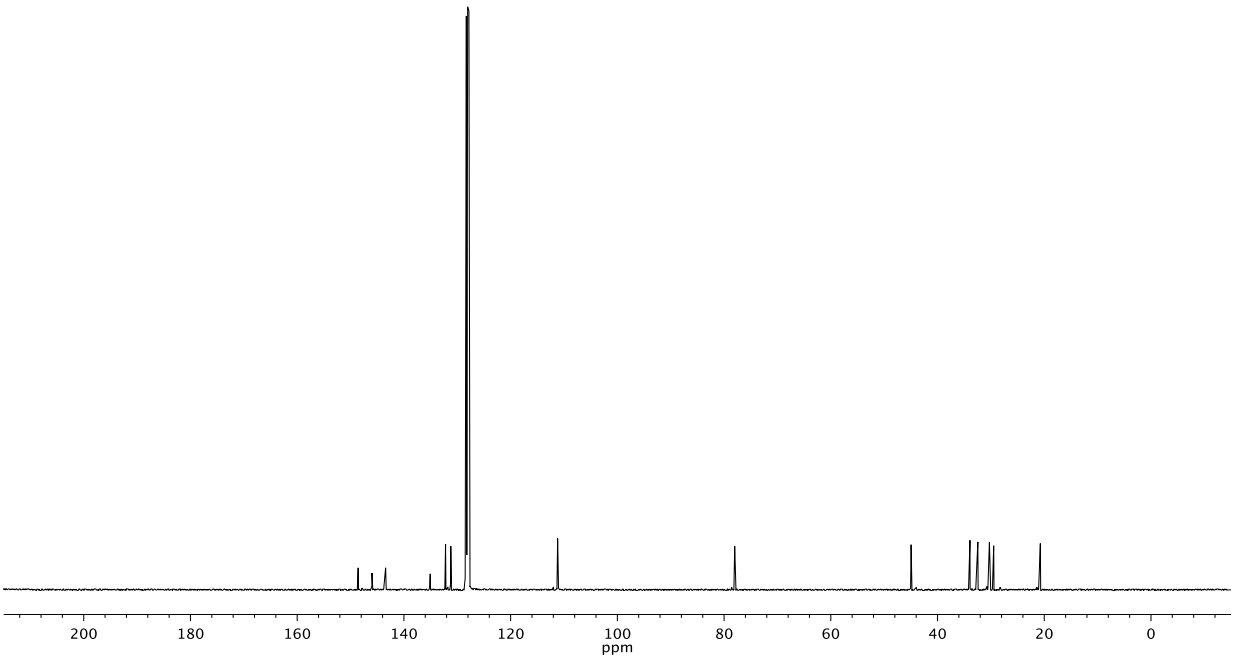

Figure A2.9 ^{13}C NMR (101 MHz, C_6D_6) of compound **87**

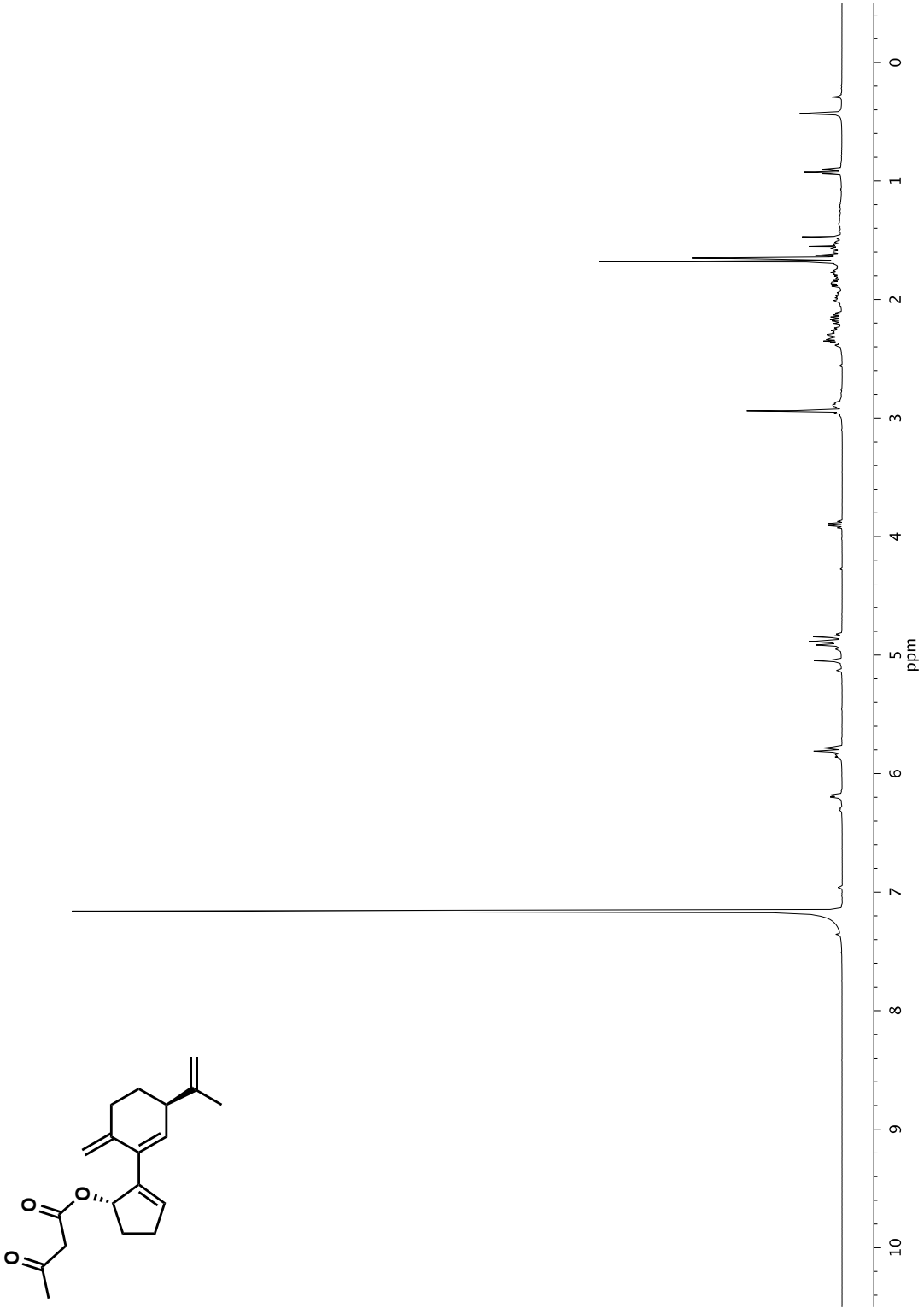

Figure A2.10 ^{1}H NMR (400 MHz, C_6D_6) of compound **33**

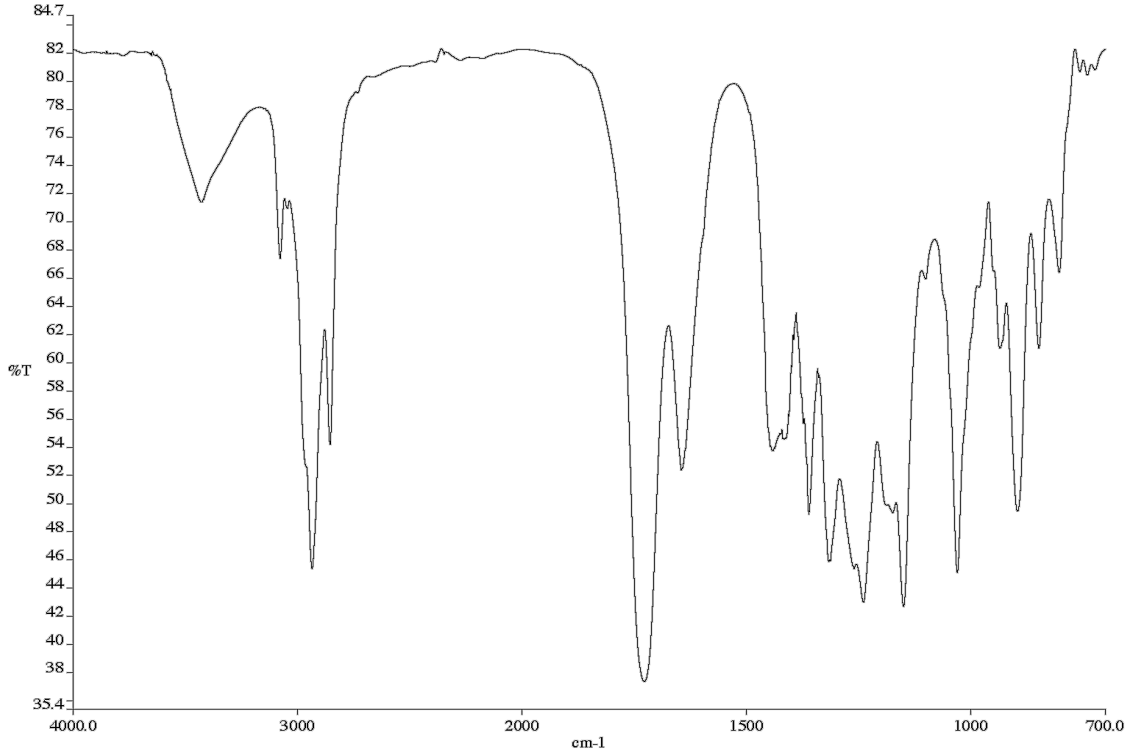

Figure A2.11 Infrared spectrum (Thin Film, NaCl) of compound **33**

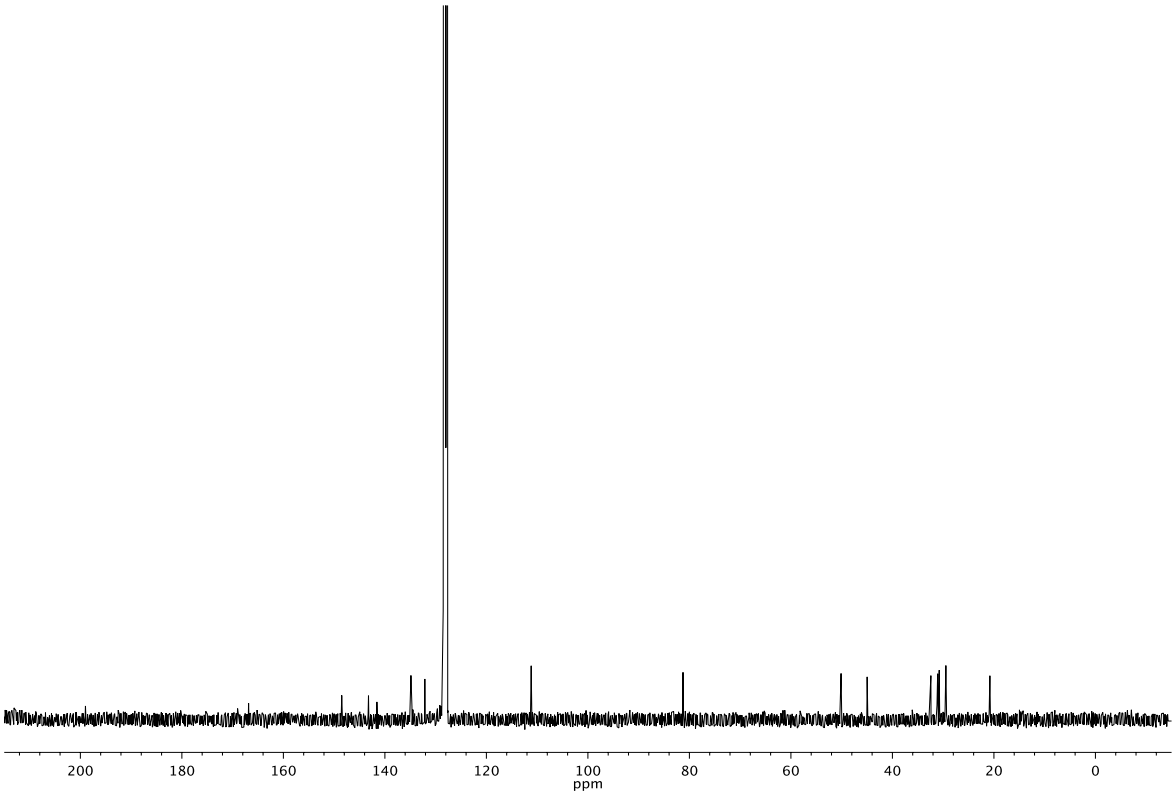

Figure A2.12 ^{13}C NMR (101 MHz, $CDCl_3$) of compound **33**

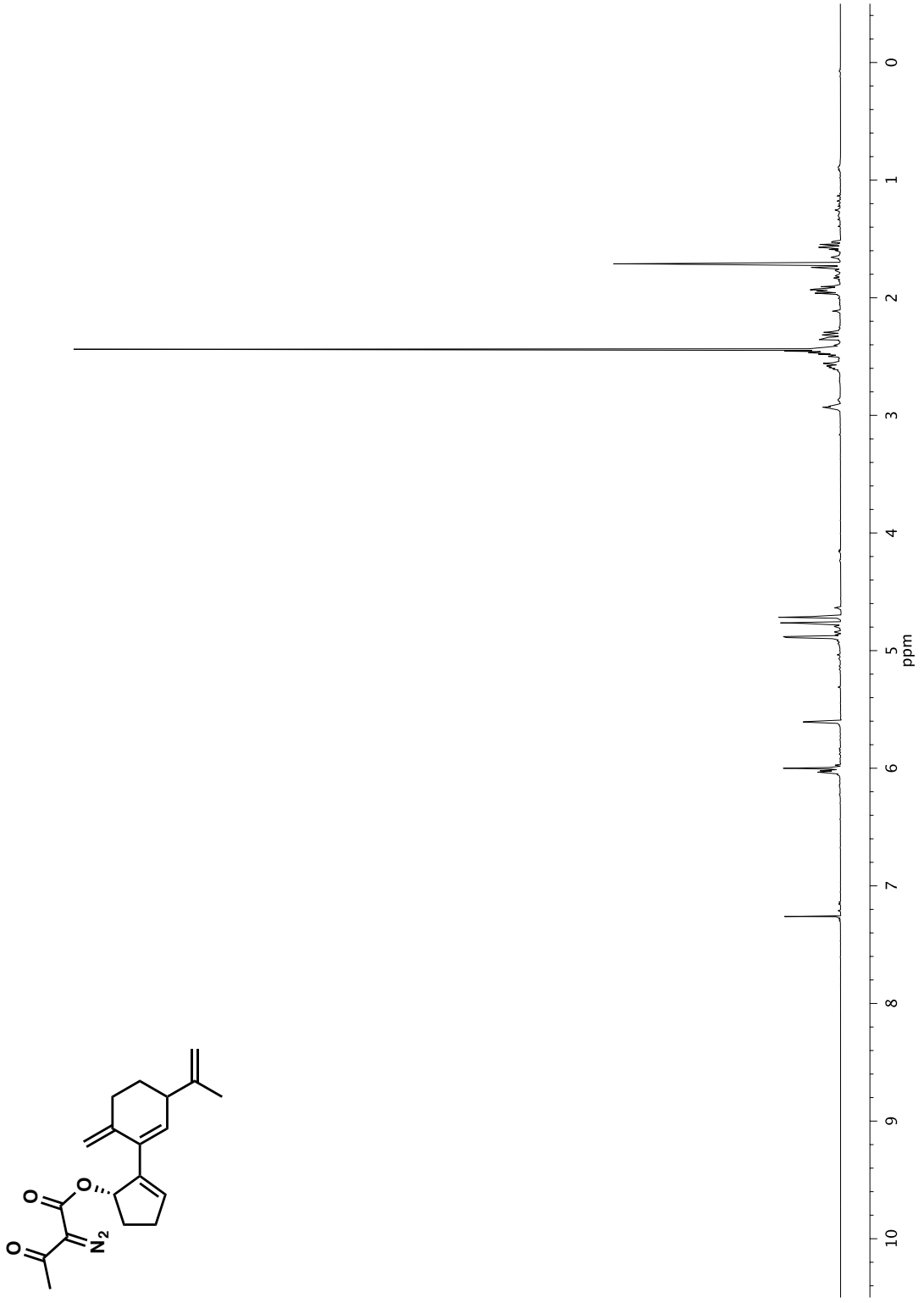

Figure A2.13 ^{1}H NMR (500 MHz, $CDCl_3$) of compound **34**

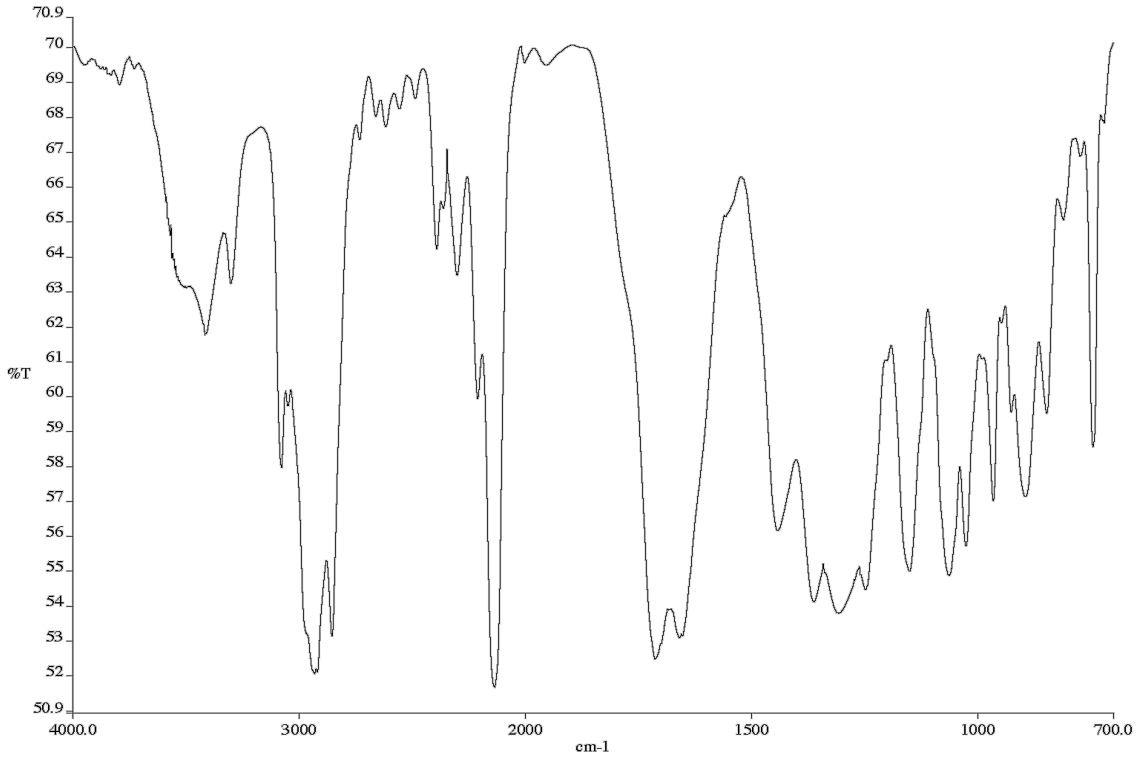

Figure A2.14 Infrared spectrum (Thin Film, NaCl) of compound **34**

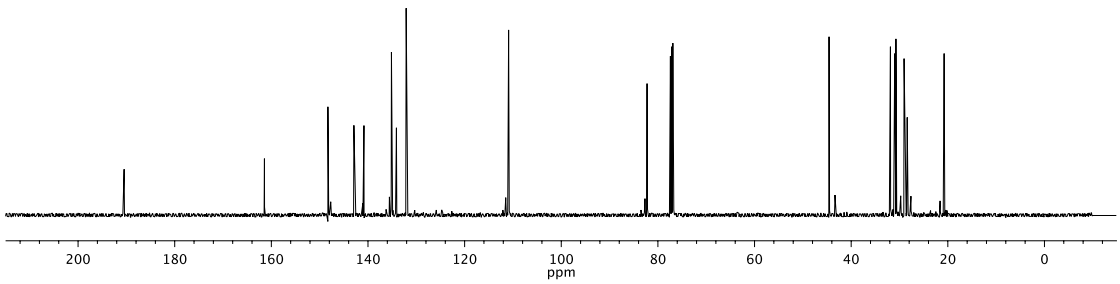

Figure A2.15 ^{13}C NMR (126 MHz, $CDCl_3$) of compound **34**

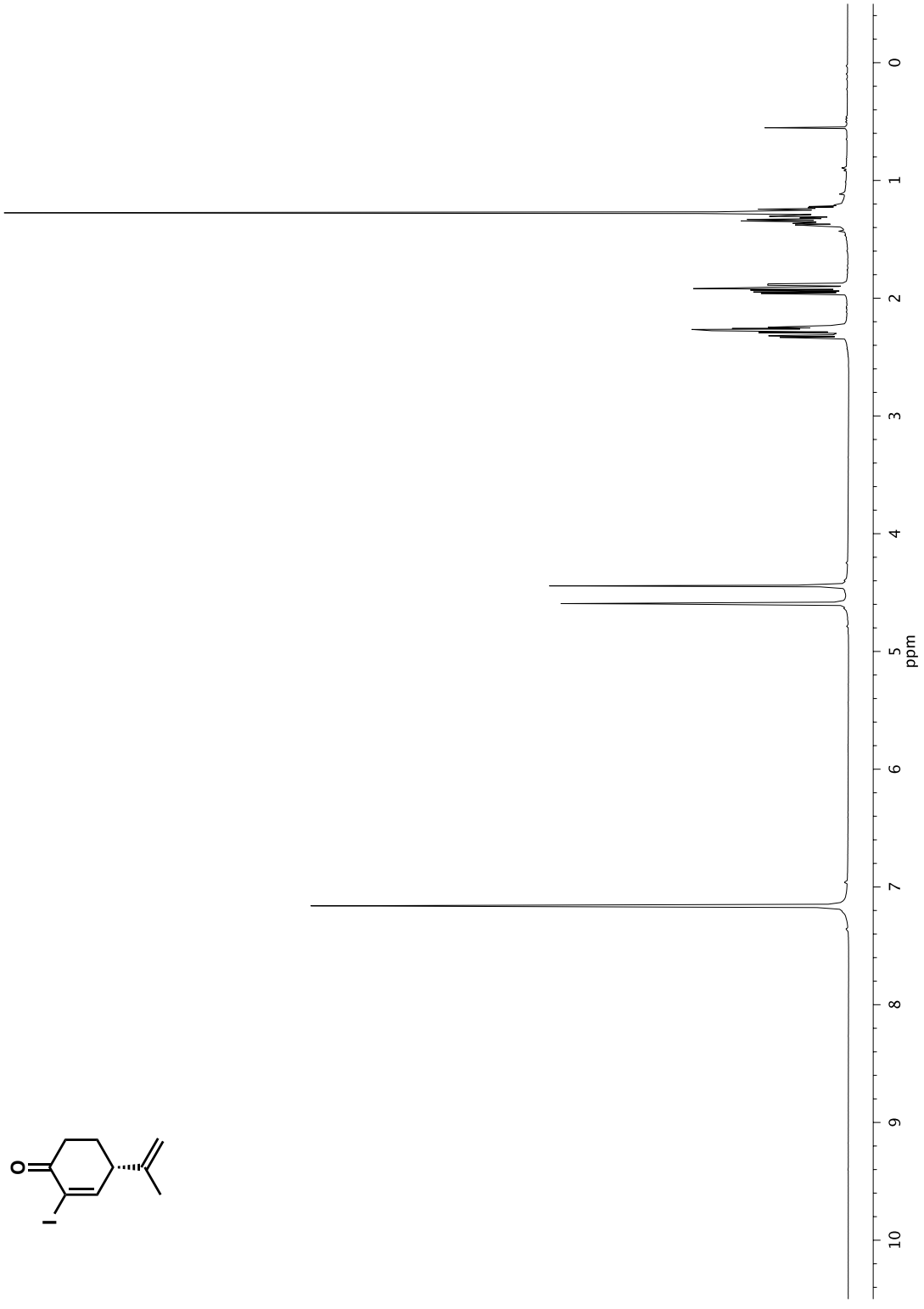

Figure A2.16 ^{1}H NMR (400 MHz, C_6D_6) of compound **38**

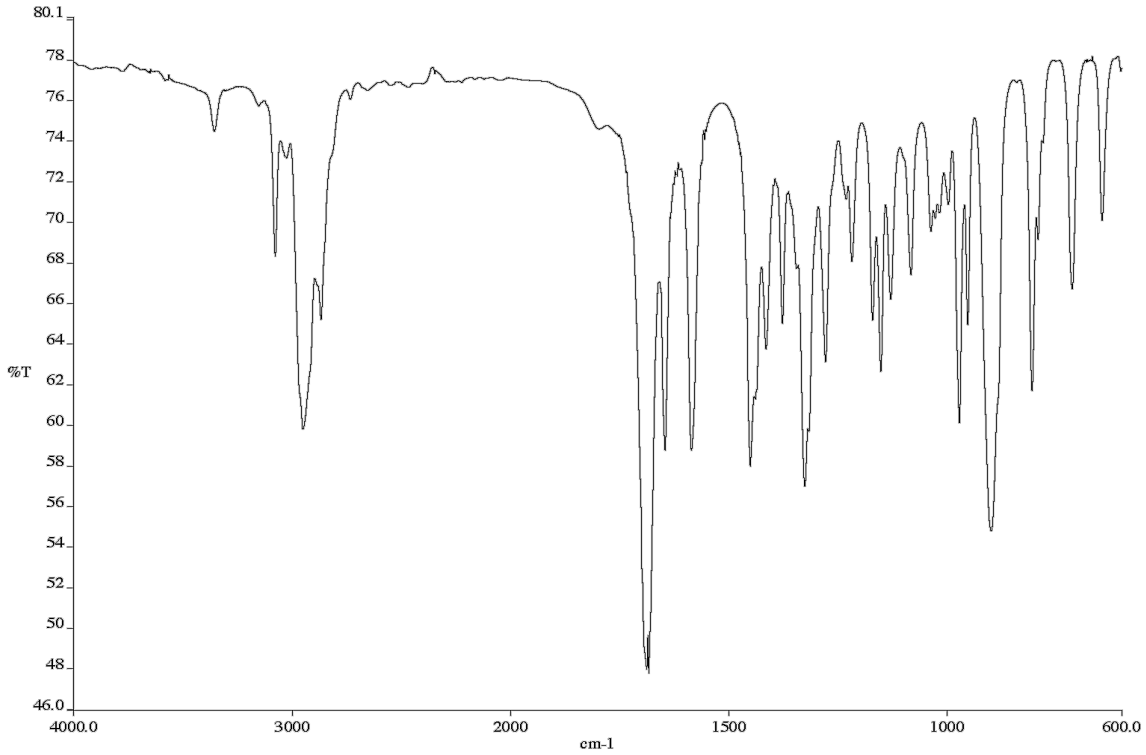

Figure A2.17 Infrared spectrum (Thin Film, NaCl) of compound **38**

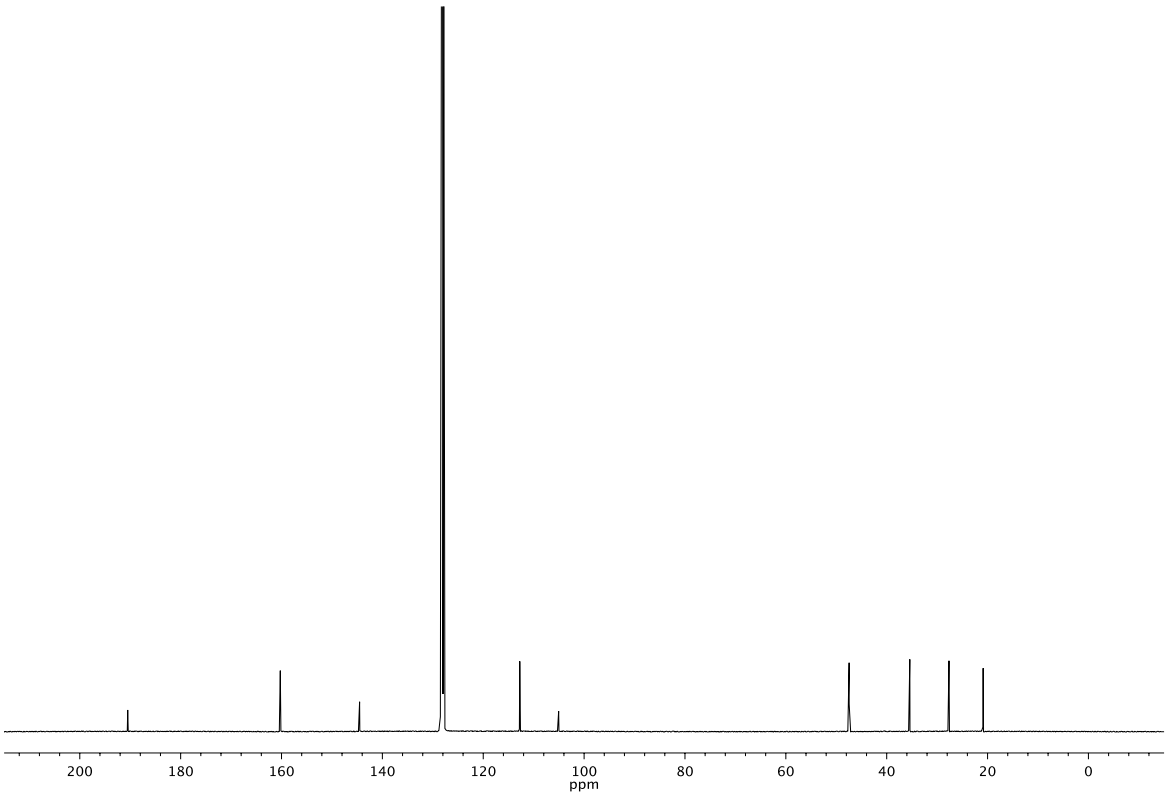

Figure A2.18 ^{13}C NMR (101 MHz, C_6D_6) of compound **38**

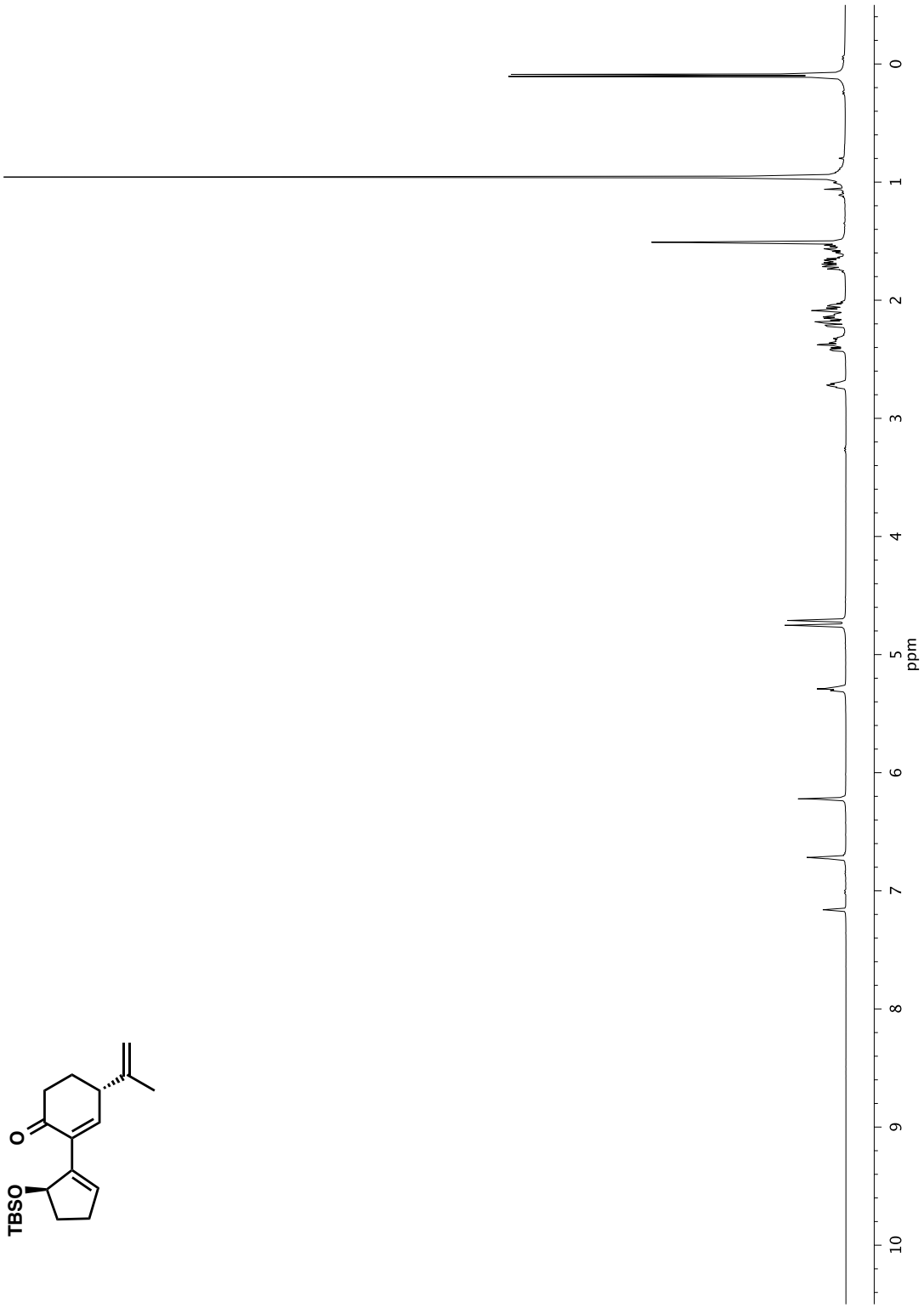

Figure A2.19 ^{1}H NMR (400 MHz, C_6D_3) of compound **39**

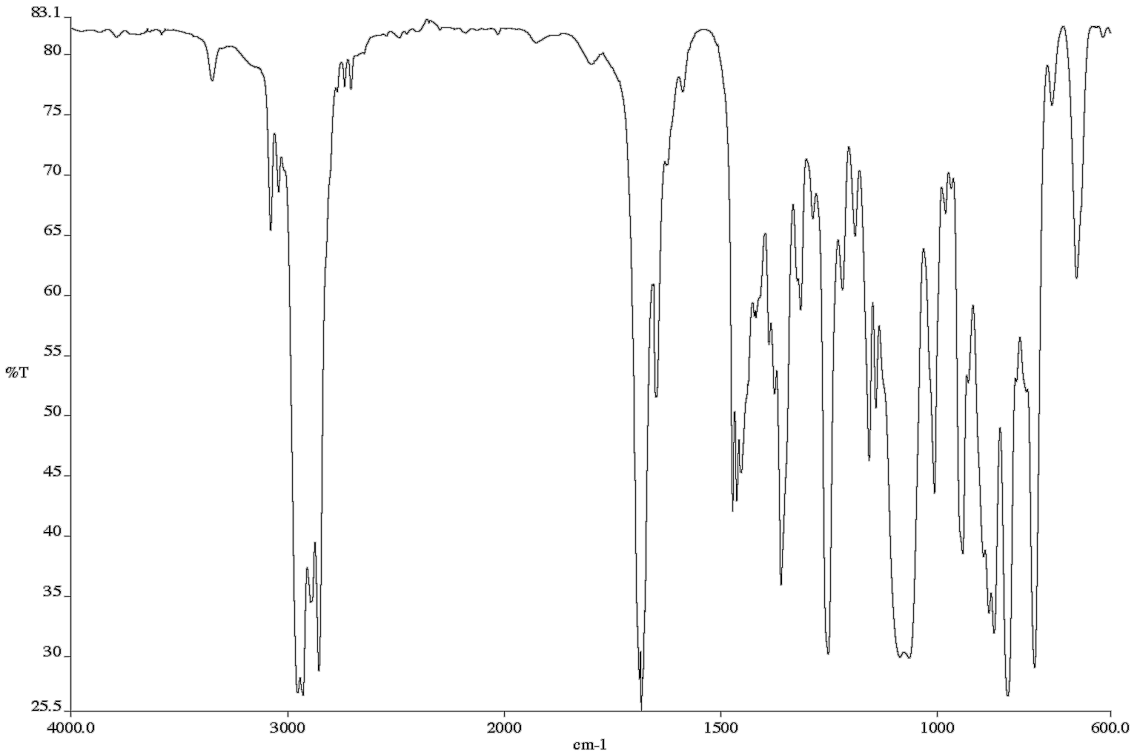

Figure A2.20 Infrared spectrum (Thin Film, NaCl) of compound **39**

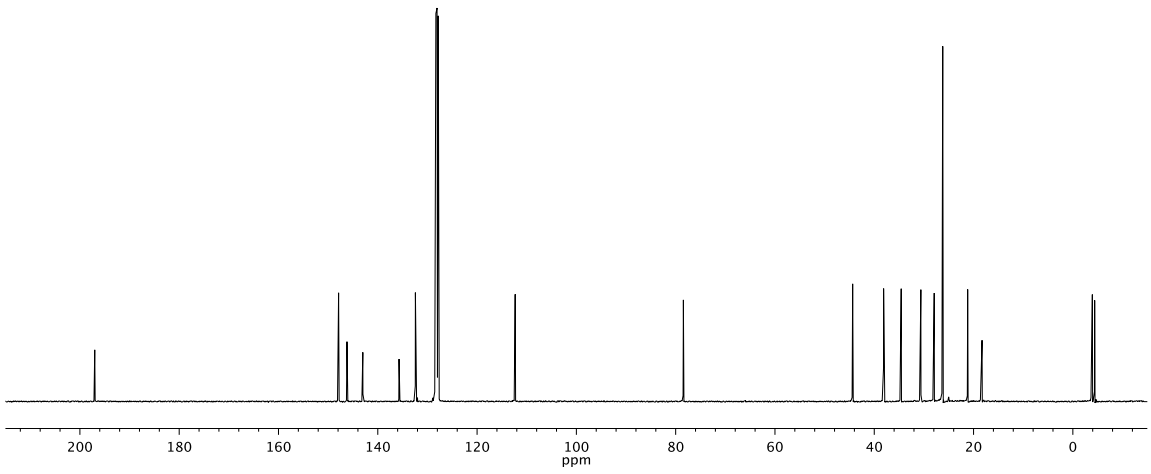

Figure A2.21 ^{13}C NMR (101 MHz, C_6D_6) of compound **39**

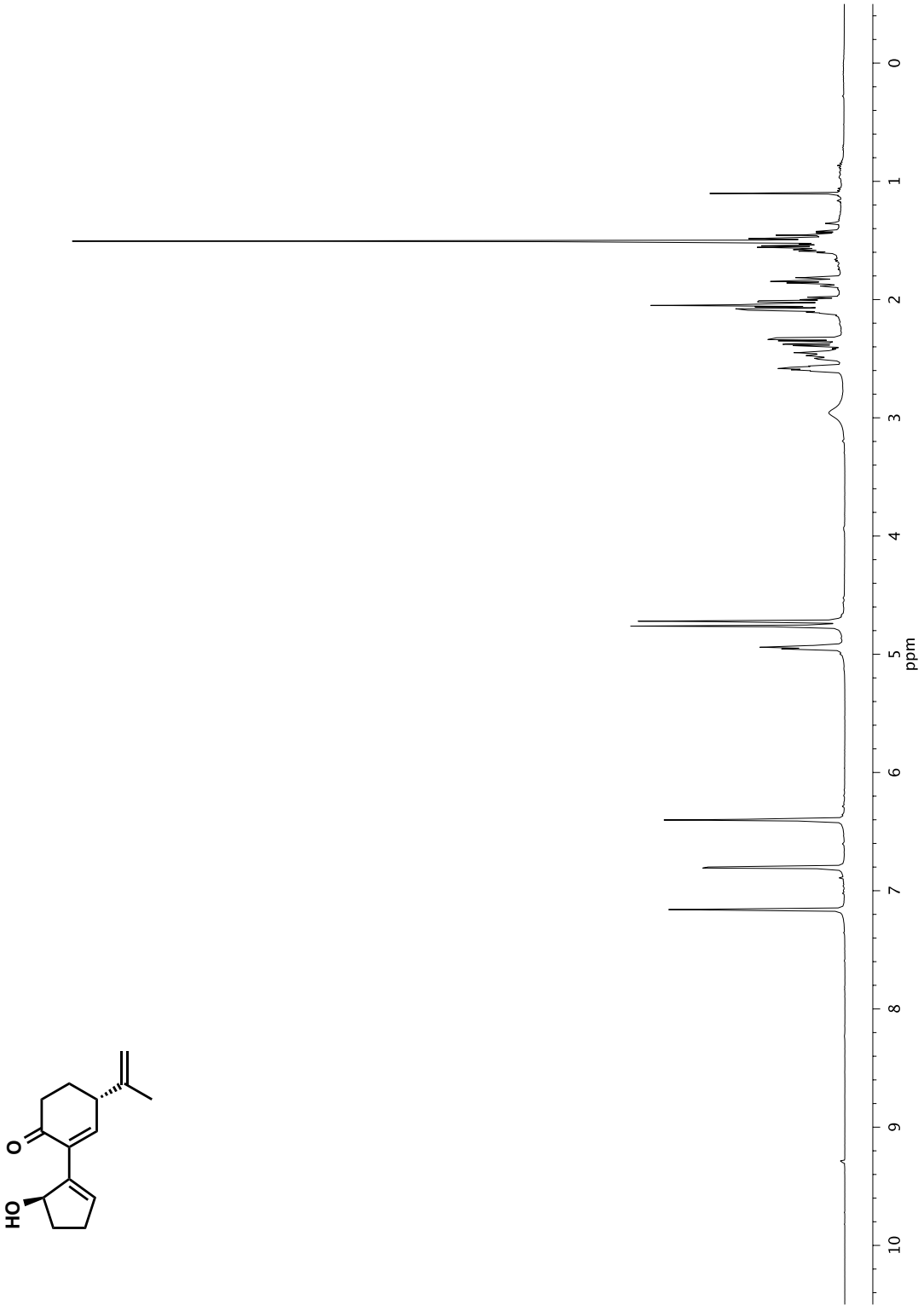

Figure A2.22 ^{1}H NMR (400 MHz, C_6D_6) of compound **88**

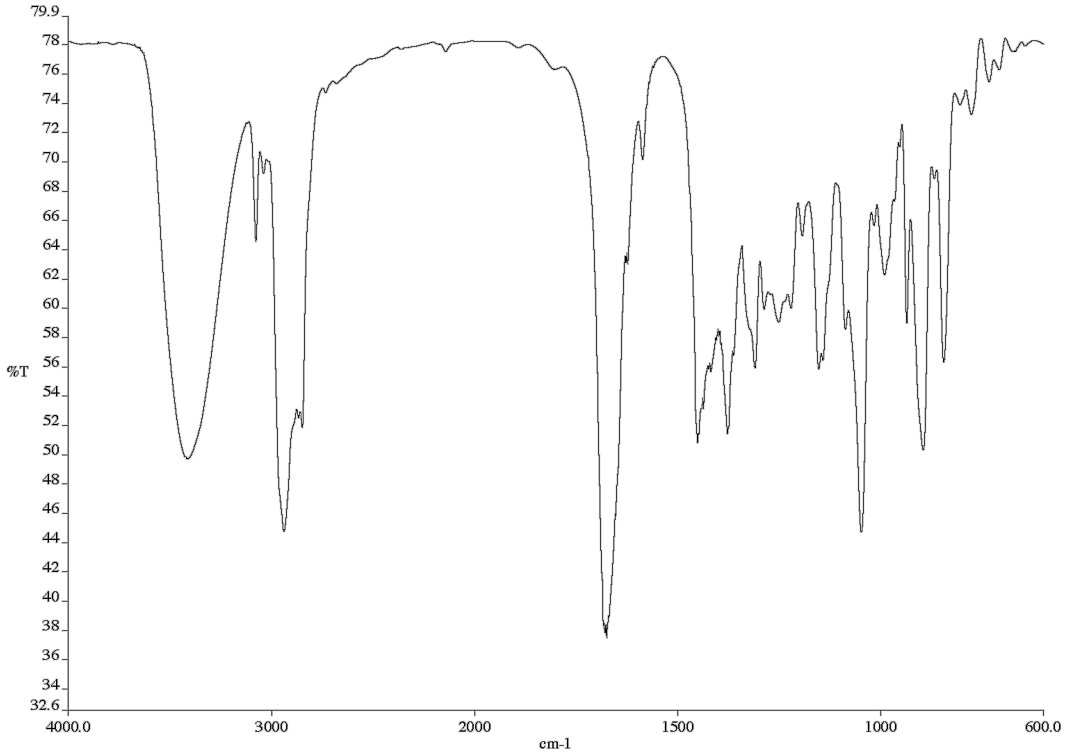

Figure A2.23 Infrared spectrum (Thin Film, NaCl) of compound **88**

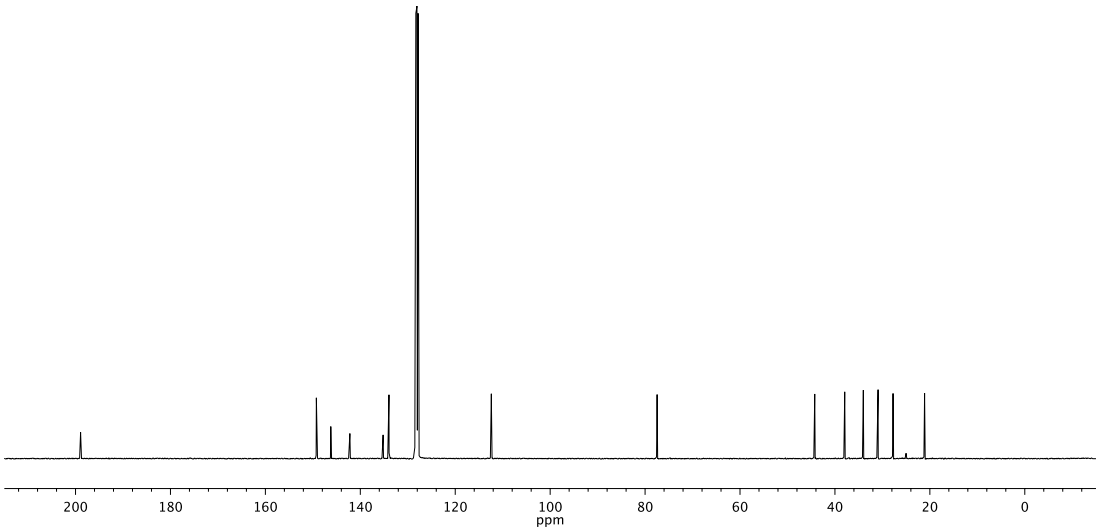

Figure A2.24 ^{13}C NMR (101 MHz, $CDCl_3$) of compound **88**

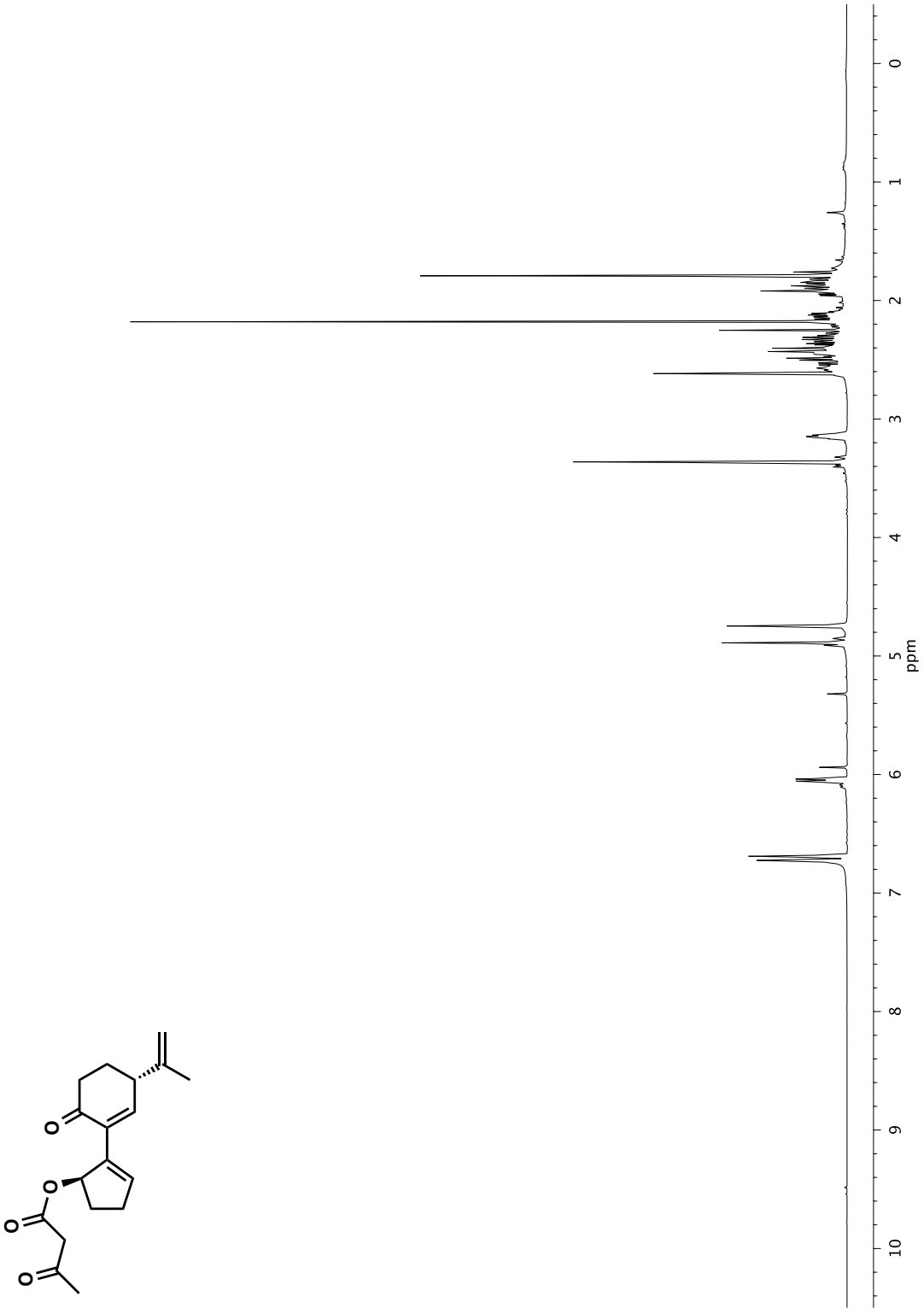

Figure A2.25 ^{1}H NMR (400 MHz, CD_2Cl_2) of compound **40**

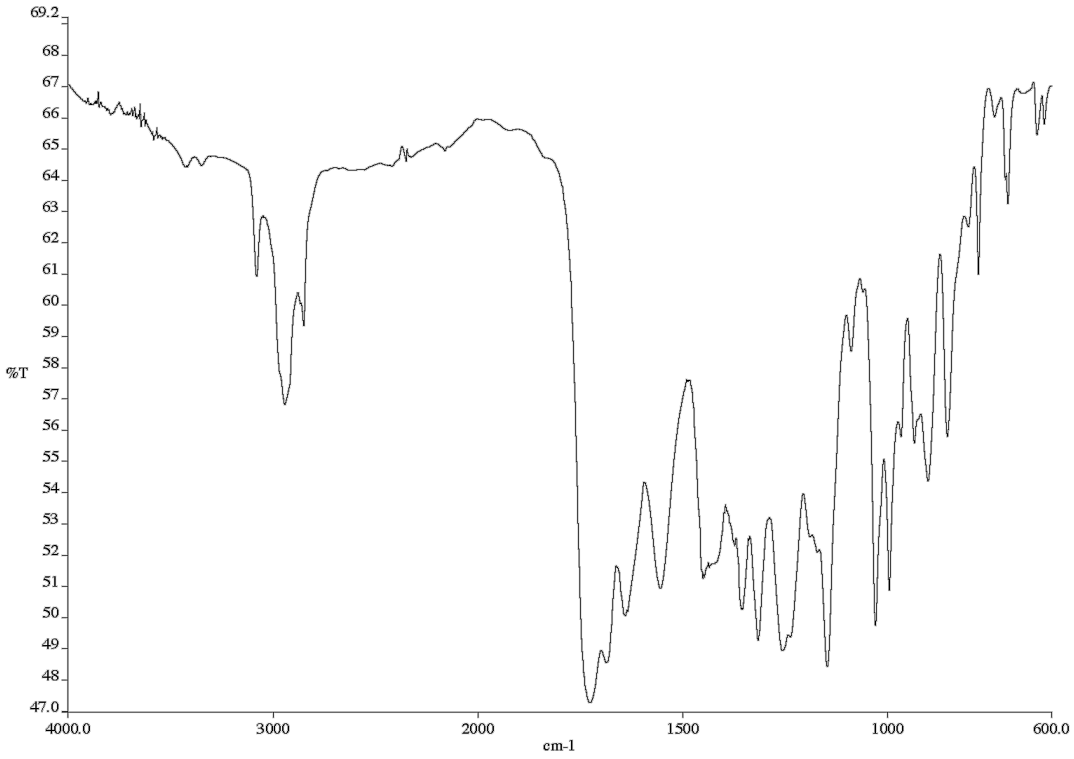

Figure A2.26 Infrared spectrum (Thin Film, NaCl) of compound **40**

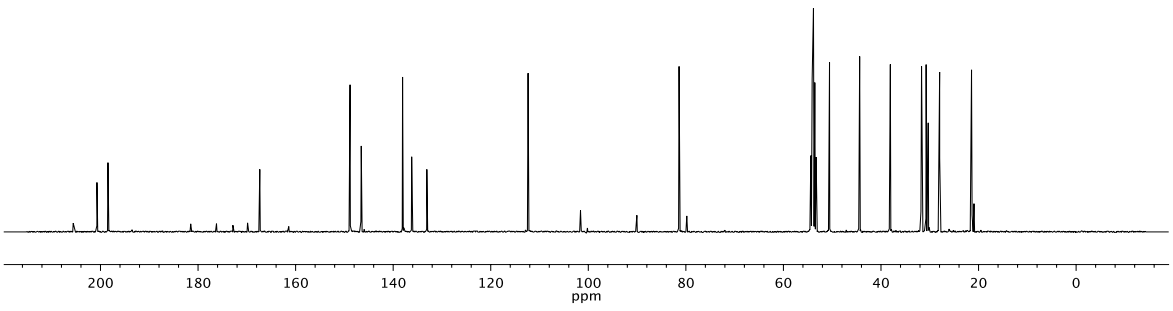

Figure A2.27 ^{13}C NMR (101 MHz, CD_2Cl_2) of compound **40**

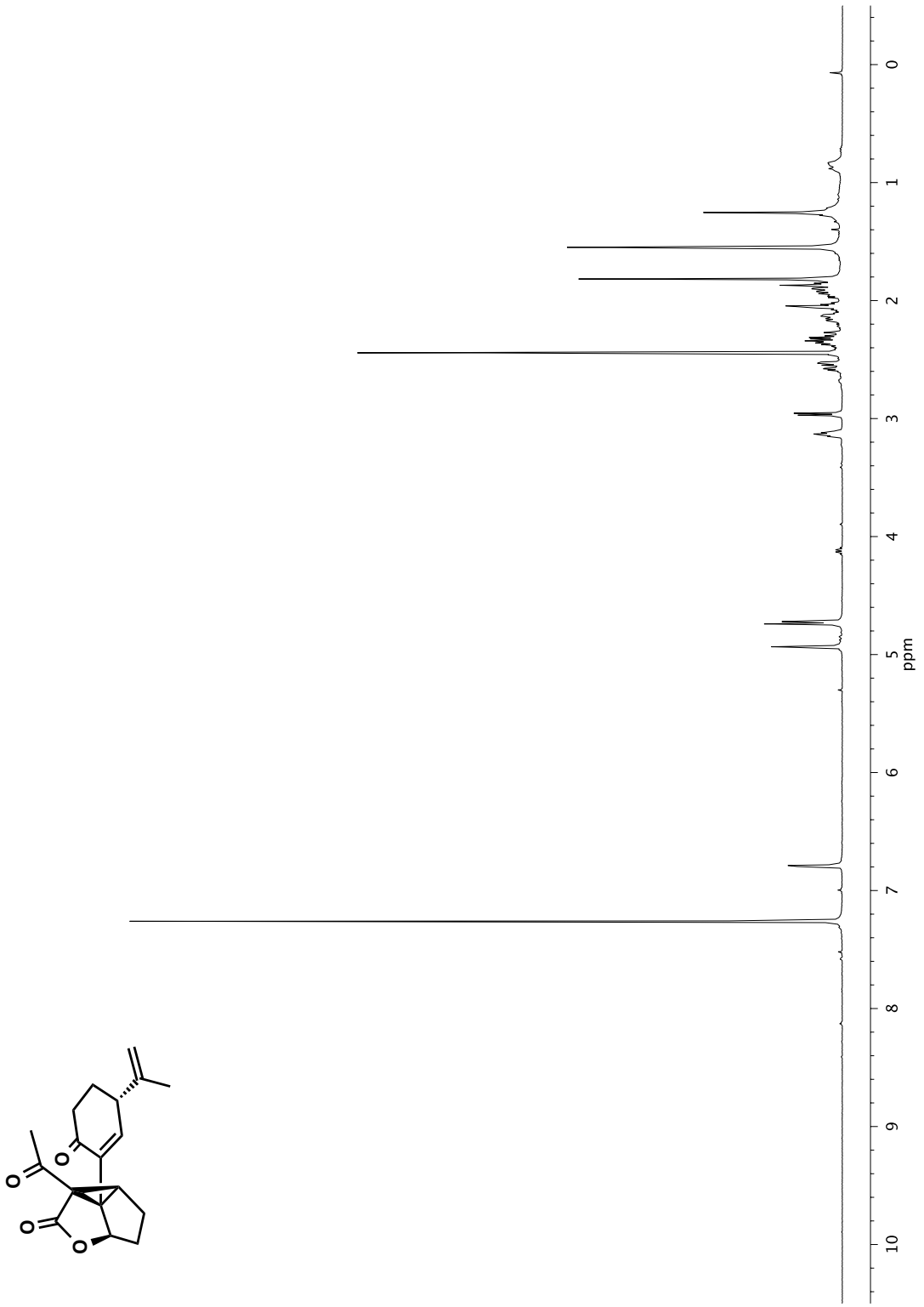

Figure A2.28 ^{1}H NMR (400 MHz, $CDCl_3$) of compound **41**

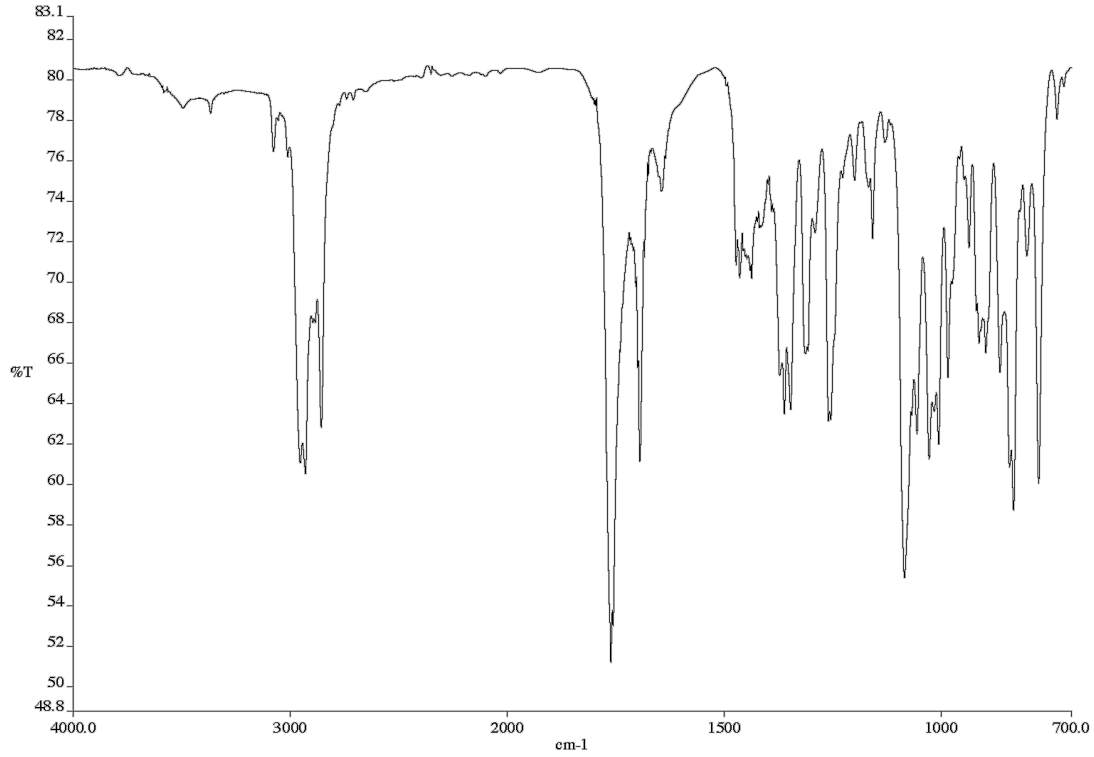

Figure A2.29 Infrared spectrum (Thin Film, NaCl) of compound **41**

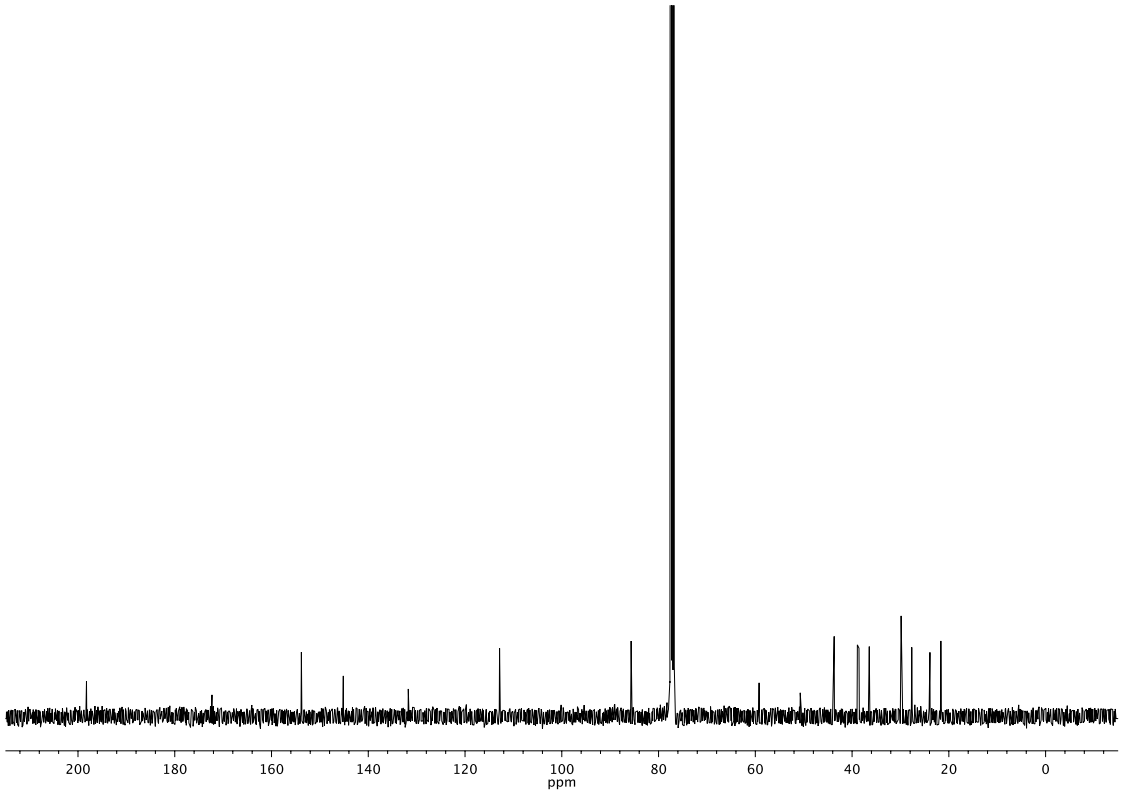

Figure A2.30 ^{13}C NMR (101 MHz, $CDCl_3$) of compound **41**

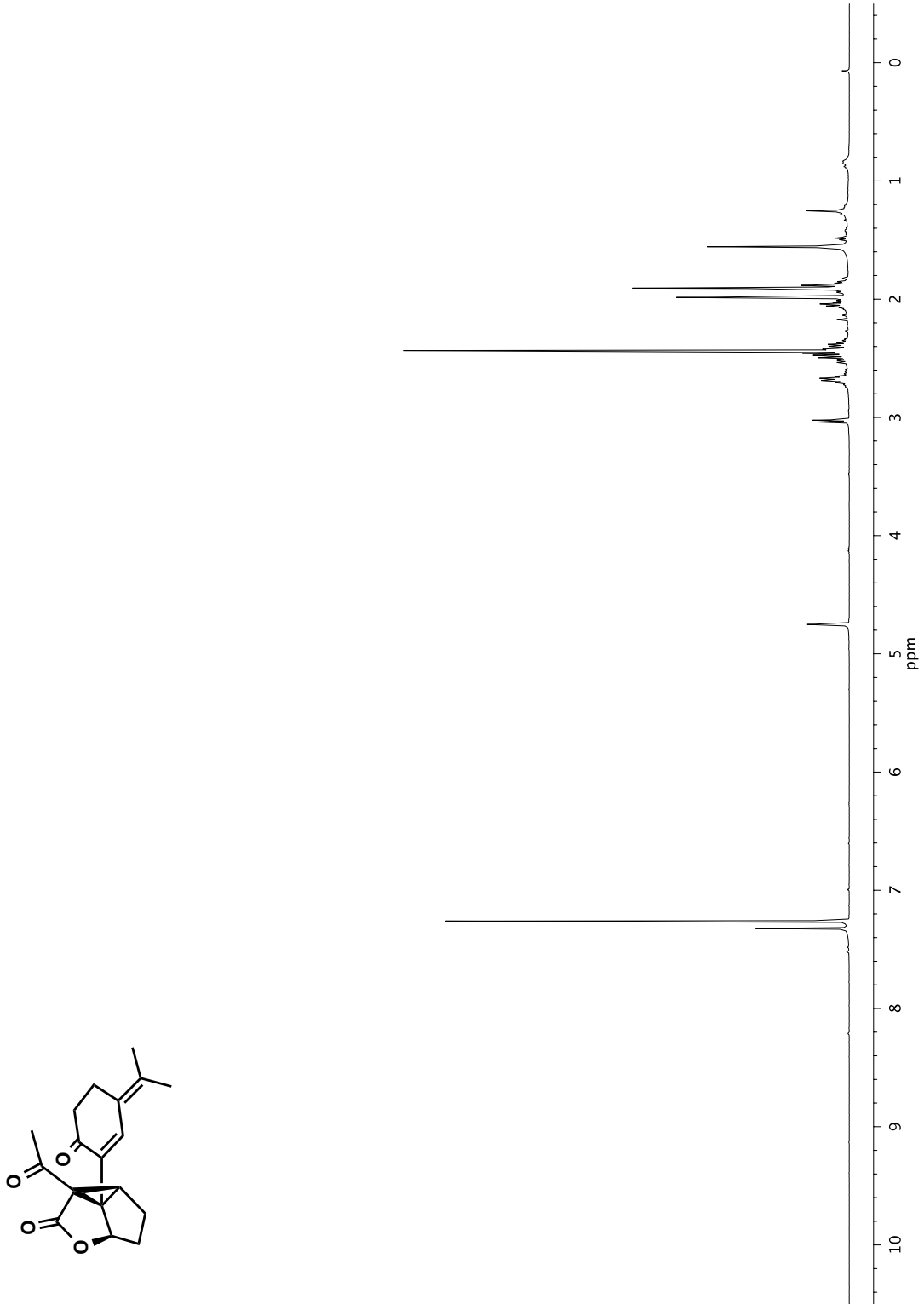

Figure A2.31 ^{1}H NMR (400 MHz, $CDCl_3$) of compound **42**

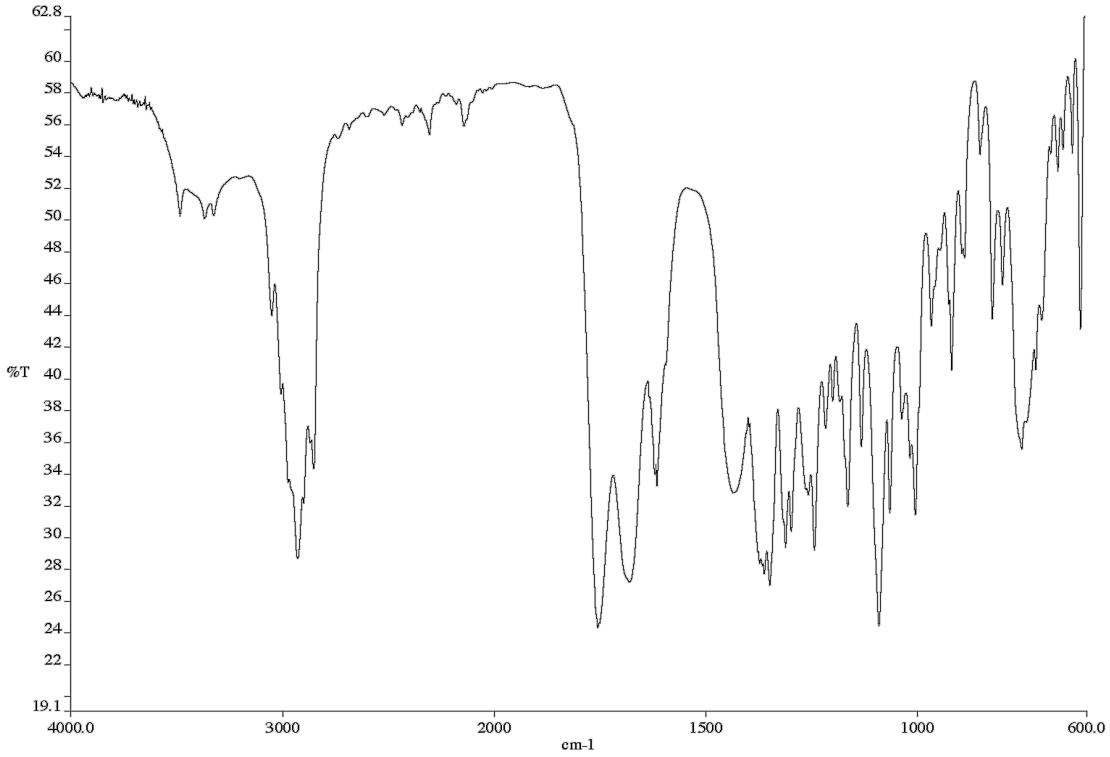

Figure A2.32 Infrared spectrum (Thin Film, NaCl) of compound **42**

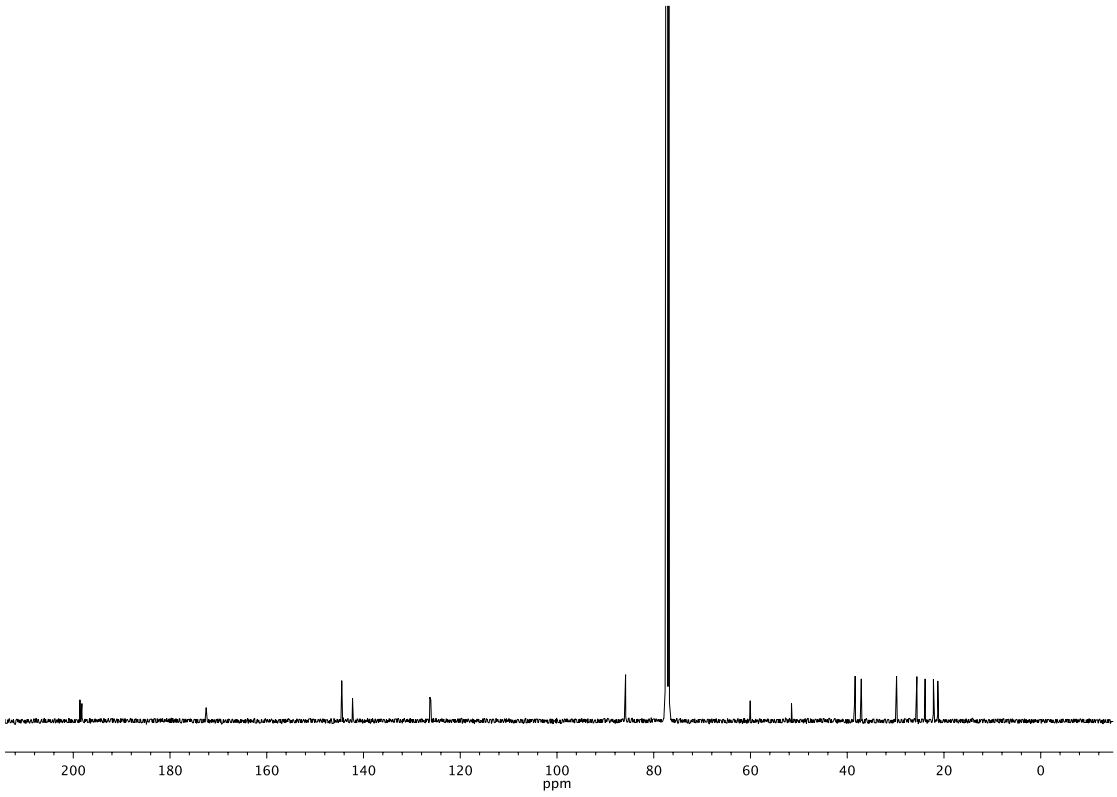

Figure A2.33 ^{13}C NMR (101 MHz, $CDCl_3$) of compound **42**

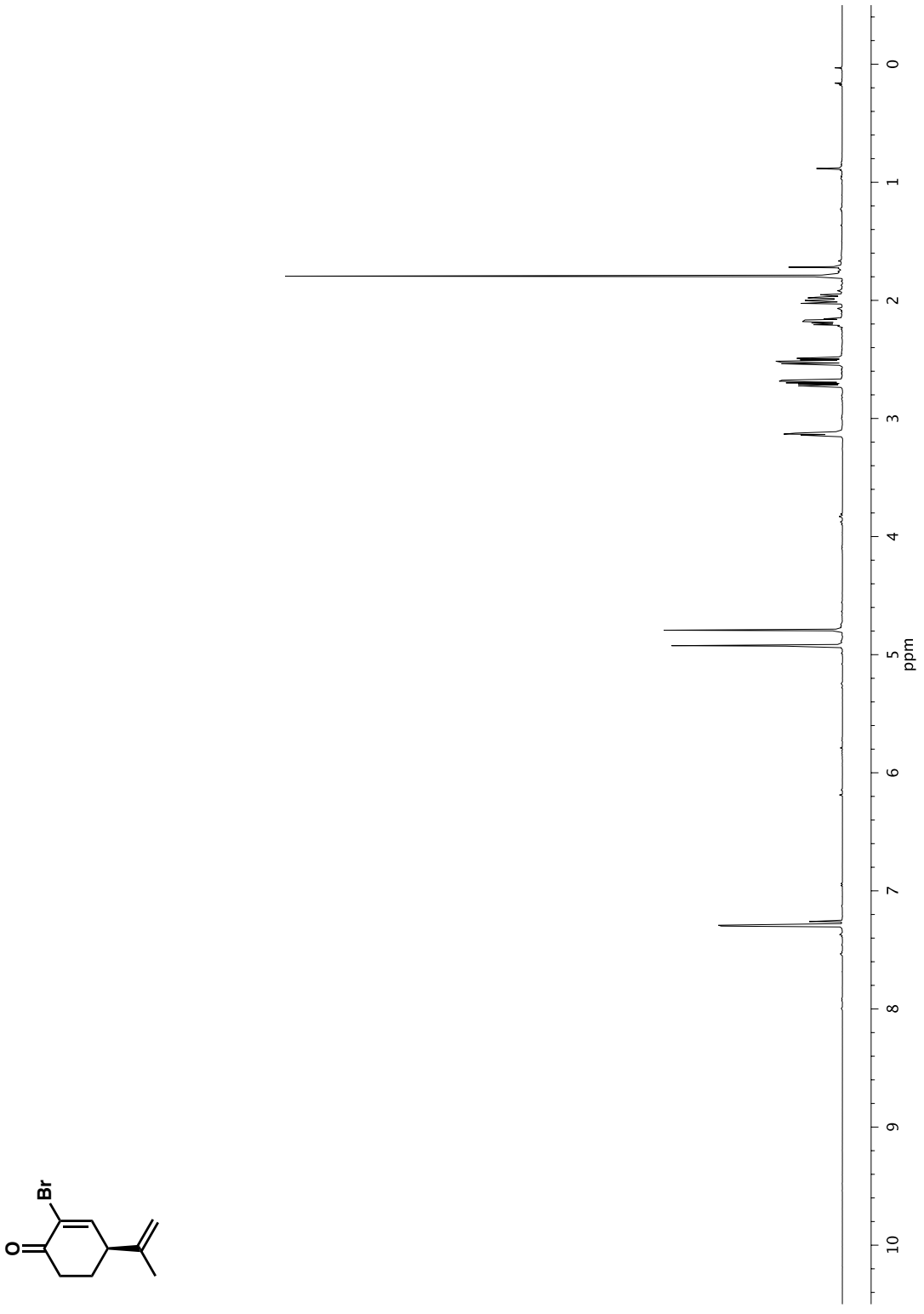

Figure A2.34 ^{1}H NMR (500 MHz, $CDCl_3$) of compound **43**

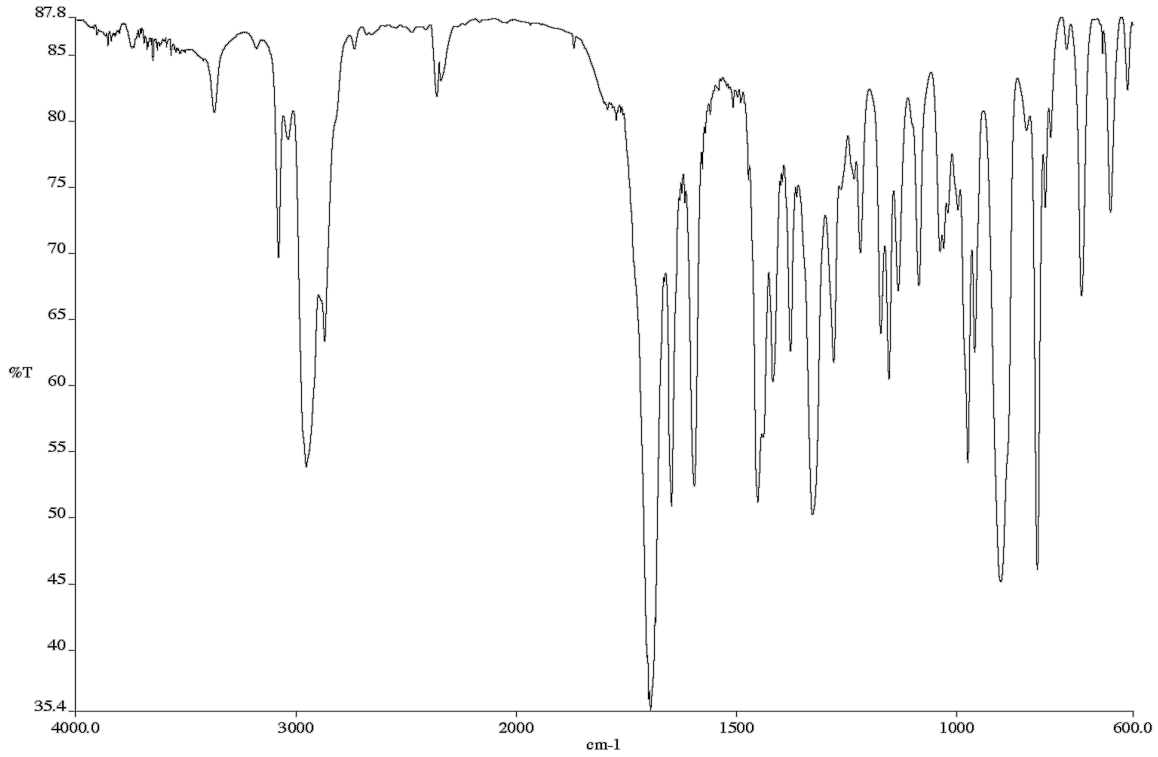

Figure A2.35 Infrared spectrum (Thin Film, NaCl) of compound **43**

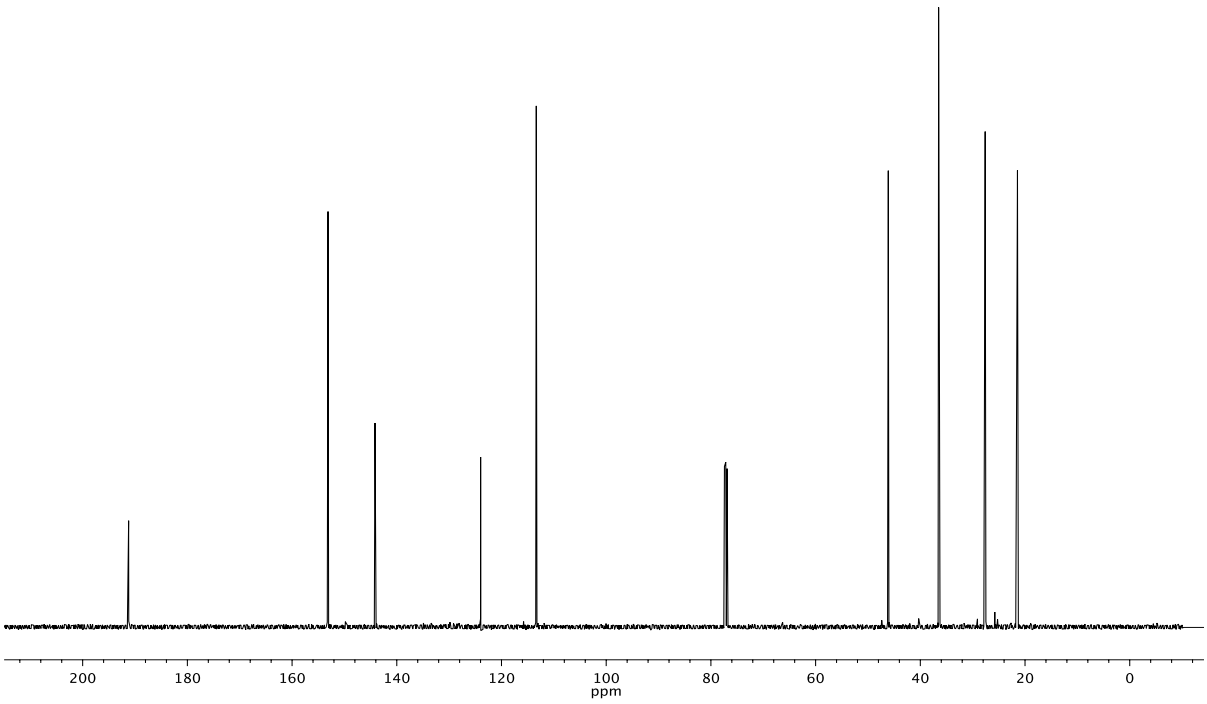

Figure A2.36 ^{13}C NMR (126 MHz, $CDCl_3$) of compound **43**

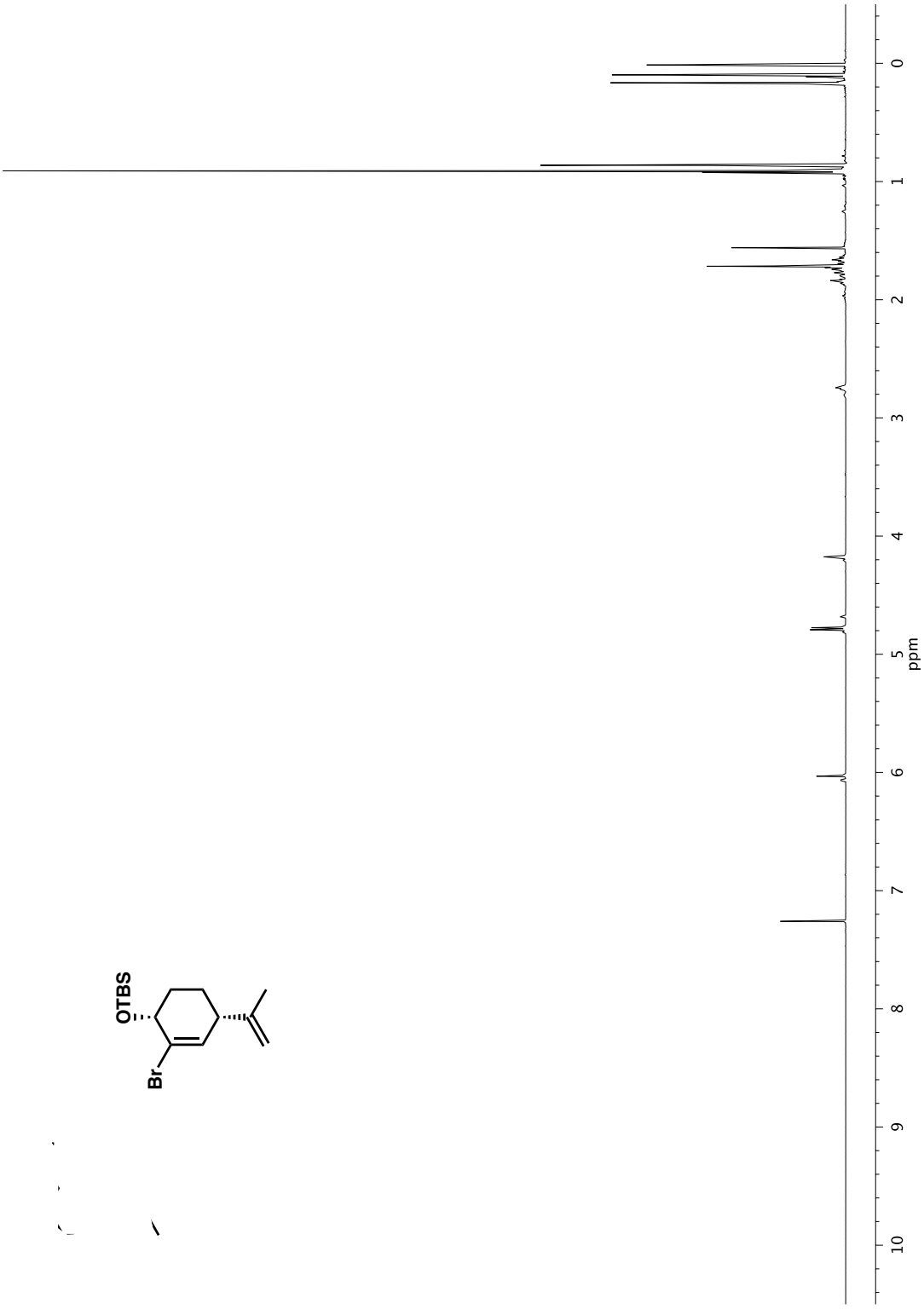

Figure A2.37 ^{1}H NMR (500 MHz, $CDCl_3$) of compound **21**

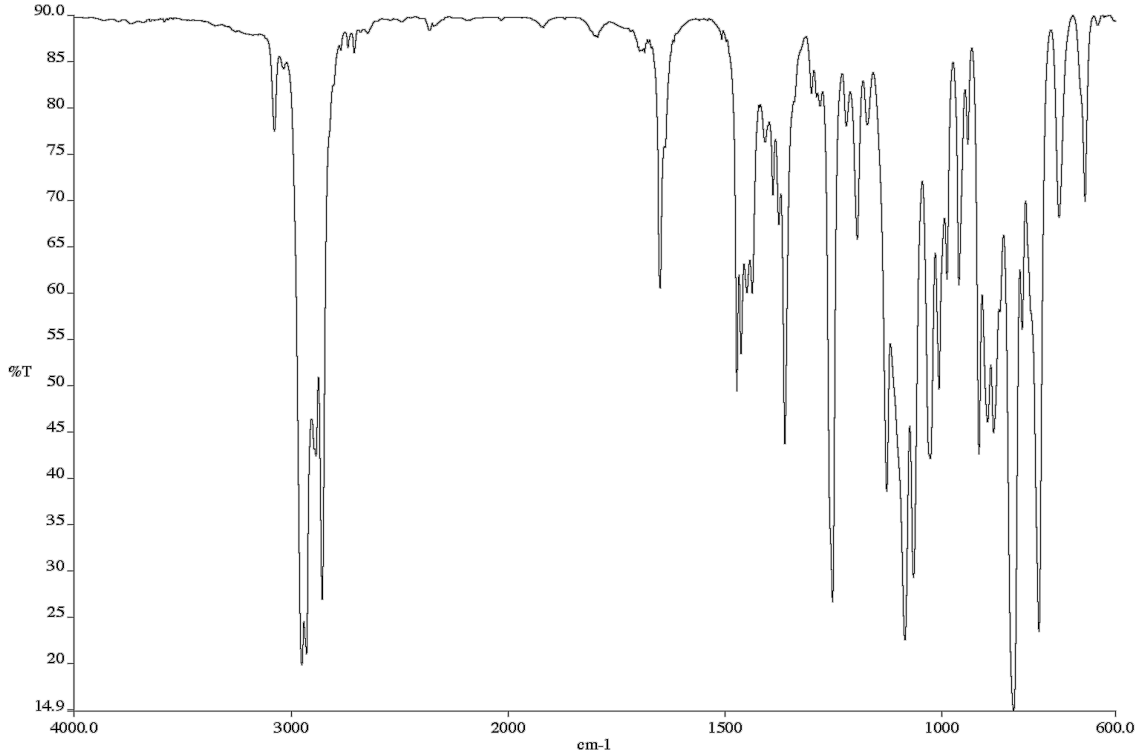

Figure A2.38 Infrared spectrum (Thin Film, NaCl) of compound **21**

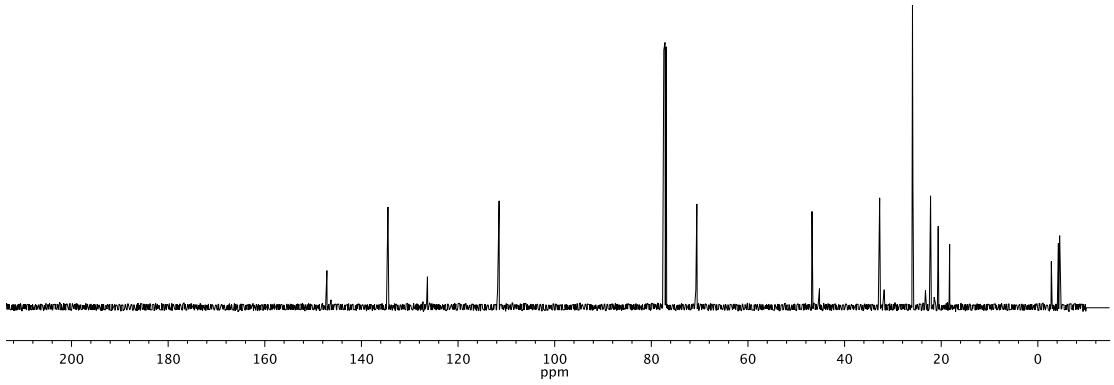

Figure A2.39 ^{13}C NMR (126 MHz, $CDCl_3$) of compound **21**

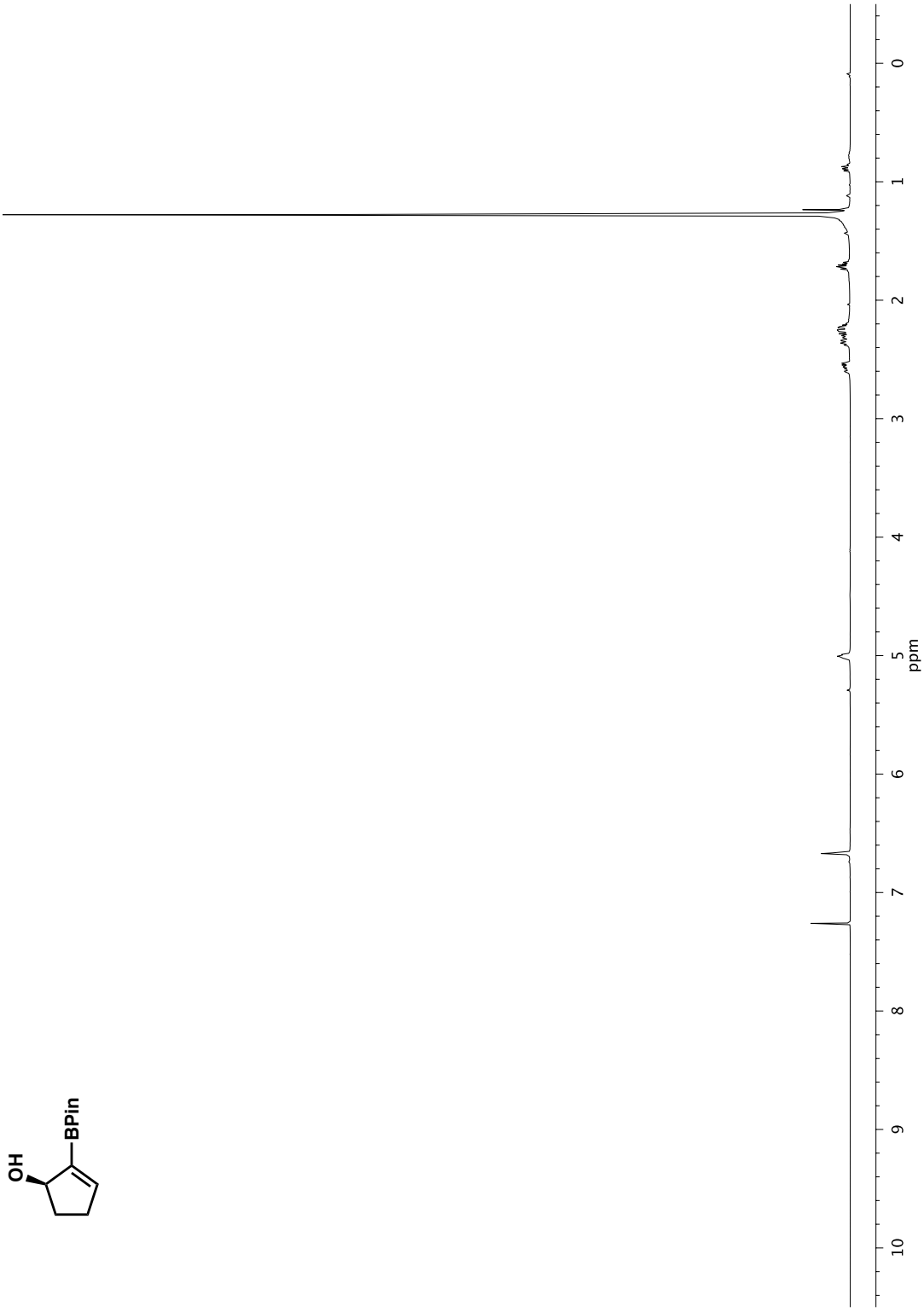

Figure A2.40 ^{1}H NMR (500 MHz, $CDCl_3$) of compound **44**

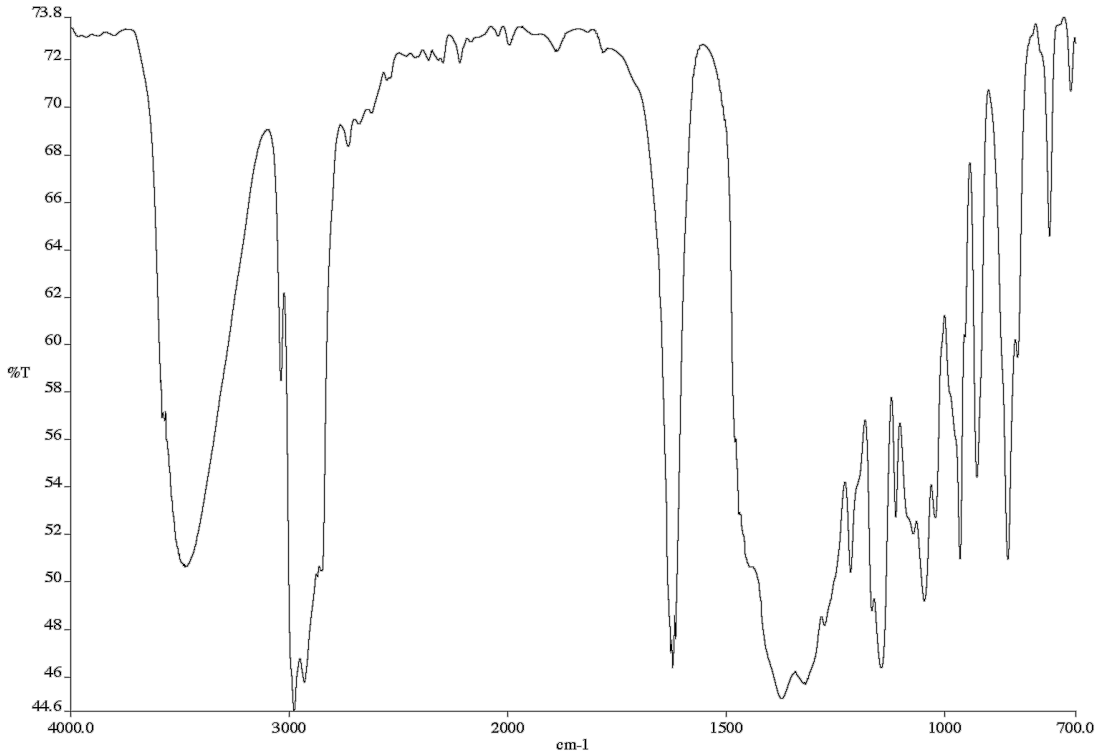

Figure A2.41 Infrared spectrum (Thin Film, NaCl) of compound **44**

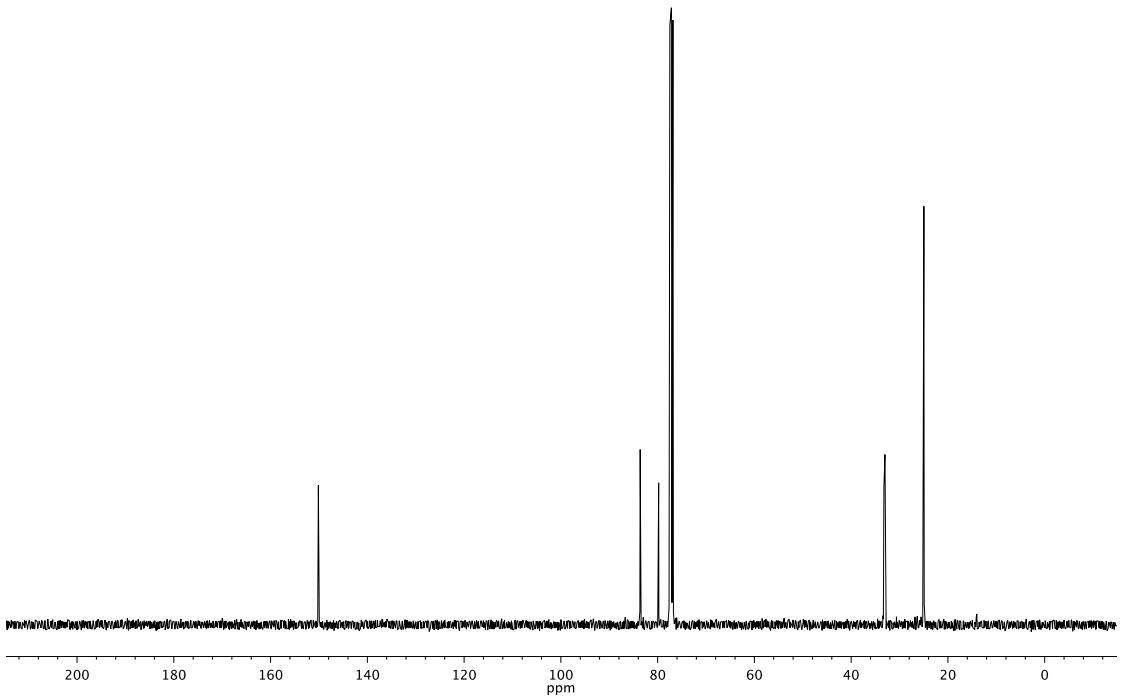

Figure A2.42 ^{13}C NMR (126 MHz, $CDCl_3$) of compound **44**

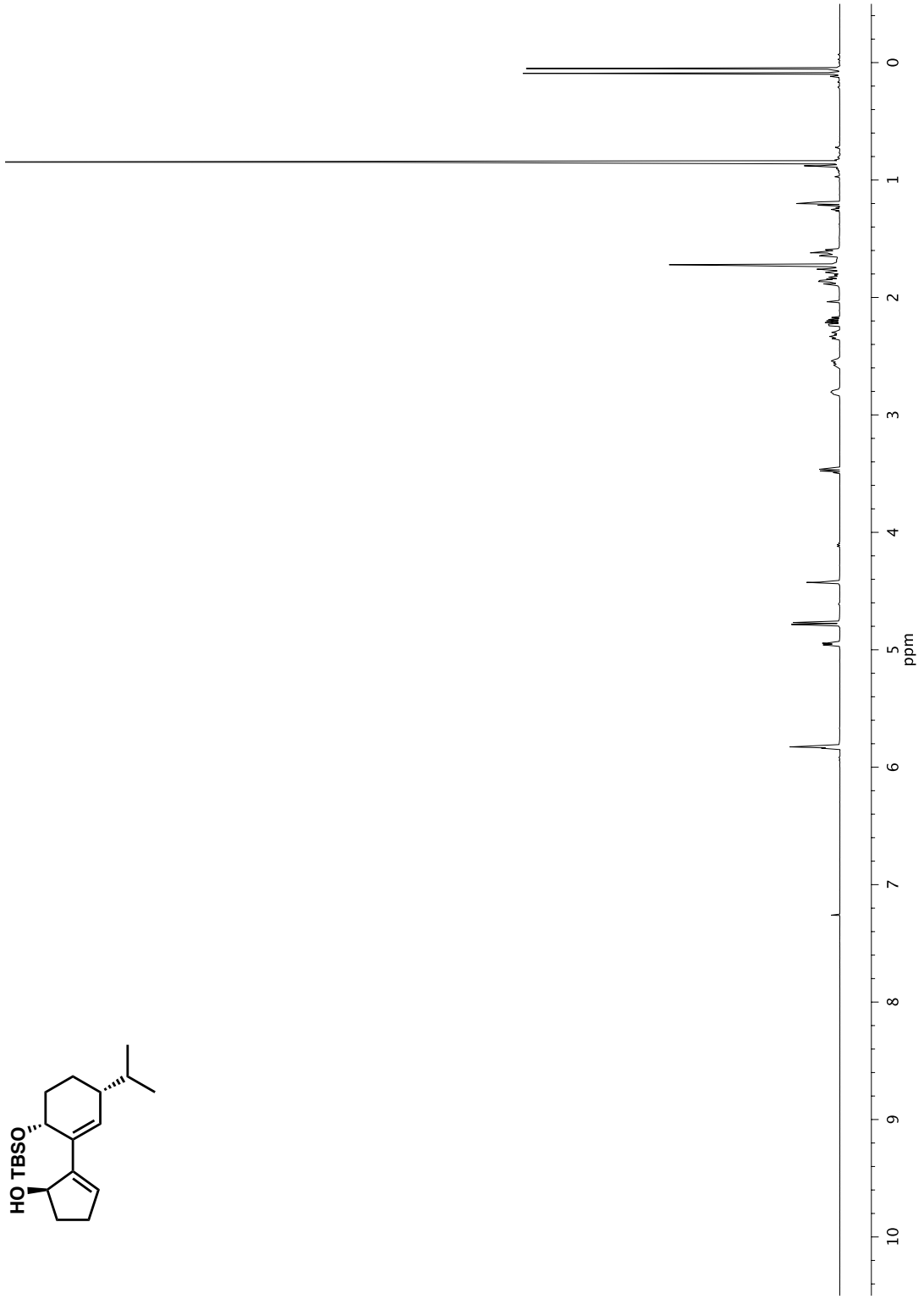

Figure A2.43 ^{1}H NMR (500 MHz, $CDCl_3$) of compound **19**

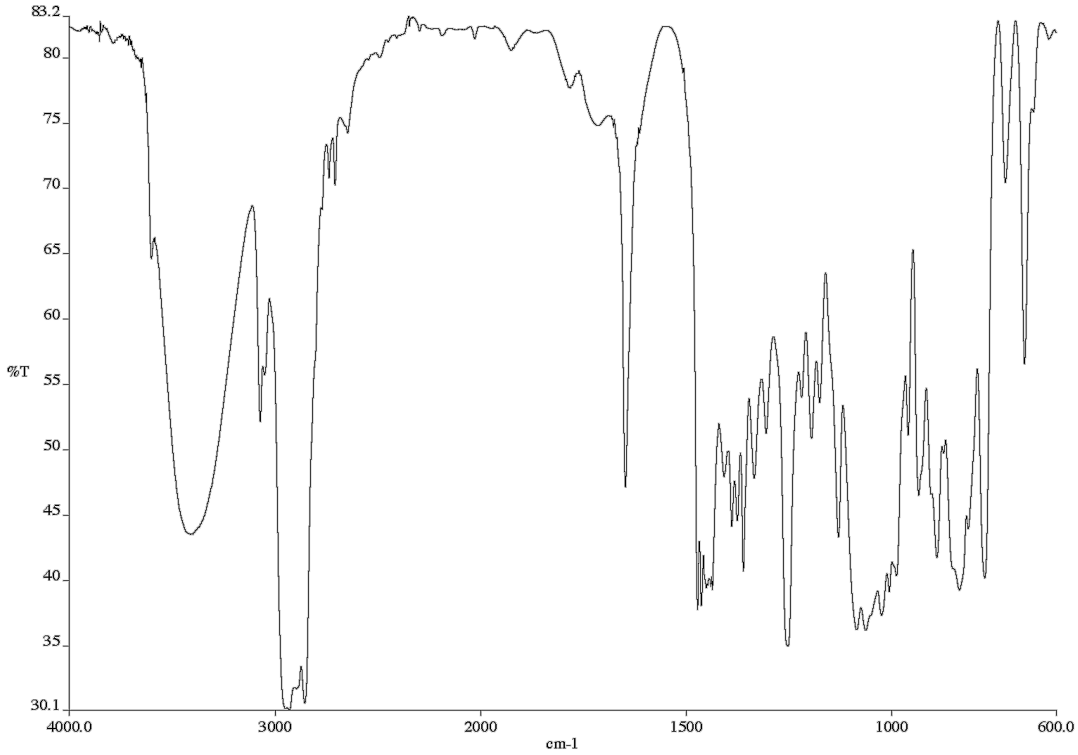

Figure A2.44 Infrared spectrum (Thin Film, NaCl) of compound **19**

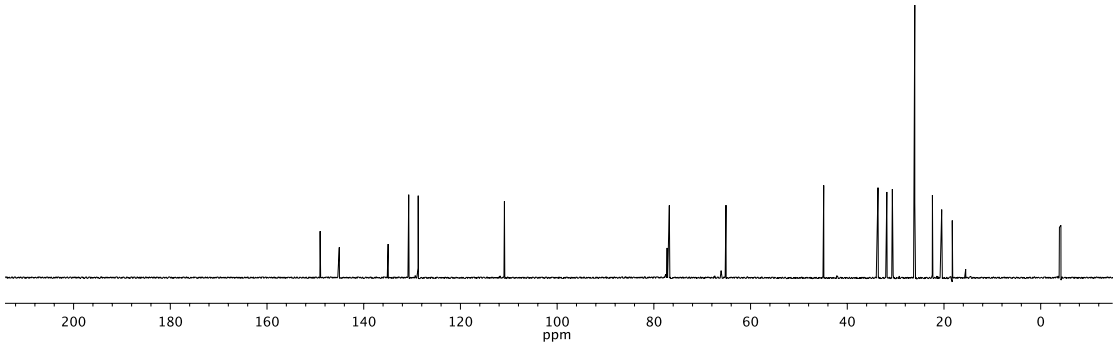

Figure A2.45 ^{13}C NMR (126 MHz, $CDCl_3$) of compound **19**

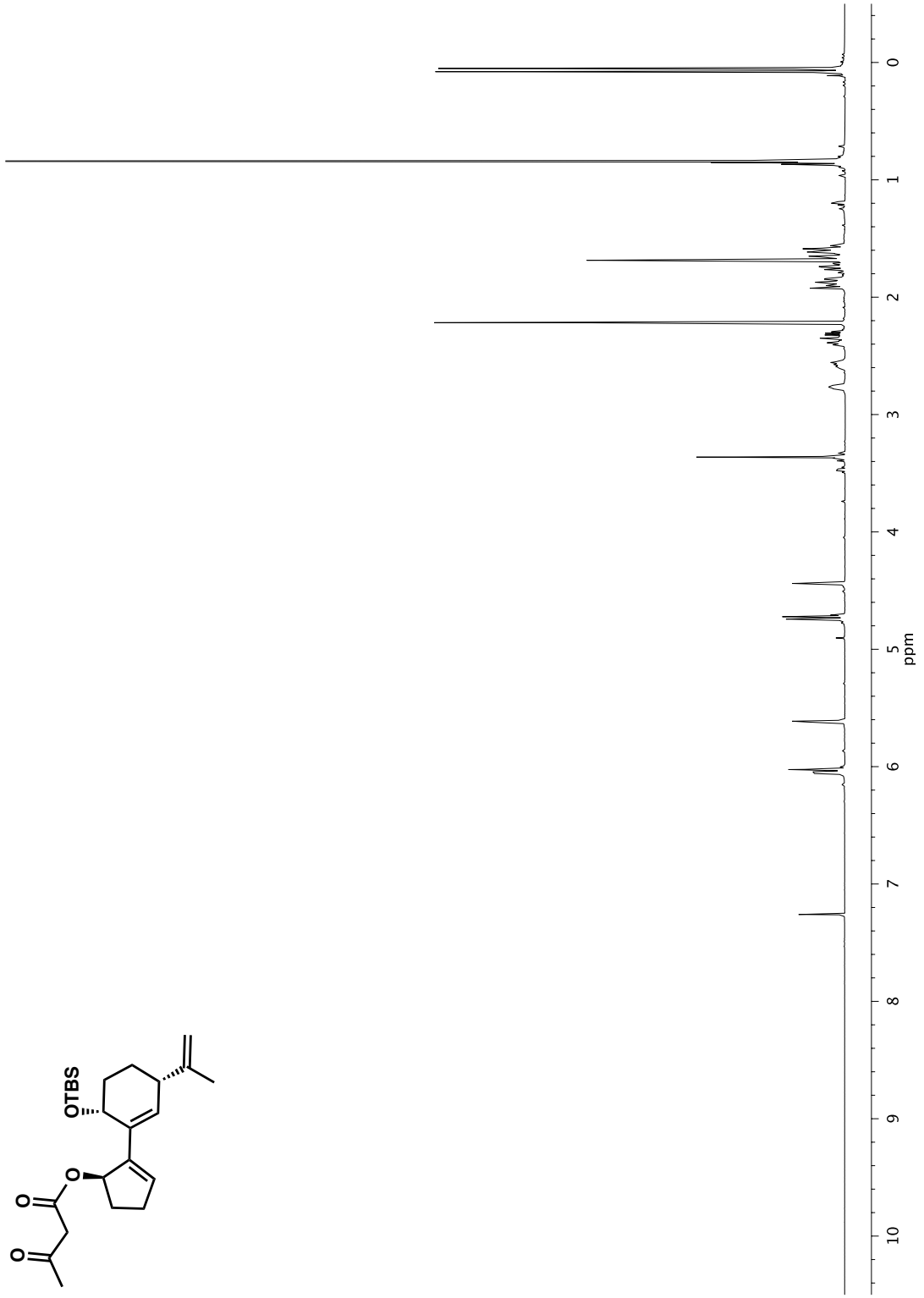

Figure A2.46 ^{1}H NMR (500 MHz, $CDCl_3$) of compound **45**

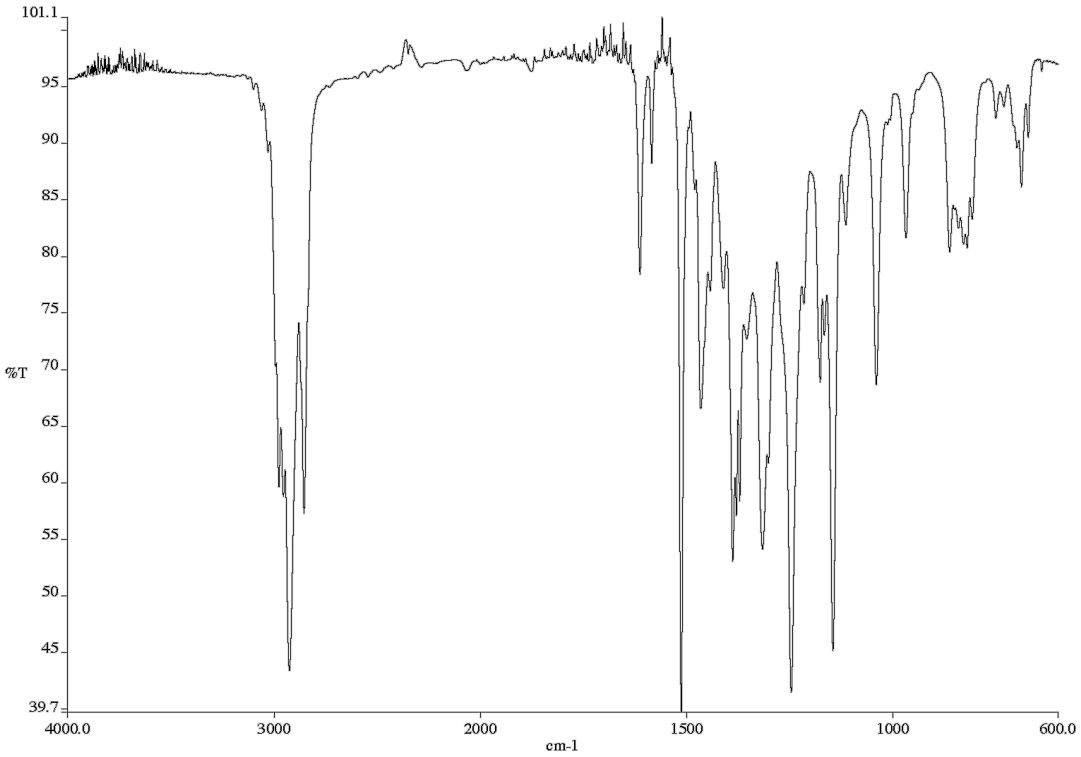

Figure A2.47 Infrared spectrum (Thin Film, NaCl) of compound **45**

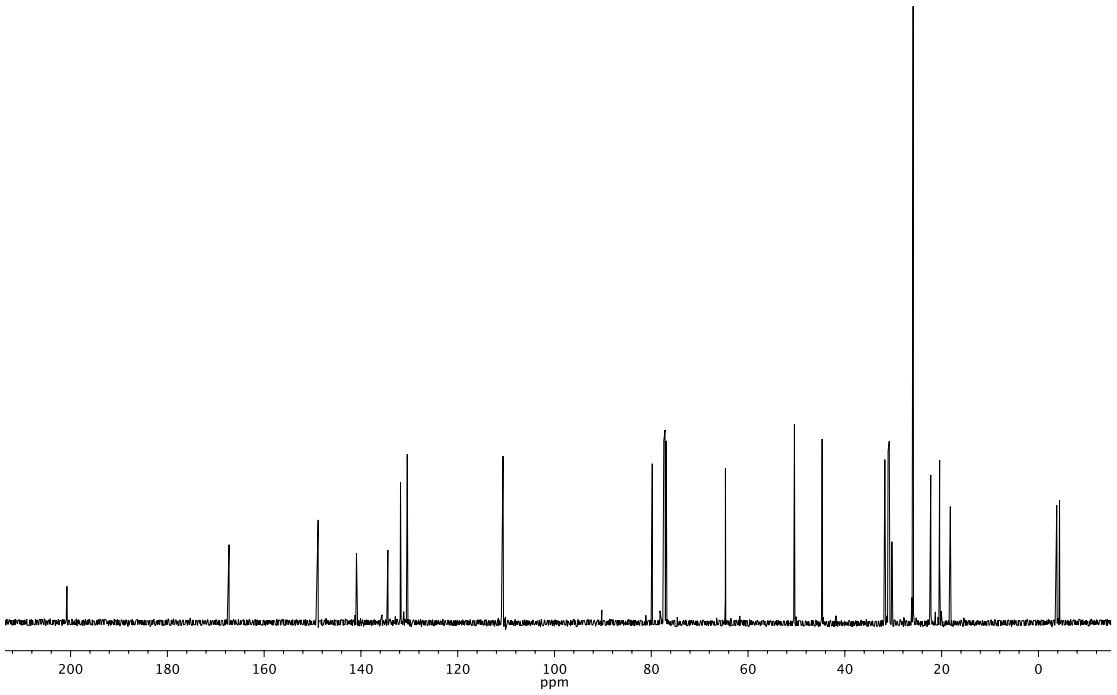

Figure A2.48 ^{13}C NMR (126 MHz, $CDCl_3$) of compound **45**

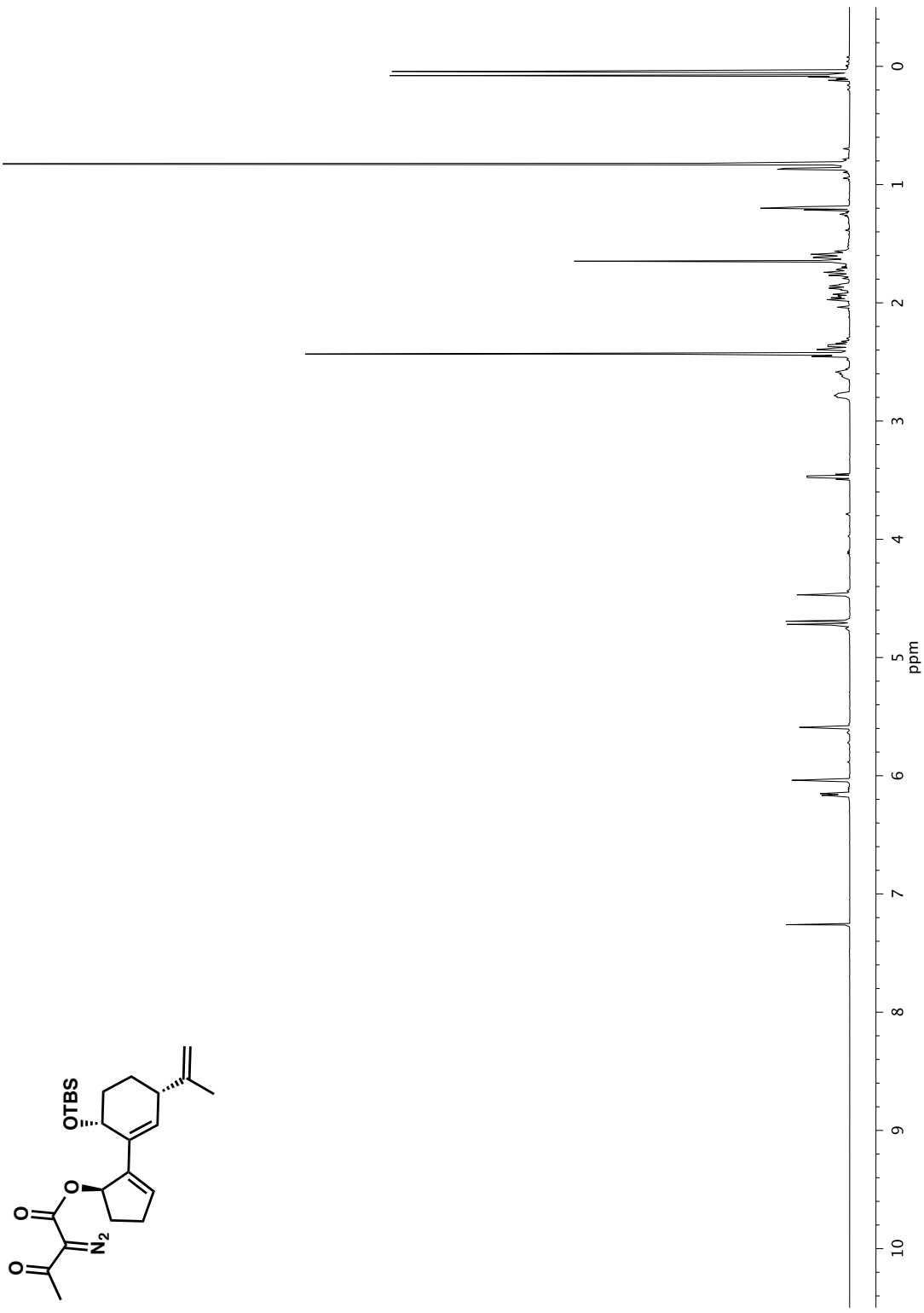

Figure A2.49 ^{1}H NMR (500 MHz, $CDCl_3$) of compound **18**

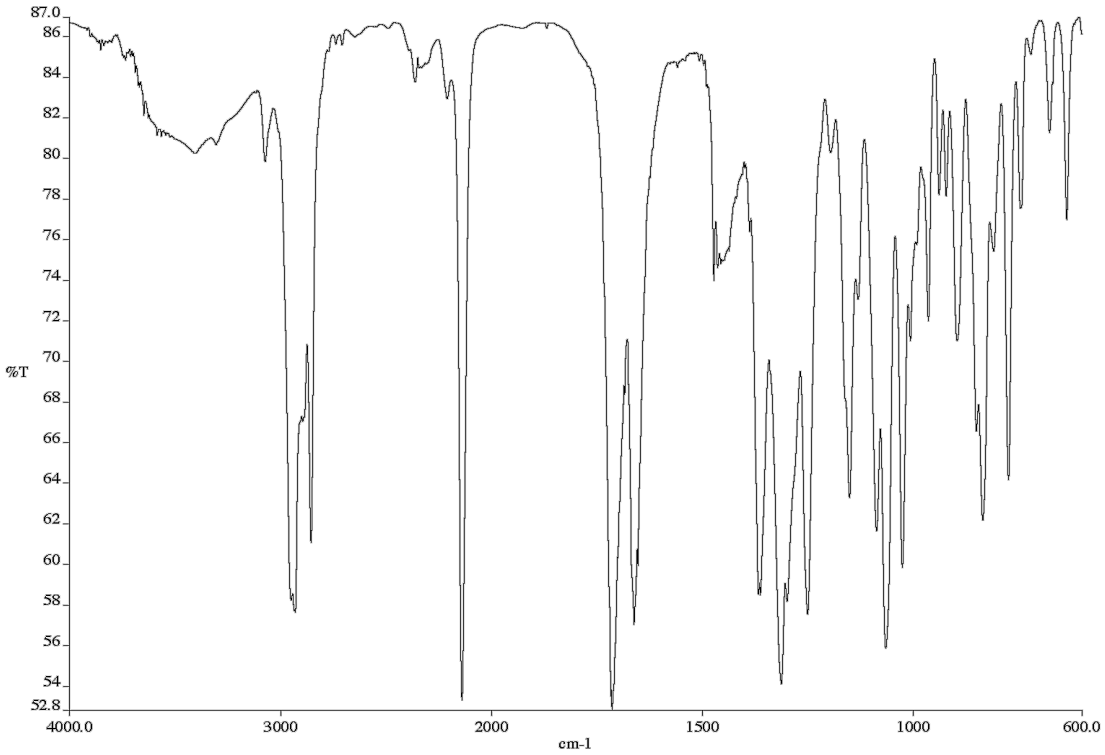

Figure A2.50 Infrared spectrum (Thin Film, NaCl) of compound **18**

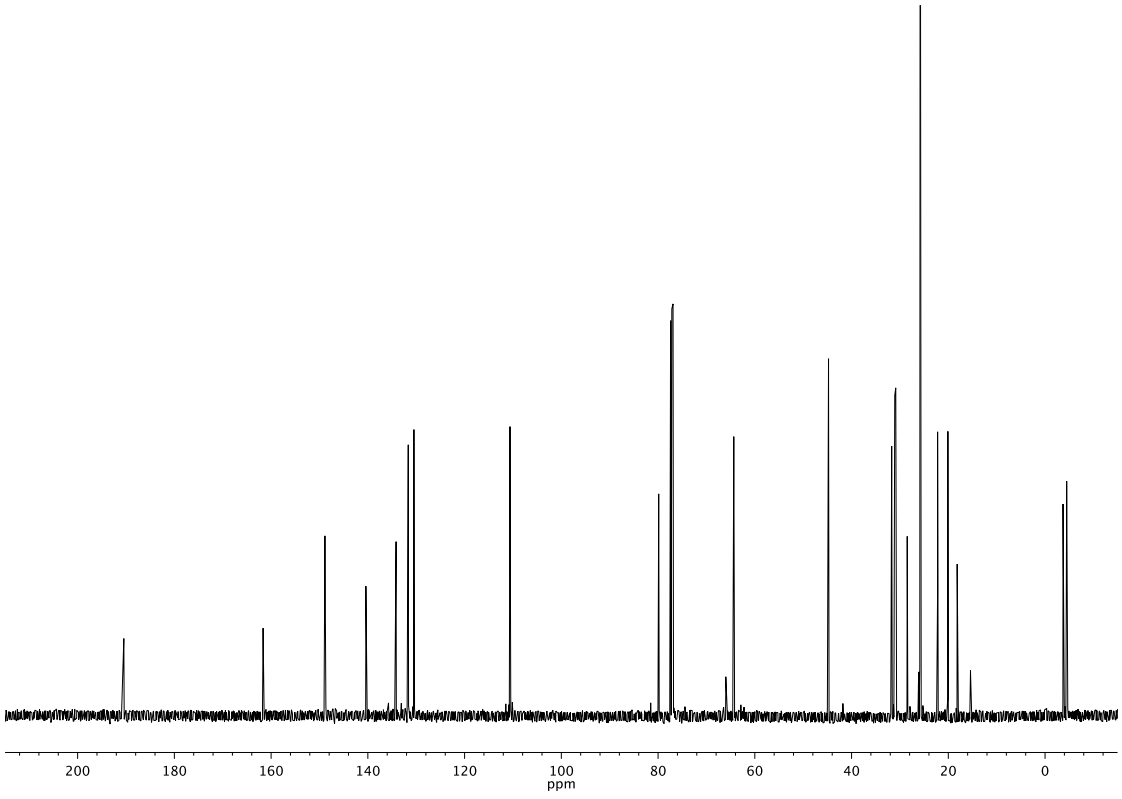

Figure A2.51 ^{13}C NMR (126 MHz, $CDCl_3$) of compound **18**

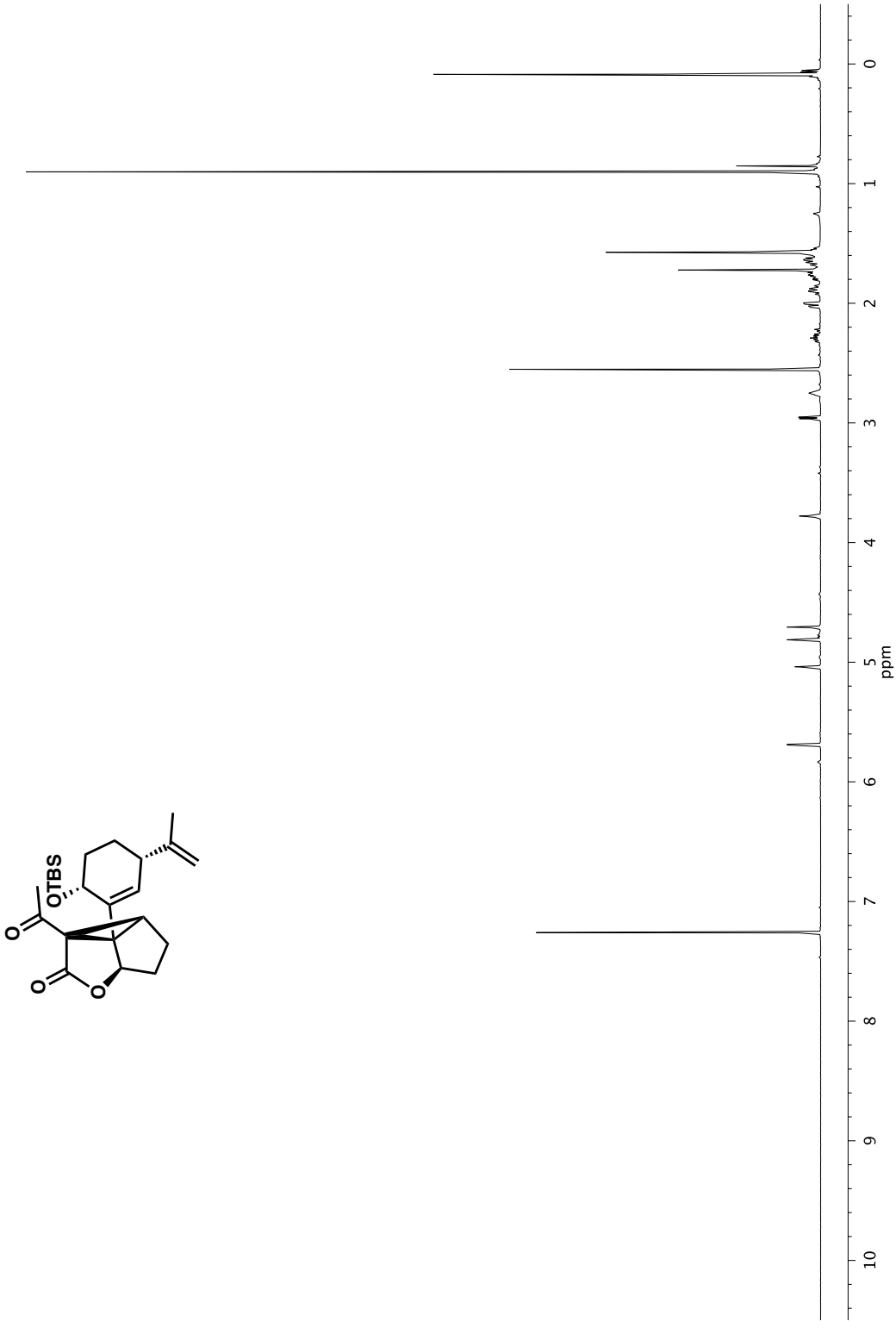

Figure A2.52 ^{1}H NMR (500 MHz, $CDCl_3$) of compound **46**

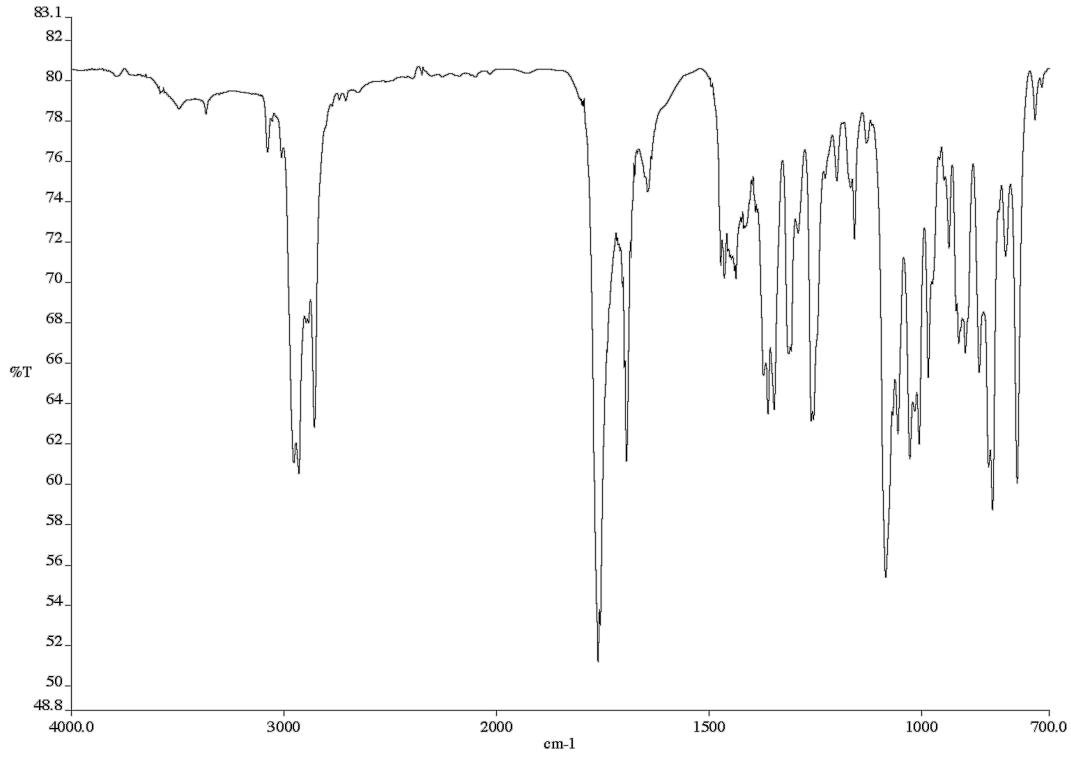

Figure A2.53 Infrared spectrum (Thin Film, NaCl) of compound **46**

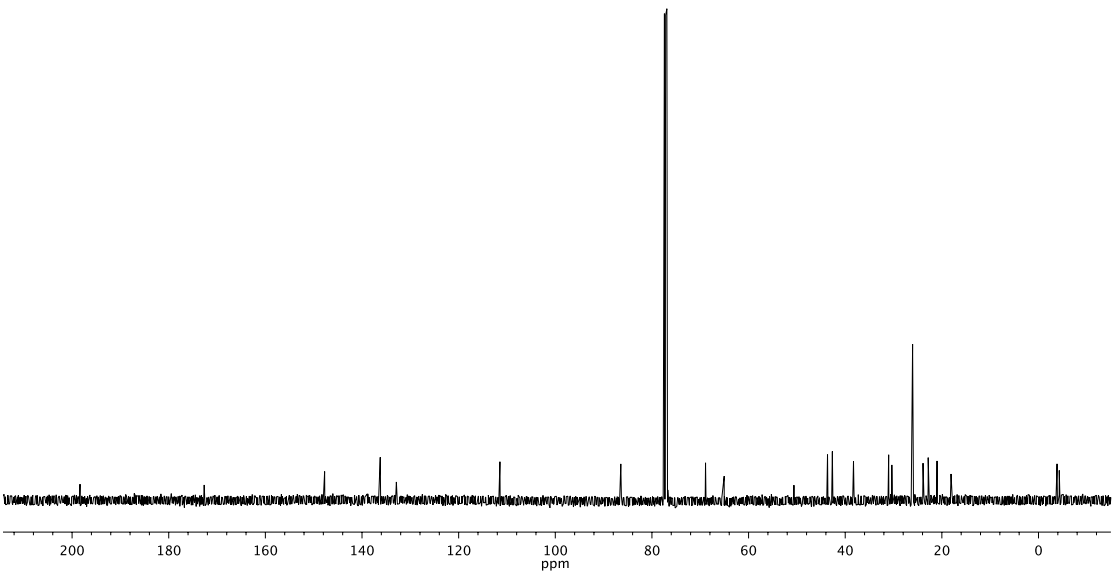

Figure A2.54 ^{13}C NMR (126 MHz, $CDCl_3$) of compound **46**

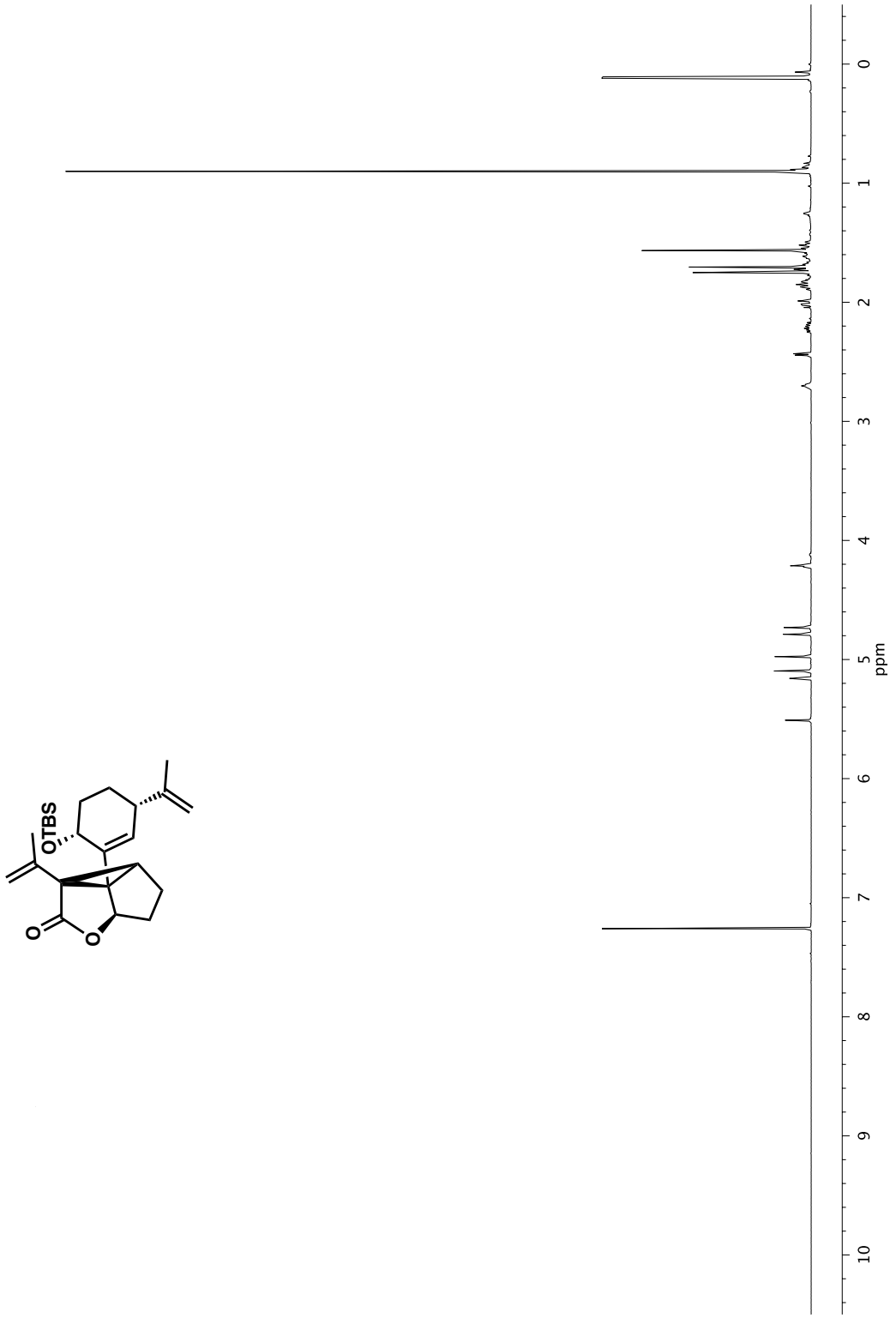

Figure A2.55 ^{1}H NMR (500 MHz, $CDCl_3$) of compound **47**

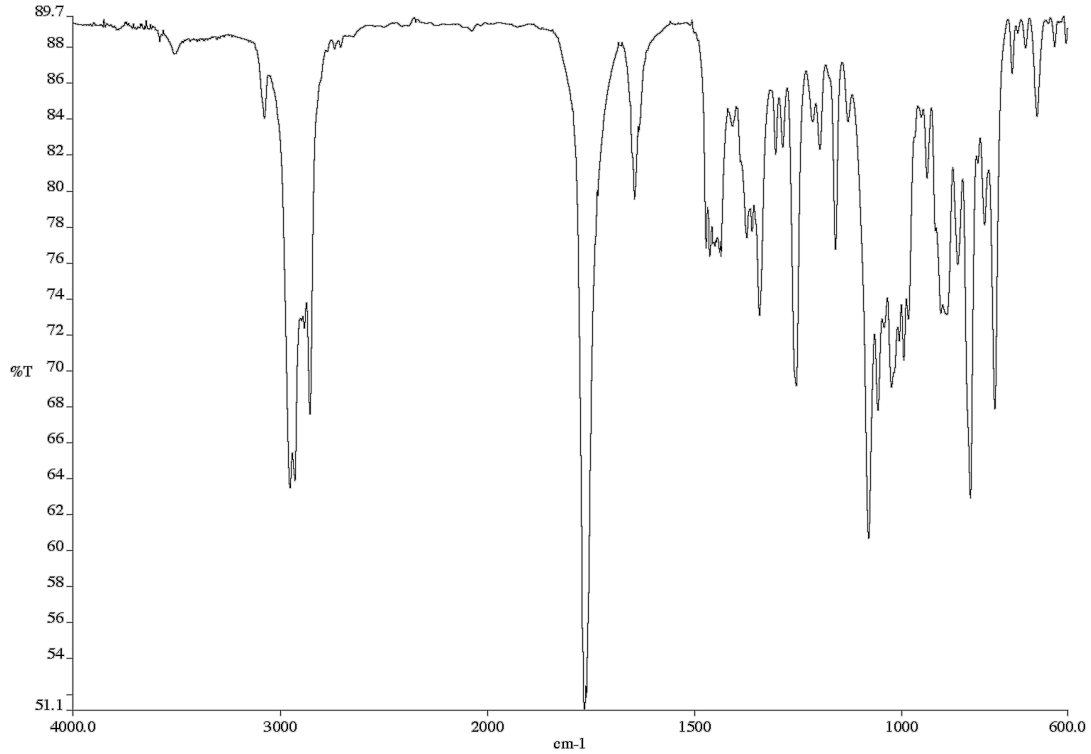

Figure A2.56 Infrared spectrum (Thin Film, NaCl) of compound **47**

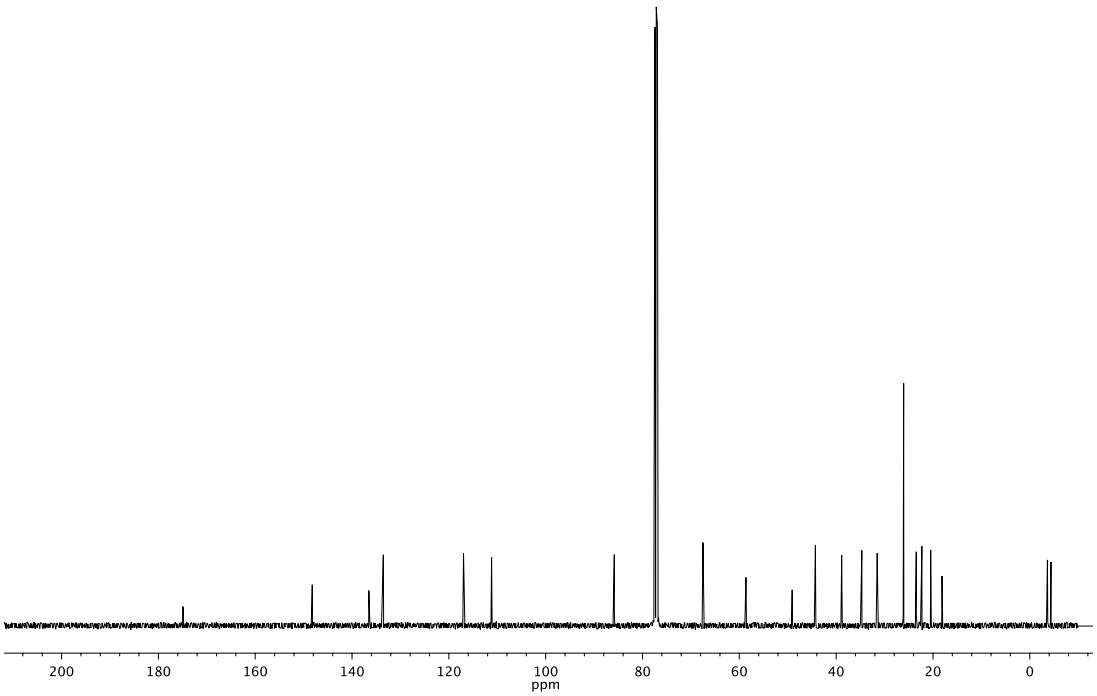

Figure A2.57 ^{13}C NMR (126 MHz, $CDCl_3$) of compound **47**

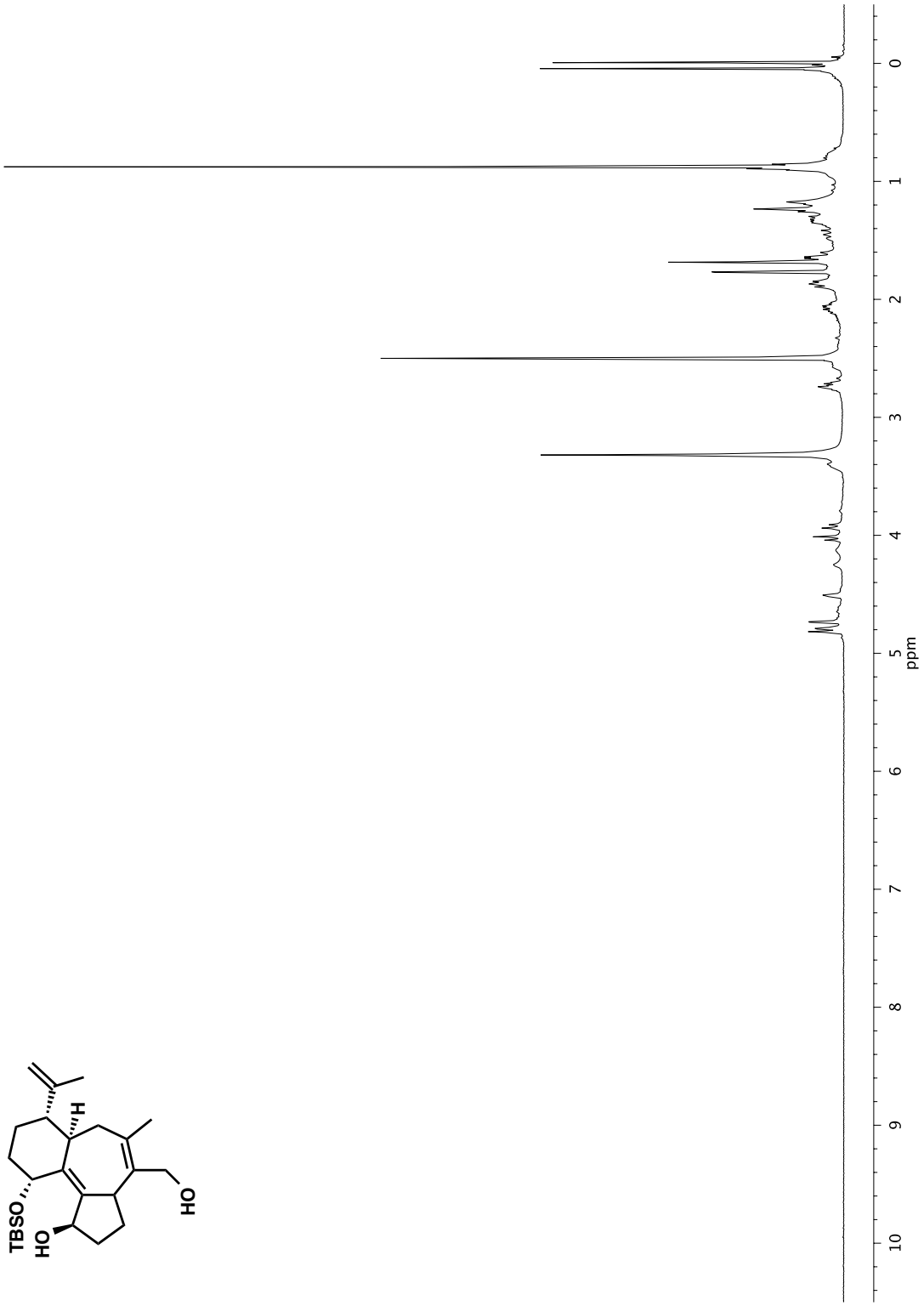

Figure A2.58 ^{1}H NMR (500 MHz, DMSO-*d6*) of compound **49**

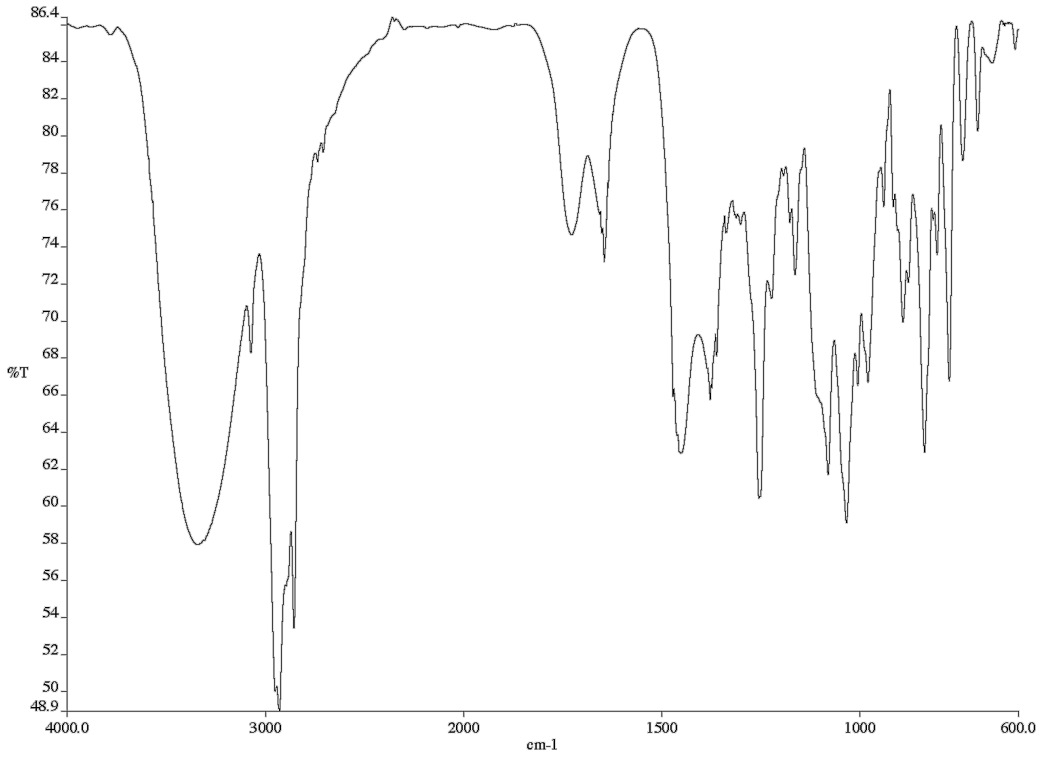

Figure A2.59 Infrared spectrum (Thin Film, NaCl) of compound **49**

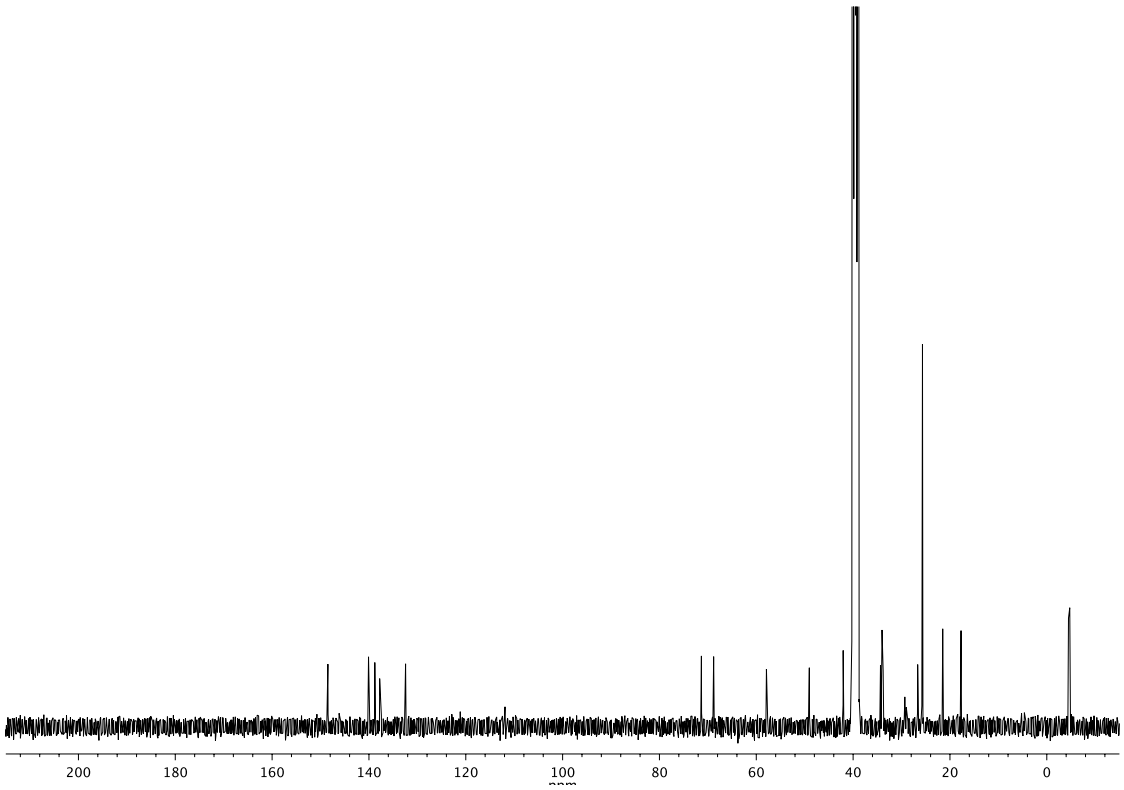

Figure A2.60 ^{13}C NMR (126 MHz, DMSO-*d6*) of compound **49**

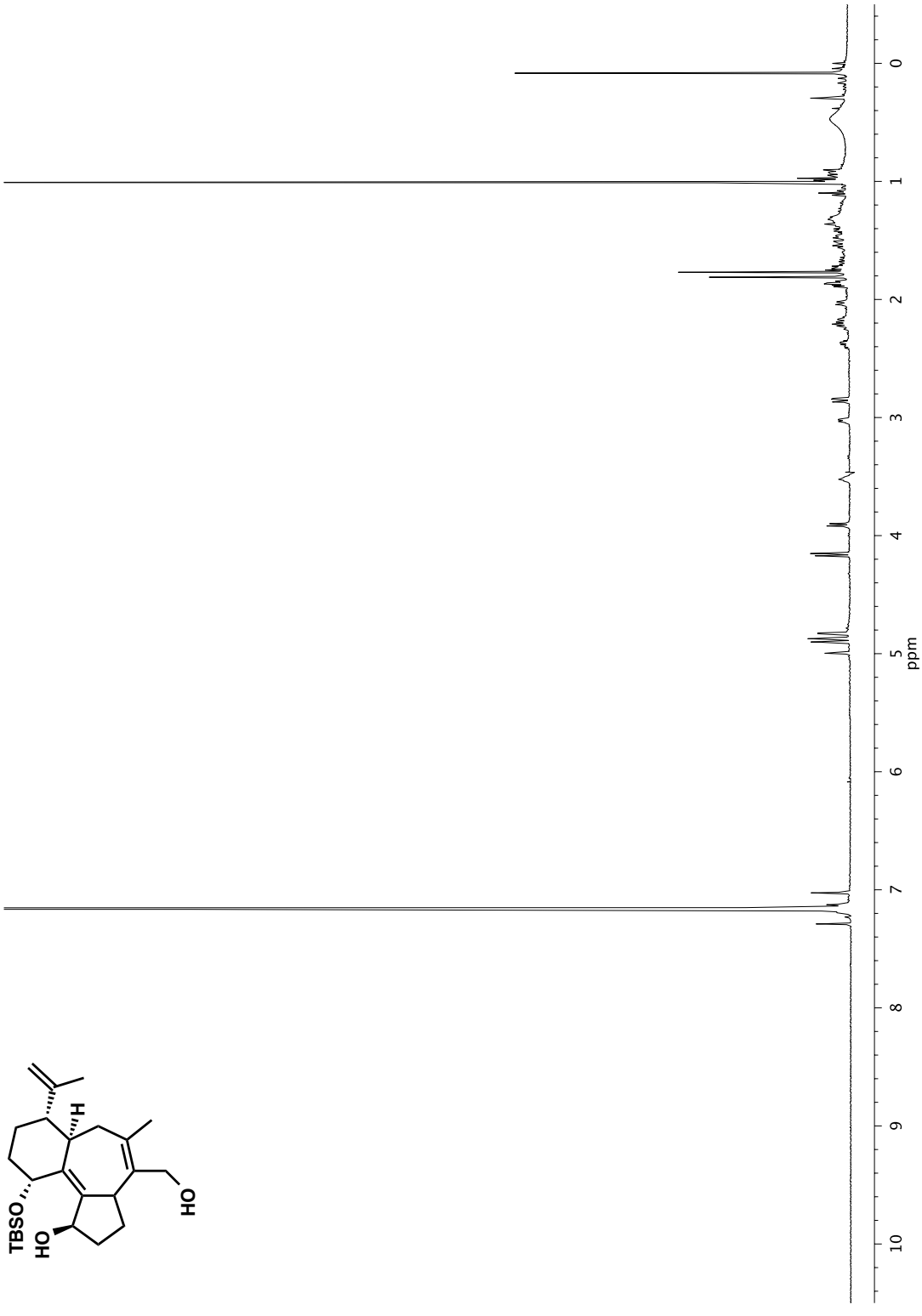

Figure A2.61 ^{1}H NMR (500 MHz, C_6D_6) of compound **49**

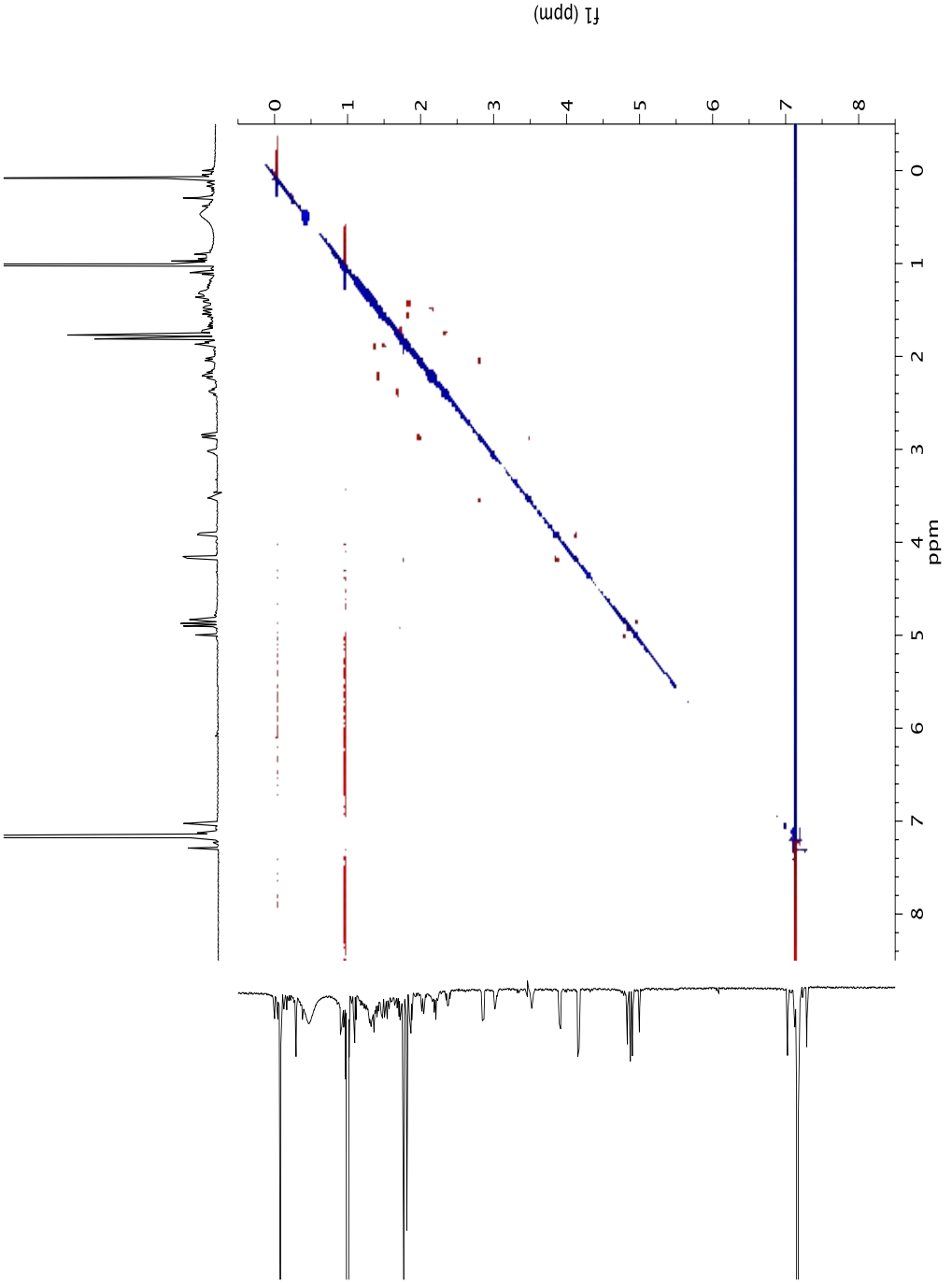

Figure A2.62 NOESY (600 MHz, C_6D_6) of compound **49**

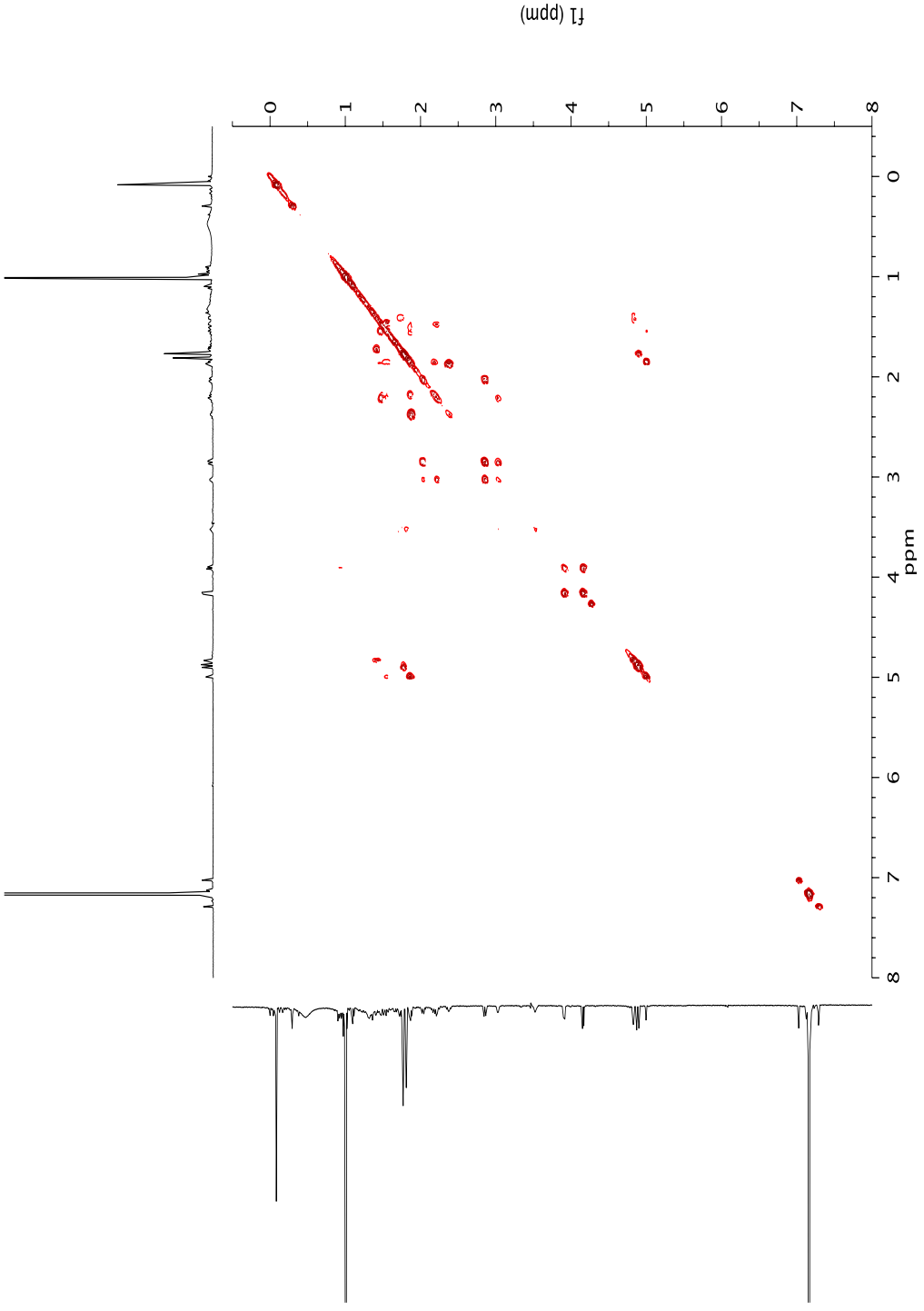

Figure A2.63 ^{1}H–^{1}H gCOSY NMR (600 MHz, C_6D_6) of compound **49**

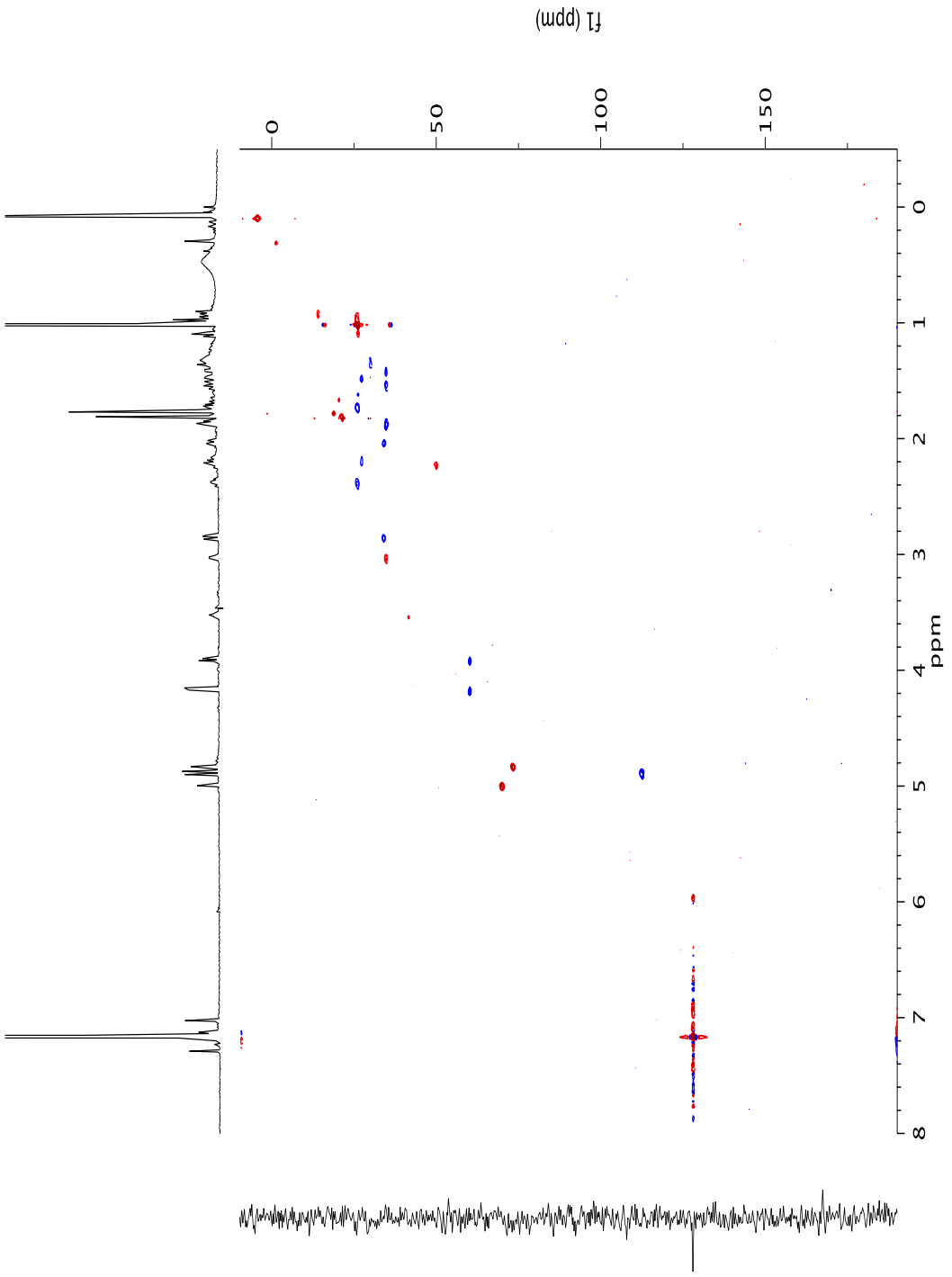

Figure A2.64 ^{1}H–^{13}C HSQC NMR (600 MHz, C_6D_6) of compound **49**

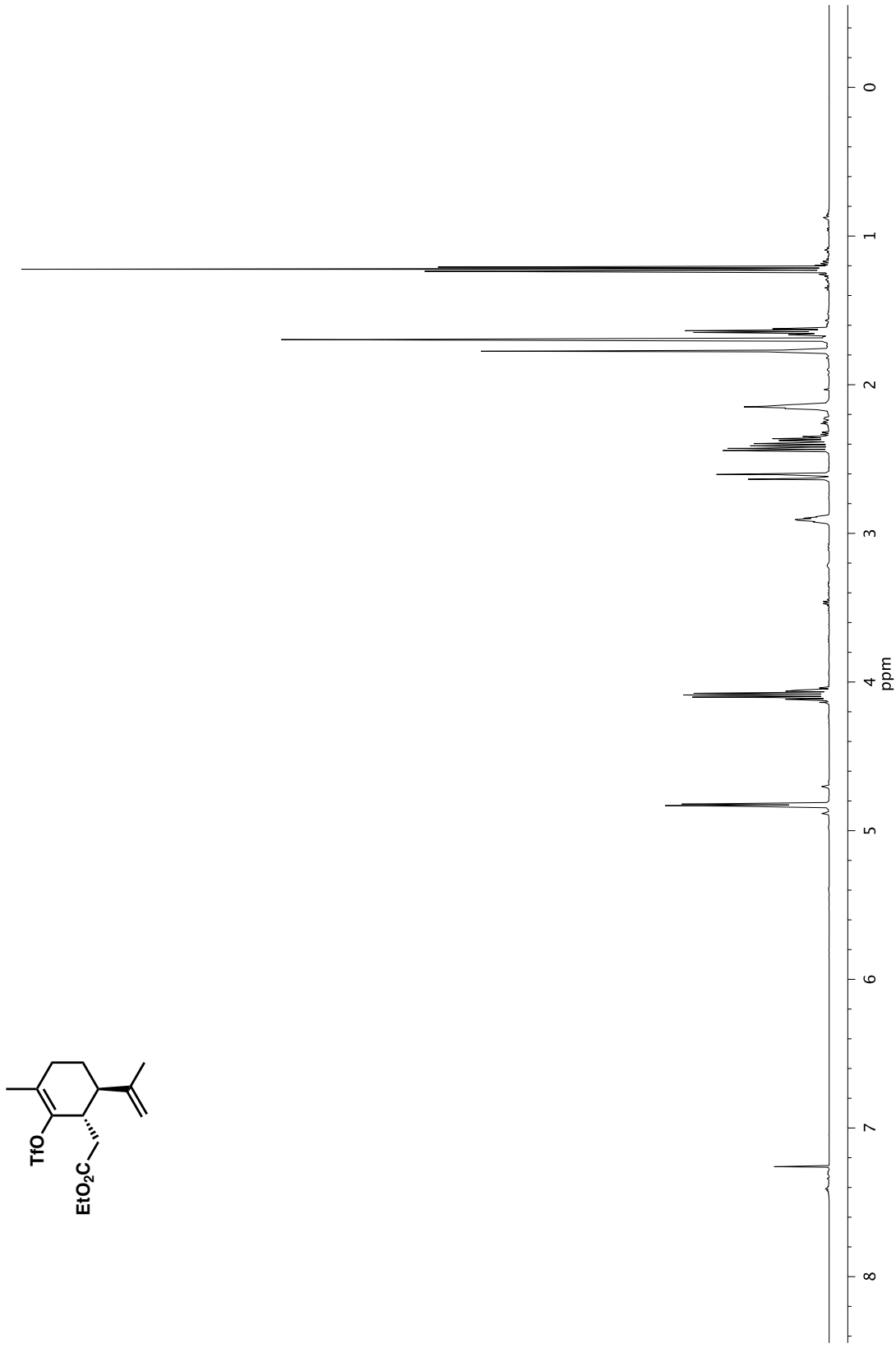

Figure A2.65 ^{1}H NMR (500 MHz, $CDCl_3$) of compound **60**

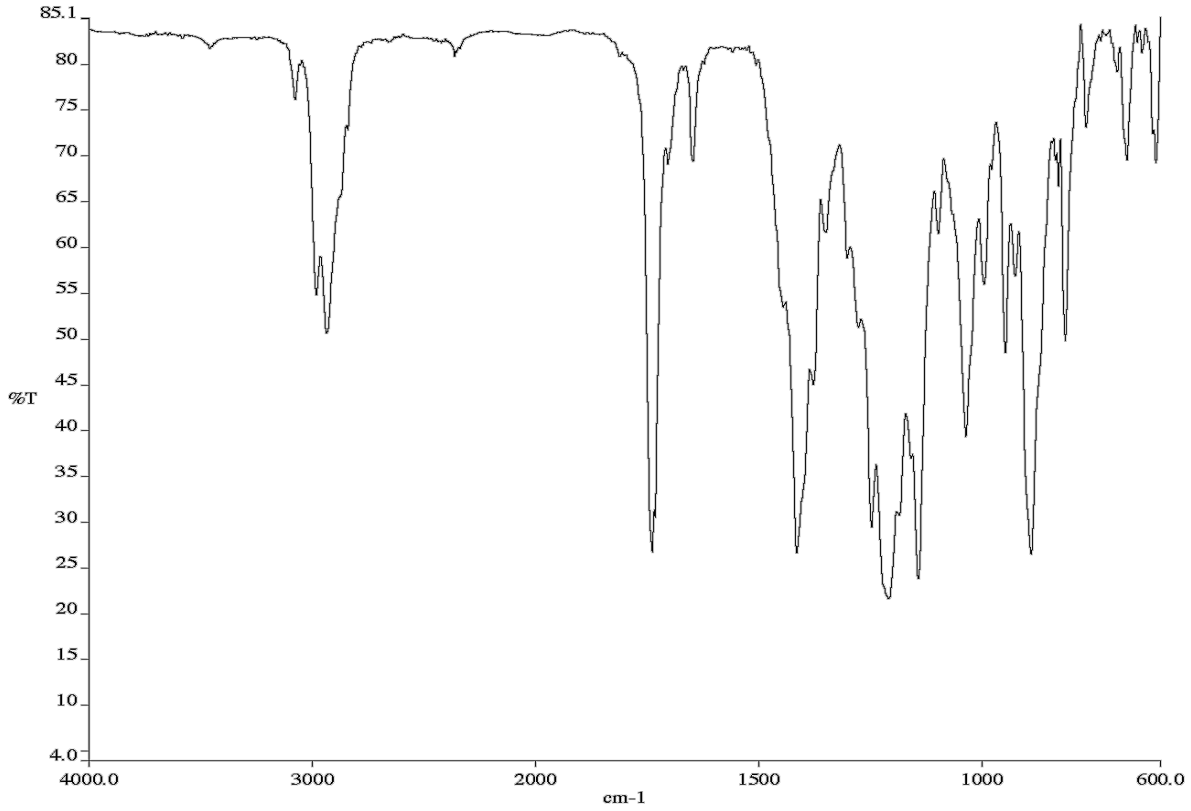

Figure A2.66 Infrared spectrum (Thin Film, NaCl) of compound **60**

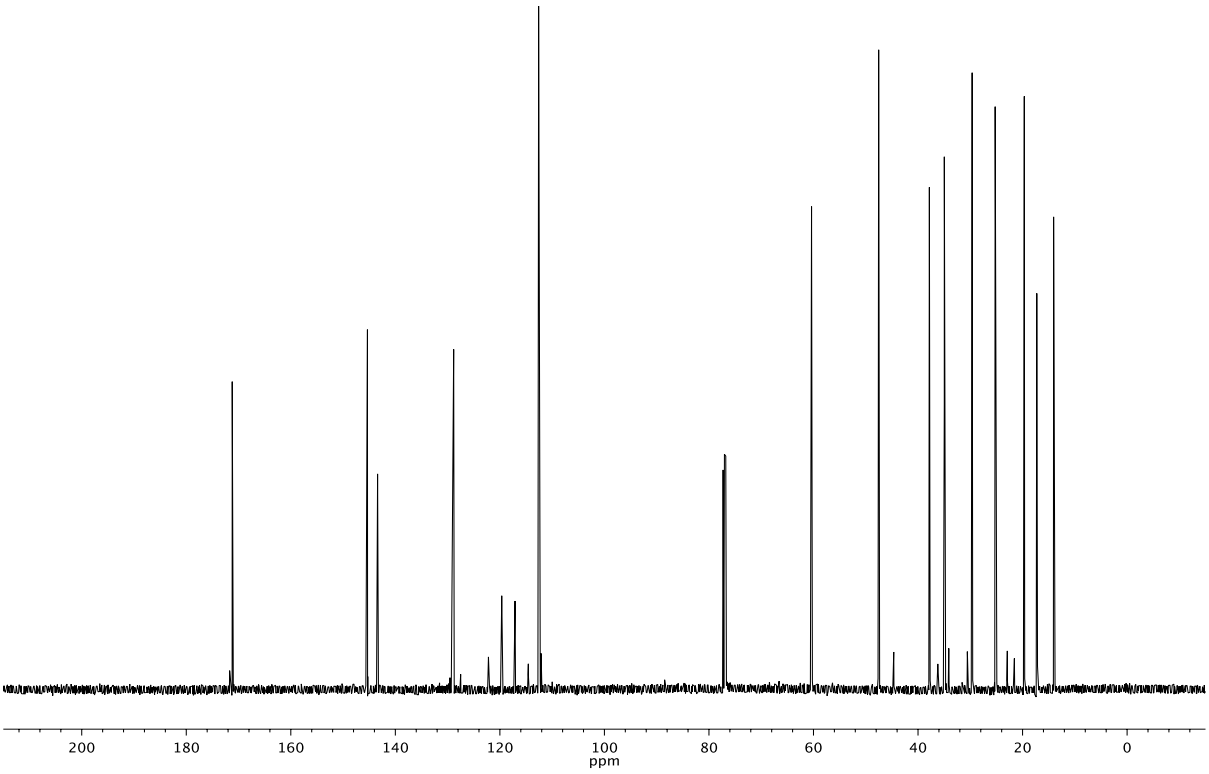

Figure A2.67 ^{13}C NMR (126 MHz, $CDCl_3$) of compound **60**

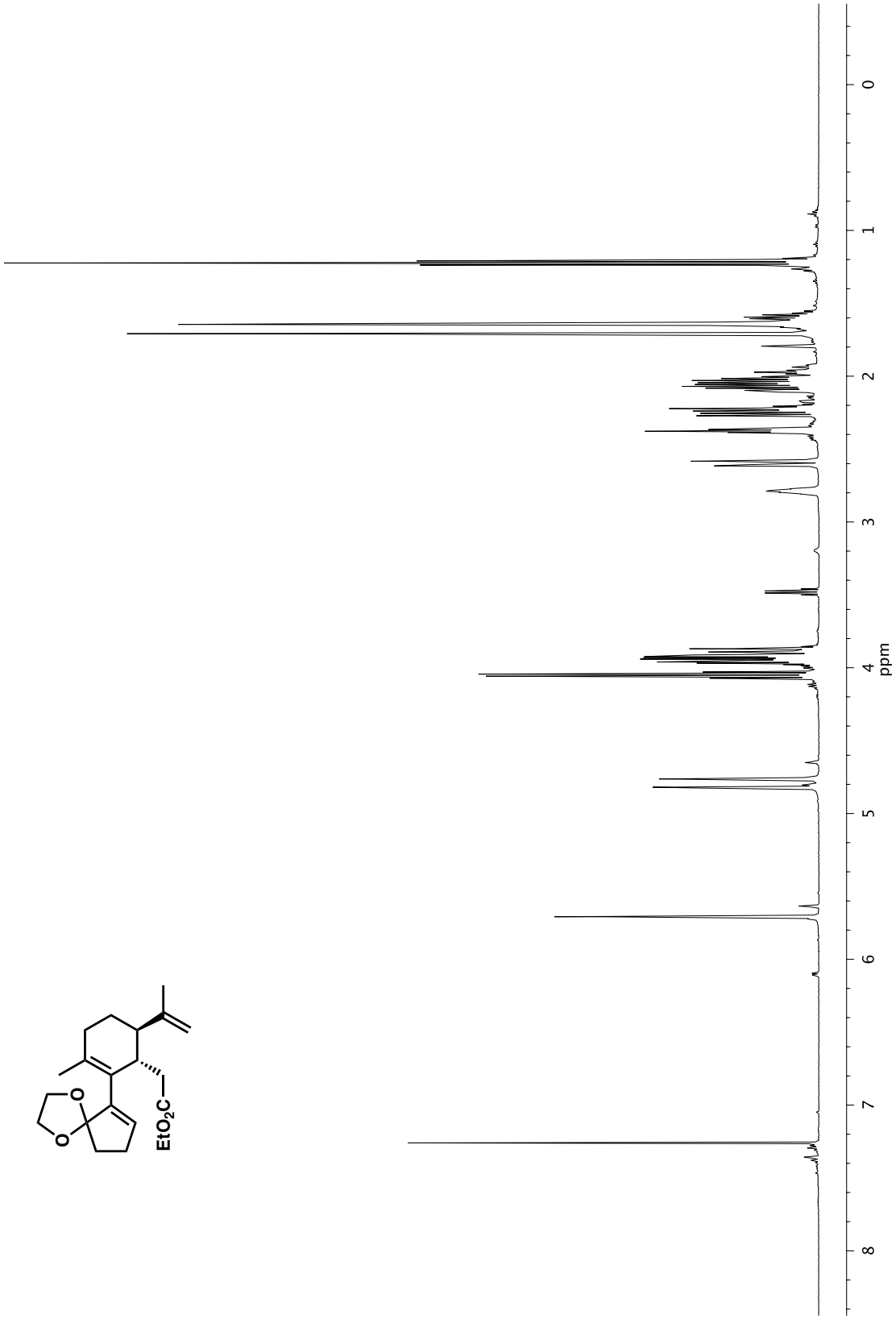

Figure A2.68 ^{1}H NMR (500 MHz, $CDCl_3$) of compound **58**

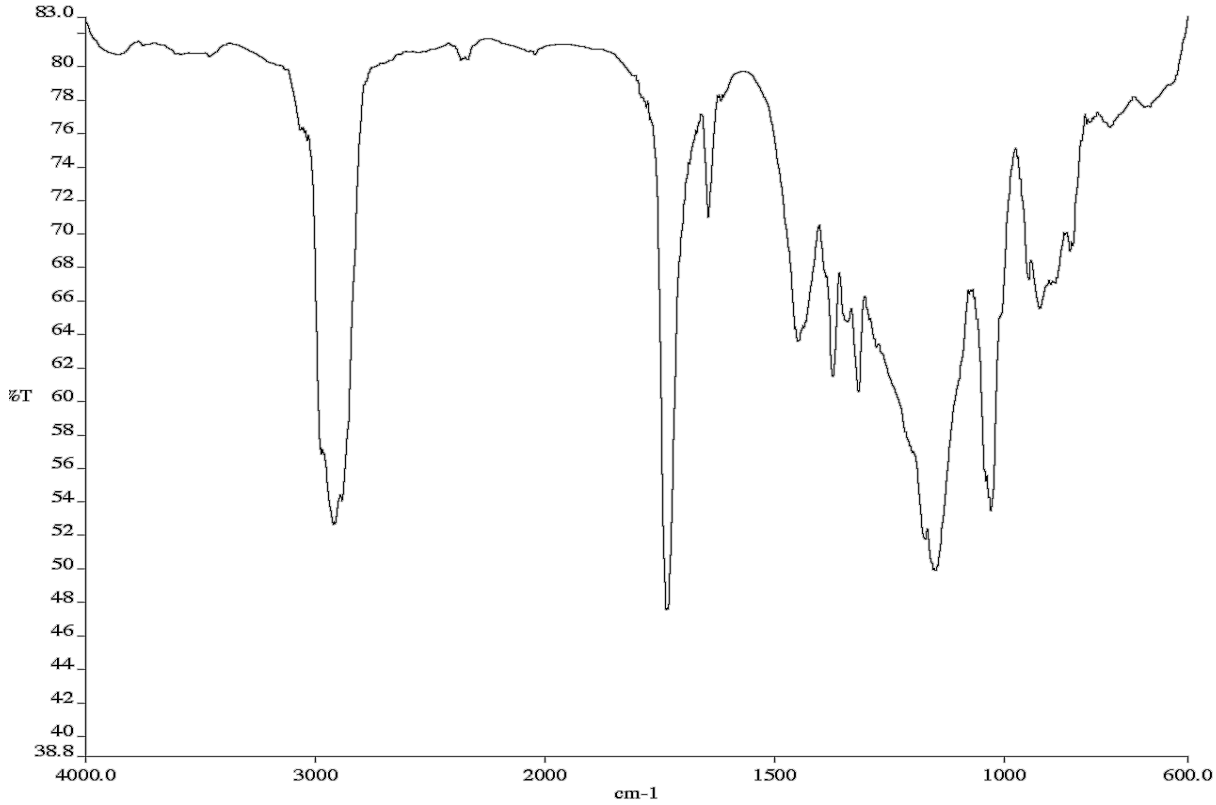

Figure A2.69 Infrared spectrum (Thin Film, NaCl) of compound **58**

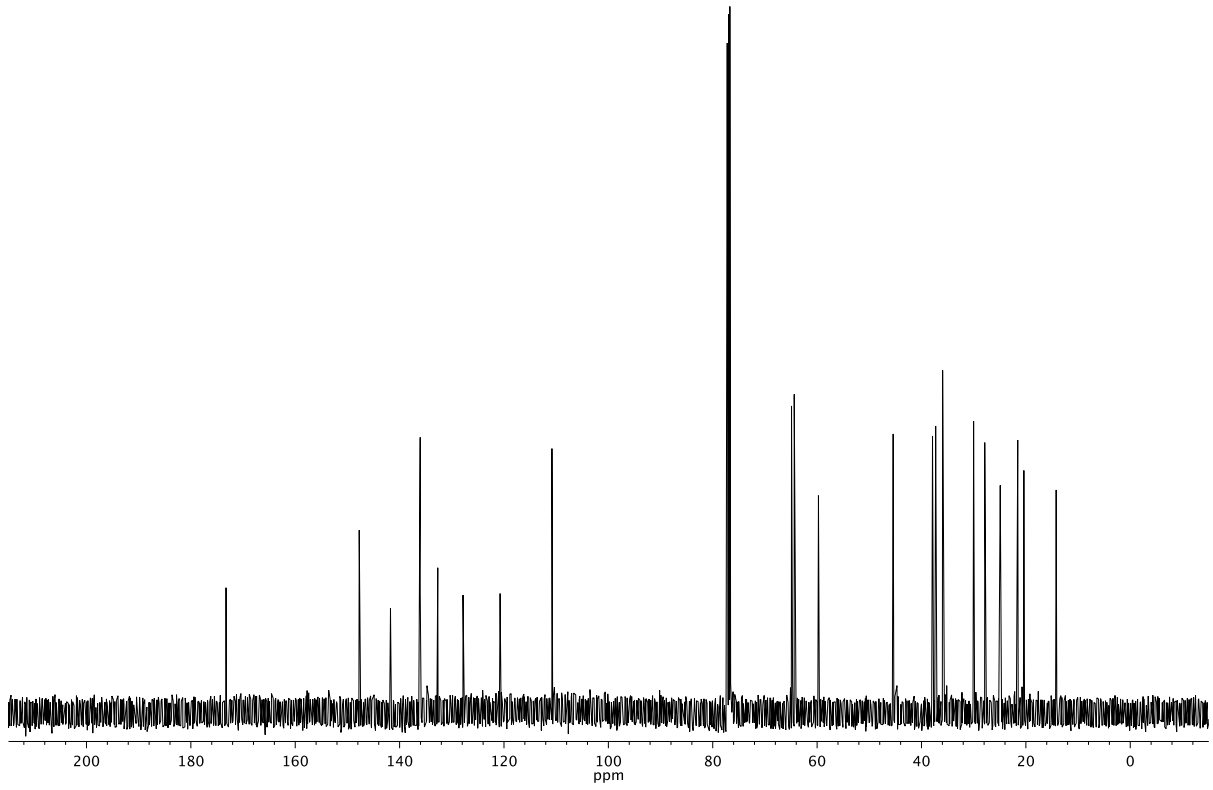

Figure A2.70 ^{13}C NMR (126 MHz, $CDCl_3$) of compound **58**

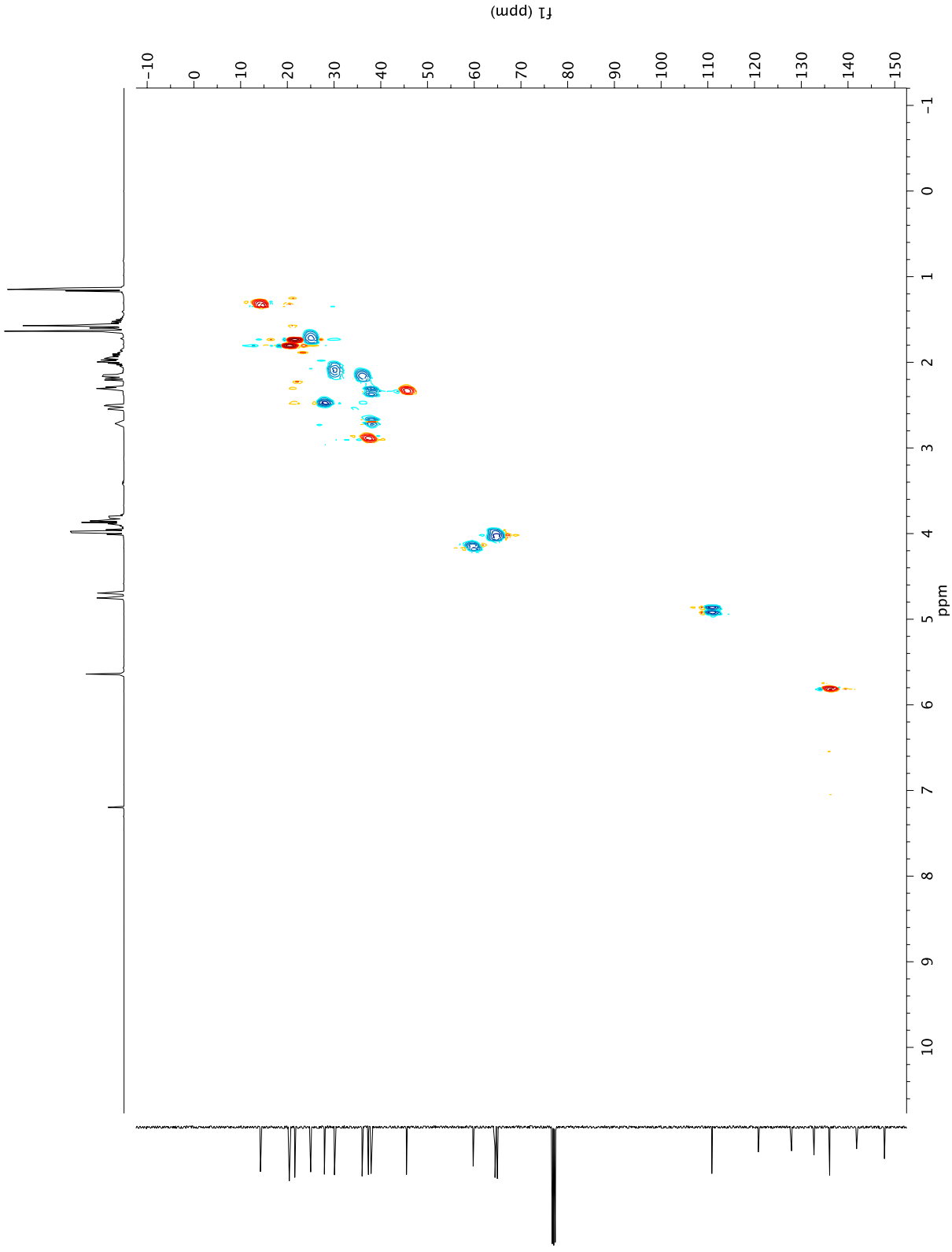

Figure A2.71 $^{1}H–^{13}C$ HSQC NMR (400 MHz, $CDCl_3$) of compound **58**

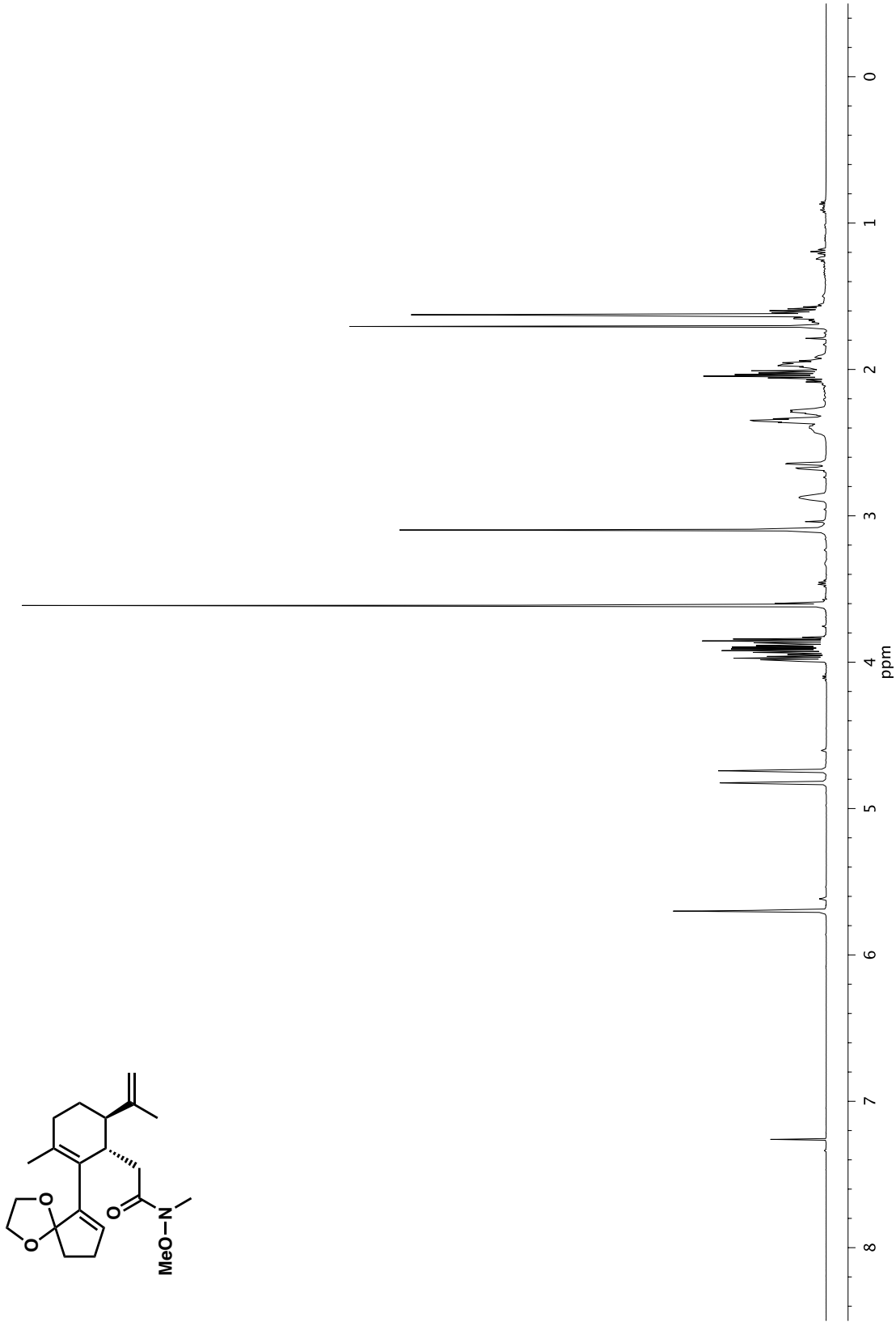

Figure A2.72 ^{1}H NMR (500 MHz, $CDCl_3$) of compound **67**

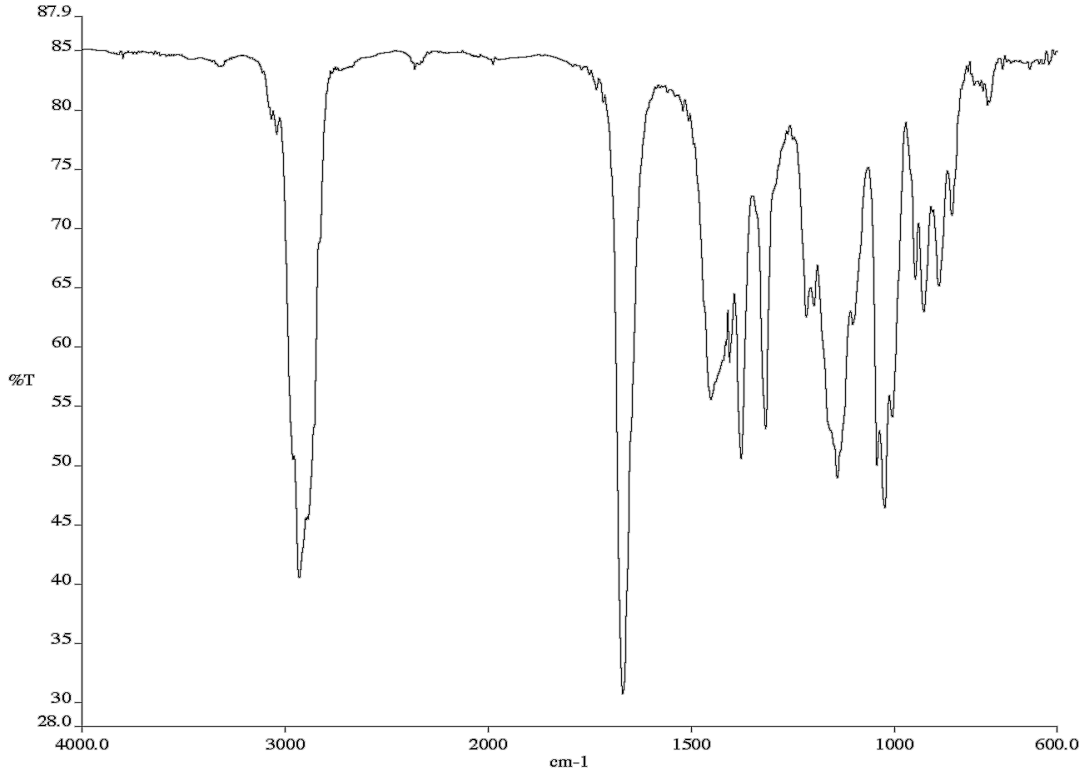

Figure A2.73 Infrared spectrum (Thin Film, NaCl) of compound **67**

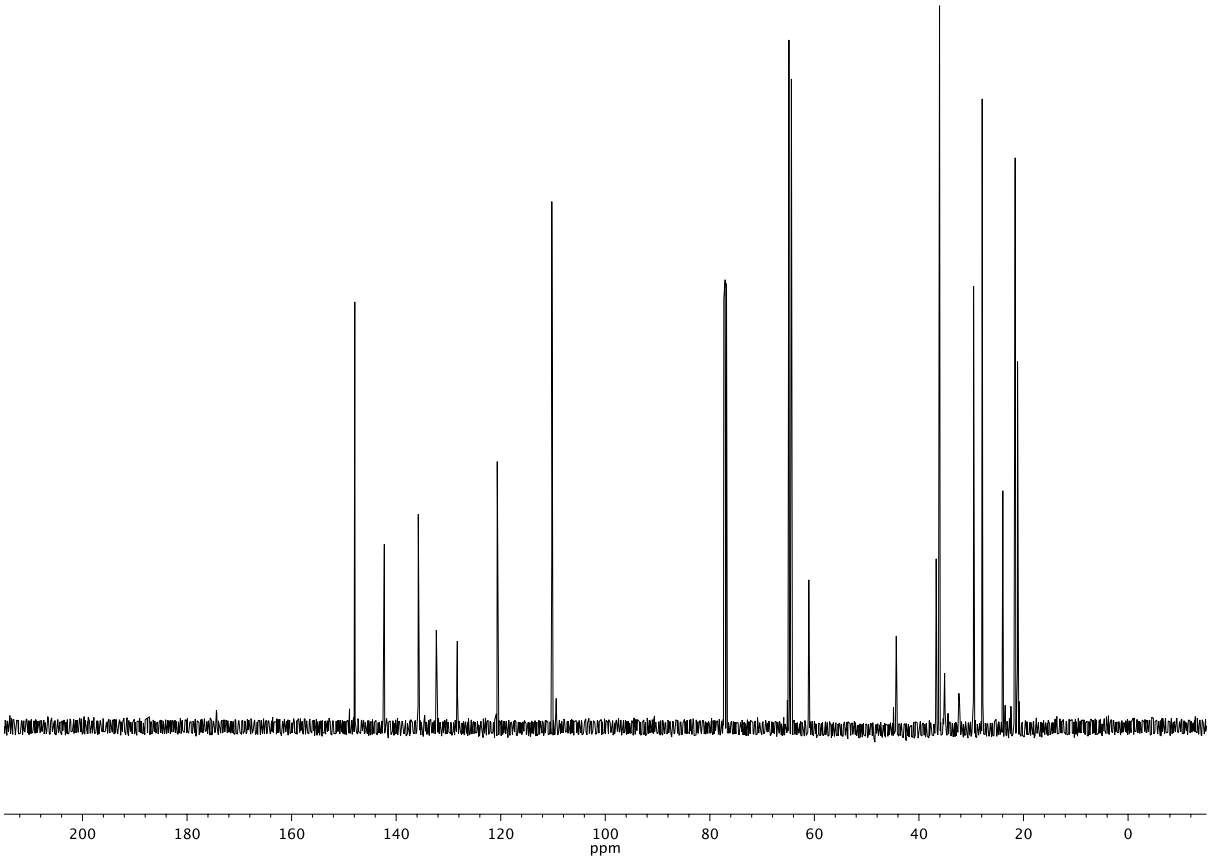

Figure A2.74 ^{13}C NMR (126 MHz, $CDCl_3$) of compound **67**

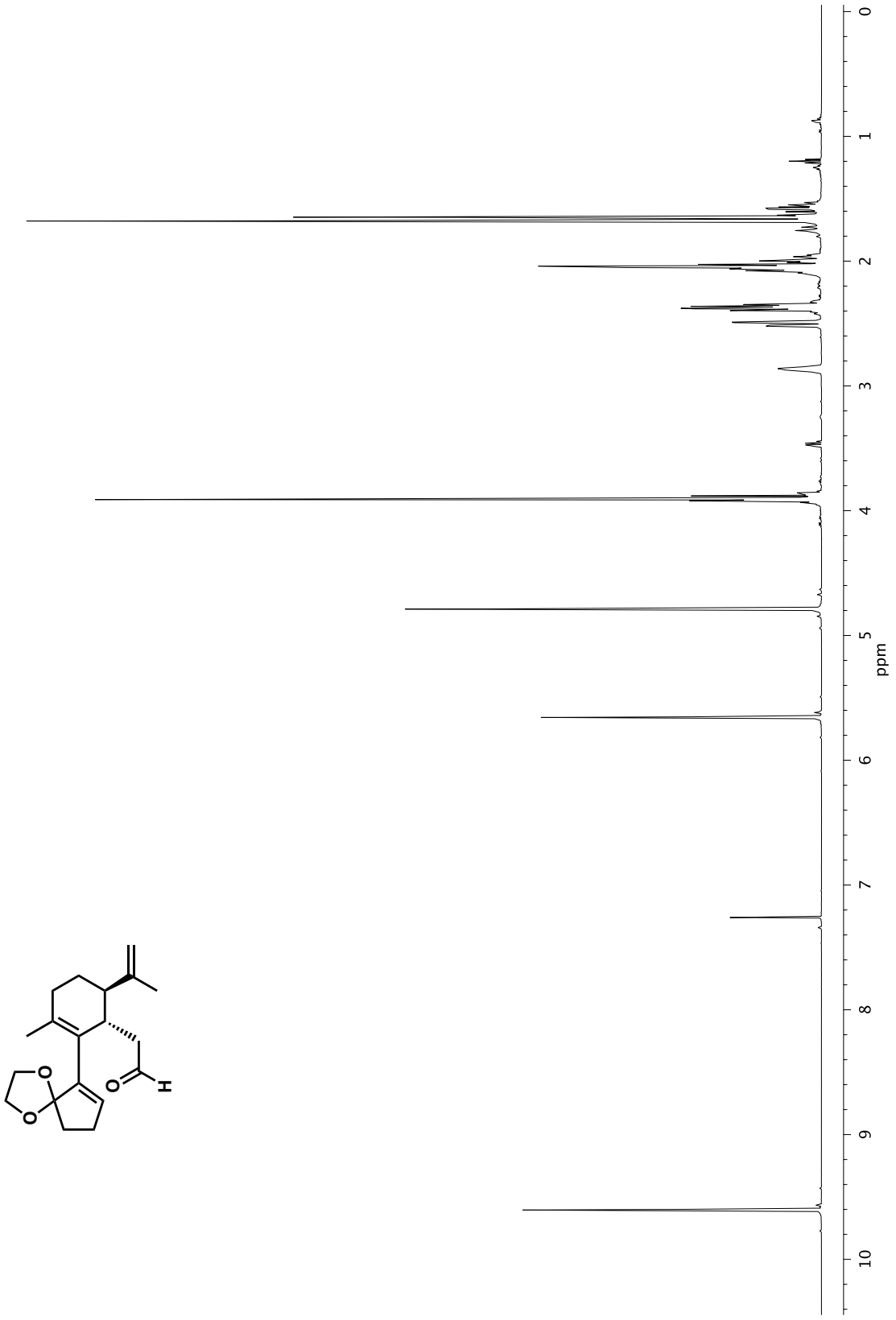

Figure A2.75 ^{1}H NMR (500 MHz, $CDCl_3$) of compound **68**

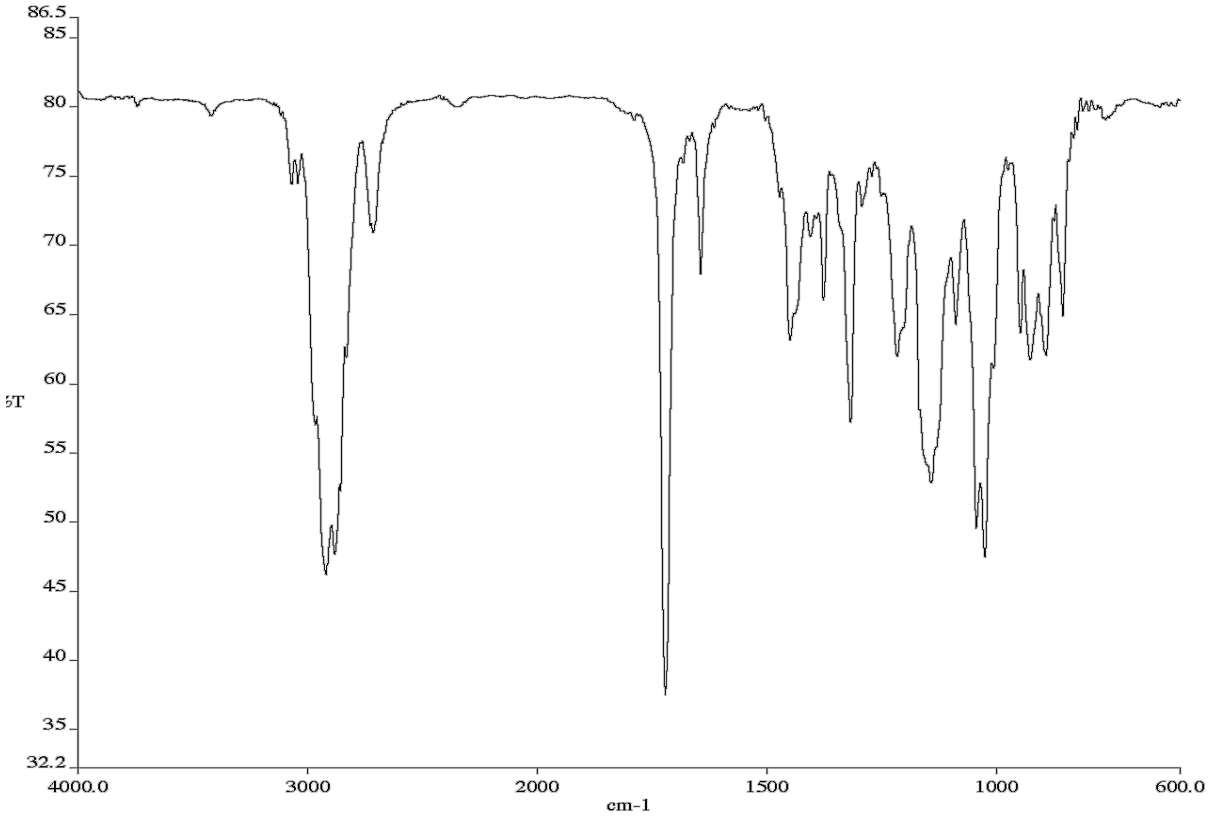

Figure A2.76 Infrared spectrum (Thin Film, NaCl) of compound **68**

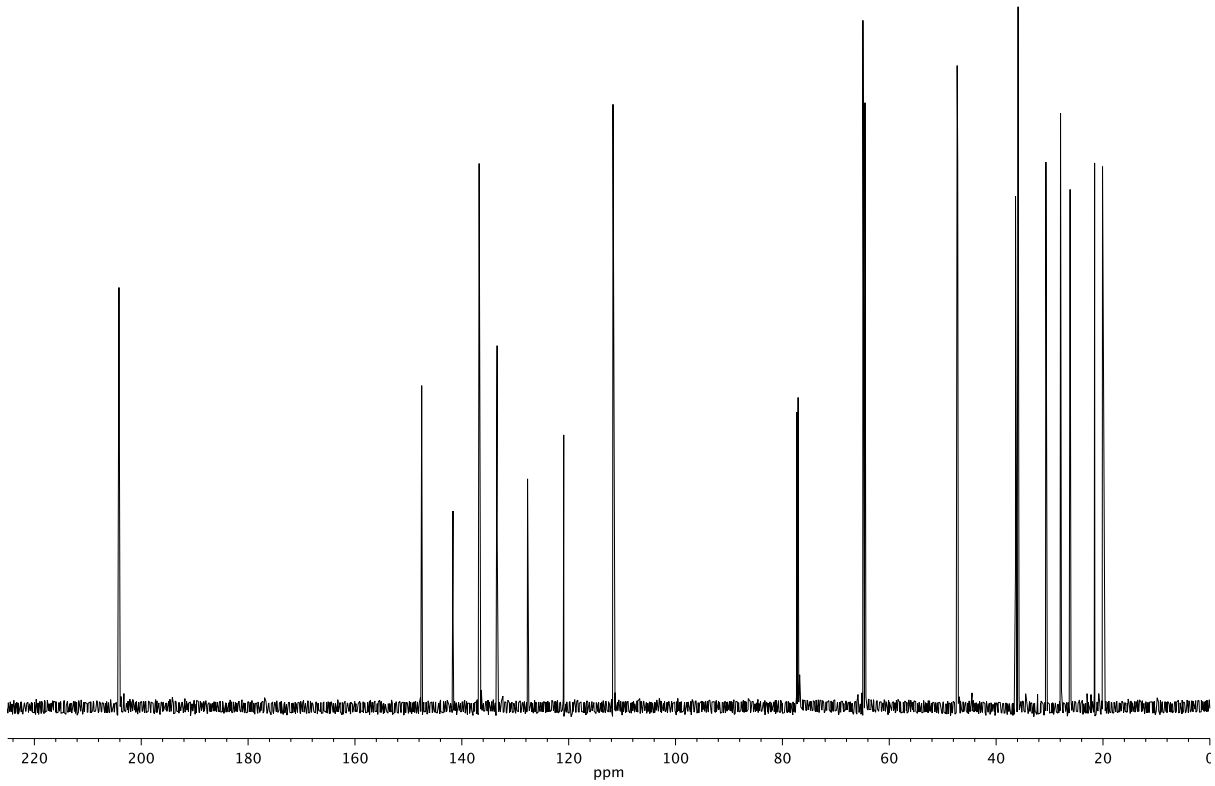

Figure A2.77 ^{13}C NMR (126 MHz, $CDCl_3$) of compound **68**

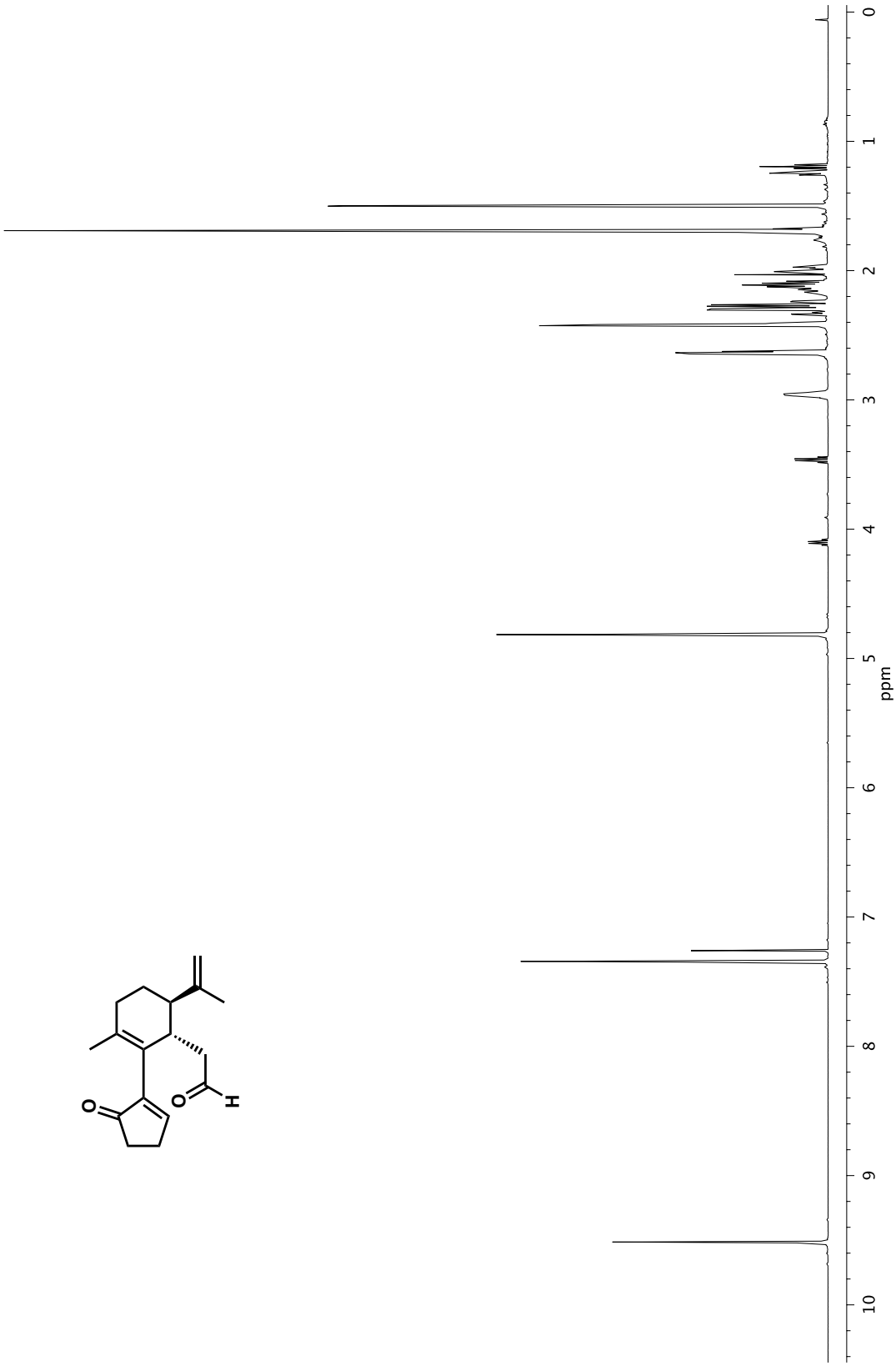

Figure A2.78 ^{1}H NMR (500 MHz, $CDCl_3$) of compound **57**

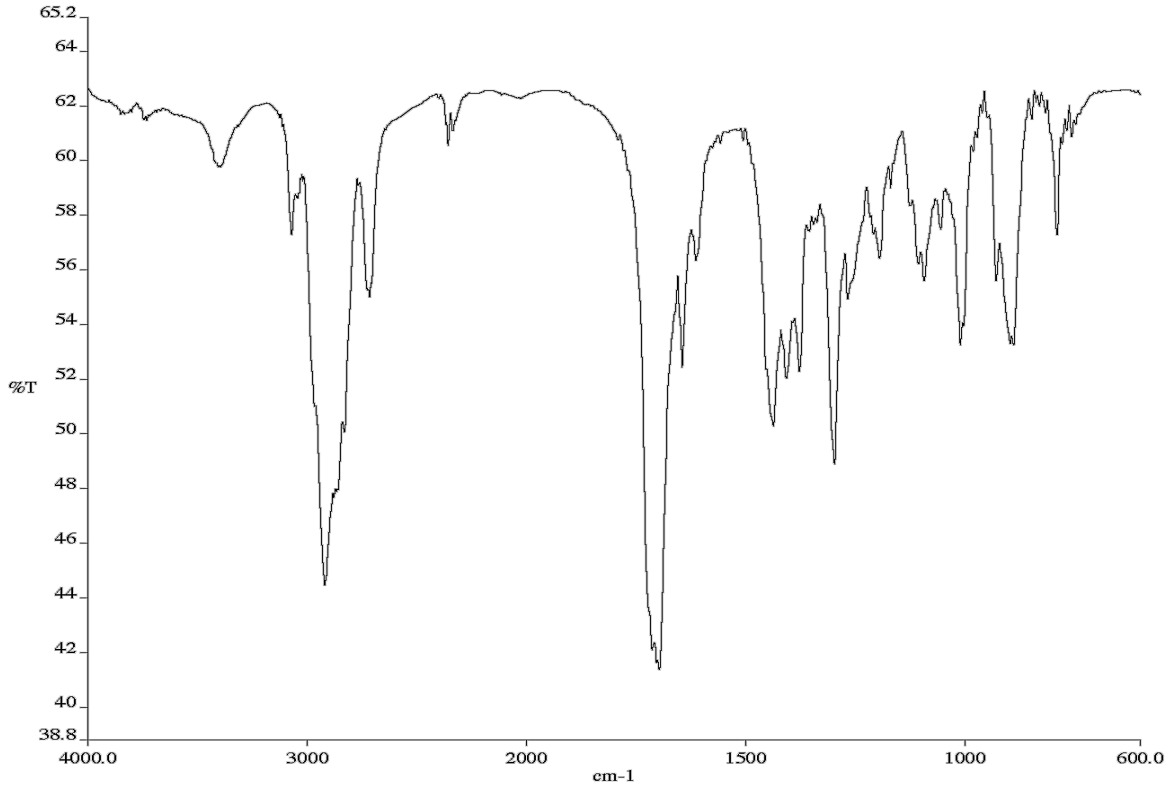

Figure A2.79 Infrared spectrum (Thin Film, NaCl) of compound **57**

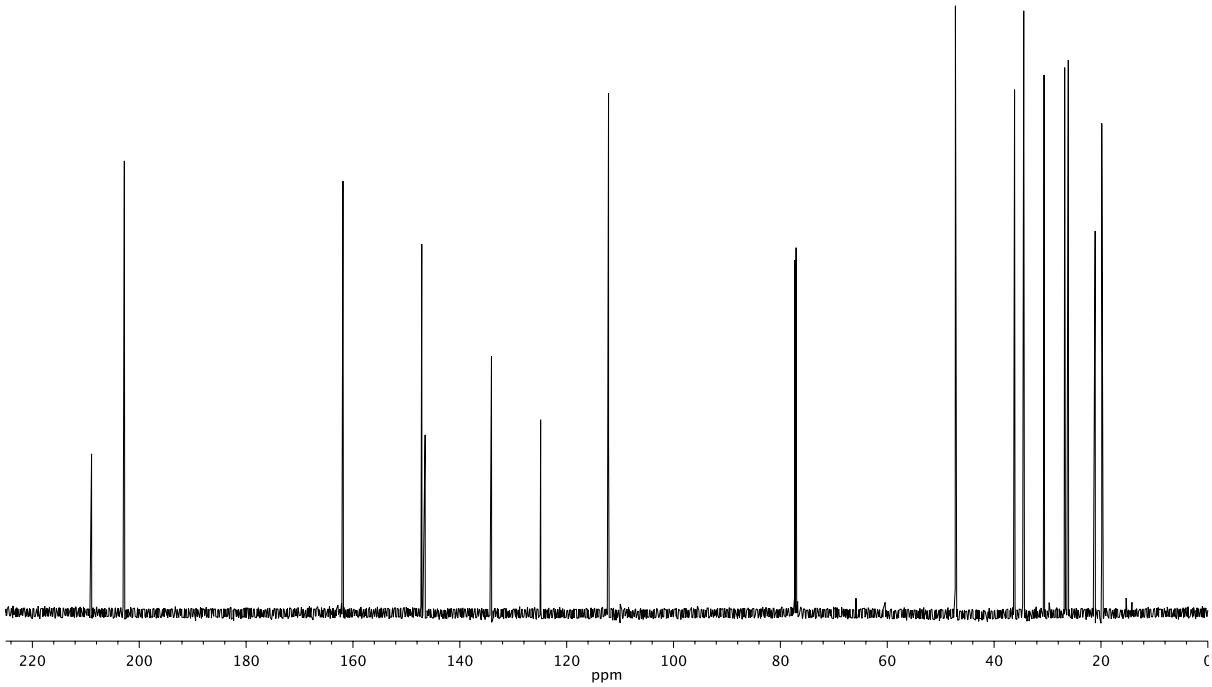

Figure A2.80 ^{13}C NMR (126 MHz, $CDCl_3$) of compound **57**

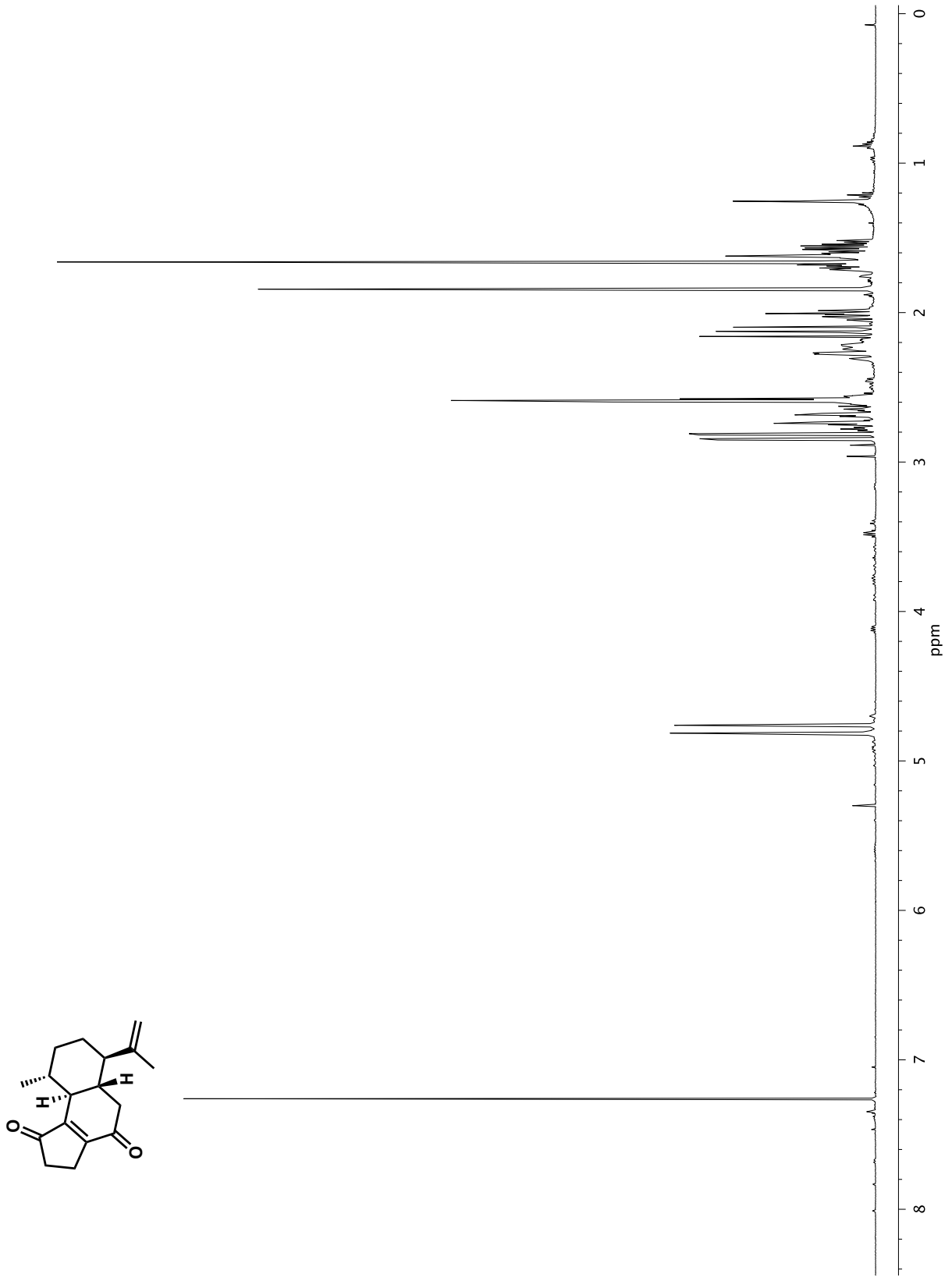

Figure A2.81 ^{1}H NMR (500 MHz, $CDCl_3$) of compound **63**

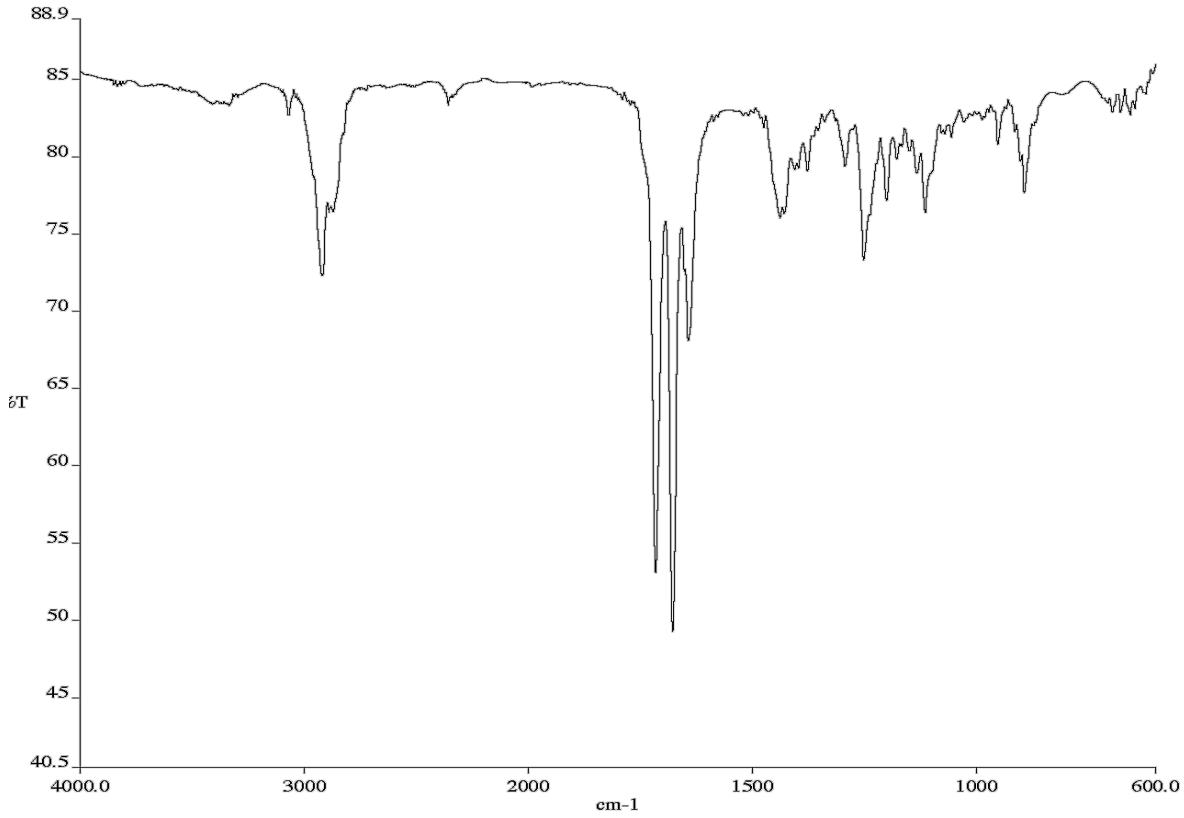

Figure A2.82 Infrared spectrum (Thin Film, NaCl) of compound **63**

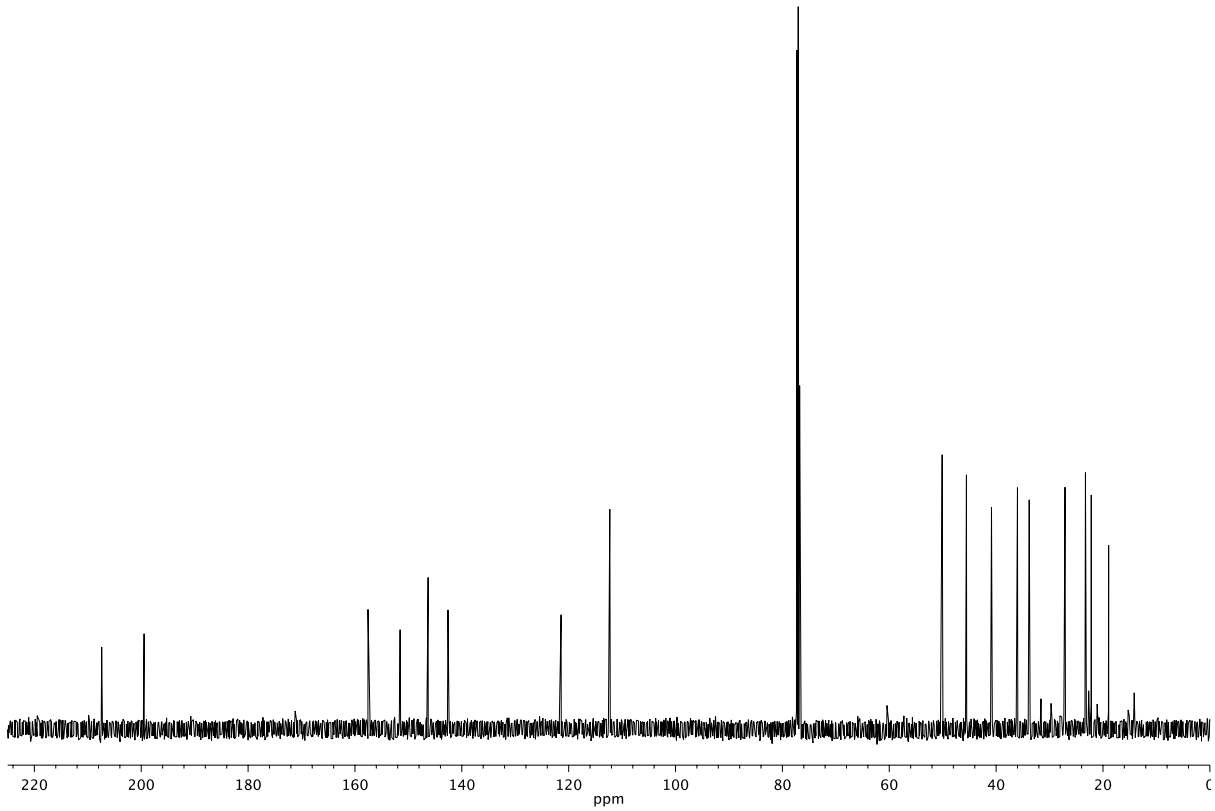

Figure A2.83 ^{13}C NMR (126 MHz, $CDCl_3$) of compound **63**

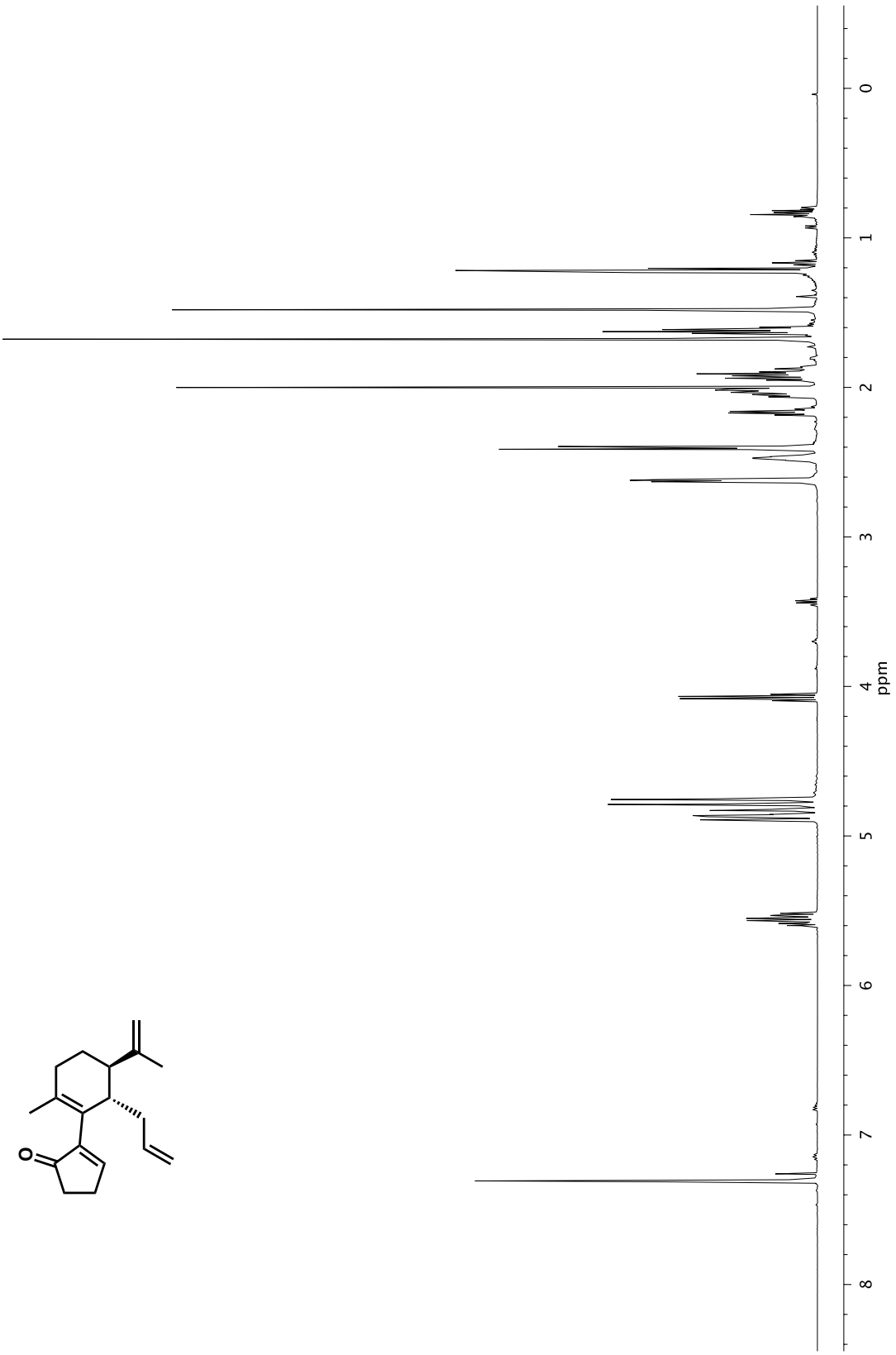

Figure A2.84 ^{1}H NMR (500 MHz, $CDCl_3$) of compound **72**

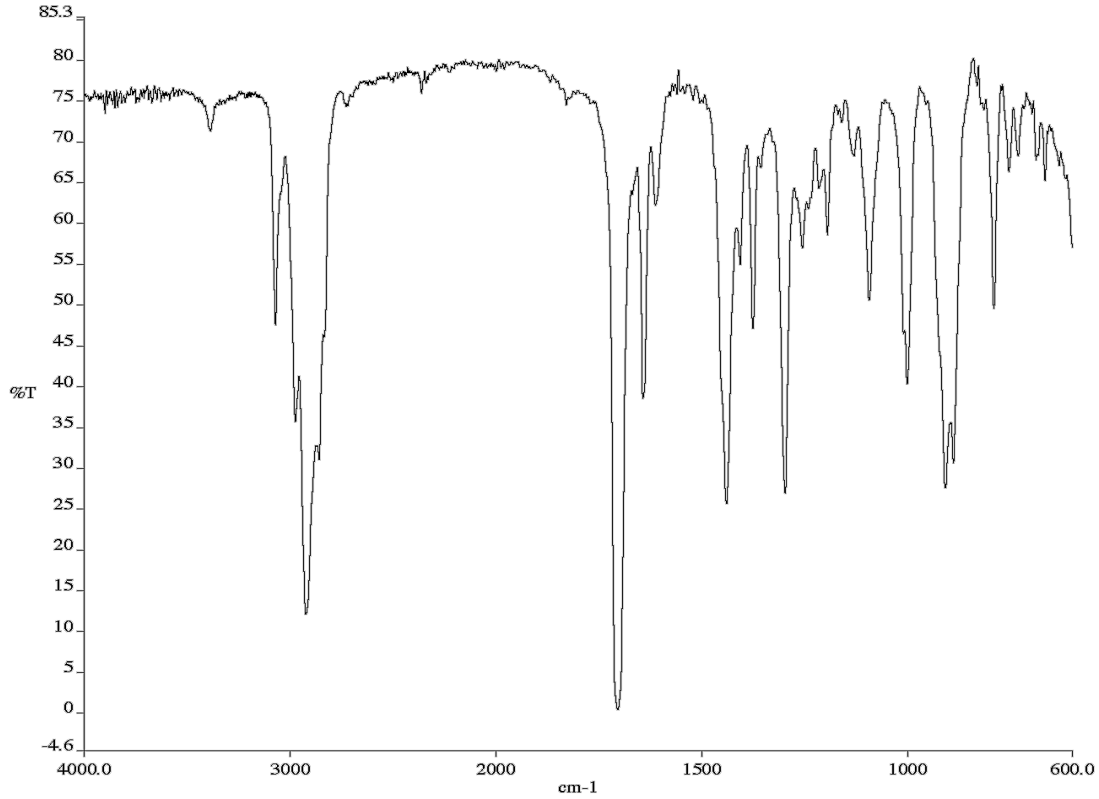

Figure A2.85 Infrared spectrum (Thin Film, NaCl) of compound **72**

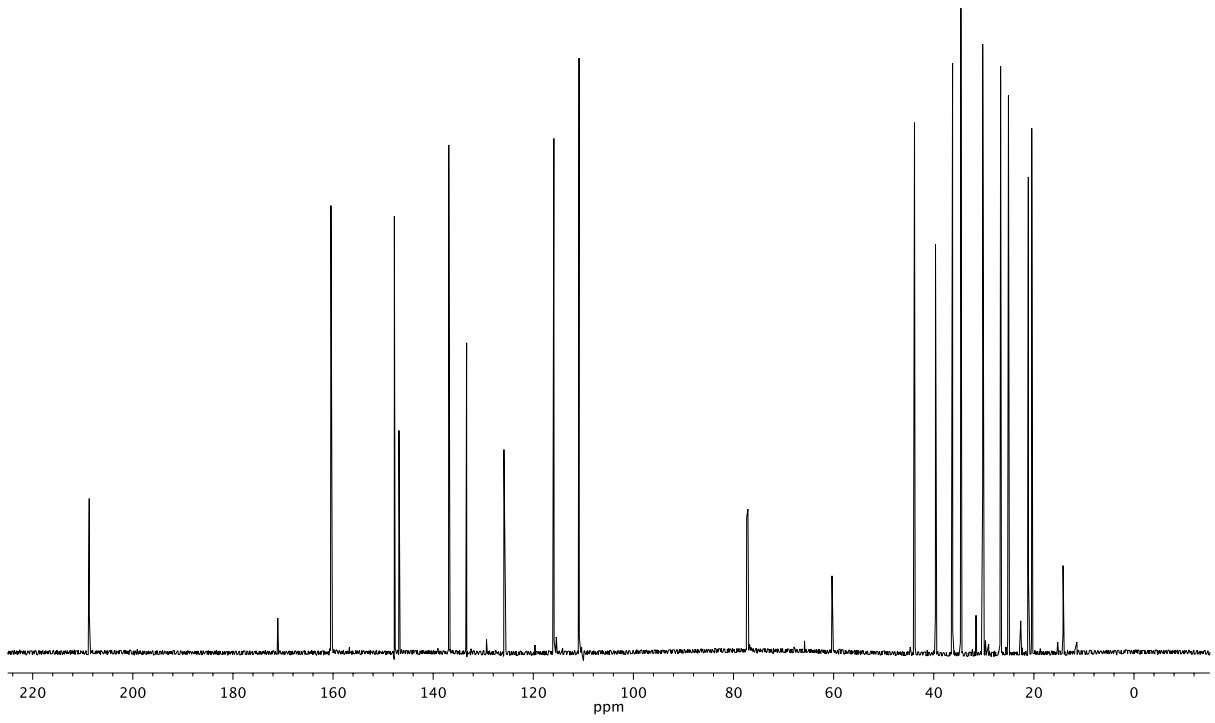

Figure A2.86 ^{13}C NMR (126 MHz, $CDCl_3$) of compound **72**

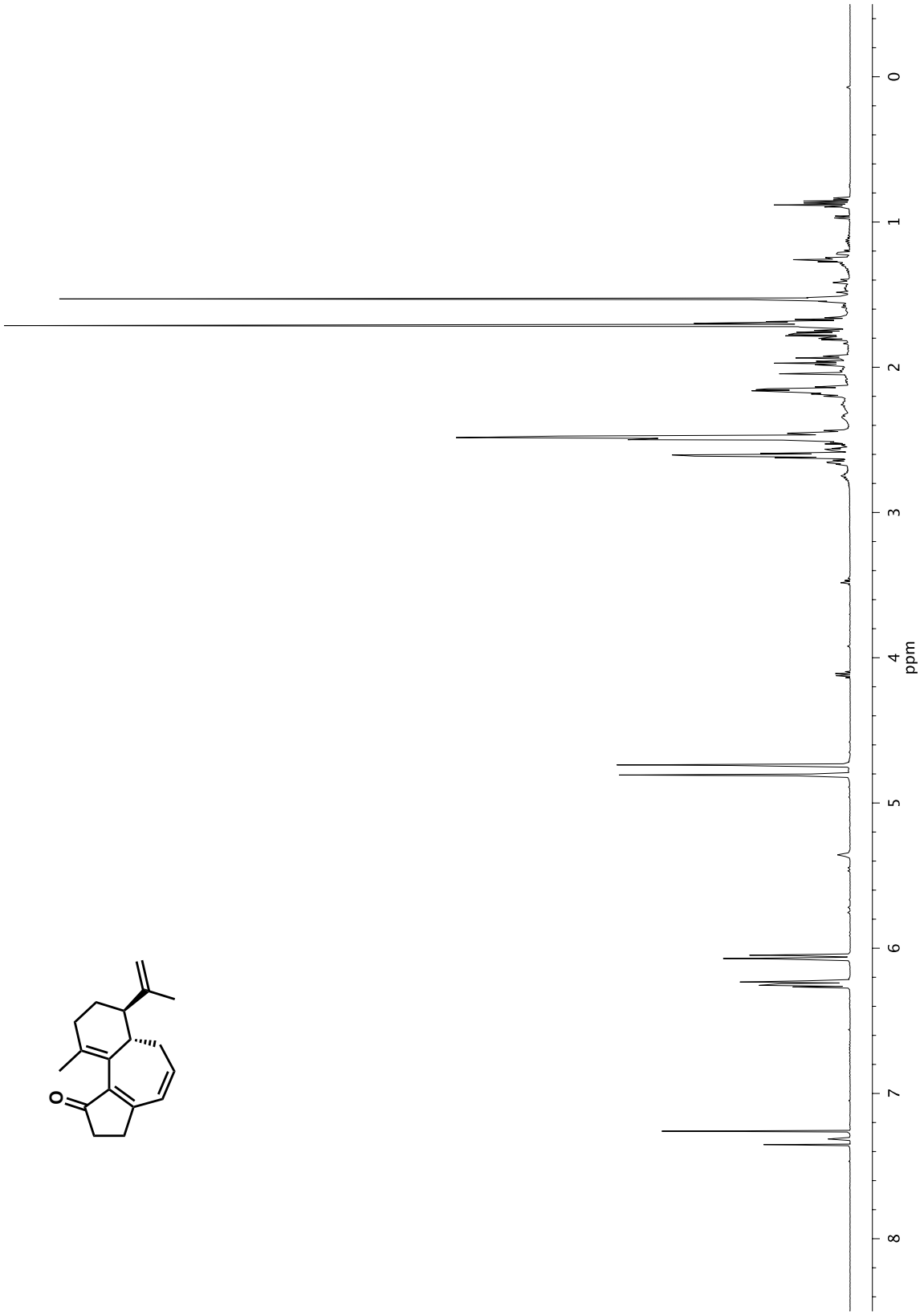

Figure A2.87 ^{1}H NMR (500 MHz, $CDCl_3$) of compound **73**

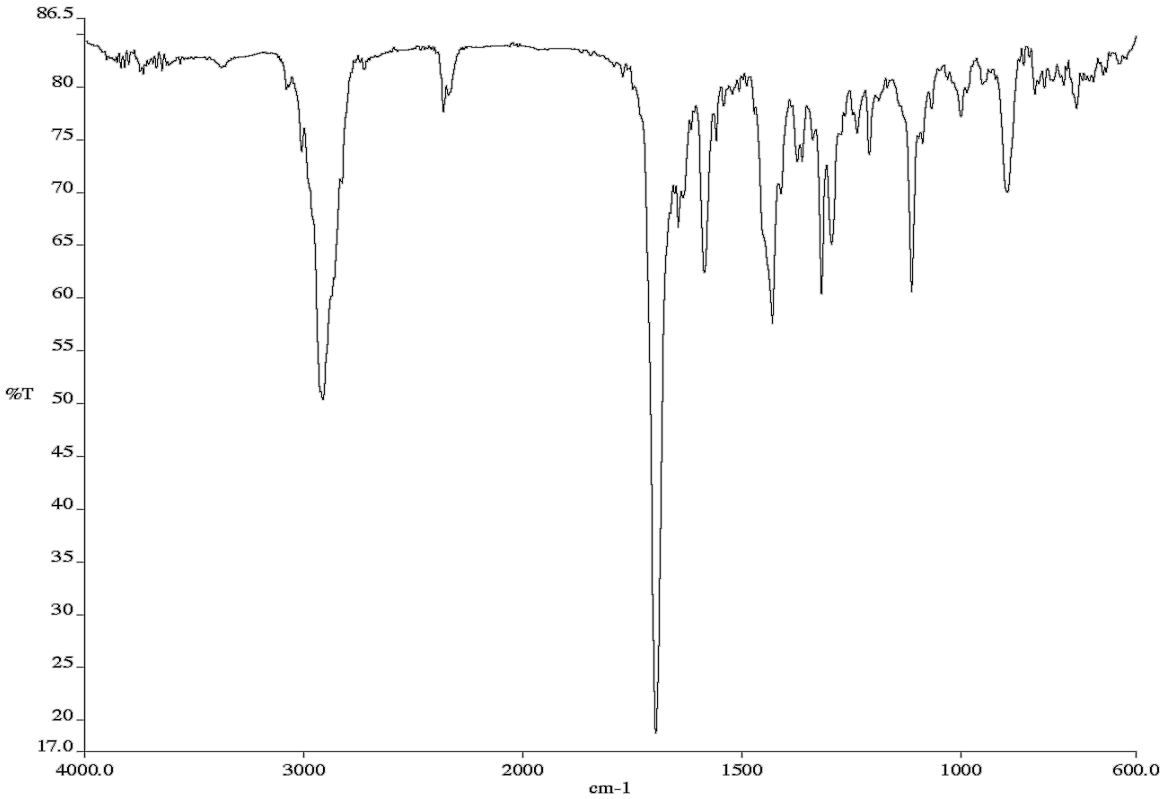

Figure A2.88 Infrared spectrum (Thin Film, NaCl) of compound **73**

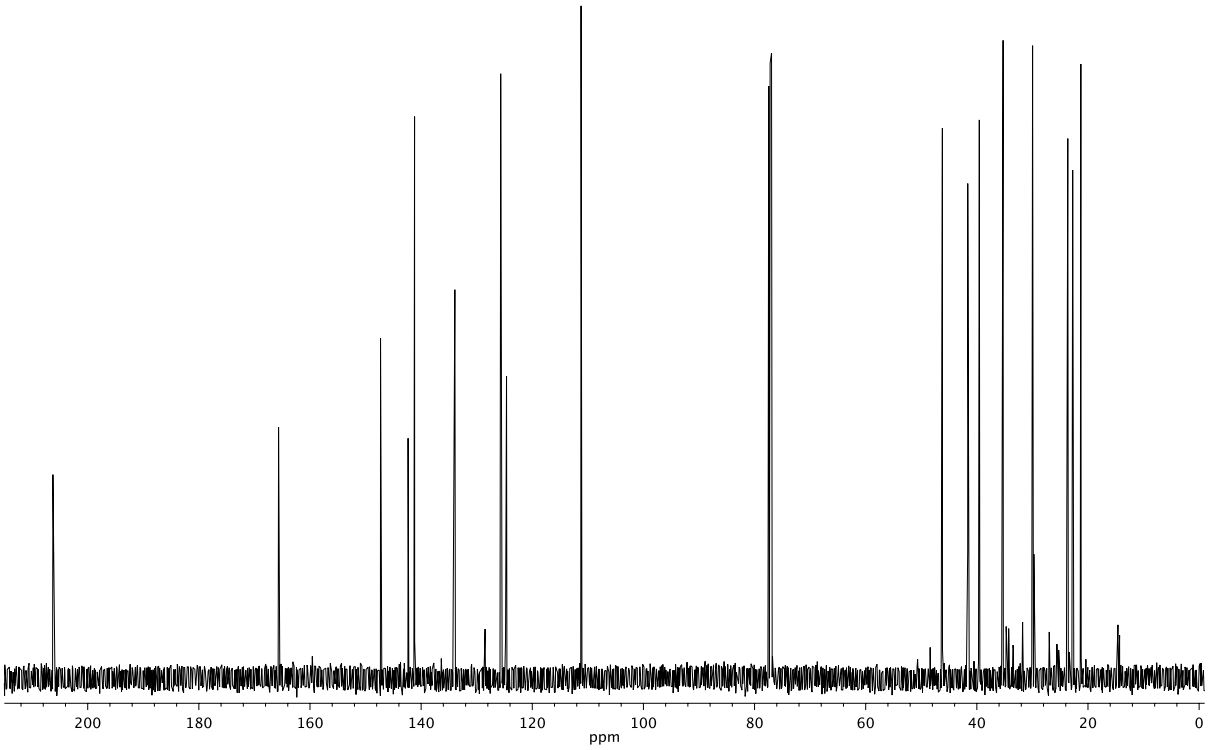

Figure A2.89 ^{13}C NMR (126 MHz, $CDCl_3$) of compound **73**

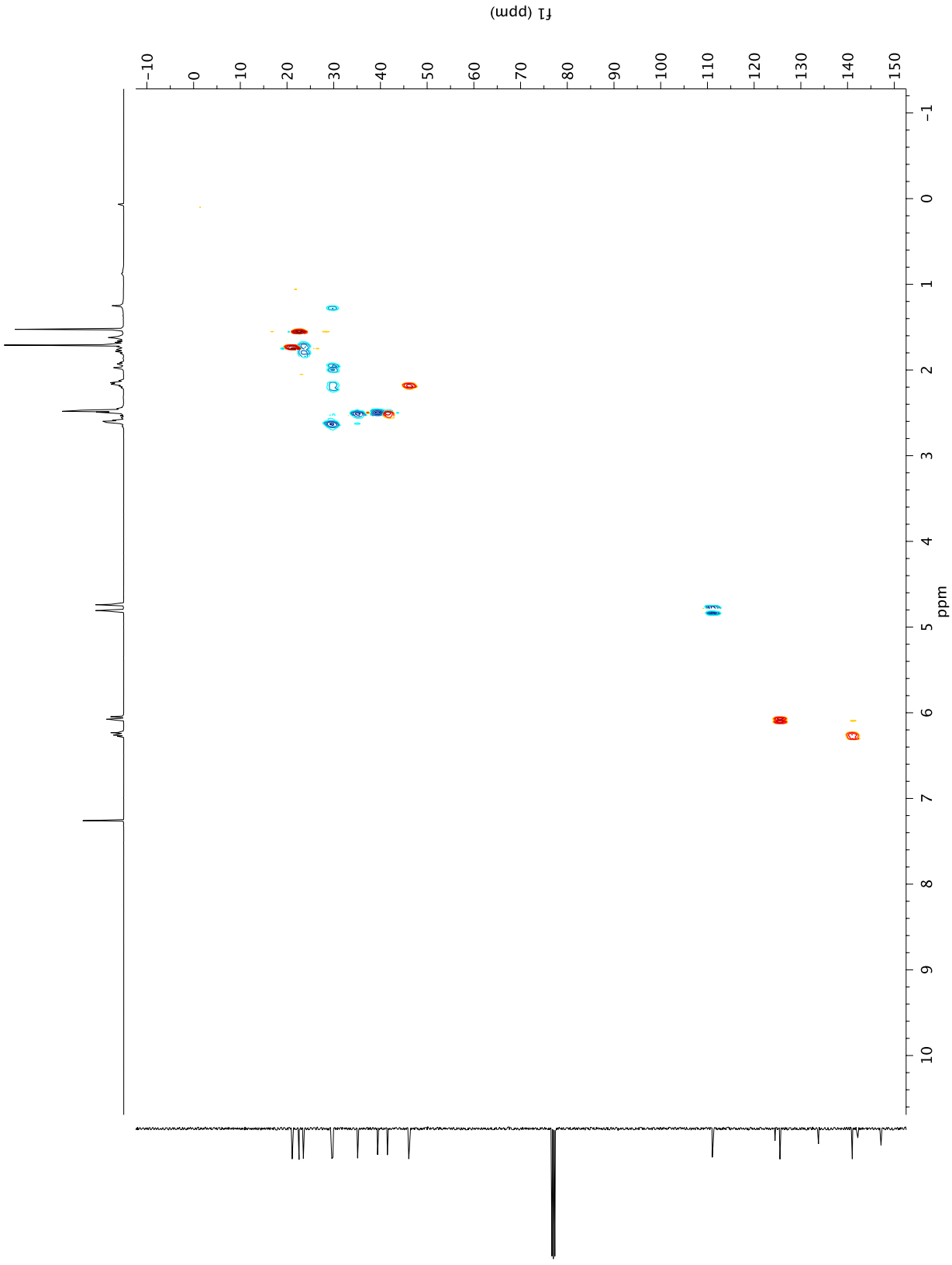

Figure A2.90 ^{1}H–^{13}C HSQC NMR (400 MHz, $CDCl_3$) of compound **73**

APPENDIX 3

X-Ray Crystallography Data

Relevant to Chapter 1

A3.1 CRYSTAL STRUCTURE ANALYSIS OF 73

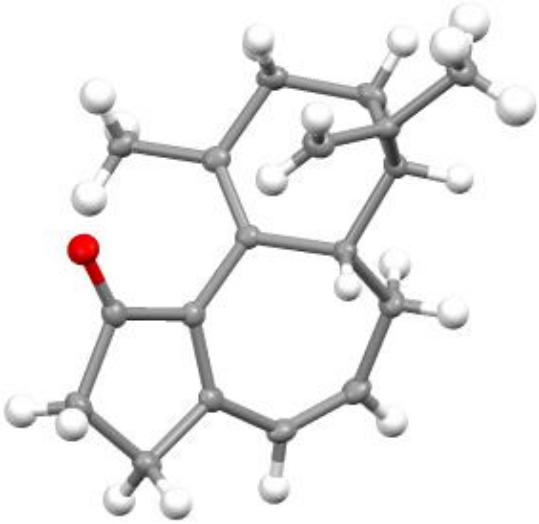

73

Low-temperature diffraction data (f- and w-scans) were collected on a Bruker AXS D8 VENTURE KAPPA diffractometer coupled to a PHOTON II CPAD detector with Cu K_a radiation (l = 1.54178 Å) from an IμS micro-source for the structure of compound **73**. The structure was solved by direct methods using SHELX[1] and refined against F^2 on all data by full-matrix least squares with SHELXL-2017[2] using established refinement techniques.[3] All non-hydrogen atoms were refined anisotropically. All hydrogen atoms were included into the model at geometrically calculated positions and refined using a riding model. The isotropic displacement parameters of all hydrogen atoms were fixed to 1.2 times the *U* value of the atoms they are linked to (1.5 times for methyl groups). Compound **73** crystallizes in the orthorhombic space group $P2_12_12_1$ with one molecule in the asymmetric unit.

*Table A3.1.1. Crystal data and structure refinement for **73**.*

Identification code	**73**	
Empirical formula	C18 H22 O	
Formula weight	254.35	
Temperature	100(2) K	
Wavelength	1.54178 Å	
Crystal system	Orthorhombic	
Space group	$P2_12_12_1$	
Unit cell dimensions	a = 6.7708(6) Å	a= 90°.
	b = 10.8979(10) Å	b= 90°.
	c = 19.414(2) Å	g = 90°.
Volume	1432.5(2) Å^3	
Z	4	

Density (calculated)	1.179 Mg/m^3
Absorption coefficient	0.541 mm^{-1}
F(000)	552
Crystal size	0.350 x 0.300 x 0.150 mm^3
Theta range for data collection	4.555 to 74.559°.
Index ranges	-8<=h<=8, -13<=k<=13, -24<=l<=24
Reflections collected	48838
Independent reflections	2938 [R(int) = 0.0345]
Completeness to theta = 67.679°	99.9 %
Absorption correction	Semi-empirical from equivalents
Max. and min. transmission	0.7538 and 0.6977
Refinement method	Full-matrix least-squares on F^2
Data / restraints / parameters	2938 / 0 / 174
Goodness-of-fit on F^2	1.059
Final R indices [I>2sigma(I)]	R1 = 0.0282, wR2 = 0.0699
R indices (all data)	R1 = 0.0283, wR2 = 0.0700
Absolute structure parameter	0.10(4)
Extinction coefficient	n/a
Largest diff. peak and hole	0.172 and -0.158 $e.Å^{-3}$

Table A3.1.2. Atomic coordinates (x 10^4) and equivalent isotropic displacement parameters (Å^{2}x 10^3) for ***73****. U(eq) is defined as one third of the trace of the orthogonalized U^{ij} tensor.*

	x	y	z	U(eq)
C(1)	7111(2)	2852(1)	6676(1)	16(1)
C(2)	5291(2)	2699(1)	7094(1)	18(1)
O(1)	4865(2)	1814(1)	7449(1)	25(1)
C(3)	4012(2)	3832(1)	6999(1)	23(1)
C(4)	5034(2)	4576(1)	6436(1)	22(1)
C(5)	6946(2)	3901(1)	6303(1)	17(1)
C(6)	8389(2)	4420(1)	5831(1)	20(1)
C(7)	9894(2)	3860(1)	5516(1)	21(1)
C(8)	10489(2)	2534(1)	5518(1)	22(1)
C(9)	9146(2)	1577(1)	5867(1)	16(1)
C(10)	10099(2)	302(1)	5786(1)	18(1)
C(15)	8664(2)	-766(1)	5788(1)	18(1)
C(16)	6898(2)	-743(1)	6084(1)	22(1)
C(17)	9404(3)	-1896(1)	5419(1)	27(1)
C(11)	11718(2)	133(1)	6336(1)	21(1)
C(12)	10898(2)	276(1)	7063(1)	20(1)
C(13)	9533(2)	1357(1)	7152(1)	17(1)

C(18)	9244(2)	1734(1)	7891(1)	21(1)
C(14)	8673(2)	1915(1)	6613(1)	15(1)

Table A3.1.3. Bond lengths [Å] and angles [°] for ***73****.*

C(1)-C(5)	1.3575(18)
C(1)-C(14)	1.4751(18)
C(1)-C(2)	1.4843(18)
C(2)-O(1)	1.2201(18)
C(2)-C(3)	1.5198(19)
C(3)-C(4)	1.526(2)
C(3)-H(3A)	0.9900
C(3)-H(3B)	0.9900
C(4)-C(5)	1.5119(19)
C(4)-H(4A)	0.9900
C(4)-H(4B)	0.9900
C(5)-C(6)	1.454(2)
C(6)-C(7)	1.335(2)
C(6)-H(6)	0.9500
C(7)-C(8)	1.500(2)
C(7)-H(7)	0.9500
C(8)-C(9)	1.5408(18)
C(8)-H(8A)	0.9900
C(8)-H(8B)	0.9900
C(9)-C(14)	1.5278(18)
C(9)-C(10)	1.5411(17)

C(9)-H(9)	1.0000
C(10)-C(15)	1.5166(19)
C(10)-C(11)	1.5414(19)
C(10)-H(10)	1.0000
C(15)-C(16)	1.327(2)
C(15)-C(17)	1.5105(19)
C(16)-H(16A)	0.9500
C(16)-H(16B)	0.9500
C(17)-H(17A)	0.9800
C(17)-H(17B)	0.9800
C(17)-H(17C)	0.9800
C(11)-C(12)	1.524(2)
C(11)-H(11A)	0.9900
C(11)-H(11B)	0.9900
C(12)-C(13)	1.5073(19)
C(12)-H(12A)	0.9900
C(12)-H(12B)	0.9900
C(13)-C(14)	1.3436(18)
C(13)-C(18)	1.5048(19)
C(18)-H(18A)	0.9800
C(18)-H(18B)	0.9800
C(18)-H(18C)	0.9800
C(5)-C(1)-C(14)	126.68(12)

C(5)-C(1)-C(2)	108.52(12)
C(14)-C(1)-C(2)	124.24(11)
O(1)-C(2)-C(1)	126.43(13)
O(1)-C(2)-C(3)	125.18(13)
C(1)-C(2)-C(3)	108.39(11)
C(2)-C(3)-C(4)	105.08(12)
C(2)-C(3)-H(3A)	110.7
C(4)-C(3)-H(3A)	110.7
C(2)-C(3)-H(3B)	110.7
C(4)-C(3)-H(3B)	110.7
H(3A)-C(3)-H(3B)	108.8
C(5)-C(4)-C(3)	104.58(11)
C(5)-C(4)-H(4A)	110.8
C(3)-C(4)-H(4A)	110.8
C(5)-C(4)-H(4B)	110.8
C(3)-C(4)-H(4B)	110.8
H(4A)-C(4)-H(4B)	108.9
C(1)-C(5)-C(6)	127.50(13)
C(1)-C(5)-C(4)	112.91(12)
C(6)-C(5)-C(4)	119.56(12)
C(7)-C(6)-C(5)	128.54(13)
C(7)-C(6)-H(6)	115.7
C(5)-C(6)-H(6)	115.7

C(6)-C(7)-C(8)	130.09(13)
C(6)-C(7)-H(7)	115.0
C(8)-C(7)-H(7)	115.0
C(7)-C(8)-C(9)	119.62(12)
C(7)-C(8)-H(8A)	107.4
C(9)-C(8)-H(8A)	107.4
C(7)-C(8)-H(8B)	107.4
C(9)-C(8)-H(8B)	107.4
H(8A)-C(8)-H(8B)	106.9
C(14)-C(9)-C(8)	112.21(11)
C(14)-C(9)-C(10)	113.70(11)
C(8)-C(9)-C(10)	108.55(11)
C(14)-C(9)-H(9)	107.4
C(8)-C(9)-H(9)	107.4
C(10)-C(9)-H(9)	107.4
C(15)-C(10)-C(9)	115.06(11)
C(15)-C(10)-C(11)	111.22(11)
C(9)-C(10)-C(11)	109.56(11)
C(15)-C(10)-H(10)	106.9
C(9)-C(10)-H(10)	106.9
C(11)-C(10)-H(10)	106.9
C(16)-C(15)-C(17)	121.35(13)
C(16)-C(15)-C(10)	124.36(13)

C(17)-C(15)-C(10)	114.29(12)
C(15)-C(16)-H(16A)	120.0
C(15)-C(16)-H(16B)	120.0
H(16A)-C(16)-H(16B)	120.0
C(15)-C(17)-H(17A)	109.5
C(15)-C(17)-H(17B)	109.5
H(17A)-C(17)-H(17B)	109.5
C(15)-C(17)-H(17C)	109.5
H(17A)-C(17)-H(17C)	109.5
H(17B)-C(17)-H(17C)	109.5
C(12)-C(11)-C(10)	111.74(11)
C(12)-C(11)-H(11A)	109.3
C(10)-C(11)-H(11A)	109.3
C(12)-C(11)-H(11B)	109.3
C(10)-C(11)-H(11B)	109.3
H(11A)-C(11)-H(11B)	107.9
C(13)-C(12)-C(11)	114.21(11)
C(13)-C(12)-H(12A)	108.7
C(11)-C(12)-H(12A)	108.7
C(13)-C(12)-H(12B)	108.7
C(11)-C(12)-H(12B)	108.7
H(12A)-C(12)-H(12B)	107.6
C(14)-C(13)-C(18)	124.23(12)

C(14)-C(13)-C(12)	122.00(12)
C(18)-C(13)-C(12)	113.77(12)
C(13)-C(18)-H(18A)	109.5
C(13)-C(18)-H(18B)	109.5
H(18A)-C(18)-H(18B)	109.5
C(13)-C(18)-H(18C)	109.5
H(18A)-C(18)-H(18C)	109.5
H(18B)-C(18)-H(18C)	109.5
C(13)-C(14)-C(1)	124.00(12)
C(13)-C(14)-C(9)	122.59(12)
C(1)-C(14)-C(9)	113.32(11)

Table A3.1.4. Anisotropic displacement parameters ($Å^2 x\ 10^3$) for ***73****. The anisotropic displacement factor exponent takes the form:* $-2p^2[\ h^2\ a^{*2}U^{11} + \ldots + 2\ h\ k\ a^*\ b^*\ U^{12}\ ]$

	U^{11}	U^{22}	U^{33}	U^{23}	U^{13}	U^{12}
C(1)	19(1)	14(1)	14(1)	-3(1)	-2(1)	-2(1)
C(2)	20(1)	18(1)	17(1)	-3(1)	-1(1)	0(1)
O(1)	25(1)	23(1)	28(1)	5(1)	6(1)	-2(1)
C(3)	24(1)	21(1)	24(1)	-3(1)	2(1)	5(1)
C(4)	26(1)	18(1)	22(1)	-2(1)	-2(1)	5(1)
C(5)	22(1)	14(1)	15(1)	-4(1)	-3(1)	0(1)
C(6)	28(1)	14(1)	18(1)	2(1)	-4(1)	-3(1)
C(7)	26(1)	18(1)	19(1)	4(1)	1(1)	-6(1)
C(8)	26(1)	18(1)	21(1)	2(1)	7(1)	-1(1)
C(9)	17(1)	14(1)	16(1)	2(1)	1(1)	0(1)
C(10)	18(1)	16(1)	18(1)	0(1)	4(1)	2(1)
C(15)	23(1)	16(1)	17(1)	1(1)	-2(1)	2(1)
C(16)	21(1)	19(1)	27(1)	-1(1)	-2(1)	-3(1)
C(17)	34(1)	18(1)	30(1)	-4(1)	2(1)	2(1)
C(11)	14(1)	19(1)	30(1)	1(1)	0(1)	2(1)
C(12)	19(1)	18(1)	24(1)	4(1)	-5(1)	0(1)
C(13)	16(1)	16(1)	19(1)	1(1)	-2(1)	-4(1)
C(18)	28(1)	19(1)	17(1)	2(1)	-5(1)	-3(1)

C(14)	15(1)	13(1)	16(1)	1(1)	0(1)	-3(1)

Table A3.1.5. Hydrogen coordinates (x 10^4) and isotropic displacement parameters (Å^{2}x 10^3) for ***73****.*

	x	y	z	U(eq)
H(3A)	3934	4309	7432	28
H(3B)	2659	3601	6856	28
H(4A)	4214	4607	6015	26
H(4B)	5293	5425	6594	26
H(6)	8241	5270	5734	24
H(7)	10716	4384	5250	25
H(8A)	11803	2480	5739	26
H(8B)	10660	2280	5032	26
H(9)	7869	1565	5608	19
H(10)	10775	294	5328	21
H(16A)	6071	-1447	6066	27
H(16B)	6461	-23	6314	27
H(17A)	8433	-2558	5465	41
H(17B)	10662	-2156	5622	41
H(17C)	9599	-1708	4930	41
H(11A)	12311	-693	6287	25
H(11B)	12773	747	6261	25
H(12A)	10176	-482	7187	24
H(12B)	12017	364	7387	24
H(18A)	8262	2394	7915	32
H(18B)	10501	2027	8080	32

H(18C)	8782	1029	8159	32

*Table A3.1.6. Torsion angles [°] for **73**.*

C(5)-C(1)-C(2)-O(1)	173.96(14)
C(14)-C(1)-C(2)-O(1)	2.0(2)
C(5)-C(1)-C(2)-C(3)	-5.26(15)
C(14)-C(1)-C(2)-C(3)	-177.21(12)
O(1)-C(2)-C(3)-C(4)	-172.03(14)
C(1)-C(2)-C(3)-C(4)	7.20(14)
C(2)-C(3)-C(4)-C(5)	-6.34(14)
C(14)-C(1)-C(5)-C(6)	-9.2(2)
C(2)-C(1)-C(5)-C(6)	179.09(13)
C(14)-C(1)-C(5)-C(4)	172.73(12)
C(2)-C(1)-C(5)-C(4)	1.03(15)
C(3)-C(4)-C(5)-C(1)	3.51(15)
C(3)-C(4)-C(5)-C(6)	-174.72(12)
C(1)-C(5)-C(6)-C(7)	20.2(2)
C(4)-C(5)-C(6)-C(7)	-161.89(14)
C(5)-C(6)-C(7)-C(8)	4.0(3)
C(6)-C(7)-C(8)-C(9)	6.5(2)
C(7)-C(8)-C(9)-C(14)	-53.97(17)
C(7)-C(8)-C(9)-C(10)	179.52(12)
C(14)-C(9)-C(10)-C(15)	81.49(14)
C(8)-C(9)-C(10)-C(15)	-152.87(11)

C(14)-C(9)-C(10)-C(11)	-44.68(15)
C(8)-C(9)-C(10)-C(11)	80.97(14)
C(9)-C(10)-C(15)-C(16)	-24.94(19)
C(11)-C(10)-C(15)-C(16)	100.38(16)
C(9)-C(10)-C(15)-C(17)	155.08(12)
C(11)-C(10)-C(15)-C(17)	-79.61(15)
C(15)-C(10)-C(11)-C(12)	-70.33(14)
C(9)-C(10)-C(11)-C(12)	58.00(14)
C(10)-C(11)-C(12)-C(13)	-44.76(16)
C(11)-C(12)-C(13)-C(14)	18.31(18)
C(11)-C(12)-C(13)-C(18)	-161.66(12)
C(18)-C(13)-C(14)-C(1)	-9.3(2)
C(12)-C(13)-C(14)-C(1)	170.73(12)
C(18)-C(13)-C(14)-C(9)	174.39(13)
C(12)-C(13)-C(14)-C(9)	-5.6(2)
C(5)-C(1)-C(14)-C(13)	138.53(14)
C(2)-C(1)-C(14)-C(13)	-51.01(19)
C(5)-C(1)-C(14)-C(9)	-44.87(18)
C(2)-C(1)-C(14)-C(9)	125.60(13)
C(8)-C(9)-C(14)-C(13)	-104.09(14)
C(10)-C(9)-C(14)-C(13)	19.59(18)
C(8)-C(9)-C(14)-C(1)	79.25(14)
C(10)-C(9)-C(14)-C(1)	-157.07(11)

(1) Sheldrick, G. M. *Acta Cryst.* **1990**, A46, 467–473.
(2) Sheldrick, G. M. *Acta Cryst.* **2015**, C71, 3–8.
(3) Müller, P. *Crystallography Reviews* **2009**, *15*, 57–83.

CHAPTER 2

Acyl-Amination of Arenes via Aryne Formation[i]

2.1 INTRODUCTION AND BACKGROUND

Over the past 50 years, arynes have been of considerable interest to synthetic chemists owing to their diverse modes of reactivity. Although numerous procedures for their preparation are known, the majority of these approaches relies on high temperatures or strong base additives (Scheme 2.1.1).[1] However, in 1983 the Kobayashi group disclosed a comparatively mild procedure for *in situ* aryne preparation utilizing *o*-silylaryl triflates (highlighted in blue).[2] Thus, treatment with fluoride will result in desilylation with concomitant triflate elimination, providing a highly reactive benzyne intermediate **91**.

(i) This research was a collaborative effort between A. C. Wright, C. K. Haley, and G. Lapointe, see reference 14.

*Scheme 2.1.1. Classical Preparative Procedures for Benzyne (**91**)*

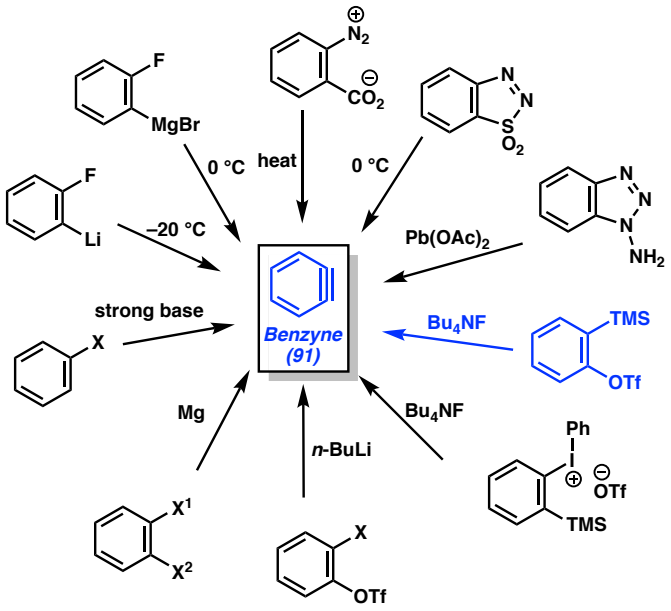

The insertion of aromatic systems into carbon–carbon and carbon–heteroatom σ bonds is a desirable transformation in organic synthesis.[3] In 2005, our group reported an insertion of arenes into β-ketoesters to form acyl-alkylated products using arynes generated *in situ* from *o*-silylphenyl triflates such as **92** under Kobayashi conditions (Scheme 2.1.2).[4] Following this report, other aryne insertions were disclosed using a variety of substrates, including malononitriles,[5] α-cyanocarbonyls,[6] acylated fluorenes[7] and β-ketosulfones.[8] More recently, Saito and co-workers developed a procedure for inserting pyridynes into cyclic ureas in order to construct various bicyclic heterocycles.[9] Herein, we expand the scope of this aryne reaction manifold to include acyclic imides and anhydrides **95** in order to produce ketoamido- and ketoacyloxyarenes **96**. The ketoamide products accessed by this method have been used to generate a variety of valuable structural motifs such as quinolones (**98**),[10] *ortho*-acylanilines (**99**)[11] and indoles[12] (**100**, Scheme 2.1.3). Work from the Greaney group demonstrated that the insertion of amides into arynes

afforded similar acyl-aminated products.[13] However, the scope of their method was limited to *N*-arylated amide substrates, prohibiting subsequent derivatization.

Scheme 2.1.2. Aryne Insertion Methods

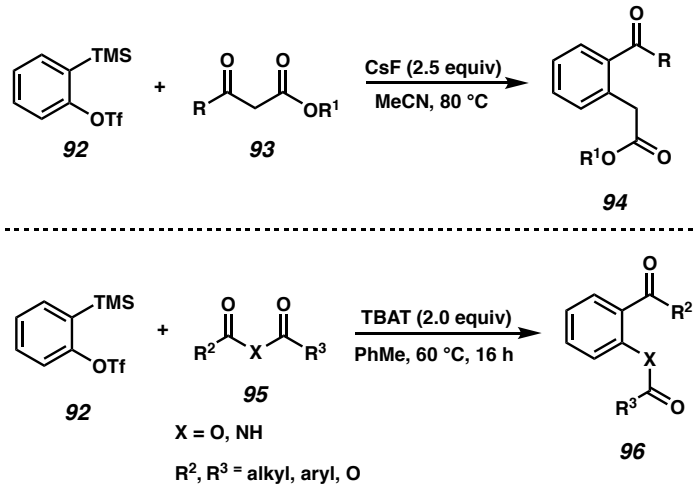

*Scheme 2.1.3. Derivatization of Aryl Ketoamides **97***

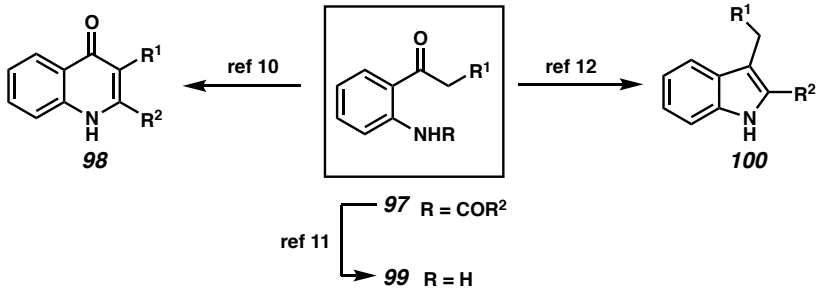

2.2 RESULTS AND DISCUSSION

We initiated our synthetic studies by optimizing conditions for the insertion reaction using acetylacetamide (**101**) and silylaryl triflate **92** (Table 2.2.1).[14] Implementing CsF as the fluoride source to trigger aryne generation, we observed a mixture of the desired ketoamide **102** and undesired imide byproduct **103**. Presumably, **103** is formed via nucleophilic addition of **101** to aryne **91** followed by proton quenching of the resultant aryl anion intermediate (Scheme 2.2.1).

Although all three fluoride reagents afforded the desired product, KF and tetrabutylammonium difluorotriphenylsilicate (TBAT) substantially improved selectivity for the desired amide. Additional screening of solvent and temperature demonstrated that using TBAT in PhMe at 60 °C maximized product yields and minimized byproduct formation (entry 4).

Table 2.2.1. Reaction Optimization

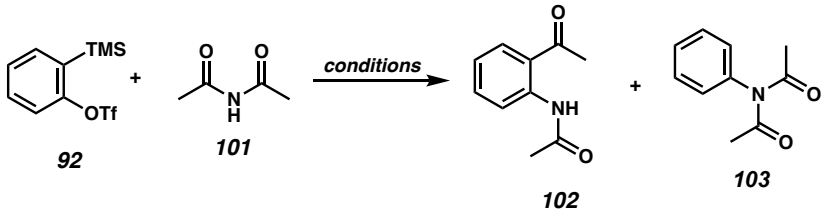

entry	fluoride source	solvent	yield (%)	*102*:*103*
1	CsF	MeCN	49	1.25:1
2	KF/18-crown-6	THF	37	10:1
3	TBAT	THF	21	10:1
4	TBAT	PhMe	62	>20:1

*Scheme 2.2.1. Plausible Mechanism for Formation of Desired **102** and Byproduct **103***

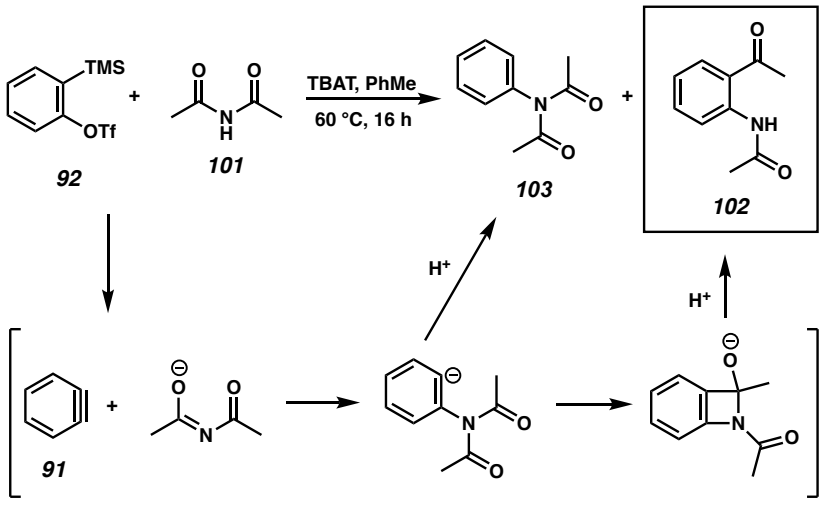

With optimized conditions in hand, we explored the substrate scope with respect to the imide substrate (Table 2.2.2). Imides possessing either aliphatic or aromatic substituents afforded the

corresponding ketoamides in moderate to good yields (entries 1–5). An acylated urethane also underwent insertion, albeit with reduced yield (entry 6). However, *N*-substituted imides afforded no product (entry 7). Acetic anhydride was found to be a suitable substrate, delivering the corresponding ketoacyloxyarene (entry 8) in 54% yield. Unfortunately, benzoic anhydride failed to provide any insertion product (entry 9).

Table 2.2.2. Imide Substrate Scope[a]

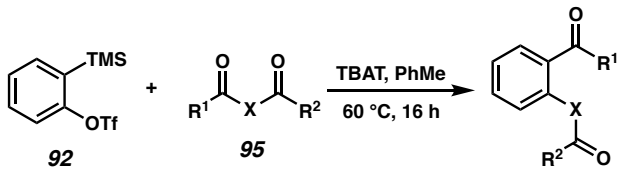

entry	product	R^1	R^2	X	yield (%)[b]
1	***102***	Me	Me	NH	89
2	***104a***	Et	Et	NH	88
3	***104b***	Ph	Ph	NH	68
4	***104c***	*i*-Pr	*i*-Pr	NH	78
5	***104d***	*i*-Bu	*i*-Bu	NH	79
6	***104e***	OMe	Bn	NH	24
7	***104f***	Me	Me	NMe	0
8	***104g***	Me	Me	O	54
9	***104h***	Ph	Ph	O	0

[a]Reaction conditions: TBAT (2.0 equiv), **95** (0.08 M in PhMe), and **92** (1.5 equiv), 60 °C, 16 h. [b]All reported yields are for isolated products.

We next investigated the tolerance of the reaction to other aryne precursors (Table 2.2.3). Gratifyingly, substituted carbocyclic substrates (**105a**–**d**) offered moderate yields of the corresponding aryl ketoamide product (**106a**–**d**). Furthermore, we observed that insertion into an unsymmetrical aryne formed from methoxylated **105d** occurred with good regioselectivity. Unfortunately, the presence of electron-withdrawing fluoride substituents in substrate **105e** failed to undergo insertion.

Table 2.2.3. Aryne Substrate Scope[a]

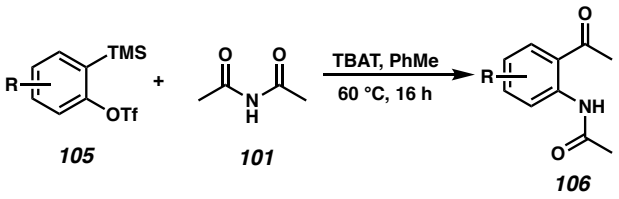

entry	aryne precursor	major product	yield (%)[b]
1	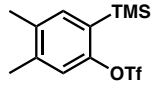 ***105a***	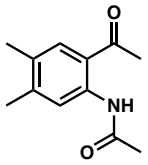 ***106a***	31
2	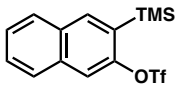 ***105b***	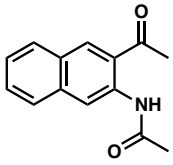 ***106b***	44
3	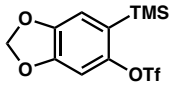 ***105c***	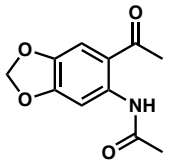 ***106c***	65
4	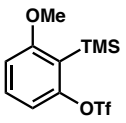 ***105d***	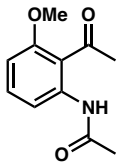 ***106d***	47
5	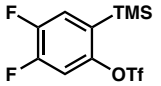 ***105e***	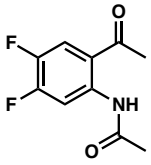 ***106e***	0

[a]TBAT (2.0 equiv), **101** (0.08 M in PhMe), and **105** (1.5 equiv), 60 °C, 16 h. [b]All reported yields are for isolated products.

To demonstrate the synthetic utility of this method, we elaborated several of these acylamide insertion products to substituted quinolones via a base-initiated Camps cyclization in a two-step,

one-pot sequence (Figure 2.2.1).[8] Gratifyingly, quinolones **107a–c** were delivered in moderate yield. Moreover, formation of **107b** and **107c** occurred with high regioselectivity for the aryne insertion, producing a single isolable structural isomer in each case.

Figure 2.2.1 Camps Cyclization of Insertion Products to Provide Quinolones

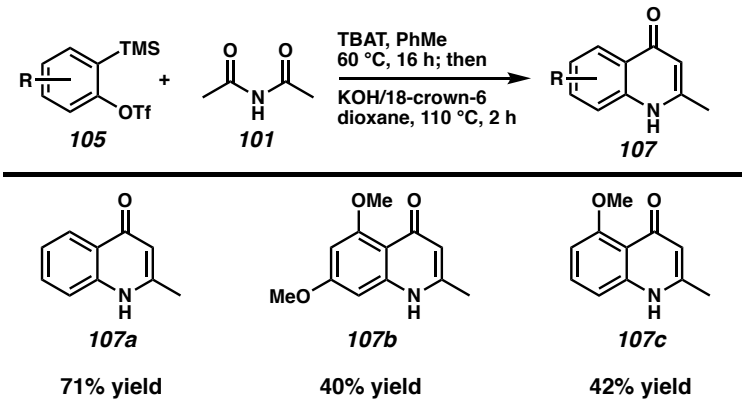

2.3 CONCLUSION

In summary, we have developed a method for inserting arynes into acyclic imides and anhydrides to generate aryl ketoamides and ketoacyloxyarenes, respectively. These products are capable of further derivatization to provide an array of useful scaffolds such as quinolones, indoles, and ketoanilines. Our laboratory is pursuing further development of this technology as it relates to other derivatizations and application in multi-step synthesis.

2.4 EXPERIMENTAL SECTION

2.4.1 MATERIALS AND METHODS

Unless otherwise stated, reactions were performed in flame-dried glassware under nitrogen atmosphere using dry, deoxygenated solvents (distilled or passed over a column of activated alumina). Reaction temperatures were controlled by an IKAmag temperature modulator. Thin layer chromatography (TLC) was performed using E. Merck silica gel 60 F254 precoated plates (0.25 mm) and visualized by UV fluorescence quenching. Silia*Flash* P60 Academic Silica gel (particle size 0.040-0.063 mm) was used for flash chromatography. ^{1}H and ^{13}C NMR spectra were recorded either on a Bruker AV III HD spectrometer equipped with a Prodigy liquid nitrogen temperature cryoprobe (400 MHz and 101 MHz, respectively) or on a Varian Inova 500 (500 MHz and 125 MHz, respectively) and are reported relative to Me_4Si (δ 0.0). IR spectra were recorded on a Perkin Elmer Paragon 1000 Spectrometer and are reported in frequency of absorption (cm^{-1}). Preparatory HPLC was performed using an Agilent 1100 Series HPLC utilizing a Zorbax XDB-C18 column purchased from Agilent Technologies. HRMS were acquired using an Agilent 6200 Series TOF with an Agilent G1978A Multimode source in electrospray ionization (ESI), atmospheric pressure chemical ionization (APCI) or mixed (MM) ionization mode or with a JEOL JMS-600H in fast atom bombardment (FAB+).

2.4.2 PREPARATIVE PROCEDURES

Imide Synthesis and Characterization Data

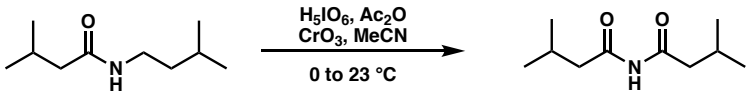

108 ***109***

Imide 109: In air, H_5IO_6 (4.42 g, 19.4 mmol, 6.0 equiv), CrO_3 (16.2 mg, 0.16 mmol, 5.0 mol %), and MeCN (46 mL) were sequentially added to a round bottom flask equipped with a magnetic stir bar. The reaction mixture was stirred for 30 minutes at ambient temperature, at which point acetic anhydride (1.8 mL, 19.4 mmol, 6.0 equiv) was added. The mixture was cooled to 0 °C, and **108** (553 mg, 3.23 mmol, 1.0 equiv) was added slowly. The resulting mixture was allowed to warm to ambient temperature over 12 h. The reaction was quenched with ice water and extracted with EtOAc (4 x 40 mL). The resulting organic layers were concentrated in vacuo and purified by column chromatography (20% EtOAc in hexanes) to afford **109** (89 mg, 15% yield) as a white solid; R_f = 0.15 (10% EtOAc in hexanes); ^{1}H NMR (400 MHz, $CDCl_3$) δ 8.72 (br s, 1H), 2.47 (d, *J* = 9.4, 4H), 2.14 (heptet, *J* = 9.0 Hz, 2H), 0.98 (s, 12 H); ^{13}C (101 MHz, $CDCl_3$) δ 173.9, 46.3, 25.2, 22.4. IR (Neat Film, NaCl) 3272.4, 3170.7, 2957.7, 2871.5, 1728.6, 1505.7, 1466.8, 1386.4, 1367.0, 1294.4, 1246.8, 1181.5, 1160.6, 1120.1, 1090.0 cm^{-1}; HRMS (FAB+) *m/z* calc'd for $C_{10}H_{20}NO_2$ $[M+H]^+$: 186.1494, found 186.1500.

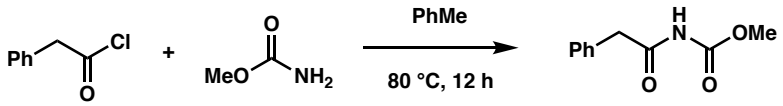

110 ***111*** ***112***

Urethane 112: In air, 2-phenylacetyl chloride (**110**, 309.2 mg, 0.26 mL, 2.00 mmol, 1.0 equiv), methyl carbamate (**111**, 450.4 mg, 6.00 mmol, 3.0 equiv), and PhMe (10 mL) were added.

The reaction vessel was heated to 80 °C for 12 h. The reaction was cooled to 23 °C, concentrated, and purified by column chromatography (10% EtOAc in hexanes) to afford **112** (34.1 mg, 9% yield) as white solid; R_f = 0.40 (50% EtOAc in hexanes); ^{1}H NMR (500 MHz, $CDCl_3$) δ 7.48 (br s, 1H), 7.36–7.33 (m, 2H), 7.31–7.27 (m, 3H), 4.07 (s, 2H), 3.78 (s, 3H); ^{13}C (126 MHz, $CDCl_3$) δ 152.0, 138.5, 133.3, 129.6, 128.6, 127.4, 110.0, 53.1. IR (Neat Film, NaCl) 3246.1, 3172.3, 3014.0, 2259.7, 1788.1, 1757.5, 1686.2, 1520.2, 1455.7, 1257.2, 1216.1, 1192.1, 1144.1, 1049.9, 781.9, 705.3 cm^{-1}; HRMS (ESI-APCI) *m/z* calc'd for $C_{10}H_{12}NO_3$ $[M+H]^+$: 194.0817, found 194.0817.

Aryl Ketoamide Synthesis and Characterization Data

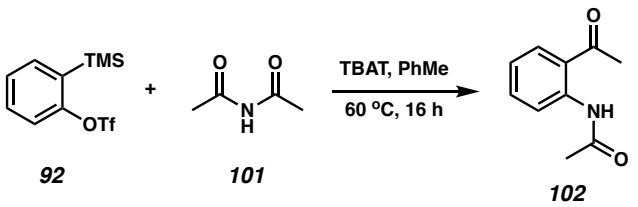

Representative Procedure for Acylamination

A 2-dram vial equipped with a magnetic stir bar was charged with TBAT (144.7 mg, 0.268 mmol, 2.0 equiv) and imide **101** (13.6 mg, 0.134 mmol, 1.0 equiv). The vial was purged with nitrogen, and PhMe (1.6 mL) was added via syringe followed by silyl triflate **92** (60.0 mg, 0.201 mmol, 1.5 equiv). The vial was sealed and placed in an aluminum block preheated to 60 °C. The reaction mixture was stirred at this temperature for 16 h, then it was allowed to cool to 23 °C. The mixture was concentrated in vacuo and purified by column chromatography (10% EtOAc in hexanes) to afford **102** (23.6 mg, 89% yield) as a white solid. Characterization data match those previously reported;[15] ^{1}H NMR (300 MHz, $CDCl_3$) δ 11.70 (s, 1H), 8.74 (d, *J* = 8.6 Hz, 1H), 7.90 (d, *J* = 8.2 Hz, 1H), 7.56 (dd, *J* = 7.3, 8.6 Hz, 1H), 7.12 (dd, *J* = 8.2, 7.3 Hz, 1H), 2.67 (s, 3H), 2.23 (s, 3H).

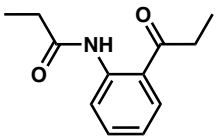

104a

Ethyl ketone 104a: Prepared according to the representative procedure using *N*-propionylpropionamide (17.3 mg, 0.134 mmol, 1.0 equiv) and silyl triflate **92** (60.0 mg, 0.201 mmol, 1.5 equiv). The reaction was purified by column chromatography (10% EtOAc in hexanes) to afford **104a** (24.0 mg, 88% yield) as a white solid. Characterization data match those previously reported.[16] ^{1}H NMR (300 MHz, $CDCl_3$) δ 11.78 (s, 1H), 8.78 (d, *J* = 9.0 Hz, 1H), 7.93 (d, *J* = 9.0 Hz, 1H), 7.57–7.51 (m, 1H), 7.13–7.07 (m, 1H), 3.06 (q, *J* = 7.2 Hz, 2H), 2.50 (q, *J* = 7.6, 2H), 1.31–1.20 (m, 6H).

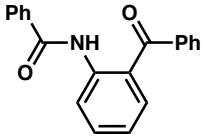

104b

Phenyl ketone 104b: Prepared according to the representative procedure using *N*-benzoylbenzamide (30.2 mg, 0.134 mmol, 1.0 equiv) and silyl triflate **92** (60.0 mg, 0.201 mmol, 1.5 equiv). The reaction was purified by column chromatography (10% EtOAc in hexanes) to afford **104b** (27.4 mg, 68% yield) as a white solid. Characterization data match those previously reported.[17] ^{1}H NMR (400 MHz, $CDCl_3$) δ 12.00 (s, 1H), 8.92 (d, *J* = 8.2 Hz, 1H), 8.11–8.08 (m, 2H), 7.74 (t, *J* = 4.3 Hz, 2H), 7.66–7.59 (m, 3H), 7.56–7.49 (m, 5H), 7.14 (s, 1H).

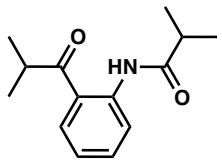

104c

Isopropyl ketone 104c: Prepared according to the representative procedure using *N*-isobutyrylisobutyramide (23.6 mg, 0.150 mmol, 1.0 equiv) and silyl triflate **92** (67.1 mg, 0.225 mmol, 1.5 equiv). Purification was achieved by preparatory HPLC to afford **104c** (27.3 mg, 78% yield) as a white solid; R_f = 0.4 (10% EtOAc in hexanes); ^{1}H NMR (400 MHz, $CDCl_3$) δ 11.80 (br s, 1H), 8.79 (d, *J* = 6 Hz, 1H), 7.93 (d, *J* = 6 Hz, 1H), 7.53 (t, *J* = 4.5 Hz, 1H), 7.10 (t, *J* = 6 Hz, 1H), 3.65 (sept, *J* = 6 Hz, 1H), 2.62 (sept, *J* = 6 Hz, 1H), 1.28 (d, *J* = 6 Hz, 6H), 1.23 (d, *J* = 6.0 Hz, 6H); ^{13}C (101 MHz, $CDCl_3$) δ 209.2, 176.6, 141.7, 134.8, 130.6, 122.2, 121.1, 120.7, 37.6, 36.3, 19.6 (2 unresolved signals); IR (Neat Film, NaCl) 3251.4, 2970.8, 2903.3, 2872.9, 1700.1, 1653.0, 1604.8, 1583.4, 1521.7, 1517.1, 1467.7, 1450.3, 1383.3, 1356.5, 1350.9, 1301.9, 1239.0, 1211.6, 1157.4, 1099.6, 1083.7, 976.8, 755.1 cm^{-1}; HRMS (MM: ESI-APCI) *m/z* calc'd for $C_{14}H_{20}NO_2$ $[M+H]^+$: 234.1489, found: 234.1490.

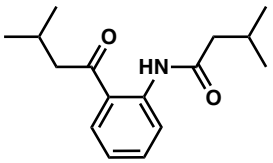

104d

Isobutyryl ketone 104d: Prepared according to the representative procedure using corresponding imide **109** (37.1 mg, 0.200 mmol, 1.0 equiv) and silyl triflate **92** (89.5 mg, 0.300 mmol, 1.5 equiv). Purification was achieved by preparatory HPLC to afford **104d** (41.3 mg, 79% yield) as a white solid. R_f = 0.30 (10% EtOAc in hexanes); ^{1}H NMR (400 MHz, $CDCl_3$) δ 11.73 (br s, 1H), 8.77 (d, *J* = 1.6 Hz, 1H), 7.90 (d, *J* = 10.8 Hz, 1H), 7.53 (t, *J* = 9.8 Hz, 1H), 7.10 (t, *J* =

9.8 Hz, 1H), 2.88 (d, *J* = 9.2 Hz, 2H), 2.33–2.19 (m, 4H), 1.03–0.99 (m, 12H); ^{13}C (126 MHz, $CDCl_3$) 205.0, 172.1, 141.0, 134.9, 130.4, 122.2, 121.92, 120.9, 49.0, 48.1, 26.3, 25.6, 22.7, 22.5. IR (Neat Film, NaCl) 3255.4, 2957.6, 2929.9, 2870.7, 1698.8, 1651.9, 1583.5, 1520.0, 1450.7, 1386.2, 1366.0, 1298.9, 1281.3, 1258.1, 1201.8, 1163.5, 1114.3, 1003.9, 947.5, 754.1 cm^{-1}; HRMS (MM: ESI-APCI) *m/z* calc'd for $C_{16}H_{24}NO_2$ $[M+H]^+$: 262.1802, found: 262.1804.

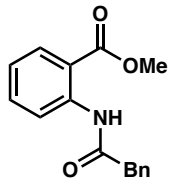

104e

Ester 104e: Prepared according to the representative procedure using carbamate **112** (25.9 mg, 0.134 mmol, 1.0 equiv) and silyl triflate **92** (60.0 mg, 0.201 mmol, 1.5 equiv). The reaction was purified by column chromatography (10% EtOAc in hexanes) to afford **104e** (8.7 mg, 24% yield) as a white solid. R_f = 0.30 (10% EtOAc in hexanes); ^{1}H NMR (400 MHz, $CDCl_3$) δ 11.04 (br s, 1H), 8.70 (dd, *J* = 8.0 Hz, 1.2 Hz, 1H), 7.99 (dd, *J* = 8.0, 1.2 Hz, 1H), 7.54–7.49 (m, 1H), 7.41–7.28 (m, 5H), 7.08–7.01 (m, 1H), 3.86 (s, 3H), 3.76 (s, 2H); ^{13}C (101 MHz, $CDCl_3$) 170.0, 168.5, 141.4, 134.6, 134.4, 130.8, 129.5, 129.3, 128.9, 127.3, 122.6, 120.4, 52.3, 45.9. IR (Neat Film, NaCl) 2917.9, 1687.6, 1588.4, 1523.0, 1448.6, 1309.3, 1263.3, 1193.6, 1088.9, 756.5 cm^{-1}; HRMS (MM: ESI-APCI) *m/z* calc'd for $C_{16}H_{15}NO_3$ $[M+H]^+$: 270.1125, found: 270.1129.

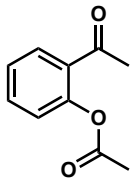

104g

Methyl ketone 104g: Prepared according to the representative procedure using acetic anhydride (13.7 mg, 0.134 mmol, 1.0 equiv) and silyl triflate **92** (60.0 mg, 0.201 mmol, 1.5 equiv). The reaction was purified by column chromatography (10% EtOAc in hexanes) to afford **104g** (12.8 mg, 54% yield) as a white solid. Characterization data match those previously reported.[18] ^{1}H NMR (300 MHz, $CDCl_3$) δ 7.78 (d, *J* = 7.8 Hz, 1H), 7.50 (t, *J* = 7.7 Hz, 1H), 7.28 (t, *J* = 7.6 Hz, 1H), 7.10 (d, *J* = 8.0 Hz, 1H), 2.52 (s, 3H), 2.32 (s, 3H).

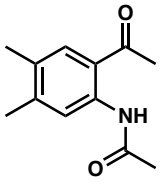

106a

Amide 106a: Prepared according to the representative procedure using imide **101** (8.4 mg, 0.083 mmol, 1.0 equiv) and silyl triflate **105a** (40.5 mg, 0.124 mmol, 1.5 equiv). Purified by column chromatography (10% EtOAc in hexanes) to afford **106a** (6.5 mg, 31% yield) as a white solid. R_f = 0.15 (10% EtOAc in hexanes); ^{1}H NMR (400 MHz, $CDCl_3$) δ 11.63 (br s, 1H), 8.53 (s, 1H), 7.61 (s, 1H), 2.63 (s, 3H), 2.31 (s, 3H), 2.26 (s, 3H), 2.21 (s, 3H); ^{13}C (101 MHz, $CDCl_3$) δ 202.4, 169.4, 145.3, 139.1, 132.4, 130.6, 121.5, 119.8, 28.6, 25.6, 20.6, 19.4. IR (Neat Film, NaCl) 3238.4, 2917.3, 1692.5, 1643.4, 1579.0, 1514.1, 1450.2, 1397.3, 1353.6, 1286.8, 1270.0, 1235.1, 1018.7, 876.4, 758.9, 659.3 cm^{-1}; HRMS (MM: ESI-APCI) *m/z* calc'd for $C_{12}H_{16}NO_2$ $[M+H]^+$: 206.1176, found: 206.1171.

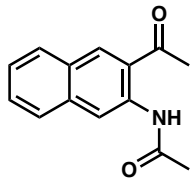

106b

Amide 106b: Prepared according to the representative procedure using imide **101** (29.0 mg, 0.287 mmol, 1.0 equiv) and silyl triflate **105b** (150.0 mg, 0.431 mmol, 1.5 equiv). Purification was achieved by preparatory HPLC to afford **106b** (28.7 mg, 44% yield) as a white solid; R_f = 0.35 (30% EtOAc in hexanes); ^{1}H NMR (400 MHz, $CDCl_3$) δ 11.50 (br s, 1H), 9.12, (s, 1H), 8.44 (s, 1H), 7.83 (d, *J* = 9.0 Hz, 2H), 7.57 (t, *J* = 7.5 Hz, 1H), 7.43 (t, *J* = 7.5 Hz, 1H), 2.80 (s, 3H), 2.27 (s, 3H); ^{13}C (101 MHz, $CDCl_3$) 203.0, 169.3, 136.7, 136.1, 134.3, 129.7, 128.9, 128.2, 127.7, 125.6, 122.7, 117.7, 28.7, 25.6; IR (Neat Film, NaCl) 3217.8, 1682.2, 1654.4, 1577.0, 1546.1, 1480.7, 1437.2, 1352.5, 1386.4, 1286.3, 1277.9, 1203.7, 1148.0, 1020.5, 953.6, 885.1, 742.1, 656.2 cm^{-1}; HRMS (MM: ESI-APCI) *m/z* calc'd for $C_{14}H_{14}NO_2$ $[M+H]^+$: 228.1019, found: 228.1022.

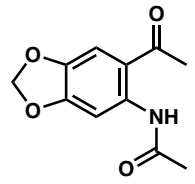

106c

Dioxolane 106c: Prepared according to the representative procedure using imide **101** (20.4 mg, 0.201 mmol, 1.0 equiv) and silyl triflate **105c** (103.4 mg, 0.302 mmol, 1.5 equiv). Purification was achieved by preparatory HPLC to afford **106c** (28.9 mg, 65% yield) as a white solid; R_f = 0.55 (50% EtOAc in hexanes); ^{1}H NMR (400 MHz, $CDCl_3$) δ 12.08 (br s, 1H), 8.37 (s, 1H), 7.25 (s, 1H), 6.02 (s, 2H), 2.57 (s, 3H), 2.20 (s, 3H); ^{13}C NMR (75 MHz, CDCl3) δ 200.6, 169.5, 152.9, 142.4, 139.3, 115.1, 109.6, 102.1, 101.5, 28.8, 25.6. IR (Neat Film, NaCl) 2916.7, 1692.6, 1611.8,

1502.7, 1483.5, 1433.8, 1370.2, 1342.5, 1243.2, 1178.9, 1118.8, 1044.8, 927.0 cm^{-1}; HRMS (MM: ESI-APCI) *m/z* calc'd for $C_{11}H_{12}NO_4$ $[M+H]^+$: 222.0761, found: 222.0766.

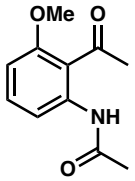

106d

Methyl ether 106d: Prepared according to the representative procedure using imide **101** (13.6 mg, 0.134 mmol, 1.0 equiv) and silyl triflate **105d** (66.0 mg, 0.201 mmol, 1.5 equiv). The reaction was purified by column chromatography (10% EtOAc in hexanes) to afford **106d** (13.0 mg, 47% yield) as a white solid; R_f = 0.20 (20% EtOAc in hexanes); ^{1}H NMR (500 MHz, $CDCl_3$) δ 10.49 (s, 1H), 8.07 (d, *J* = 8.3 Hz, 1H), 7.40 (td, *J* = 8.4, 0.5 Hz, 1H), 6.69 (dd, *J* = 8.4, 0.9 Hz, 1H), 2.57 (s, 3H), 3.90 (s, 3H), 2.61 (s, 3H); ^{13}C NMR (126 MHz, $CDCl_3$) δ 204.6, 169.2, 160.0, 139.2, 133.7, 116.5, 114.0, 106.2, 55.8, 33.7, 25.5; IR (Neat Film, NaCl) 3086.8, 2947.7, 1698.6, 1639.6, 1634.0, 1528.8, 1470.6, 1403.5, 1273.1, 1243.4, 1195.9, 1093.2, 1017.3, 967.4, 802.3, 735.2, 610.8 cm^{-1}; HRMS (MM: ESI-APCI) *m/z* calc'd for $C_{11}H_{14}NO_3$ $[M+H]^+$: 262.1802, found: 262.1804.

Quinolone Synthesis and Characterization Data

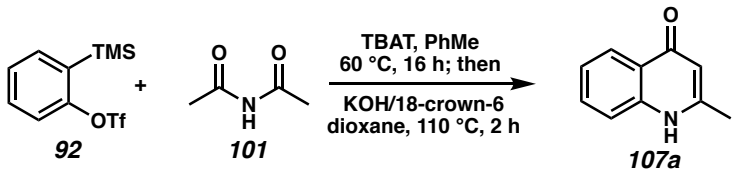

92 ***101*** ***107a***

Representative Procedure for Quinolone Synthesis

A 2-dram vial equipped with a magnetic stir bar was charged with TBAT (144.7 mg, 0.268 mmol, 2.0 equiv) and imide **101** (13.6 mg, 0.134 mmol, 1.0 equiv). The vial was purged with

nitrogen, and PhMe (1.6 mL) was added via syringe followed by silyl triflate **92** (60.0 mg, 0.201 mmol, 1.5 equiv). The vial was sealed and placed in an aluminum block preheated to 60 °C. The reaction mixture was stirred at this temperature for 16 h, then it was allowed to cool to 23 °C. The mixture was concentrated in vacuo and then charged with dioxane (1.6 mL), KOH (22.6 mg, 0.402 mmol, 3.0 equiv), and 18-crown-6 (106.3 mg, 0.402 mmol, 3.0 equiv). The reaction vial was sealed and heated to 110 °C and stirred for 2 h. The reaction was allowed to cool, diluted with CH_2Cl_2 (10 mL), neutralized to pH ~7, and washed with brine (10 mL). The layers were separated, and the aqueous layer was back-extracted with CH_2Cl_2 (2 x 10 mL). The combined organic layers were dried (Na_2SO_4), concentrated, and purified by column chromatography (CH_2Cl_2 to 5% MeOH in CH_2Cl_2) to provide **107a** (15.1 mg, 71% yield) as a yellow solid. Characterization data match those previously reported.[19] ^{1}H NMR (400 MHz, $CDCl_3$) δ 12.04 (s, 1H), 7.79 (d, *J* = 10.8 Hz, 1H), 7.65–7.62 (m, 2H), 7.40–7.36 (m, 1H), 6.74 (s, 1H), 2.61 (d, *J* = 1.4 Hz, 3H).

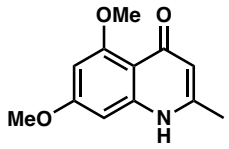

107b

Quinolone 107b: Prepared according to the representative procedure using imide **101** (13.6 mg, 0.134 mmol, 1.0 equiv) and 3,5-dimethoxy-2-(trimethylsilyl)phenyl trifluoromethanesulfonate (66.0 mg, 0.201 mmol, 1.5 equiv) to provide quinolone **107b** (11.8 mg, 40% yield) as a brown solid. Characterization data match those previously reported.[20] ^{1}H NMR (400 MHz, $CDCl_3$) δ 7.08 (s, 1H), 6.75 (s, 1H), 6.74 (s, 1H), 6.24–6.23 (m, 1H), 3.78 (s, 6H), 2.17 (s, 3H).

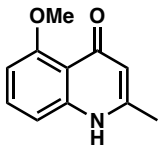

107c

Quinolone 107c: Prepared according to the representative procedure using imide **101** (13.6 mg, 0.134 mmol, 1.0 equiv) and silyl triflate **105d** (66.0 mg, 0.201 mmol, 1.5 equiv) to provide quinolone **107c** (10.6 mg, 42% yield) as a beige solid. $R_f = 0.35$ (10% MeOH in CH_2Cl_2); ^{1}H NMR (400 MHz, $CDCl_3$) δ 7.29–7.27 (m, 1H), 7.21 (t, *J* = 8.2, 1H), 7.11 (br s, 1H), 6.95 (d, *J* = 8.0 Hz, 1H), 6.67 (dd, *J* = 12.0, 11.2 Hz, 1H), 3.81 (s, 3H), 2.18 (s, 3H); ^{13}C (126 MHz, $CDCl_3$) 168.2, 160.2, 139.1, 134.8, 129.7, 111.8, 110.1, 105.6, 100.0 55.3, 24.8. IR (Neat Film, NaCl) 2920.7, 1664.8, 1598.3, 1548.7, 1492.8, 1425.9, 1369.9, 1252.6, 1156.1, 1044.1, 775.1 cm^{-1}; HRMS (MM: ESI-APCI) *m/z* calc'd for $C_{11}H_{12}NO_2$ $[M+H]^+$: 190.0863, found: 190.0866.

Preparatory HPLC Conditions

Entry	Product	Conditions	Retention Time (min)
1	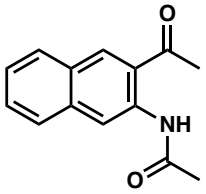 ***106b***	HPLC Zorbax XDB-C18 column 20% to 60% MeCN in H_2O 15 min, 30.0 mL/min	13.90
2	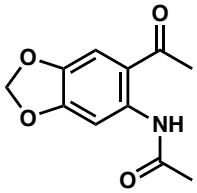 ***106c***	HPLC Zorbax XDB-C18 column 20% to 60% MeCN in H_2O 15 min, 30.0 mL/min	12.75
3	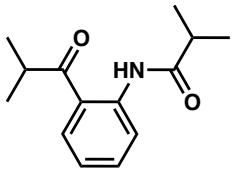 ***104c***	HPLC Zorbax XDB-C18 column 40% to 80% MeCN in H_2O 15 min, 30.0 mL/min	14.36
4	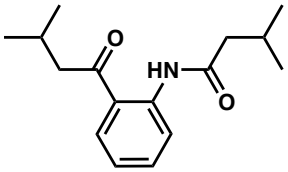 ***104d***	HPLC Zorbax XDB-C18 column 40% to 80% MeCN in H_2O 20 min, 30.0 mL/min	17.35
5	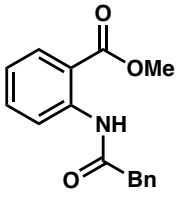 ***104e***	HPLC Zorbax XDB-C18 column 0% to 80% MeCN in H_2O 10 min, 15 mL/min	9.79

2.5 NOTES AND REFERENCES

(1) For various methods for benzyne preparation, see: a) Kitamura, T.; Yamane, M. *J. Chem. Soc. Chem. Commun.* **1995**, 983–984; b) Campbell, C. D.; Rees, C. W. *J. Chem. Soc.* **1969**, 742–747; c) Matsumoto, T.; Hosoya, T.; Katsuki, M.; Suzuki, K. *Tetrahedron Lett.* **1991**, *32*, 6735–6736; d) Friedman, L.; Logullo, F. M. *J. Am. Chem. Soc.* **1963**, *85*, 1792–1797; e) Logullo, F. M.; Seitz, A. H.; Friedman, L. *Org. Synth.* **1968**, *48*, 12–17; f) Wittig, G.; Hoffmann, R. W. *Org. Synth.* **1967**, *47*, 4–8; g) Hoffmann, R. W. *Dehydrobenzene and Cycloalkynes*; Academic Press: New York, 1967.

(2) Himeshima, Y.; Sonoda, T.; Kobayashi, H. *Chem. Lett.* **1983**, 1211–1214.

(3) For examples of aryne insertion into C–C bonds, see: a) Caubere, P.; Loubinoux, B. *Bull. Soc. Chim. Fr.* **1968**, 3008–3012; b) Guyot, M.; Molho, D. *Tetrahedron Lett.* **1973**, *14*, 3433–3436; c) Geoffrey, P.; Mouaddib, A.; Carre, M. C.; Caubere, P. *Tetrahedron Lett.* **1988**, *29*, 1385–1388; d) Pansegrau, P. D.; Rieker, W. F.; Meyers, A. I. *J. Am. Chem. Soc.* **1988**, *110*, 7178–7184; e) Jamart-Gregoire, B.; Leger, C.; Caubere, P. *Tetrahedron Lett.* **1990**, *31*, 7599–7602; f) Danheiser, R. L.; Helgason, A. L. *J. Am. Chem. Soc.* **1994**, *116*, 9471–9479; g) Shair, M. D.; Yoon, T. Y.; Mosny, K. K.; Chou, T. C.; Danishefsky, S. J. *J. Am. Chem. Soc.* **1996**, *118*, 9509–9525; h) Wang, A.; Tandel, S.; Zhang, H.; Huang, Y.; Holdeman, T. C.; Biehl, E. R. *Tetrahedron* **1998**, *54*, 3391–3400.

(4) Tambar, U. K.; Stoltz, B. M. *J. Am. Chem. Soc.* **2005**, *127*, 5340–5341.

(5) Yoshida, H.; Watanabe, M.; Ohshita, J.; Kunai, A. *Tetrahedron Lett.* **2005**, *46,* 6729–6731.

(6) Yoshida, H.; Watanabe, M.; Morishita, T.; Ohshita, J.; Kunai, A. *Chem. Commun.* **2007**, 1505–1507.

(7) Yoshida, H.; Kishida, T.; Watanabe, M.; Ohshita, J. *Chem. Commun.* **2008,** 5963–5965.

(8) Huang, X.; Xue, J. *J. Org. Chem.* **2007***, 72*, 3965–3968.

(9) Saito, N.; Nakamura, K.; Shibano, S.; Ide, S.; Minami, M.; Sato, Y. *Org. Lett.* **2013**, *15*, 386–389.

(10) Jones, C. P.; Anderson, K. W.; Buchwald, S. L. *J. Org. Chem.* **2007**, *72*, 7968–7973.

(11) Okabe, M.; Sun, R.-C. *Tetrahedron* **1995**, *51*, 1861–1866.

(12) Fürstner, A.; Jumam, D. N.; Weidmann, H. *Tetrahedron Lett.* **1991**, *32*, 6695–6696.

(13) Pintori, D. G.; Greaney, M. F. *Org. Lett.* **2010**, *12*, 168–171.

(14) Wright, A. C.; Haley, C. K.; Lapointe, G.; Stoltz, B. M. *Org. Lett.* **2016**, *18*, 2793–2795.

(15) Tobisu, M.; Ano, Y.; Chatani, N. *Org. Lett*. **2009**, *11*, 3250–3252.

(16) Canonne, P.; Boulanger, R.; Chantegrel, B. *Tetrahedron* **1987**, *43*, 663–668.

(17) Yin, Z.; Sun, P. *Org. Lett.* **2012**, *77*, 11339–11344.

(18) Rodriguez–Ramos, F.; Navarette, A.; Gonzalez–Andrade, M.; Alarcon, C.; Aguilera–Cruz, A.; Reyes–Ramirez, Adelfo. *Bioorg. Chem.* **2013**, *50*, 17–25.

(19) Cross, R. M.; Manetsch, R. *J. Org. Chem.* **2010**, *75*, 8654–8657.

(20) Liu, G.-B.; Xu, J.-L.; He, C.-C.; Chen, G.; Xu, Q.; Xu, H.-X.; Li, J.-X. *Bioorg. Med. Chem.* **2009**, *17*, 5433–5441.

APPENDIX 4

Spectra Relevant to Chapter 2:

Acyl-Amination of Arenes via Aryne Formation

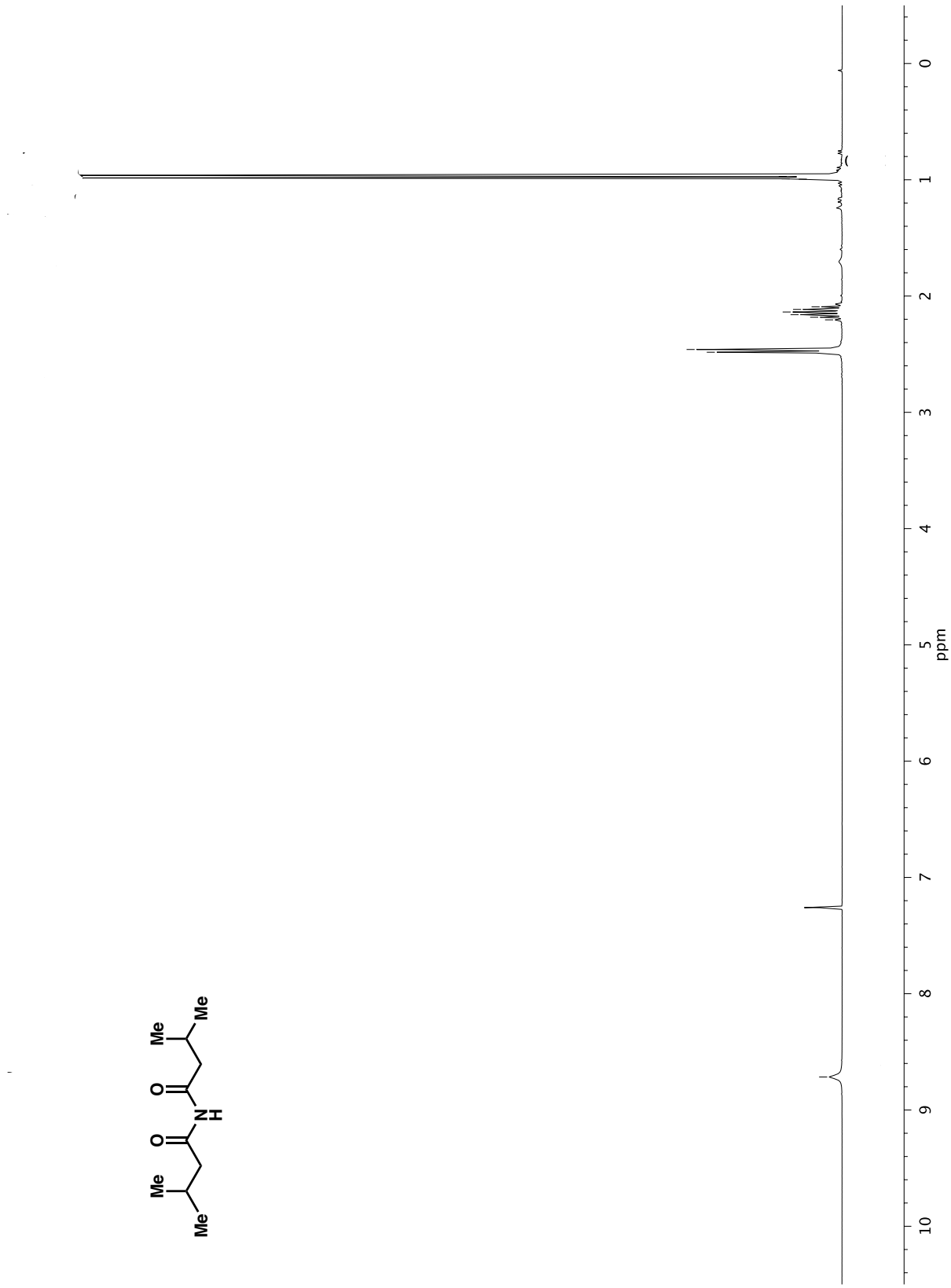

Figure A4.1 ^{1}H NMR (400 MHz, $CDCl_3$) of compound **109**

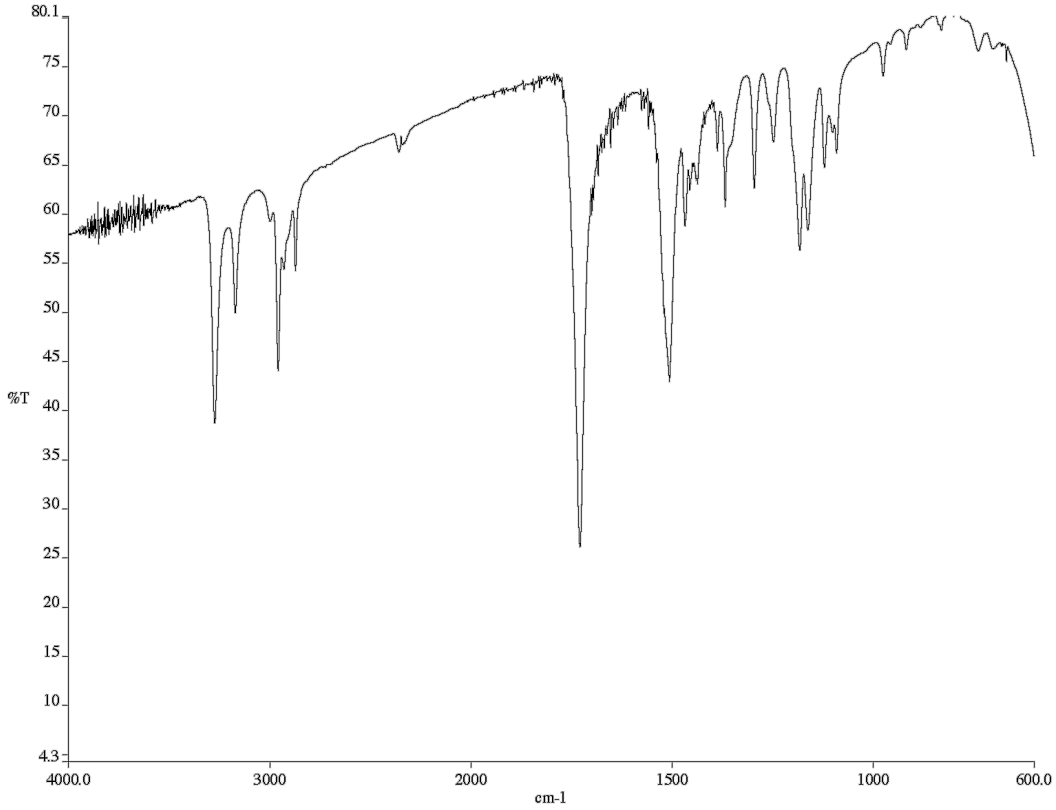

Figure A4.2 Infrared spectrum (Thin Film, NaCl) of compound **109**

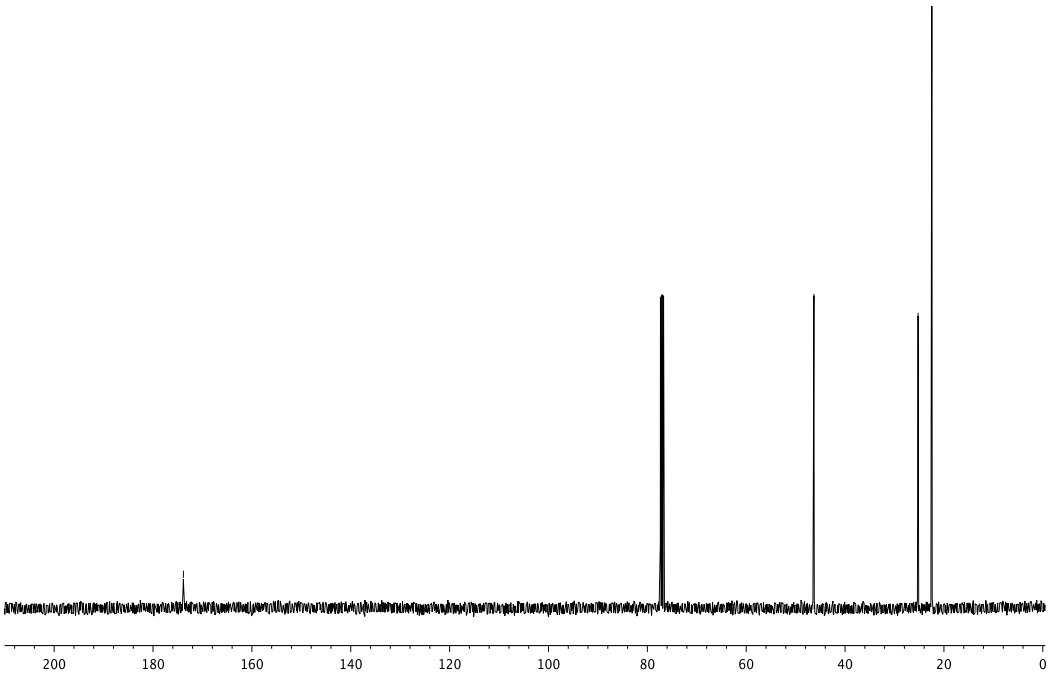

Figure A4.3 ^{13}C NMR (101 MHz, $CDCl_3$) of compound **109**

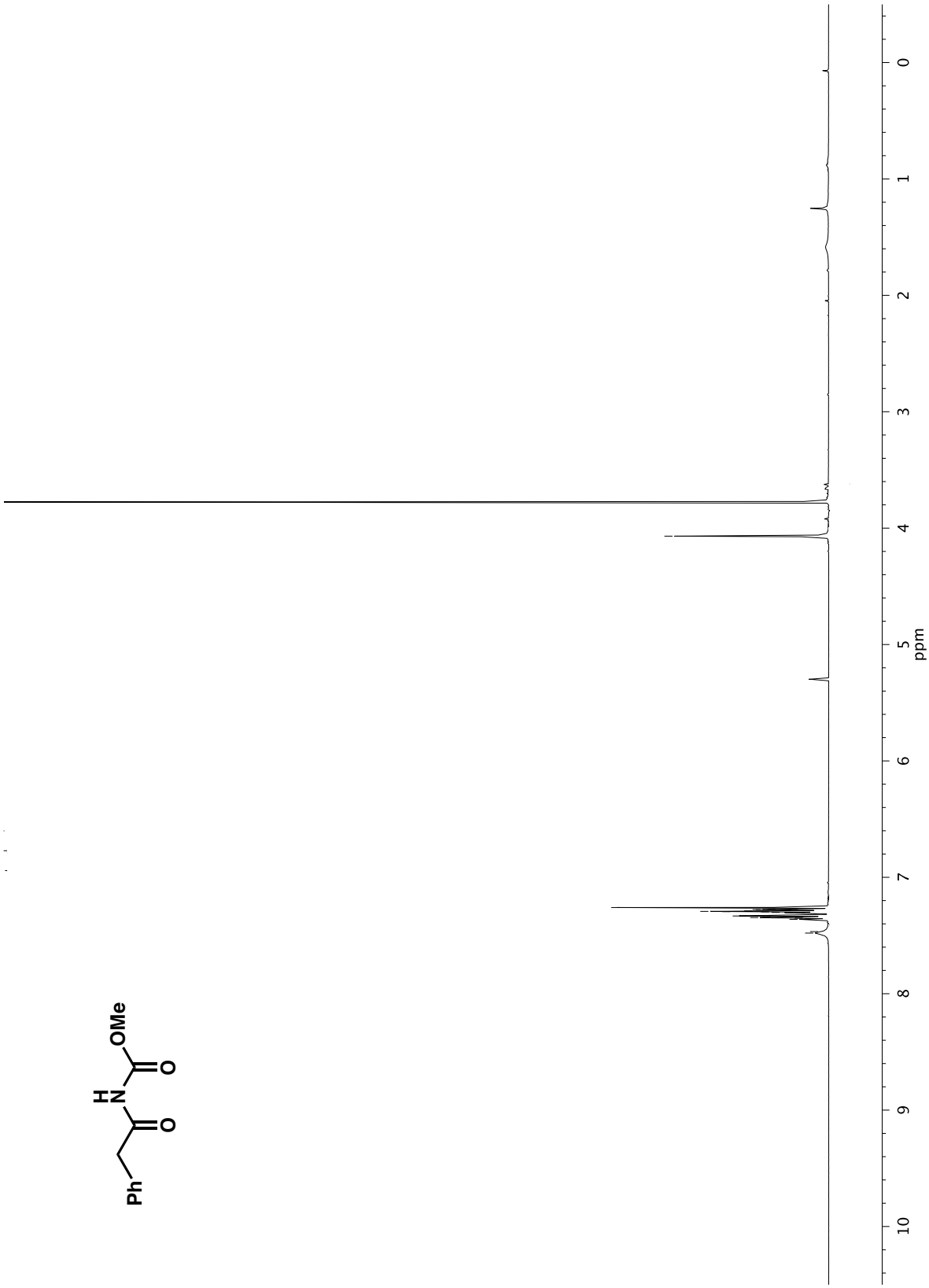

Figure A4.4 ^{1}H NMR (400 MHz, $CDCl_3$) of compound **112**

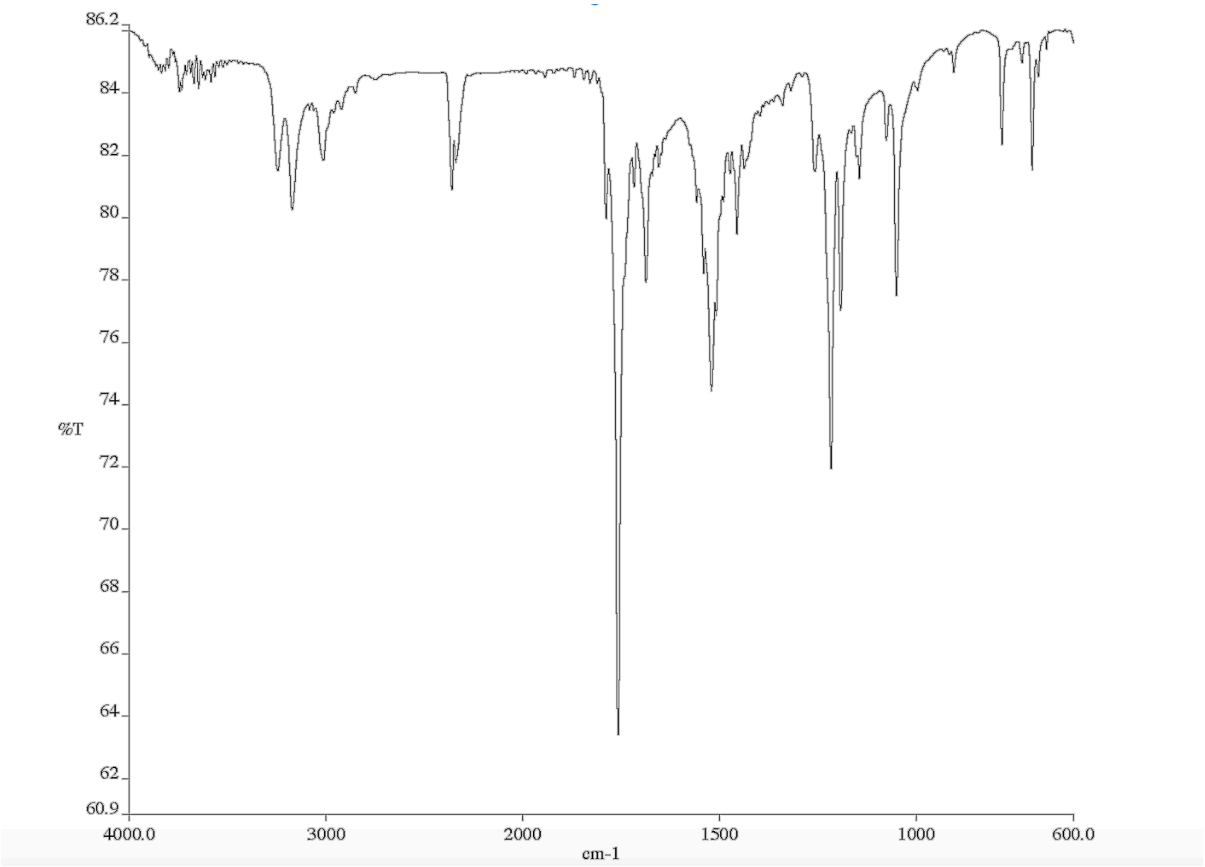

Figure A4.5 Infrared spectrum (Thin Film, NaCl) of compound **112**

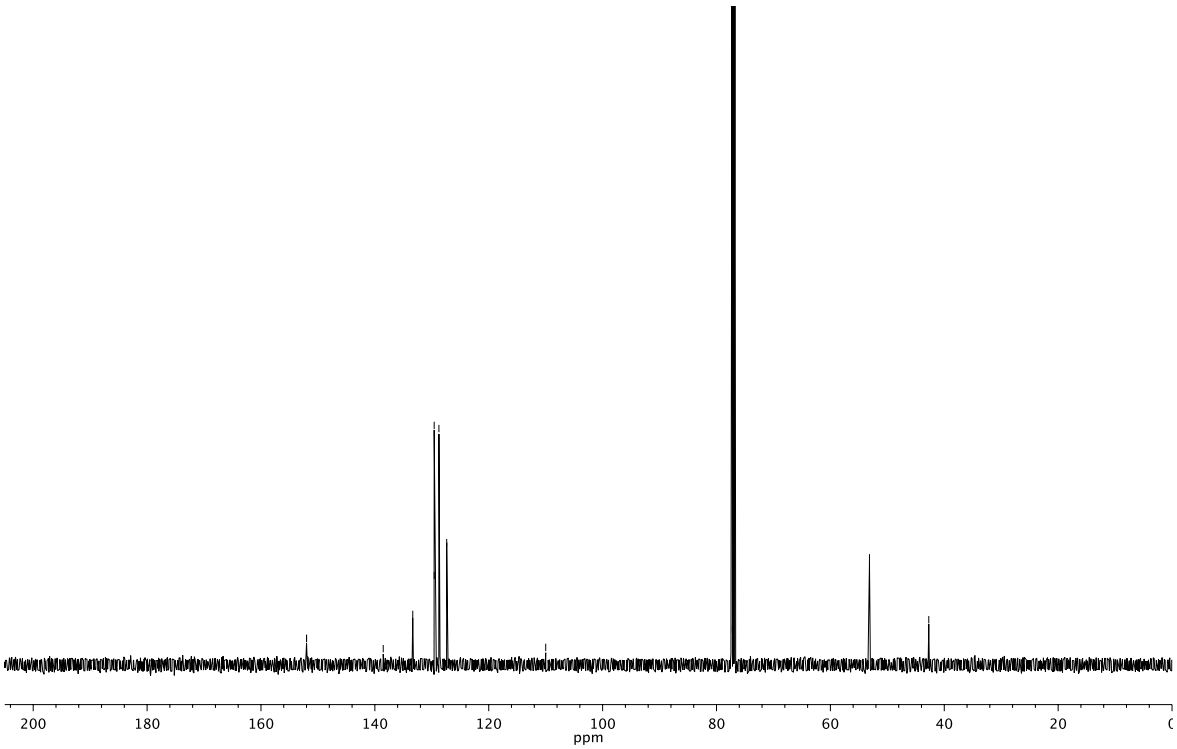

Figure A4.6 ^{13}C NMR (101 MHz, $CDCl_3$) of compound **112**

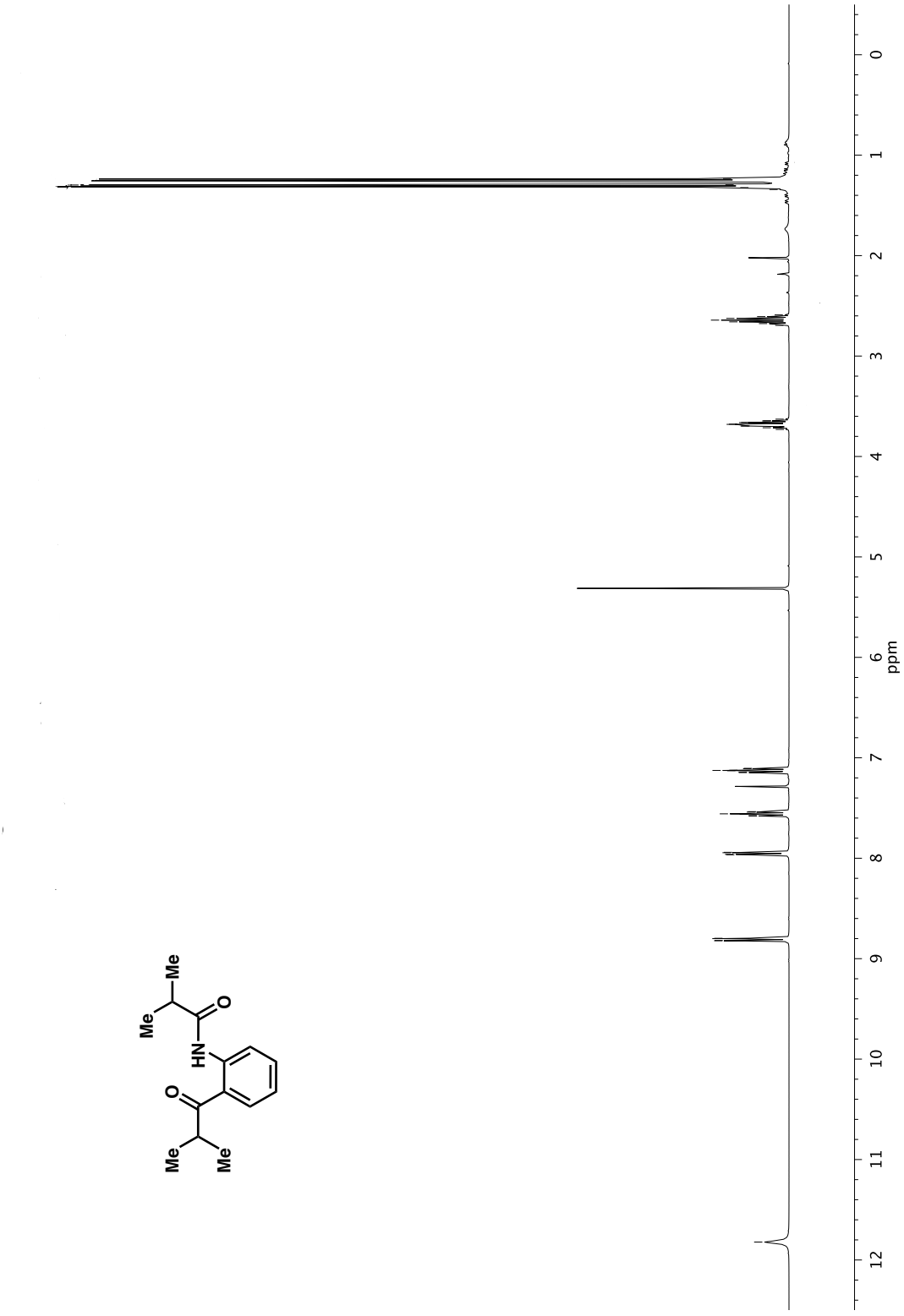

Figure A4.7 ^{1}H NMR (400 MHz, $CDCl_3$) of compound **104c**

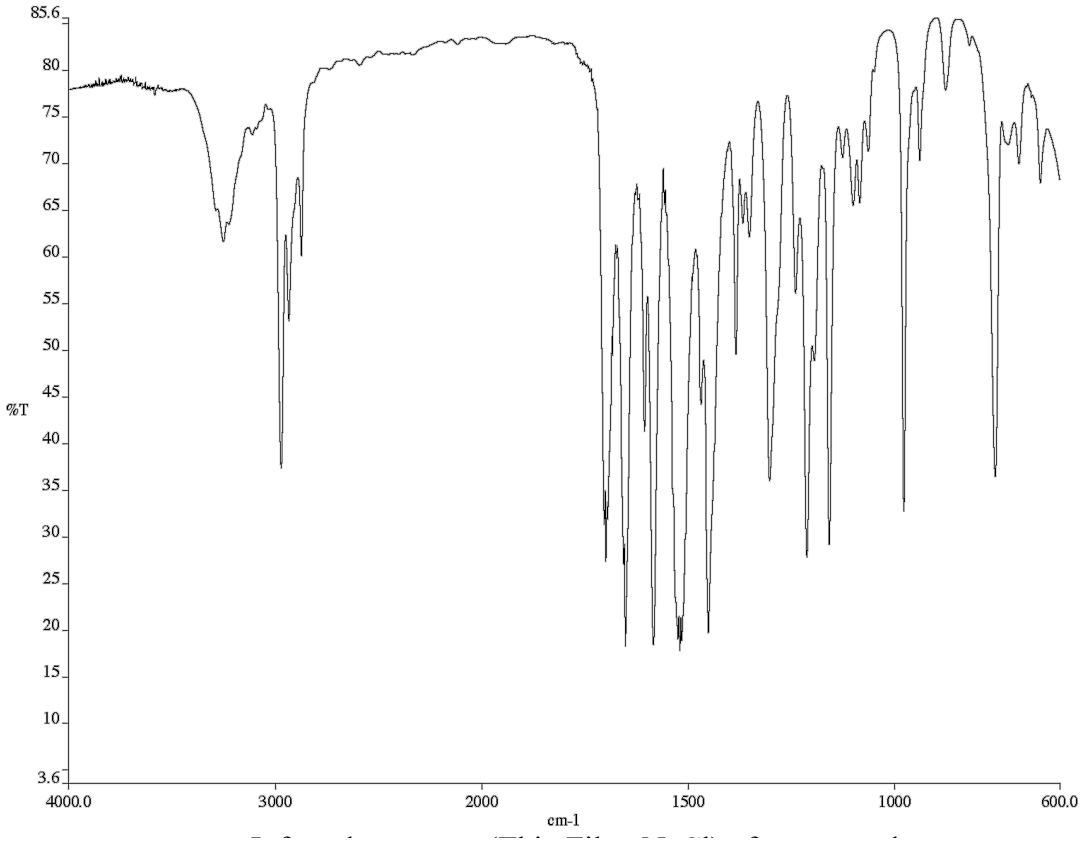

Figure A4.8 Infrared spectrum (Thin Film, NaCl) of compound **104c**

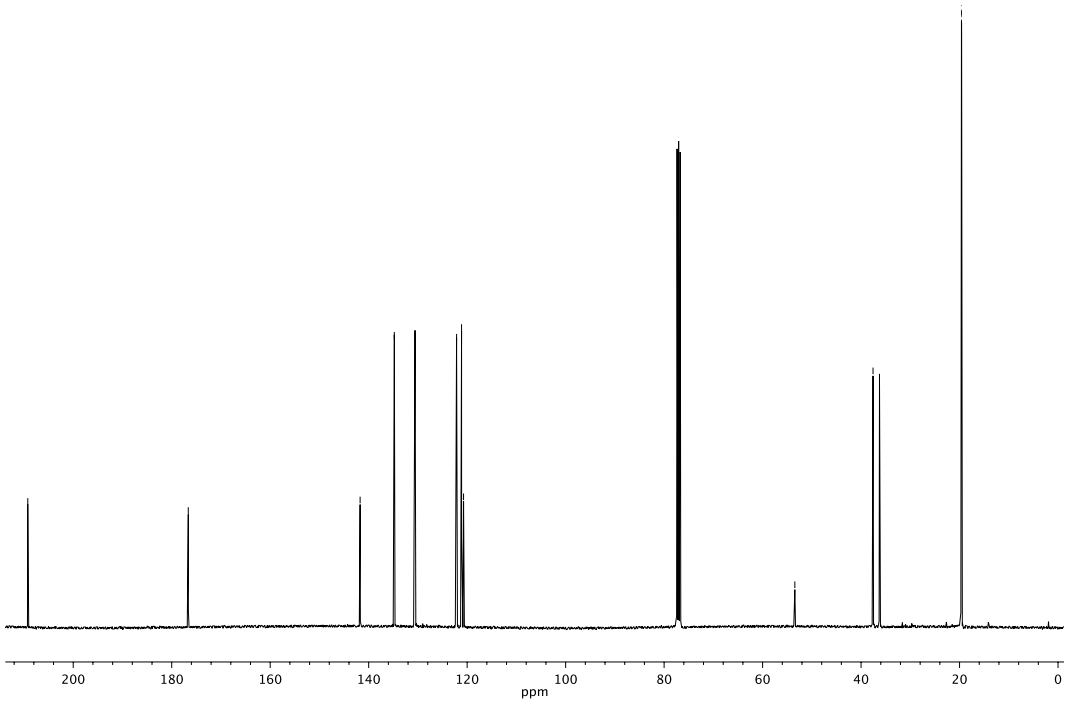

Figure A4.9 ^{13}C NMR (101 MHz, $CDCl_3$) of compound **104c**

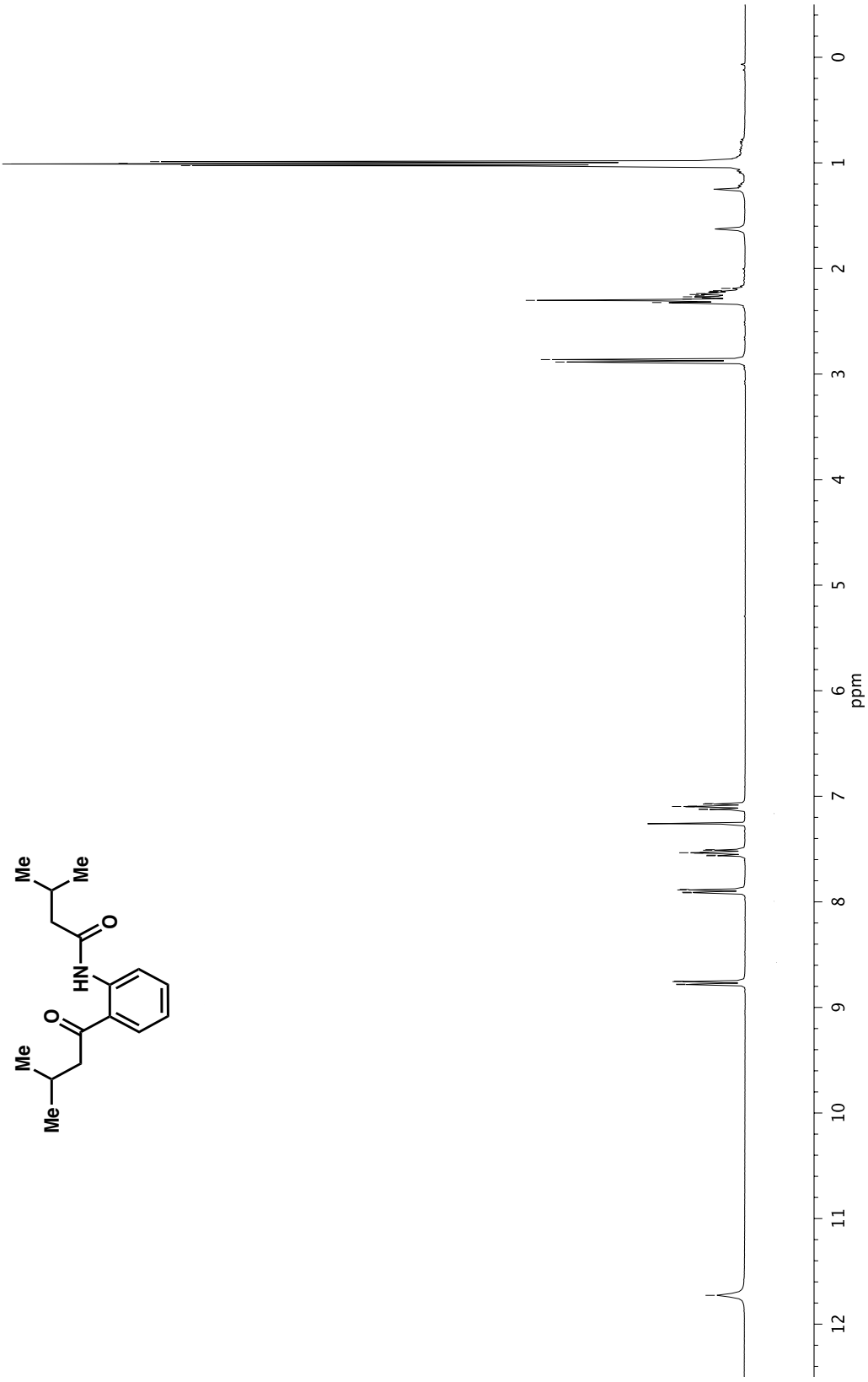

Figure A4.10 ^{1}H NMR (400 MHz, $CDCl_3$) of compound **104d**

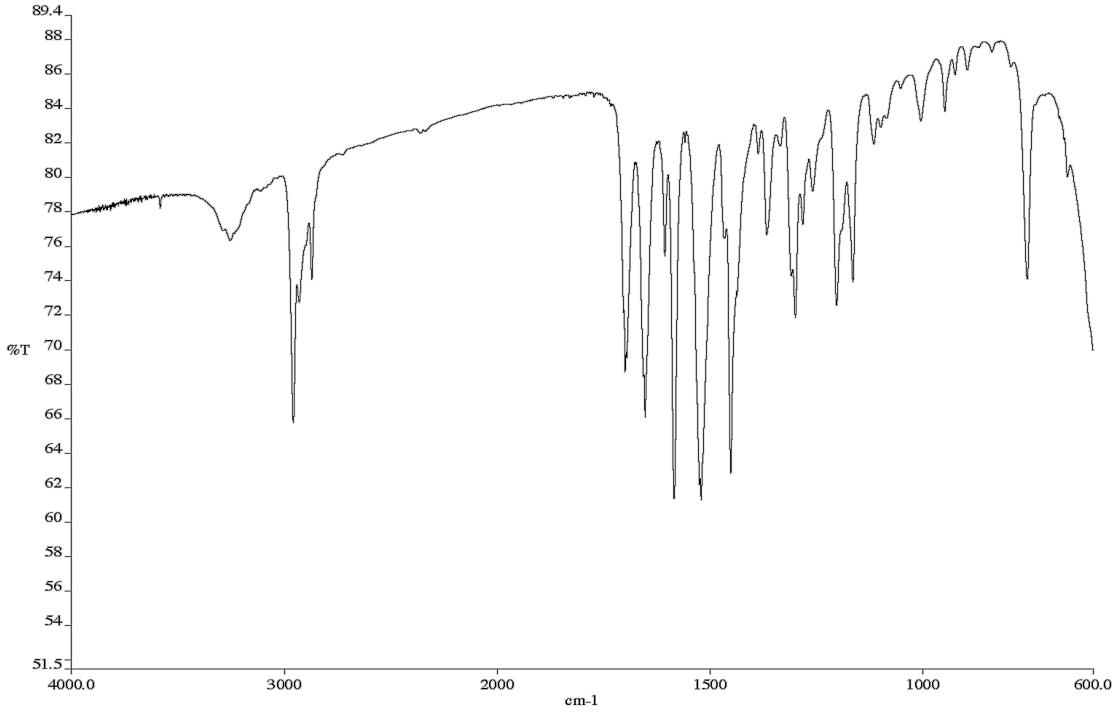

Figure A4.11 Infrared spectrum (Thin Film, NaCl) of compound **104d**

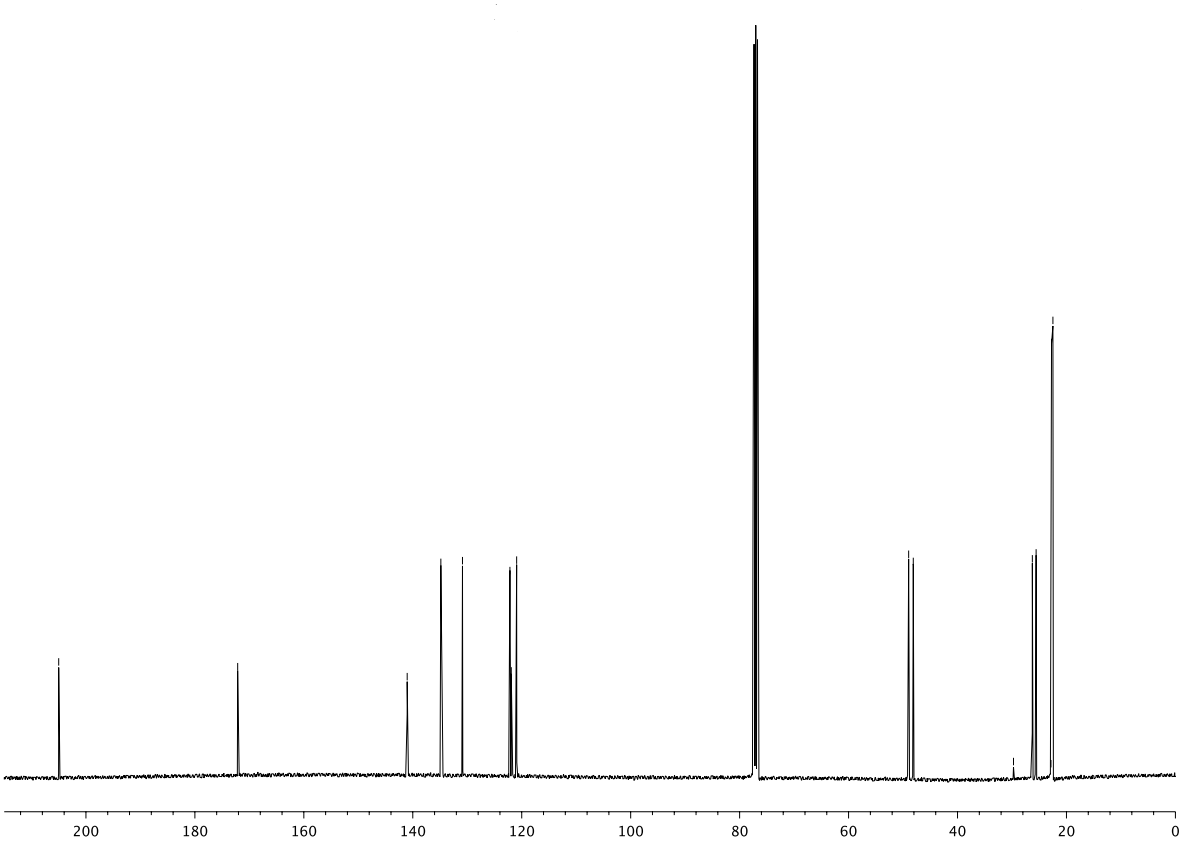

Figure A4.12 ^{13}C NMR (101 MHz, $CDCl_3$) of compound **104d**

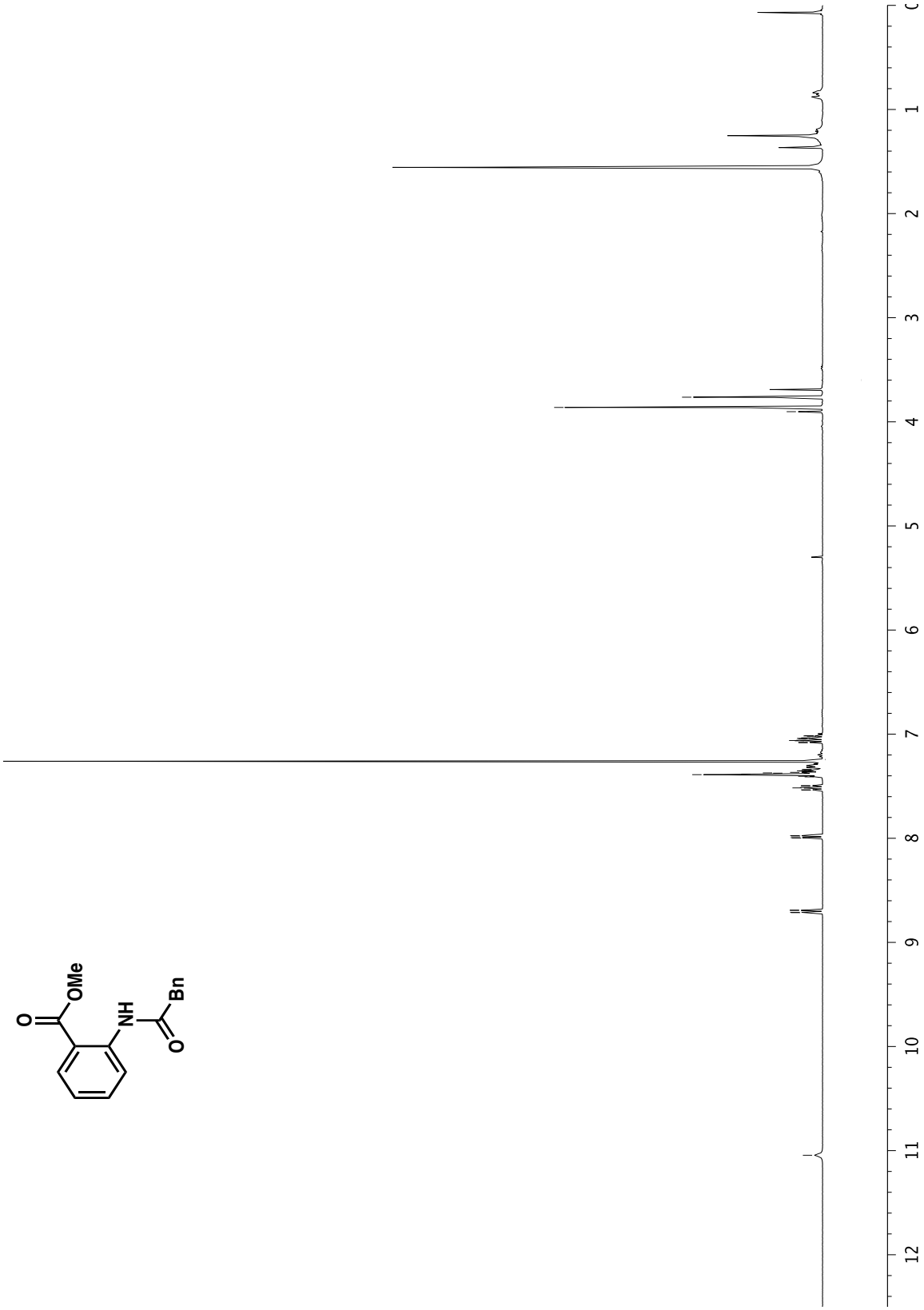

Figure A4.13 ^{1}H NMR (400 MHz, $CDCl_3$) of compound **104e**

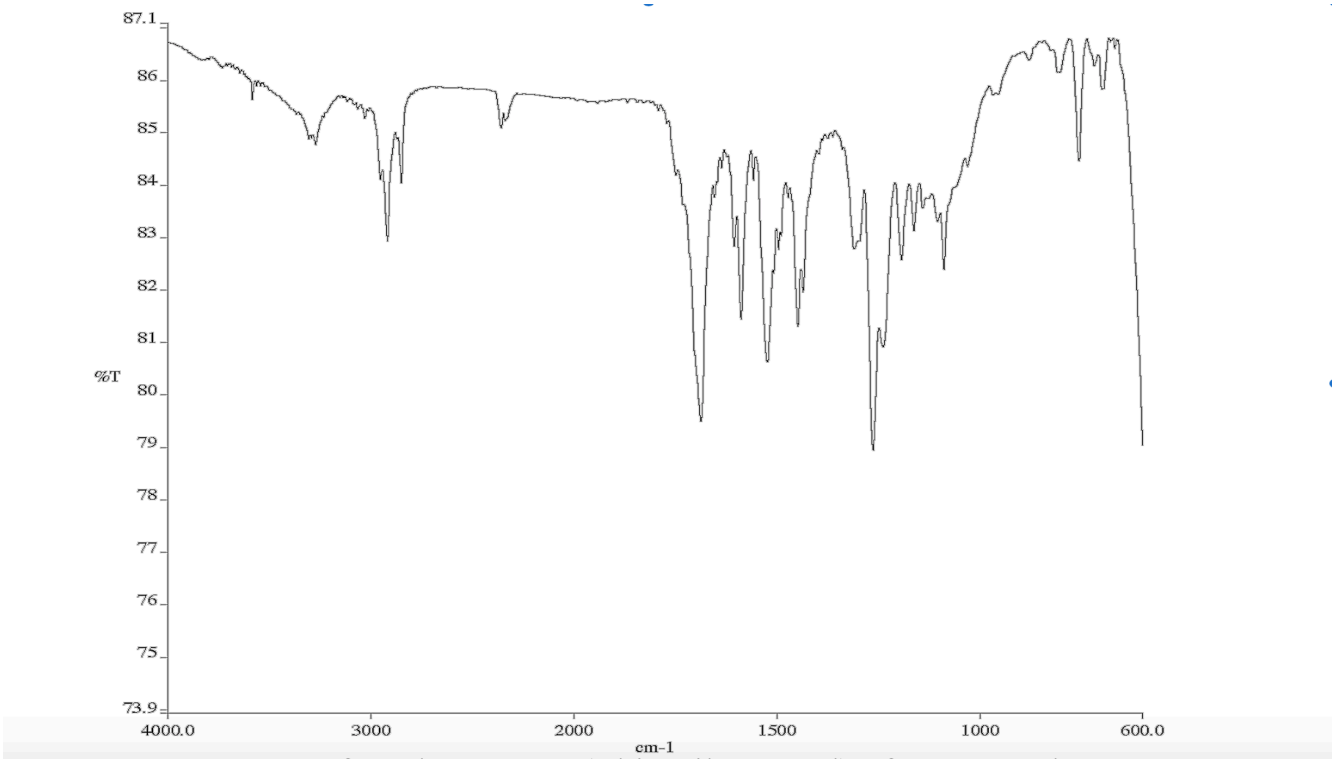

Figure A4.14 Infrared spectrum (Thin Film, NaCl) of compound **104e**

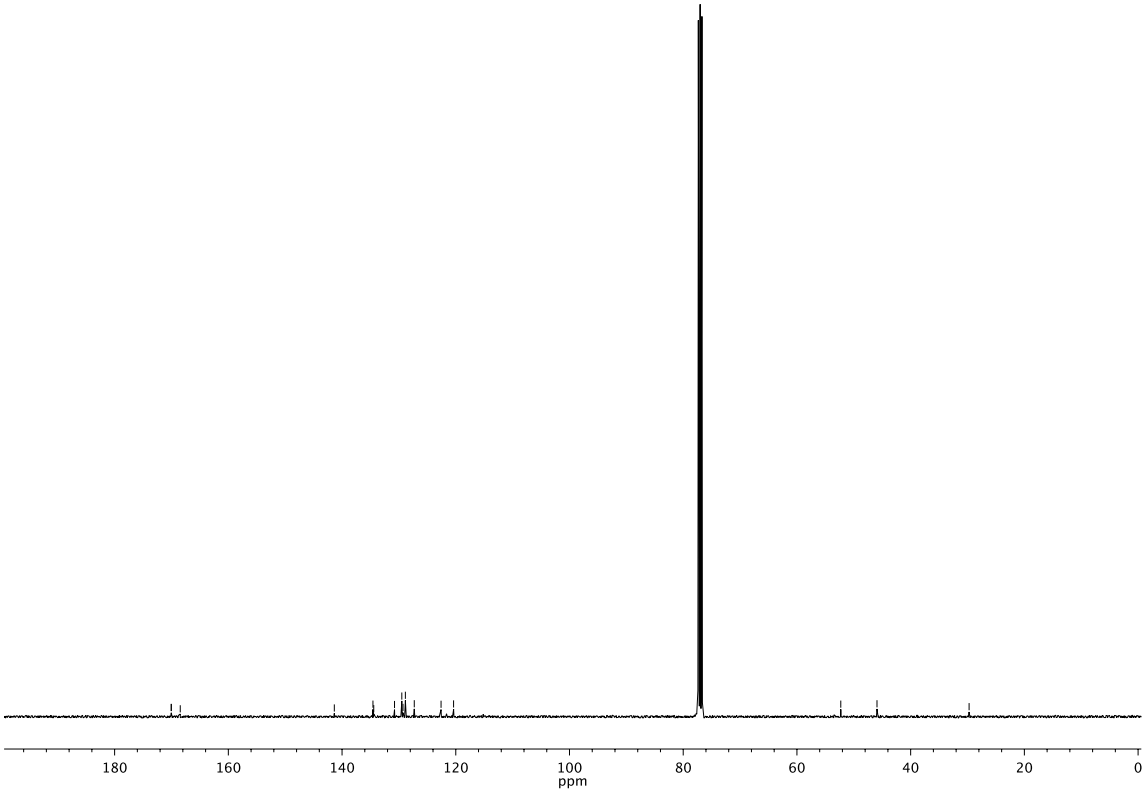

Figure A4.15 ^{13}C NMR (101 MHz, $CDCl_3$) of compound **104e**

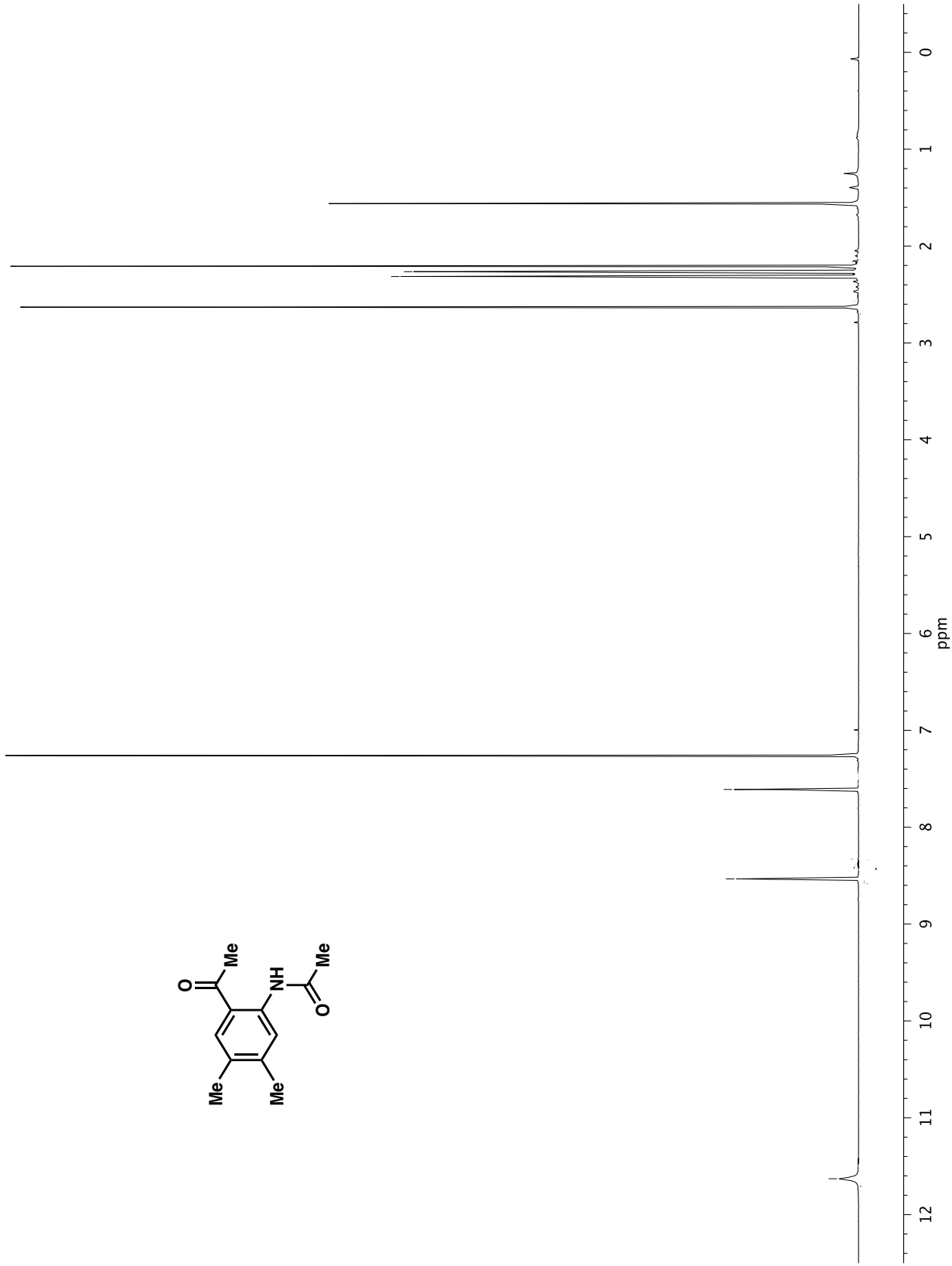

Figure A4.16 ^{1}H NMR (400 MHz, $CDCl_3$) of compound **106a**

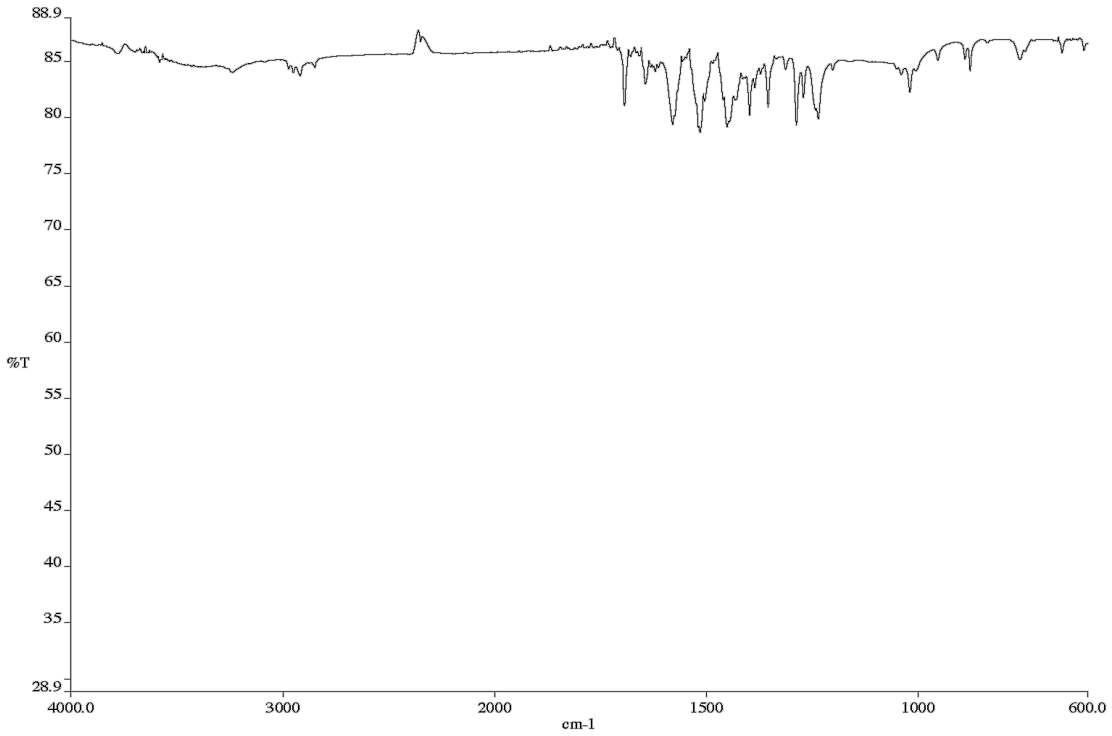

Figure A4.17 Infrared spectrum (Thin Film, NaCl) of compound **106a**

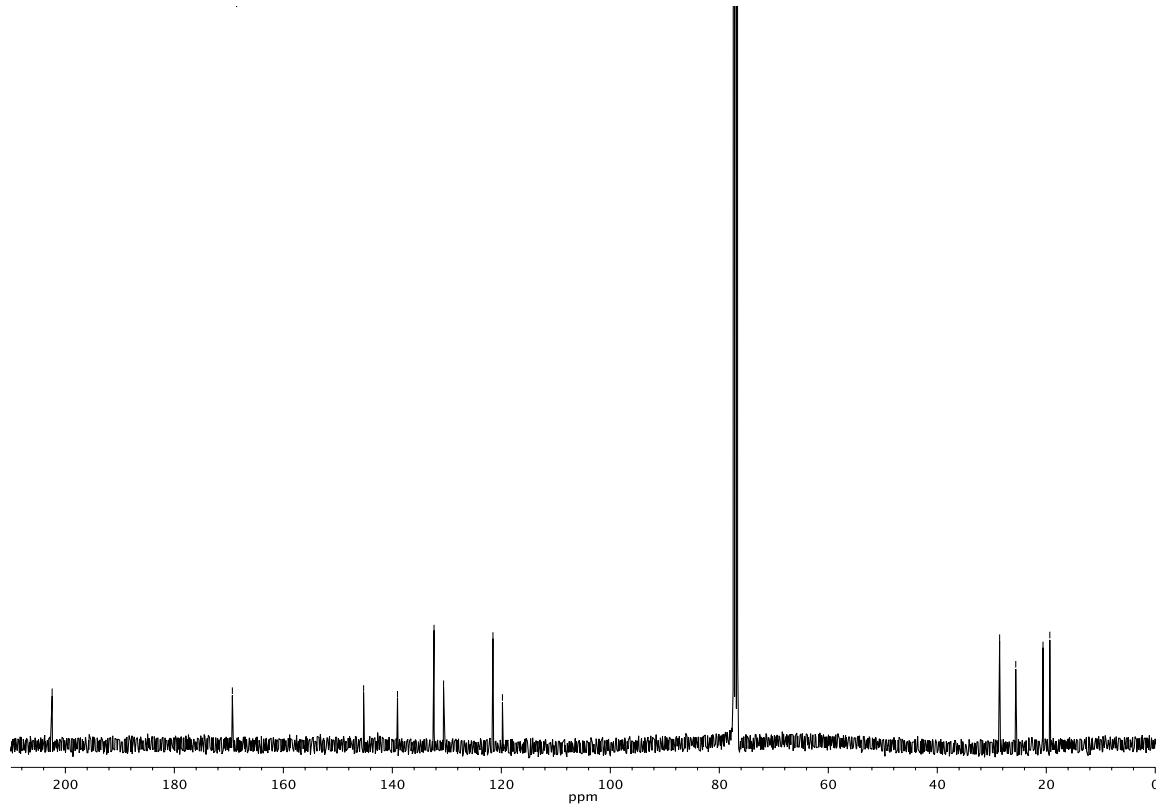

Figure A4.18 ^{13}C NMR (101 MHz, $CDCl_3$) of compound **106a**

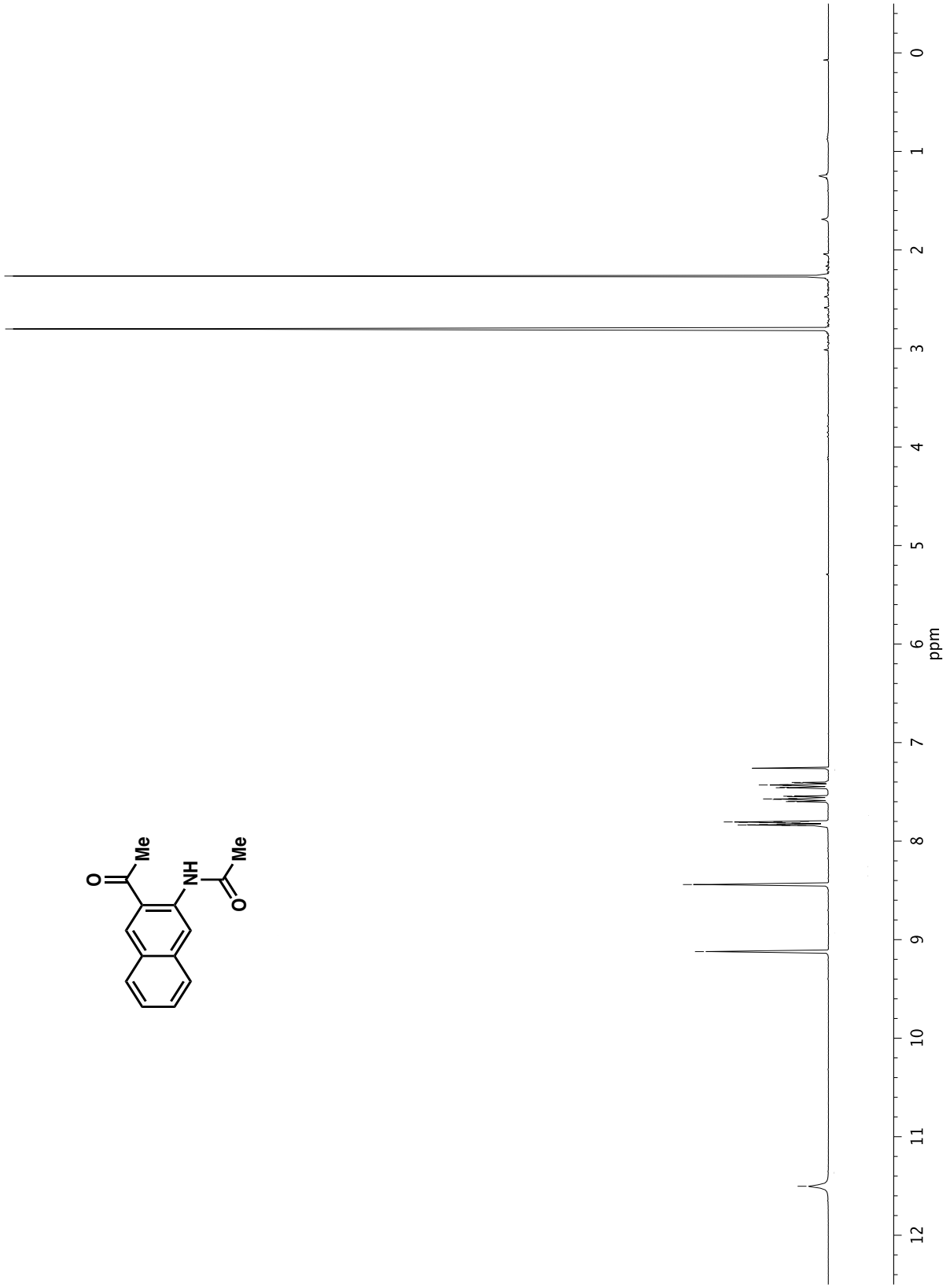

Figure A4.19 ^{1}H NMR (400 MHz, $CDCl_3$) of compound **106b**

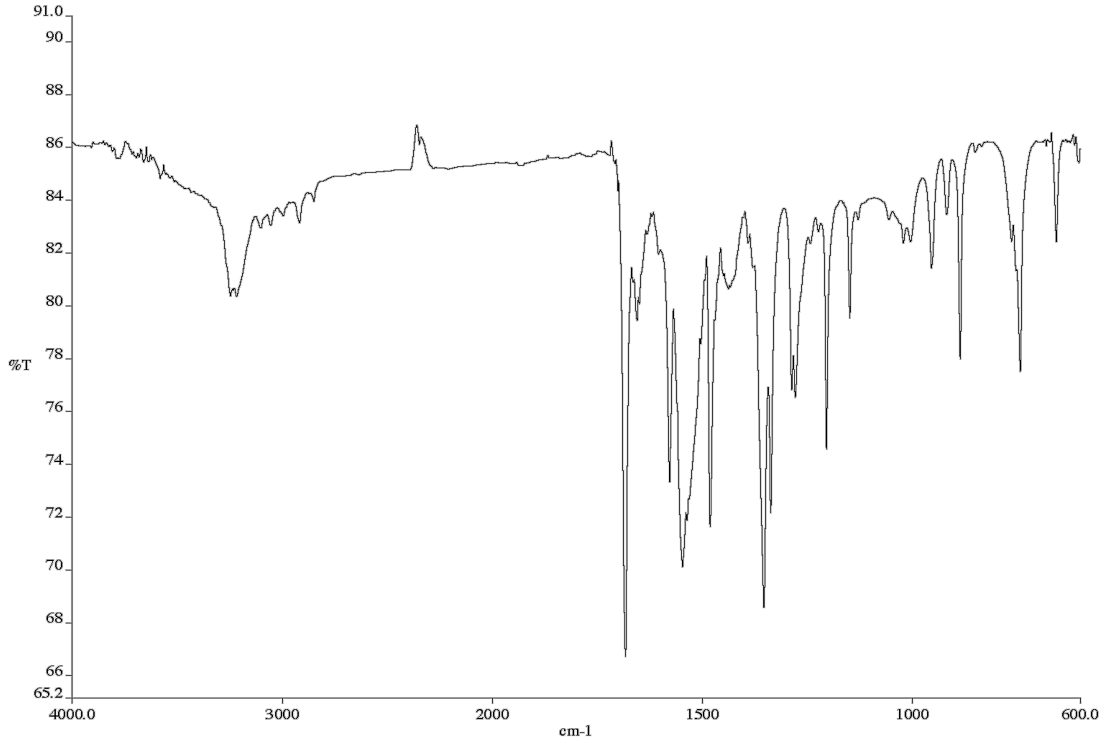

Figure A4.20 Infrared spectrum (Thin Film, NaCl) of compound **106b**

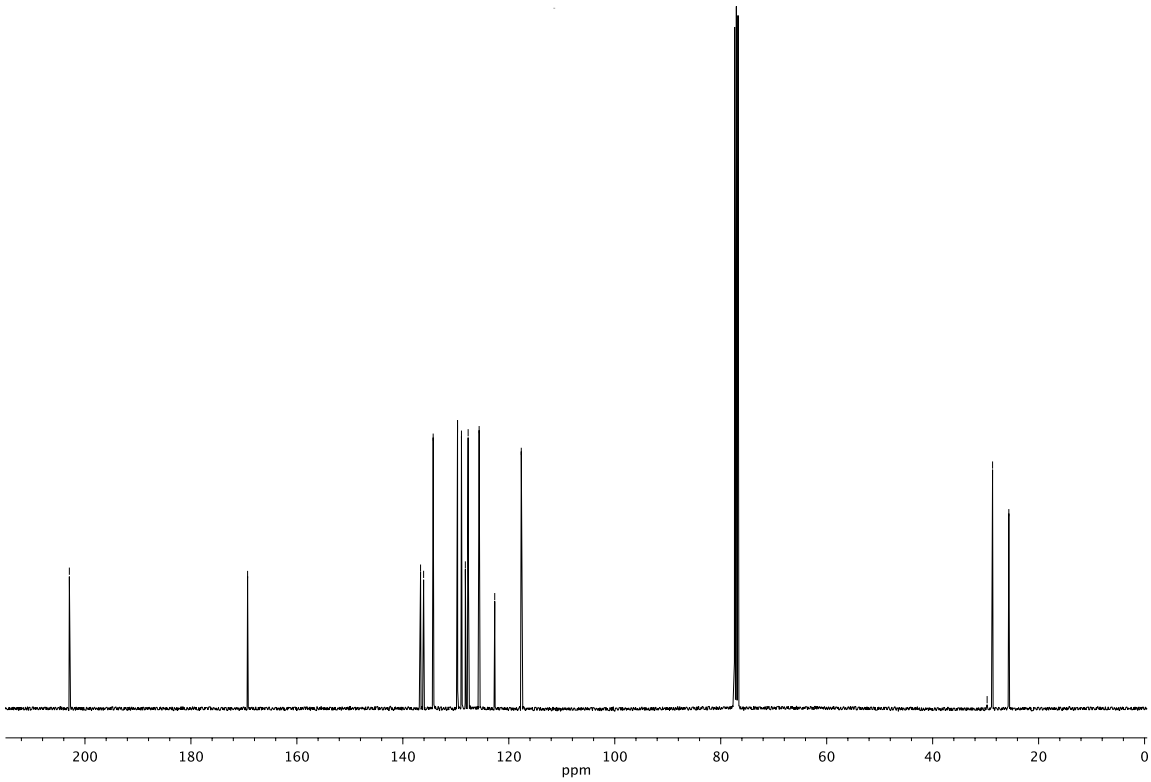

Figure A4.21 ^{13}C NMR (101 MHz, $CDCl_3$) of compound **106b**

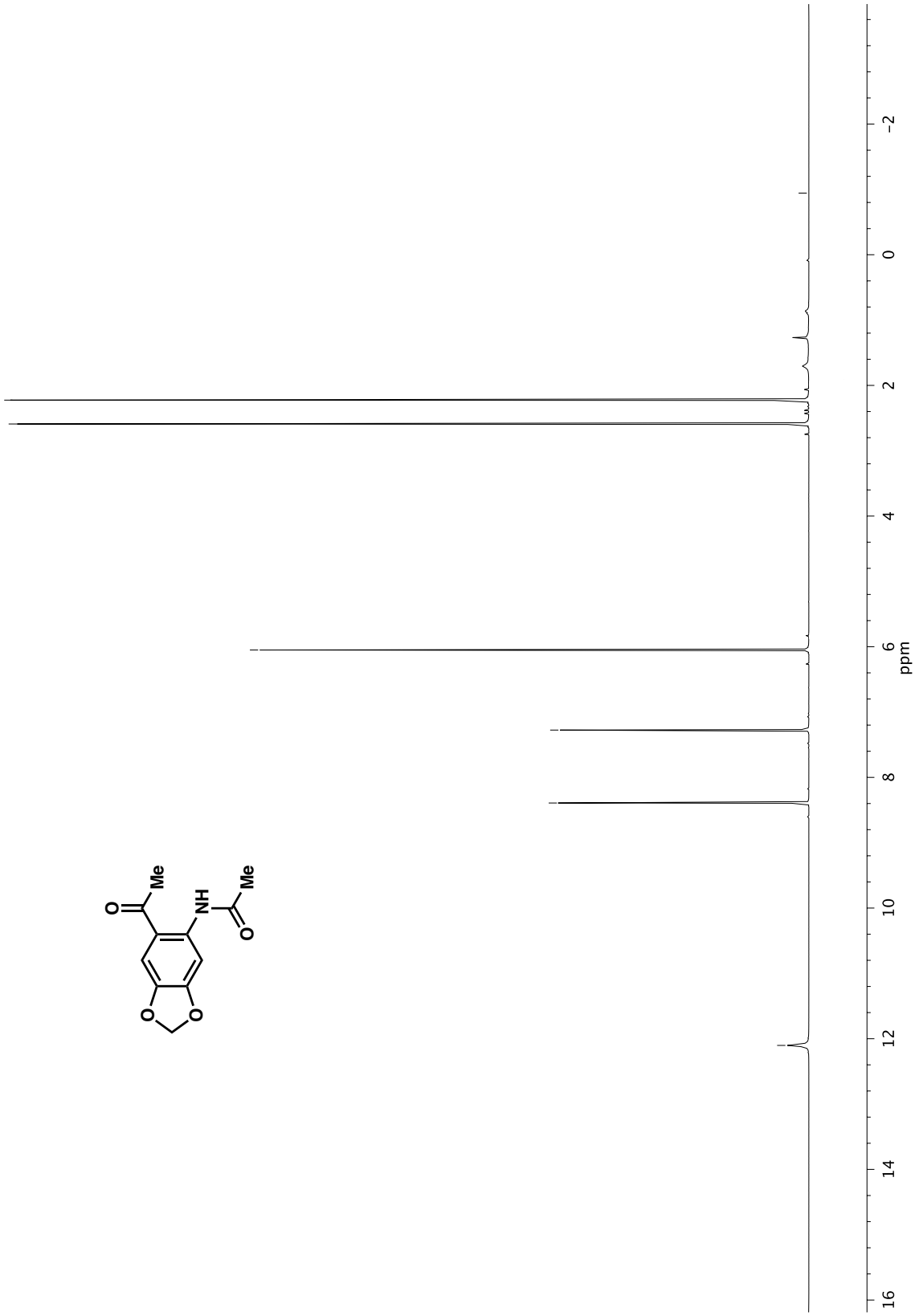

Figure A4.22 ^{1}H NMR (400 MHz, $CDCl_3$) of compound **106c**

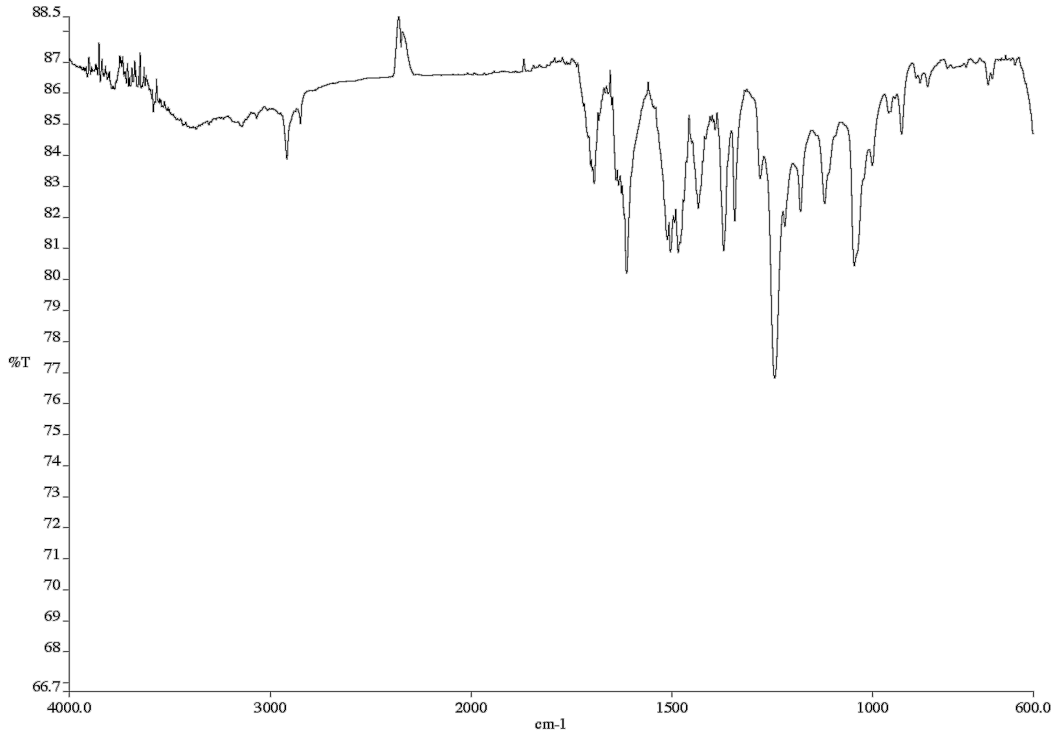

Figure A4.23 Infrared spectrum (Thin Film, NaCl) of compound **106c**

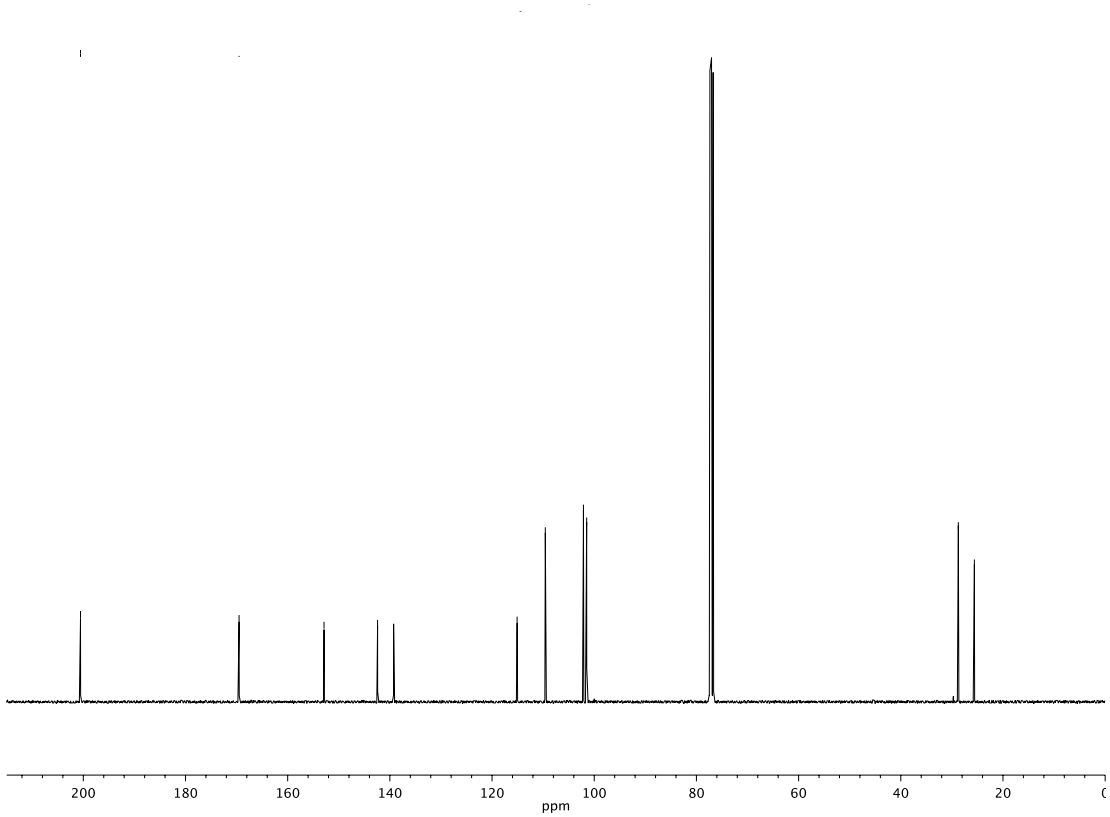

Figure A4.24 ^{13}C NMR (101 MHz, $CDCl_3$) of compound **106c**

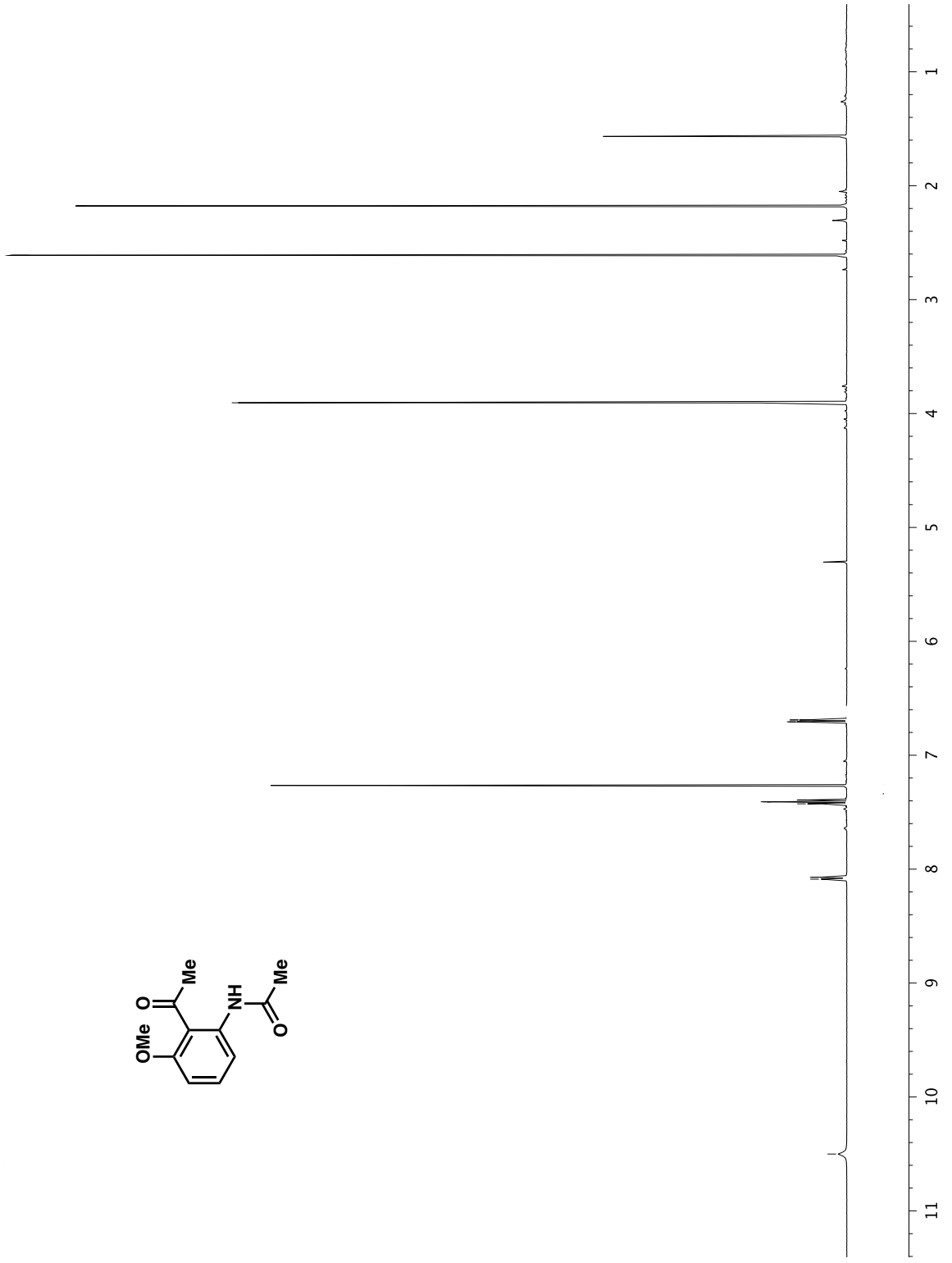

Figure A4.25 ^{1}H NMR (500 MHz, $CDCl_3$) of compound **106d**

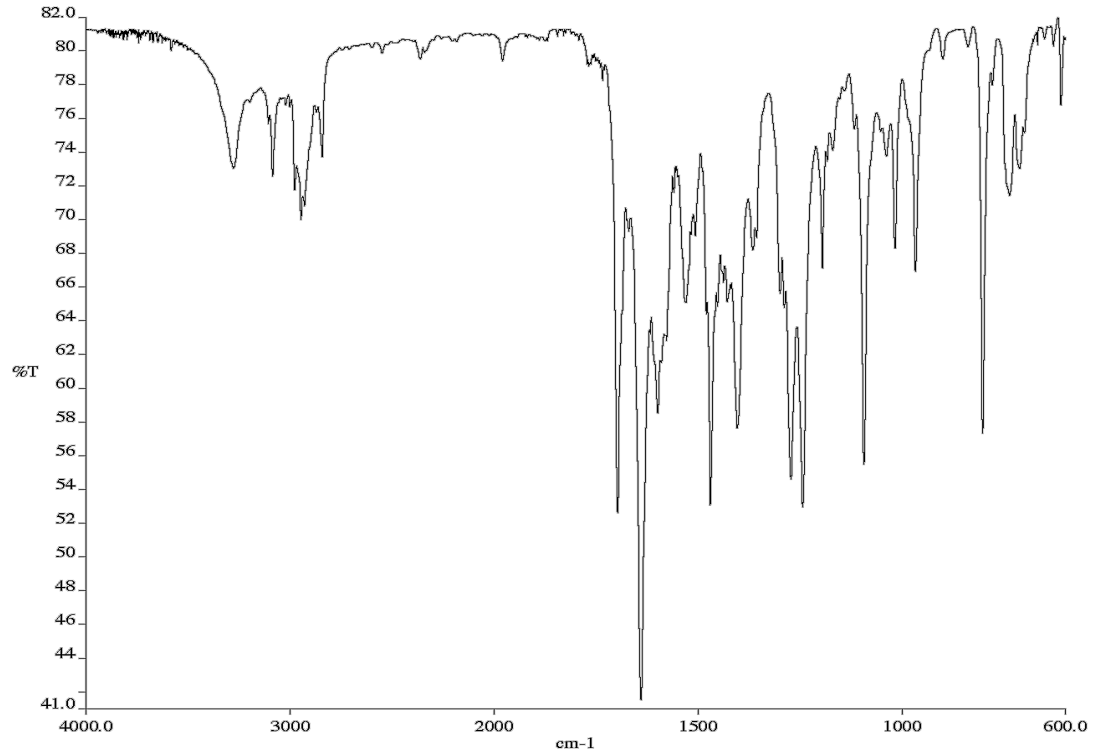

Figure A4.26 Infrared spectrum (Thin Film, NaCl) of compound **106d**

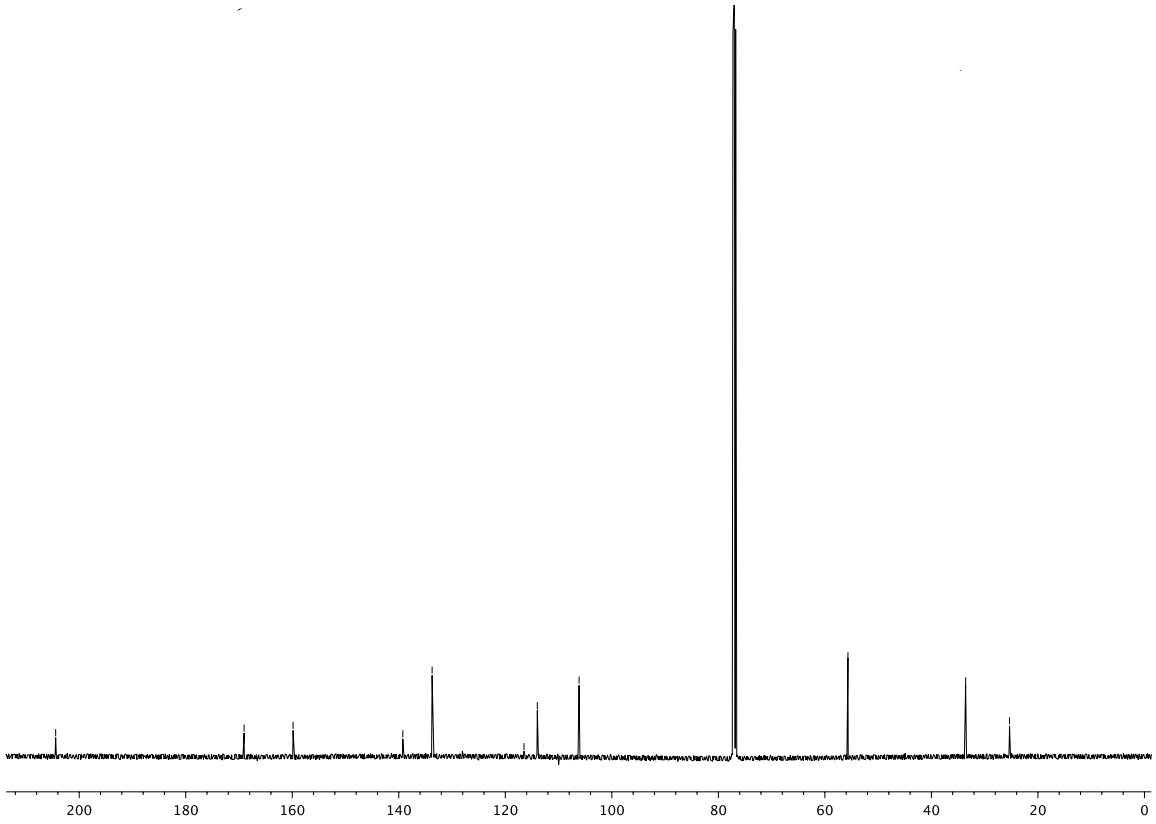

Figure A4.27 ^{13}C NMR (126 MHz, $CDCl_3$) of compound **106d**

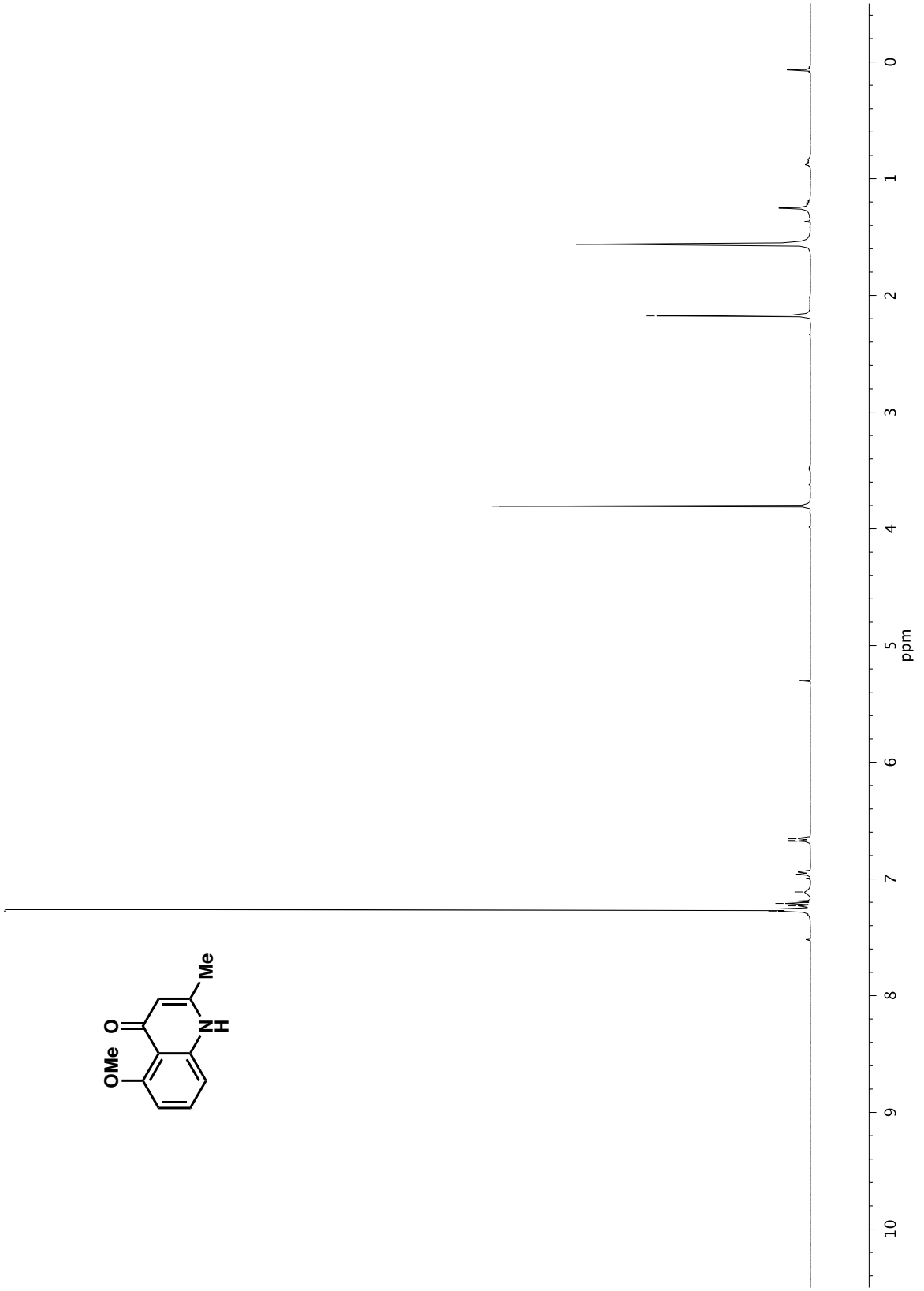

Figure A4.28 ^{1}H NMR (400 MHz, $CDCl_3$) of compound **107c**

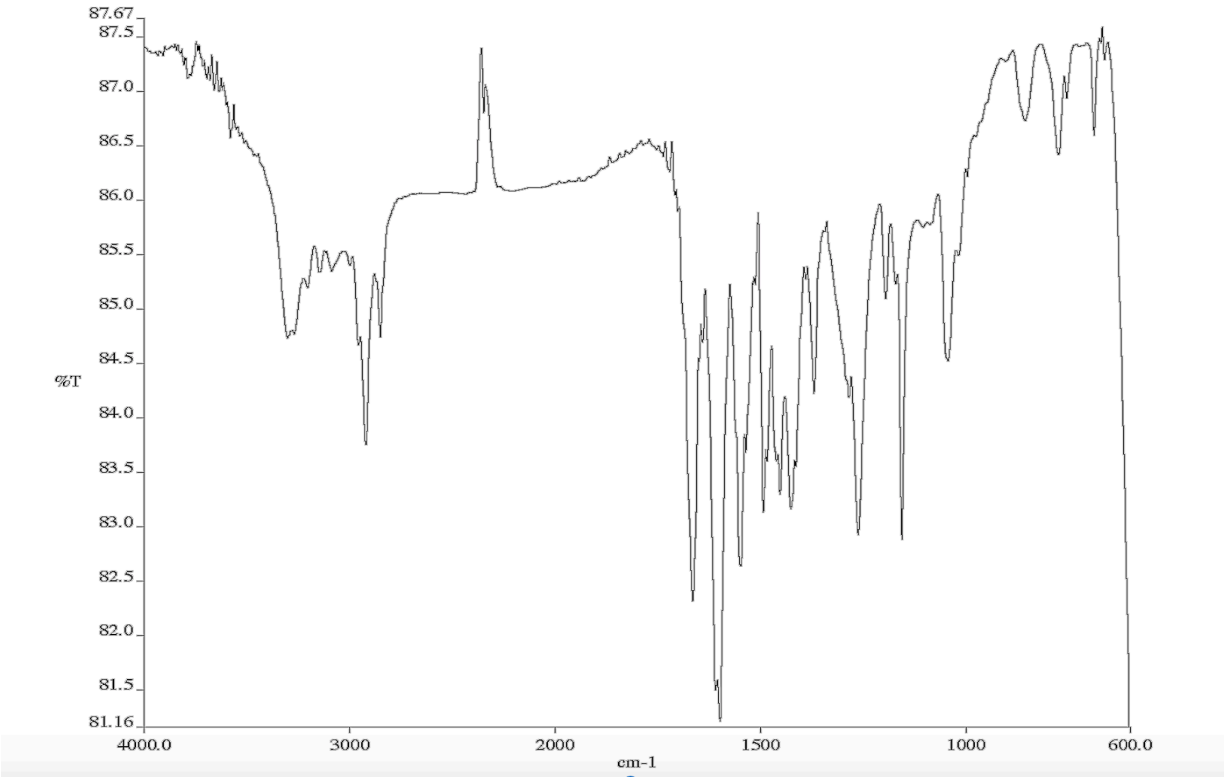

Figure A4.29 Infrared spectrum (Thin Film, NaCl) of compound **107c**

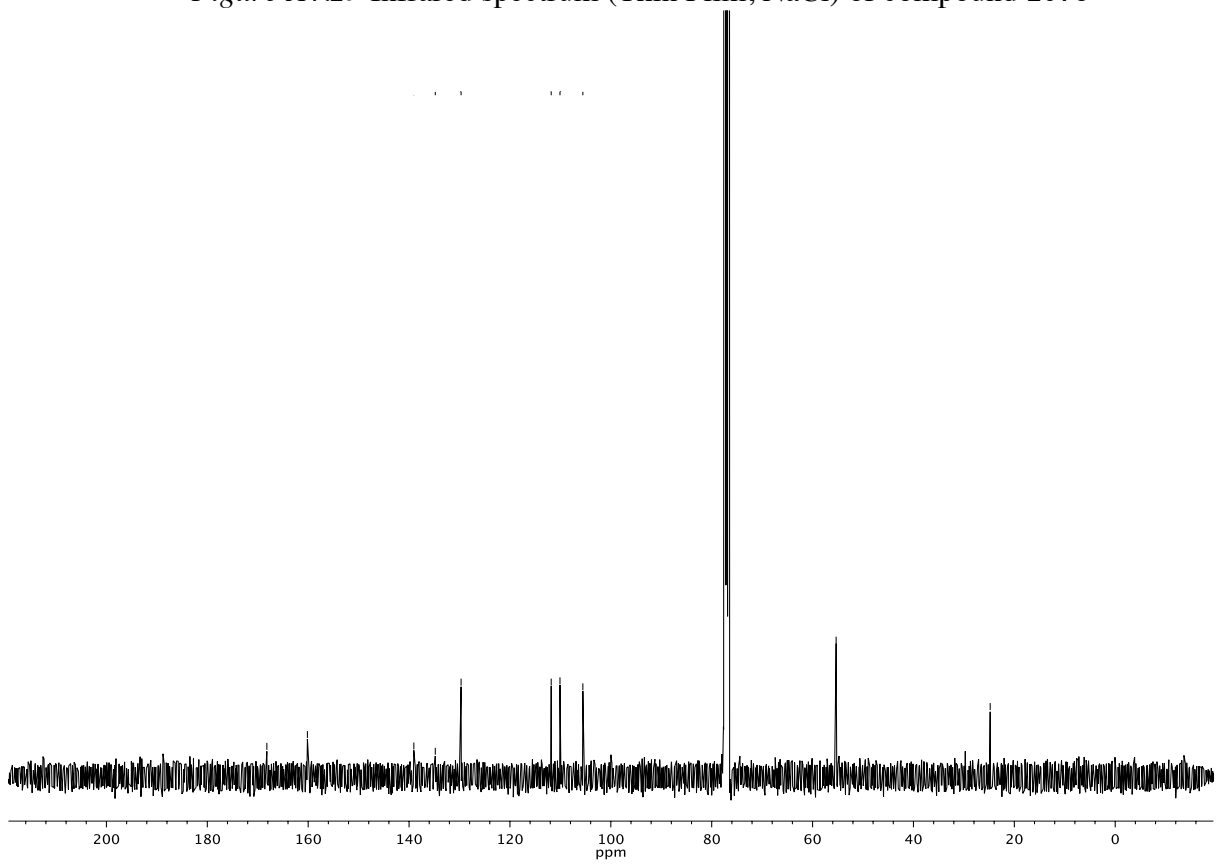

Figure A4.30 ^{13}C NMR (101 MHz, $CDCl_3$) of compound **107c**

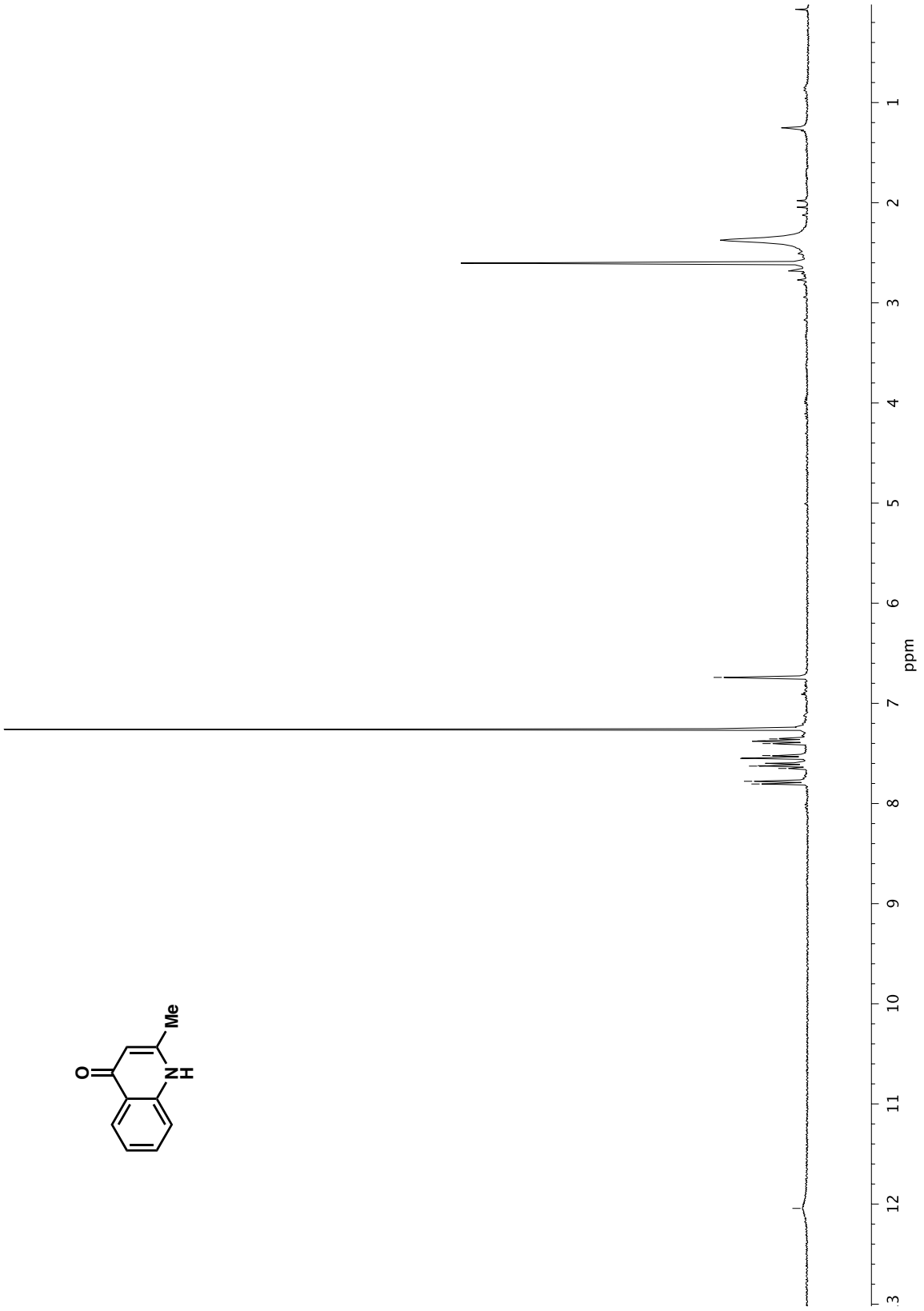

Figure A4.31 ^{1}H NMR (400 MHz, $CDCl_3$) of compound **107a**

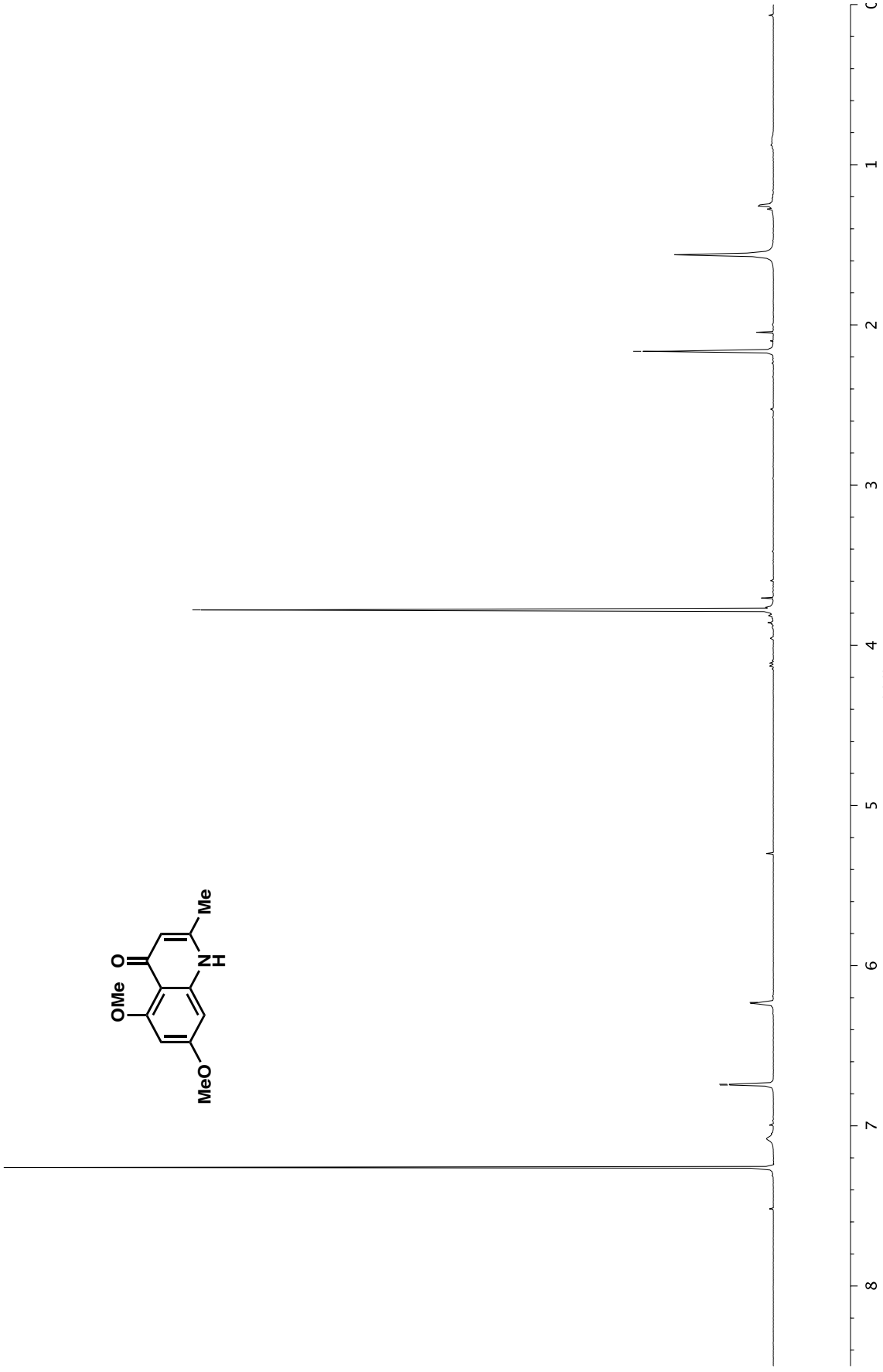

Figure A4.32 ^{1}H NMR (400 MHz, $CDCl_3$) of compound **107b**

APPENDIX 5

Notebook Cross-Reference

This section contains notebook cross-references in order to streamline perusal of all original spectroscopic data. These data are presented according to chapter, and comprise ^{1}H, ^{13}C, and 2D NMR spectra as well as IR spectra. All relevant notebooks can be found in the Stoltz group archive. Additionally, all relevant electronic data may be accessed on the Stoltz group server.

Table 5.1 Notebook Cross-Reference for Compounds in Chapter 1.2

Compound	Structure	Notebook reference	NMR and IR data files
28	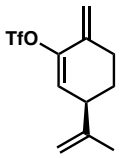	**CWL-IV-153**	**CWL-VI-129** **CWL-IV-169**
31	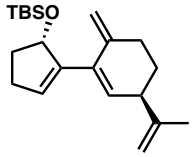	**CWL-IV-171**	**CWL-VII-41**
87	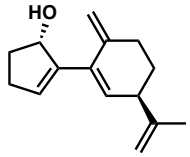	**CWL-IV-173**	**CWL-VII-37-OH**
33	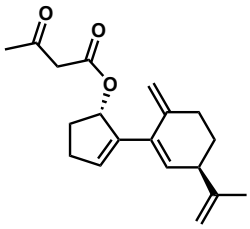	**CWL-VII-175**	**CWL-VII-39**
34	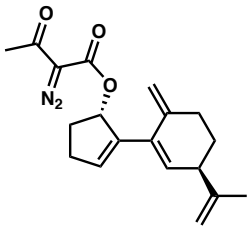	**CWL-VII-177**	**CWL-VII-37-N2**
38	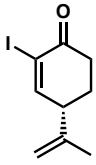	**CWL-V-63**	**CWL-VII-49**

Table 5.1 Notebook Cross-Reference for Compounds in Chapter 1.2-Continued

Compound	Structure	Notebook reference	NMR and IR data files
39	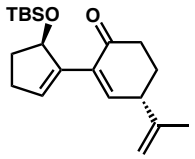	**CWL-V-49**	**CWL-VII-51**
88	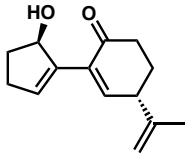	**CWL-V-95**	**CWL-VII-53**
40	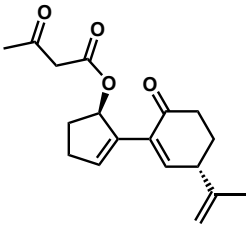	**CWL-V-133**	**CWL-VII-55**
41	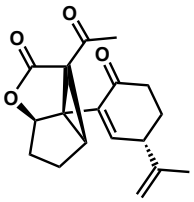	**CWL-V-113**	**CWL-V-111C**
42	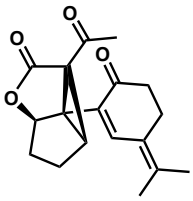	**CWL-V-113**	**CWL-V-111D**
43	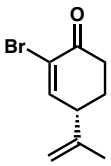	**CWL-VI-97**	**CWL-VI-97**

Table 5.1 Notebook Cross-Reference for Compounds in Chapter 1.2-Continued

Compound	Structure	Notebook reference	NMR and IR data files
21	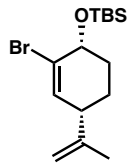	**CWL-VI-65**	**CWL-VI-101**
44	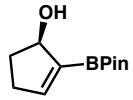	**CWL-VI-147**	**CWL-VII-15**
19	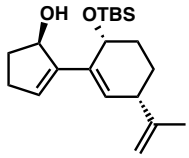	**CWL-VI-105**	**CWL-VI-105**
45	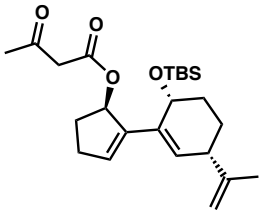	**CWL-VI-47**	**CWL-VI-107**
18	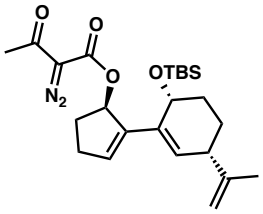	**CWL-VI-49**	**CWL-VI-109**
46	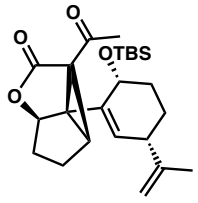	**CWL-VI-51**	**CWL-VI-111**

Table 5.1 Notebook Cross-Reference for Compounds in Chapter 1.2-Continued

Compound	Structure	Notebook reference	NMR and IR data files
47	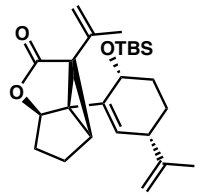	**CWL-VI-183**	**CWL-VI-113**
49	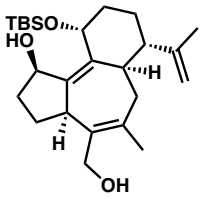	**CWL-VI-185**	**CWL-VI-115** **CWL-VI-185**

Table 5.2 Notebook Cross-Reference for Compounds in Chapter 1.3

Compound	Structure	Notebook reference	NMR and IR data files
60	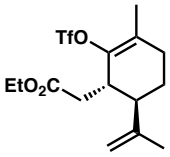	**ACW-XIX-023**	**ACW-XIX-triflatechar**
58	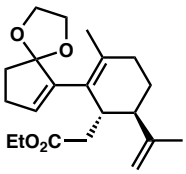	**ACW-XIX-57**	**ACW-XIX-XECchar**
67	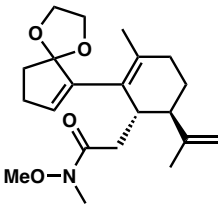	**ACW-XIX-**	**ACW-XIX-amidechar**
68	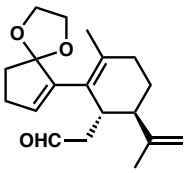	**ACW-XIX**	**ACW-XIX-ketaldehyde**
57	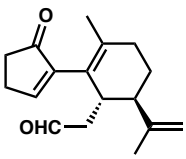	**CWL-VI-49**	**CWL-VI-109**
70	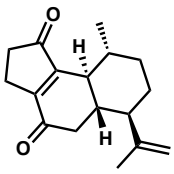	**ACW-XVI-61**	**ACW-XVI-61**

Table 5.2 Notebook Cross-Reference for Compounds in Chapter 1.3-Continued

Compound	Structure	Notebook reference	NMR and IR data files
72	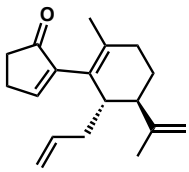	**ACW-XX-69**	**ACW-XX-69** **ACW-XX-263**
73	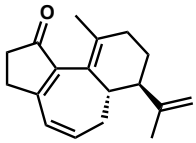	**ACW-XX-247**	**ACW-XX-247**

Table 5.3 Notebook Cross-Reference for Compounds in Chapter 2.2

Compound	Structure	Notebook reference	NMR and IR data files
95d	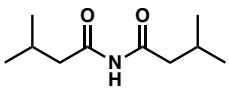	ACW-III-257	ACW-III-257
112	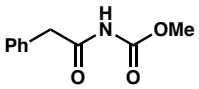	ACW-V-203	ACW-V-203-3
104c	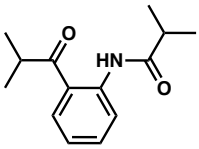	ACW-III-091	ACW-III-091
104d	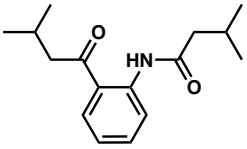	ACW-III-279	ACW-III-279
104e	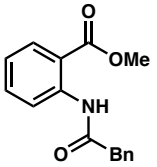	ACW-V-275	ACW-V-275
106a	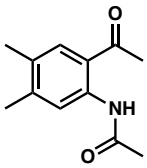	ACW-II-161	ACW-II-161
106b	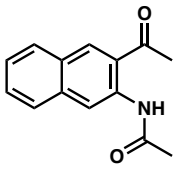	ACW-II-063	ACW-II-063

Table 5.3 Notebook Cross-Reference for Compounds in Chapter 2.2-Continued

Compound	Structure	Notebook reference	NMR and IR data files
106c	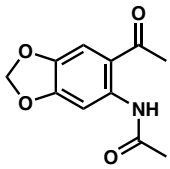	**ACW-II-87**	**ACW-II-87** **ACW-II-99**
106d	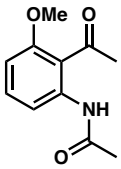	**CKH-V-061**	**CKH-V-061**
107c	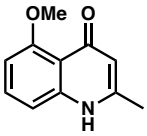	**ACW-V-259**	**ACW-V-259**
107b	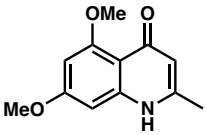	**CKH-V**	**CKH-V**
107a	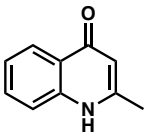	**CKH-V**	**CKH-V**

COMPREHENSIVE BIBLIOGRAPHY

Ackerman, L. K. G.; Lovell, M. M.; Weix, D. J. *Nature* **2015**, *524*, 454–457.

Anka-Lufford, L. L.; Huihui, K. M. M.; Gower, N. J.; Ackerman, L. K. G.; Weix, D. J. *Chem. Eur. J.* **2016**, *22*, 11564–11567.

Babler, J. H.; Coghlan, M. J. *Synth. Commun.* **1976**, *6*, 469–474.

Campbell, C. D.; Rees, C. W. *J. Chem. Soc.* **1969**, 742–747.

Canonne, P.; Boulanger, R.; Chantegrel, B. *Tetrahedron* **1987**, *43*, 663–668.

Caubere, P.; Loubinoux, B. *Bull. Soc. Chim. Fr.* **1968**, 3008–3012.

Charles, R. G. *J. Org. Chem.* **1957**, *22*, 677–679.

Chianese, G.; Fattorusso, E.; Aiyelaagbe, O. O.; Luciano, P.; Schröder, H. C.; Müller, W. E. G.; Taglialatela-Scafati, O. *Org. Lett.* **2011**, *13*, 316–319.

Comins, D. L.; Dehghani, A.; Foti, C. J.; Joseph, S. P. *Org. Synth.* **1997**, *74*, 77–80.

Craig II, R. A. C.; Roizen, J. L.; Smith, R. C.; Jones, A. C.; Virgil, S. C. *Chem. Sci.* **2017**, 8, 507–514.

Cross, R. M.; Manetsch, R. *J. Org. Chem.* **2010**, *75*, 8654–8657.

Danheiser, R. L.; Helgason, A. L. *J. Am. Chem. Soc.* **1994**, *116*, 9471–9479.

Dauben, W. G.; Michno, D. M. *J. Org. Chem.* **1977**, *42*, 682–685.

Davies, H. M. L.; Cantrell, R. W.; Jr.; Romines, R. K.; and Baum, S. J. *Org. Synth.* **1992**, 70, 93–100; *Coll. Vol. IX* **1998**, 422-426.

Davis, F. A. *Tetrahedron* **2018**, *74*, 3198–3214.

Denney, D. B.; Sherman, N. *J. Am. Chem. Soc.* **1965**, *30*, 3760–3761.

Everson, D. A.; Weix, D. J. *J. Org. Chem.* **2014**, *79*, 4793–4798.

Fairless, D. *Nature* **2007** 652–655.

Friedman, L.; Logullo, F. M. *J. Am. Chem. Soc.* **1963**, *85*, 1792–1797.

Fürstner, A.; Jumam, D. N.; Weidmann, H. *Tetrahedron Lett.* **1991**, *32*, 6695–6696.

Geoffrey, P.; Mouaddib, A.; Carre, M. C.; Caubere, P. *Tetrahedron Lett.* **1988**, *29*, 1385–1388.

Guyot, M.; Molho, D. *Tetrahedron Lett.* **1973**, *14*, 3433–3436.

Himeshima, Y.; Sonoda, T.; Kobayashi, H. *Chem. Lett.* **1983**, 1211–1214.

Hoffmann, R. W. *Dehydrobenzene and Cycloalkynes*; Academic Press: New York, 1967.

Huang, X.; Xue, J. *J. Org. Chem.* **2007***, 72*, 3965–3968.

Jamart-Gregoire, B.; Leger, C.; Caubere, P. *Tetrahedron Lett.* **1990**, *31*, 7599–7602.

Jones, C. P.; Anderson, K. W.; Buchwald, S. L. *J. Org. Chem.* **2007**, *72*, 7968–7973.

Kantorowski, E. J.; Kurth, M. J. *Tetrahedron* **2000***, 56*, 4317–4353.

Karaarslan, M.; Gokturk, E.; Demircan, A. *J. Chem. Res.* **2007**, 117–120.

Kauffmann, T.; Papenberg, M.; Wieschollek, R.; Sander, J. *Chem. Ber*. **1992**, *125*, 143–148.

Khan, S.; Kato, N.; Hirama, M. *Synlett* **2000**, 1494–1496.

Kitamura, T.; Yamane, M. *J. Chem. Soc. Chem. Commun.* **1995**, 983–984.

Lee, C. W.; Taylor, B. L. H.; Petrova, G. P.; Patel, A.; Morokuma, K.; Houk, K. N.; Stoltz, B. M. *J. Am. Chem. Soc.* **2019**, *141*, 6995–7004.

Levine, S. G. *J. Am. Chem. Soc.* **1958**, *80*, 6150–6151.

Li, Y.; Dai, M. *Angew. Chem. Int. Ed.* **2017**, *56*, 11624–11627.

Liu, G.-B.; Xu, J.-L.; He, C.-C.; Chen, G.; Xu, Q.; Xu, H.-X.; Li, J.-X. *Bioorg. Med. Chem.* **2009**, *17*, 5433–5441.

Liu, J.-Q.; Yang, Y.-F.; Li, X.-Y.; Liu, E.-Q.; Li, Z.-R.; Zhou, L.; Li, Y.; Qiu, M.-H., *Phytochemistry* **2013**, *96*, 265–272.

Logullo, F. M.; Seitz, A. H.; Friedman, L. *Org. Synth.* **1968**, *48*, 12–17.

Marion, N.; Díez-González, S.; Nolan, S. P. *Angew. Chem. Int. Ed.* **2007**, *46*, 2988–3000.

Matsumoto, T.; Hosoya, T.; Katsuki, M.; Suzuki, K. *Tetrahedron Lett.* **1991**, *32*, 6735–6736.

McUliffe, C. A.; Hosseiny, A.; McCullough, F. P. *Inorg*. *Chim*. *Acta* **1979**, *33*, 5–10.

Morcillo, S. P.; Miguel, D.; Campana, A. G.; de Cienfuegos, L. A.; Justicia, J.; Cuerva, J. M. *Org. Chem. Front.* **2014**, *1*, 15–33.

Müller, P. *Crystallography Reviews* **2009**, *15*, 57–83.

Naengchomnong, W.; Thebtaranonth, Y.; Wiriyachitra, P.; Okamoto, K. T.; Clardy, J. *Tetrahedron Lett.* **1986**, *27*, 2439–2442.

Oesterreich, K.; Klein, I.; Spitzner, D. *Synlett* **2002**, 1712–1713.

Okabe, M.; Sun, R.-C. *Tetrahedron* **1995**, *51*, 1861–1866.

Oldenziel, O. H.; Van Leusen, D.; Van Leusen, A. M. *J. Org. Chem.* **1977**, *42*, 3114–3118.

Olivares, A. M.; Weix, D. J. *J. Am. Chem. Soc.* **2018**, *140*, 2446–2449.

Pangborn, A. B.; Giardello, M. A.; Grubbs, R. H.; Rosen, R. K.; Timmers, F. J. *Organometallics* **1996**, *15*, 1518–1520.

Pansegrau, P. D.; Rieker, W. F.; Meyers, A. I. *J. Am. Chem. Soc.* **1988**, *110*, 7178–7184.

Picha, P.; Naengchomnong, W.; Promratanapongse, P.; Kano, E.; Hayashi, S.; Ohtsubo, T.; Zhang, S. W.; Shioura, H.; Kitai, R.; Matsumoto, H.; Kawahara, K.; Puribhat, S.; Phanthumachinda, P. *J. Exp. Clin. Cancer Res.* **1996**, *15*, 177–183.

Pintori, D. G.; Greaney, M. F. *Org. Lett.* **2010**, *12*, 168–171.

Poremba, K. E.; Kadunce, N. T.;Suzuki, N.; Cherney, A. H.; Reisman, S. E. *J. Am. Chem. Soc.* **2017**, *139*, 5684–5687.

Rodriguez–Ramos, F.; Navarette, A.; Gonzalez–Andrade, M.; Alarcon, C.; Aguilera–Cruz, A.; Reyes–Ramirez, Adelfo. *Bioorg. Chem.* **2013**, *50*, 17–25.

Saito, N.; Nakamura, K.; Shibano, S.; Ide, S.; Minami, M.; Sato, Y. *Org. Lett.* **2013**, *15*, 386–389.

Sarotti, A. M. *Org. Biomol. Chem.* **2018**, *16*, 944–950.

Seigel, C.; Gordon, P. M.; Razdan, R. K. *J. Org. Chem.* **1989**, *54*, 5428–5430.

Shair, M. D.; Yoon, T. Y.; Mosny, K. K.; Chou, T. C.; Danishefsky, S. J. *J. Am. Chem. Soc.* **1996**, *118*, 9509–9525.

Sheldrick, G. M. *Acta Cryst.* **1990**, A46, 467–473.

Sheldrick, G. M. *Acta Cryst.* **2015**, C71, 3–8.

Shi, L.-L.; Shen, H.-J.; Fang, L.-C.; Huang, J.; Li, C.-C.; Yang, Z. *Chem. Commun.* **2013**, *49*, 8806–8808.

Smith, III, A. B.; Branca, S. J.; Pilla, N. N.; Guaciaro, M. A. *Org. Lett.* **1982**, *47*, 1855–1869.

Still, W. C. *J. Am. Chem. Soc.* **1978**, *100*, 1481–1487.

Tambar, U. K.; Stoltz, B. M. *J. Am. Chem. Soc.* **2005**, *127*, 5340–5341.

Tobisu, M.; Ano, Y.; Chatani, N. *Org. Lett*. **2009**, *11*, 3250–3252.

Wang, A.; Tandel, S.; Zhang, H.; Huang, Y.; Holdeman, T. C.; Biehl, E. R. *Tetrahedron* **1998**, *54*, 3391–3400.

Wang, Q.; Fan, S. Y.; Wong, H. N. C.; Li, Z.; Fung, B. M.; Twieg, R. J.; Nguyen, H. T. *Tetrahedron Lett.* **1993**, *49*, 619–638.

Williamson, K. S.; Michaelis, D. J.; Yoon, T. P. *Chem. Rev.* **2014**, *114*, 8016–8036.

Wittig, G.; Hoffmann, R. W. *Org. Synth.* **1967**, *47*, 4–8.

Wright, A. C.; Haley, C. K.; Lapointe, G.; Stoltz, B. M. *Org. Lett.* **2016**, *18*, 2793–2795.

Wright, A. C.; Lee, C. W.; Stoltz, B. M. *Org. Lett.* **2019**, *21*, 9658–9662.

Wright, A. C.; Stoltz, B. M. *Chem. Sci*. **2019**, *10*, 10562–10565.

Xu, X.; Deng, Y.; Yim, D. N.; Zavalij, P. Y.; Doyle, M. P. *Chem. Sci.* **2015**, *6*, 2196–2201.

Yin, Z.; Sun, P. *Org. Lett.* **2012**, *77*, 11339–11344.

Yoshida, H.; Kishida, T.; Watanabe, M.; Ohshita, J. *Chem. Commun.* **2008,** 5963–5965.

Yoshida, H.; Watanabe, M.; Morishita, T.; Ohshita, J.; Kunai, A. *Chem. Commun.* **2007**, 1505–1507.

Yoshida, H.; Watanabe, M.; Ohshita, J.; Kunai, A. *Tetrahedron Lett.* **2005**, *46,* 6729–6731.

Yu, M.; Danishefsky, S. J. *J. Am. Chem. Soc.* **2008**, *130*, 2783–2785.

INDEX

A

aldehyde……..…...…….…….……12,13,19,21,51,54,60

allylic alcohol….…….…….…….5,20,22,28,31,32,36,37

annulation……...…….……..…….…….……6,18

anticancer…….……..…….…….……2

aryne……..…..…….…….……153,154,155,157,158,159

B

boronate……...…..…….…….5,8,9,30,35,41,42

bromide…....…….…….……9,14,15,16,30,34,39,41,42,49,54,55

C

Camps cyclization…….……..…….…….……158,159

carboxy-inversion……..12

carcinoma…….…….……..…….2

carvone…….…….……...…….…….14

cascade……..…….…….…….……...…….2

catalyst…….……...…….…….15,19,53,55,56,58

Cope…….…….…….…….…….5

cross-coupling…….……...…..…….…...…….14,17

cross-electrophile coupling…….…….…….…….…….13,14,25

curcusone……..…….…….…….……1,2,3,4,8,11,13,20,21,23,24,25

cycloheptadienone…….…….……....……13

cyclopentenone……20, 23

cyclopropanation……4,7,8,9,10,12,13,25

cyclopropane……4

D

Davis oxaziridine……22

deprotection……6,8,9,20,59

diastereoselectivity……14,19

diazo transfer……4,6,8,10

Diels–Alder……3,5,6

diene……6,31,36,43

diketene……8,32,37,44

diosphenol……13

diterpenoid……1,2

divinylcyclopropane……3,4,5,10,11,13,25,46

E

electrophiles……14,15

epoxidation……5,22,28

esterification……10

I

imide……155,156,157,159,161,162,164,167,168,169,170

indoles……154,159

J

J. curcas……1

K

Kauffmann olefination……..…….……..…10

ketoamide……..…….…….……..……154,155,157,159,162

ketone…….…….…….…….7,8,10,12,20,21,23,34,40,163,164,166

L

lactone…….…….…….……4,10,11,12,47,48

limonene oxide…….…….…….…….…….5

N

natural product…….…….…….……..2,3,24

O

olefination…….……..…….…….……3,7,8,10,20

oxidation…….…….…….…….3,5,12,22,23

P

perillaldehyde…….…….…..……..……7,8

protection……..……..…….…….6,9,59

Q

quinolones..……..……..…….…….…..……154,158,159,168,169,170

R

radical……..……..…….……..…..……10

rearrangement……..……...…….……3,4,5,11,12,13,20,25

reduction…..……..……..…….…….……6,13,14,16,18,22,59

regioselectivity……..…….…..…….……..……..…….20,22,23

retrosynthetic analysis……..…….…….……..……3,4,13

rhamnofolane……2

ring-closing metathesis……20

S

stereochemistry……3,5,18,19,20

stereospecific……4,5

Stetter……13,18,19

Suzuki……4,5,6,8,9

T

total synthesis……2,25

transition state……5

triflate……5,14,16,17,29,30,31,49,50

U

Umpolung……18

W

Wittig……18

X

X-ray……2,3

About the Author

Austin C. Wright was born in Scranton, PA on May 1, 1992 as the youngest of three sons of Richard and Sharon Wright. He spent his youngest years across several areas of the country, including Clarks Summit, Pennsylvania; Jonesboro, Arkansas; and Tinley Park, Illinois. He finally settled in Souderton, PA during his teenage years, where he enrolled at the Souderton Area High School. In addition to competing in track and cross-country, he grew a fondness for chemistry after taking an AP Chemistry class with an entertaining and inspiring teacher named Peter Spizzirri.

He then enrolled at the Pennsylvania State University in 2010, where he worked in the laboratory of Professor Steven Weinreb. His undergraduate research was focused on the total synthesis of geissoschizol and several related indole alkaloid natural products. Although the key nickel-catalyzed annulation step proved unsuccessful, the training he received during these studies greatly improved his experimental technique and understanding of organic synthesis.

Upon graduating in 2014 with a B.S. in Chemistry, he moved to Pasadena, California to commence graduate studies at the California Institute of Technology under the guidance of Professor Brian Stoltz. After completing a method for the insertion of arynes into imides, he then gravitated toward the total synthesis of several members of the curcusone family of natural products. During these synthetic studies, he wrote a review on the recent synthetic applications of arynes as well as a novel apparatus for performing small-scale ketalizations.

I must also mention my favorite albums:

Husker Du: ……Zen Arcade

The Residents:…….……..……God in Three Persons